# DISSERTATION / DOCTORAL THESIS

Titel der Dissertation / Title of the Doctoral Thesis

## Triangular fully packed loop configurations: Wieland drift, configurations of small excess and a generalisation

verfasst von / submitted by

### Mag.rer.nat. Sabine Beil

angestrebter akademischer Grad / in partial fulfilment of the requirements for the degree of

### Doktorin der Naturwissenschaften (Dr.rer.nat.)

Wien, Juni 2016

# Contents

# Acknowledgements

Firstly, I would like to express my deepest gratitude to my advisor Ilse Fischer for her trust in me and her constant support throughout my research and the writing of this thesis. Thank you for giving me the freedom to generate and explore ideas and guiding and advising me with such insight whenever I needed help! I can think of no better advisor for my PhD study.

Besides my advisor I would like to thank Philippe Nadeau who contributed to the paper *Wieland drift for triangular fully packed loop configurations.* Thank you for sharing your ideas with us so generously! It was a pleasure to work with you. Furthermore, I would like to thank those who have reviewed my work in the last four years. Your thoughtful comments helped me write this thesis.

I furthermore thank my colleagues for their support, the stimulating discussions and all the fun we have had in the last four years. Special thanks go to Tomack Gilmore who proofread many of the things I wrote during my PhD.

Last but not the least, I would like to thank my parents Gabriele and Willibald Beil, my brothers Josef and Maximilian and my partner Lukas Riegler for their support, I love you!

# Summary

In this thesis, we consider fully packed loop configurations (FPLs), that is, subgraphs $F$ of the $n \times n$ square grid together with $4n$ external edges such that every vertex of the grid is incident to two edges of $F$ and precisely every other external edge starting with the, say, topmost horizontal external edge on the left side is occupied by $F$. They are in one-to-one correspondence with alternating sign matrices (ASMs), hence their number is given by the famous formula for the number of ASMs proved in [**31**] and later in [**14**]. This correspondence made FPLs that were until then mainly studied in statistical mechanics known among combinatorialists.

In contrast to ASMs, FPLs allow a study in dependency on the connectivity of the occupied external edges (these connections are encoded as a link pattern, $\pi$, and the number of FPLs with such a pattern is denoted $A_\pi$). The study of the numbers $A_\pi$ was excited by the Razumov–Stroganov correspondence, which was conjectured by Razumov and Stroganov in [**25**] and proved by Cantini and Sportiello in [**9**]. It relates the numbers $A_\pi$ to the XXZ quantum spin chain at anisotropy parameter $\Delta = -\frac{1}{2}$, Temperley-Lieb random walks and the dense $\mathcal{O}(1)$ loop model. In addition, various beautiful properties of the numbers $A_\pi$ have been proved in recent years. For instance, it was conjectured in [**35**] and proved in [**10**] that for link patterns $\pi \cup m$ made up of a link pattern $\pi$ and $m$ nested arches, $A_{\pi \cup m}$ is polynomial in $m$.

Triangular fully packed loop configurations (TFPLs) – the central objects of this thesis – came up in [**10**] in the course of the proof that $A_{\pi \cup m}$ is a polynomial in $m$: for large $m$ FPLs with link pattern $\pi \cup m$ admit a decomposition as part of which TFPLs occur. From this decomposition the authors of [**10**] derive an expression for the numbers $A_{\pi \cup m}$ from which it immediately follows that $A_{\pi \cup m}$ is a polynomial in $m$. Since in this expression numbers of TFPLs show up it provides a link between the numbers of TFPLs and the numbers $A_{\pi \cup m}$. Besides this link, the many nice properties that have been discovered since the emergence of TFPLs ([**29**], [**19**], [**11**]) motivate the study of TFPLs. For instance, one such property is that the boundary of a TFPL, that is, a triple $(u, v; w)$ made up of 01-words, must satisfy

$$(0.1) \qquad\qquad \mathrm{d}(u) + \mathrm{d}(v) \leq \mathrm{d}(w),$$

where $\mathrm{d}(\omega)$ denotes the number of inversions in $\omega$. The integer $\mathrm{exc}(u, v; w) = \mathrm{d}(w) - \mathrm{d}(u) - \mathrm{d}(v)$ is in the following said to be the excess of a TFPL (with boundary $(u, v; w)$). To study TFPLs with respect to the excess of their boundary turned out to be fruitful.

In [11] enumeration results for TFPLs of excess 0 or 1 were proved. To begin with, if $\text{exc}(u, v; w) = 0$ the number of TFPLs with boundary $(u, v; w)$ is given by the Littlewood-Richardson coefficient

$$(0.2) \qquad\qquad c^{\lambda(w)}_{\lambda(u),\lambda(v)},$$

where $\lambda(u)$, $\lambda(v)$ and $\lambda(w)$ are Young diagrams assigned to $u$, $v$ and $w$. This provides a new enumeration for Littlewood-Richardson coefficients, which are important in various areas of mathematics including algebraic geometry, representation theory and algebraic combinatorics. Finally, if $\text{exc}(u, v; w) = 1$ then the number of TFPLs with boundary $(u, v; w)$ admits an expression in terms of Littlewood-Richardson coefficients.

Wieland gyration, on the other hand, is an operation on FPLs that was invented in [30] to prove the rotational invariance of the numbers of FPLs corresponding to fixed link patterns. Later it was heavily used by Cantini and Sportiello [9] to prove the Razumov–Stroganov correspondence. In connection with TFPLs, Wieland gyration first appeared in [29] and [19].

The research that this thesis is made up of is part of two published articles (Chapter 3 and Chapter 5) and an accepted article (Chapter 4). In Chapter 3 Wieland drift is defined as an operation on TFPLs that is composed of the same local operations as the usual Wieland gyration for FPLs. In addition, various properties of Wieland drift are proved: due to a finiteness argument for every TFPL $f$ the sequence $(\text{WL}^m(f))_{m \geq 0}$ made up of the images of $f$ under iterated applications of left-Wieland drift WL is eventually periodic. In Theorem 3.10, it is proved that the length of the period is always one, which means one always reaches a TFPL that is invariant under left-Wieland drift. In fact, if $N$ is the size of $f$, then less than $2N$ iterations of WL suffice to obtain such a stable configuration. A key step in the proof of Theorem 3.10 is to classify these stable TFPLs. It turns out that the stability of a TFPL depends solely on the occurrence of a certain type of edges called drifters, which is the content of Theorem 3.11. These results also hold for right-Wieland drift.

The focus in Chapter 4 lies on TFPLs of excess 2. The main result is a linear expression for the number of TFPLs of excess 2 in terms of numbers of TFPLs that are invariant under Wieland drift, see Theorem 4.2. This linear expression generalises already existing enumeration results for TFPLs of excess 0 or 1. Its proof heavily uses Wieland drift.

In the last chapter of this thesis hexagonal fully packed loop configurations (HFPLs) are introduced as a generalisation of TFPLs. Furthermore, some of the existing results for TFPLs are generalised to HFPLs. To begin with, each HFPL is assigned a sextuple $(\mathsf{l_T}, \mathsf{t}, \mathsf{r_T}; \mathsf{l_B}, \mathsf{b}, \mathsf{r_B})$ of 01-words that encodes its boundary conditions. This is done in a way that generalises the way in which the boundary conditions of a TFPL are encoded by 01-words. The necessary condition in (0.1) for the boundary of a TFPL generalises to

the necessary condition

$$(0.3) \qquad d(r_B) + d(b) + d(l_B) \geq d(l_T) + d(t) + d(r_T) + |l_T|_1 |t|_0 + |t|_1 |r_T|_0 + |r_B|_0 |l_B|_1$$

for the boundary of an HFPL (Theorem 5.11). Here, $| \cdot |_i$ denotes the number of occurrences of $i$ for $i = 0, 1$.

The excess of an HFPL with boundary $(l_T, t, r_T; l_B, b, r_B)$ is defined as $\mathrm{exc}(l_T, t, r_T; l_B, b, r_B) = d(r_B) + d(b) + d(l_B) - d(l_T) - d(t) - d(r_T) - |l_T|_1 |t|_0 - |t|_1 |r_T|_0 - |r_B|_0 |l_B|_1$. As in the case of TFPLs, (0.3) shows that the excess of an HFPL must be non-negative. Similarly Theorem 5.35 shows that HFPLs with boundary $(l_T, t, r_T; l_B, b, r_B)$ such that $\mathrm{exc}(l_T, t, r_T; l_B, b, r_B) = 0$ are enumerated by the Littlewood-Richardson coefficient

$$c^{\lambda(l_B \, b \, r_B)}_{\lambda(m(l_B) \, l_T \, t), \, \lambda(m(t) \, r_T \, m(r_B))},$$

where $m(\omega)$ denotes the 01-word of length $N$ in which the first $|\omega|_0$ letters are zero and the last $|\omega|_1$ letters are 1. Finally, an expression for the number of HFPLs of excess 1 is established in Theorem 5.49.

# Zusammenfassung

Diese Dissertation befasst sich mit Fully Packed Loop Konfigurationen (FPLen), das heißt, Teilgraphen $F$ des $n \times n$ quadratischen Rasters zusammen mit $4n$ äußeren Kanten, sodass jeder Knoten des Rasters Endknoten zweier Kanten von $F$ ist und genau jede zweite äußere Kante startend, sagen wir, mit der obersten horizontalen äußeren Kante auf der linken Seite, von $F$ belegt ist. Sie sind in eineindeutiger Beziehung zu alternierenden Vorzeichenmatrizen, somit ist ihre Anzahl gegeben durch die berühmte Formel für die Anzahl von Vorzeichenmatrizen der Größe $n$, die in [**31**] und später in [**14**] bewiesen wurde. Diese Beziehung machte FPLen, welche bis dahin hauptsächlich in der statistischen Mechanik studiert wurden, unter KombinatorikerInnen bekannt.

Im Unterschied zu alternierenden Vorzeichenmatrizen erlauben FPLen eine verfeinerte Studie in Abhängigkeit davon, welche der belegten externen Kanten miteinander verbunden sind (diese Verbindungen werden in einem Verbindungsdiagramme, $\pi$, kodiert und die Anzahl von FPLen mit Verbindungsdiagramm $\pi$ wird mit $A_\pi$ bezeichnet). Die Studie der Anzahlen $A_\pi$ wurde von der Razumov–Stroganov Beziehung, welche von Razumov und Stroganov in [**25**] vermutet und von Cantini und Sportiello in [**9**] bewiesen wurde, angeregt. Diese bringt die Zahlen $A_\pi$ in Beziehung mit der XXZ Quantum Spin Kette bei Anisotropieparameter $\Delta = -\frac{1}{2}$, Temperley-Lieb Random Walks und dem Dense $\mathcal{O}(1)$ Loop Modell. Zusätzlich wurden in den letzten Jahren viele verschiedene schöne Eigenschaften der Anzahlen $A_\pi$ bewiesen. Zum Beispiel wurde in [**35**] vermutet und in [**10**] bewiesen, dass für Verbindungsdiagramme $\pi \cup m$ bestehend aus einem Verbindungsdiagramm $\pi$ und $m$ verschachtelten Verbindungen $A_{\pi \cup m}$ polynomiell in $m$ ist.

Dreieckige Fully Packed Loop Konfigurationen (DFPLen) – die zentralen Objekte dieser Dissertation – kamen im Zuge des Beweises in [**10**], dass $A_{\pi \cup m}$ ein Polynom in $m$ ist, auf: für große $m$ erlauben FPLen mit Verbindungsdiagramm $\pi \cup m$ eine Zerlegung als Teil welcher DFPLen auftauchen. Von dieser Zerlegung leiten die Autoren von [**10**] einen Ausdruck für die Zahlen $A_{\pi \cup m}$ ab, aus dem sofort folgt, dass $A_{\pi \cup m}$ ein Polynom in $m$ ist. Da in diesem Ausdruck auch Anzahlen von DFPLen vorkommen, stellt er eine Verbindung zwischen der Abzählung von DFPLen und von FPLen mit Verbindungsdiagrammen des Typs $\pi \cup m$ dar. Neben dieser Verbindung wird die Studie von DFPLen durch ihre zahlreichen netten Eigenschaften ([**29**], [**19**] und [**11**]) motiviert. Eine solche ist, zum Beispiel, dass der Rand einer DFPL, das ist ein Tripel $(u, v; w)$ aus 01-Wörtern, stets

$$(0.4) \qquad\qquad \mathrm{d}(u) + \mathrm{d}(v) \leq \mathrm{d}(w)$$

erfüllen muss. Hier bezeichnet d(·) die Anzahl an Inversionen in einem Wort. Die Zahl $\mathrm{exc}(u,v;w) = \mathrm{d}(w) - \mathrm{d}(u) - \mathrm{d}(v)$ wird im Folgenden als der Exzess einer DFPL (mit Rand $(u,v;w)$) bezeichnet.

DFPLen unter Berücksichtigung ihres Exzesses zu studieren hat sich als ergebnisreich erwiesen. So wurden in [20] und [11] Abzählresultate für DFPLen von Exzess 0 oder 1 bewiesen. Ist zunächst $\mathrm{exc}(u,v;w) = 0$, dann ist die Anzahl von DFPLen mit Rand $(u,v;w)$ durch den Littlewood-Richardson Koeffizienten

$$(0.5) \qquad\qquad\qquad c^{\lambda(w)}_{\lambda(u),\lambda(v)}$$

gegeben, wobei $\lambda(u)$, $\lambda(v)$ und $\lambda(w)$ den 01-Wörtern $u$, $v$ und $w$ zugeordnete Young Diagramme sind. Littlewood-Richardson Koeffizienten sind in verschiedenen Feldern der Mathematik wie zum Beispiel algebraische Geometrie, Darstellungstheorie und algebraische Kombinatorik von Bedeutung. Das obige Resultat bringt sie nun auch in Zusammenhang mit DFPLen. Ist schließlich $\mathrm{exc}(u,v;w) = 1$, so kann die Anzahl von DFPLen mit Rand $(u,v;w)$ in Form von Littlewood-Richardson Koeffizienten ausgedrückt werden.

Wieland Rotation, auf der anderen Seite, ist eine Operation auf FPLen, die in [30] entwickelt wurde, um zu zeigen, dass die Anzahl von FPLen mit einem festen Verbindungsdiagramm invariant unter Rotation dieses Verbindungsdiagramms ist. Später hat sie erheblich zum Beweis der Razumov–Stroganov Beziehung [25] durch Cantini und Sportiello ([9]) beigetragen. Im Zusammenhang mit DFPLen tauchte Wieland Rotation erstmals in [29] und [19] auf.

Die Forschungsarbeit, aus welcher diese Dissertation besteht, ist Teil zweier veröffentlichter Artikel (Kapitel 3 und Kapitel 5) und eines akzeptierten Artikels (Kapitel 4). In Kapitel 3 wird Wieland Trift definiert als eine Operation auf DFPLen, die sich aus denselben lokalen Operationen wie die übliche Wieland Rotation für FPLen zusammensetzt. Des weiteren werden einige Eigenschaften von Wieland Trift bewiesen: für jede DFPL $f$ muss die Folge $(\mathrm{WL}^m(f))_{m \geq 0}$ bestehend aus den Bildern von $f$ unter iterierten Anwendungen von Links-Wieland Trift aufgrund eines Endlichkeitsarguments schließlich periodisch sein. In Theorem 3.10 wird gezeigt, dass die Periodenlänge dabei stets 1 sein muss, das heißt, durch WL wird immer eine DFPL erreicht, die invariant unter Links-Wieland Trift ist. Genauer benötigt es dazu höchstens $2N$ Iterationen von WL, wenn $N$ die Größe der DFPL bezeichnet. Ein zentraler Schritt im Beweis von Theorem 3.10 ist die Klassifizierung von DFPLen, die invariant unter WL sind: die Stabilität einer DFPL unter WL hängt ausschließlich vom Vorhandensein eines speziellen Typs an Kanten – Trifter genannt – ab (Theorem 3.11). Diese Resultate gelten auch für Rechts-Wieland Trift.

Der Fokus in Kapitel 4 liegt auf DFPLen von Exzess 2. Das Hauptresultat ist ein linearer Ausdruck für die Anzahl von DFPLen von Exzess 2 in den Anzahlen von DFPLen, die invariant unter der Anwendung von Wieland Trift sind, siehe Theorem 4.2.

Dieser lineare Ausdruck verallgemeinert bereits bekannten Abzählresultate für DFPLen von Exzess 0 oder 1. Sein Beweis beruht stark auf Wieland Trift.

Im letzten Kapitel dieser Dissertation werden Hexagonale Fully Packed Loop Konfigurationen (HFPLen) als Verallgemeinerung von DFPLen eingeführt. Des weiteren werden einige der bereits bekannten Resultate für DFPLen für HFPLen formuliert und bewiesen. Zunächst wird jeder HFPL ein Sextupel $(\mathsf{l_T}, \mathsf{t}, \mathsf{r_T}; \mathsf{l_B}, \mathsf{b}, \mathsf{r_B})$, das den Rand der HFPL kodiert, zugeordnet. Das wird in einer Art und Weise getan, die das Kodieren des Randes einer DFPL durch Wörter verallgemeinert. Die notwendige Bedingung in (0.4) für den Rand $(u, v; w)$ einer DFPL wird dann zu der notwendigen Bedingung

$$(0.6) \qquad \mathrm{d}(\mathsf{r_B}) + \mathrm{d}(\mathsf{b}) + \mathrm{d}(\mathsf{l_B}) \geq \mathrm{d}(\mathsf{l_T}) + \mathrm{d}(\mathsf{t}) + \mathrm{d}(\mathsf{r_T}) + |\mathsf{l_T}|_1 |\mathsf{t}|_0 + |\mathsf{t}|_1 |\mathsf{r_T}|_0 + |\mathsf{r_B}|_0 |\mathsf{l_B}|_1$$

für den Rand einer HFPL (Theorem 5.11). Hier bezeichnet $|w|_i$ die Anzahl des Vorkommens von $i$ in dem Wort $w$ für $i = 0, 1$.

Der Exzess einer HFPL mit Rand $(\mathsf{l_T}, \mathsf{t}, \mathsf{r_T}; \mathsf{l_B}, \mathsf{b}, \mathsf{r_B})$ ist definiert als $\mathrm{exc}(\mathsf{l_T}, \mathsf{t}, \mathsf{r_T}; \mathsf{l_B}, \mathsf{b}, \mathsf{r_B}) = \mathrm{d}(\mathsf{r_B}) + \mathrm{d}(\mathsf{b}) + \mathrm{d}(\mathsf{l_B}) - \mathrm{d}(\mathsf{l_T}) - \mathrm{d}(\mathsf{t}) - \mathrm{d}(\mathsf{r_T}) - |\mathsf{l_T}|_1 |\mathsf{t}|_0 - |\mathsf{t}|_1 |\mathsf{r_T}|_0 - |\mathsf{r_B}|_0 |\mathsf{l_B}|_1$. Wie auch im Falle von DFPLen folgt aus (0.6), dass der Exzess einer HFPL nicht-negativ ist. Ebenso werden HFPLen mit Rand $(\mathsf{l_T}, \mathsf{t}, \mathsf{r_T}; \mathsf{l_B}, \mathsf{b}, \mathsf{r_B})$ sodass $\mathrm{exc}(\mathsf{l_T}, \mathsf{t}, \mathsf{r_T}; \mathsf{l_B}, \mathsf{b}, \mathsf{r_B}) = 0$ durch den Littlewood-Richardson Koeffizienten

$$c^{\lambda(\mathsf{l_B}\, \mathsf{b}\, \mathsf{r_B})}_{\lambda(\mathrm{m}(\mathsf{l_B})\, \mathsf{l_T}\, \mathsf{t}),\, \lambda(\mathrm{m}(\mathsf{t})\, \mathsf{r_T}\, \mathrm{m}(\mathsf{r_B}))},$$

abgezählt, siehe Theorem 5.35. Hier bezeichnet $\mathrm{m}(\omega)$ das 01-Wort der Länge $N$, in dem die ersten $|\omega|_0$ Buchstaben 0 und die letzten $|\omega|_1$ Buchstaben 1 sind. Schlussendlich wird in Theorem 5.49 ein Ausdruck für die Anzahl von HFPLen mit Rand $(\mathsf{l_T}, \mathsf{t}, \mathsf{r_T}; \mathsf{l_B}, \mathsf{b}, \mathsf{r_B})$, wo $\mathrm{exc}(\mathsf{l_T}, \mathsf{t}, \mathsf{r_T}; \mathsf{l_B}, \mathsf{b}, \mathsf{r_B}) = 1$, bewiesen.

CHAPTER 1

# Introduction

## 1.1. Fully packed loop configurations

**1.1.1. The square-ice or six-vertex model.** In ordinary ice, each oxygen atom is tetrahedrally surrounded by four oxygen atoms at a distance of 275 pico metre. Furthermore, each water molecule is oriented so that its hydrogen atoms are directed towards two of the four nearest oxygen atoms forming hydrogen bonds. The orientations are further restricted by the requirement that only one hydrogen atom lies between two neighbouring oxygen atoms. An ice crystal can thus exist in any one of a large number of configurations, each corresponding to certain orientations of the water molecules.

Pauling ([**22**]) proposed this crystal structure of ordinary ice in 1935 to account for the *residual entropy* of ice that was measured by Ashley and Giauque ([**2**]) in 1933. For $N$ large enough the residual entropy of ice is given by $S = k_B N \log W$ where $k_B$ is Boltzmann's constant, $N$ the number of oxygen atoms in the ice crystal and $W = \lim_{n \to \infty} \sqrt[n]{Z_n}$ in which $Z_n$ denotes the number of all configurations accessible to the crystal consisting of $n$ oxygen atoms. Since the crystal structure proposed by Pauling allows multiple configurations, $Z_n > 1$ for $n > 1$ and therefore $S$ is positive.

Although Pauling did not succeed in computing $W$ he could derive the estimate $W \approx 1.5$. While this agreed well with the measurements by Ashley and Giauque Pauling's theory could not be verified until exact values for $W$ were found. Given the enumerative nature of this problem it became popular amongst combinatorialists, who found it to be very hard indeed. Only in 1967 was the first exact solution for $W$ found. Lieb ([**15**]) computed the exact value of $W$ in the 2-dimensional case, namely $W = (\frac{4}{3})^{\frac{3}{2}} \approx 1.5396007$. In higher dimensions no exact solutions for $W$ are known to this day. Numerical computations of $W$, on the other hand, exist in two and three dimensions. Nagle ([**21**]) found that $W = 1.50685 \pm 0.00015$ in the 2-dimensional case and $W = 1540 \pm 0.001$ in the 3-dimensional case.

The two-dimensional ice model that Lieb used to compute $W$ was the **square-ice** model, that is, the oxygen atoms are located at the points in the plane with integer coordinates and the hydrogen atoms lineal between the oxygen atoms. The square ice model may be represented as an oriented graph by replacing the oxygen atoms by vertices and the bonds between two oxygen atoms by arrows that indicate to which oxygen atom the hydrogen atom is covalently bonded (see Figure 1.1 for an example). In this graphical
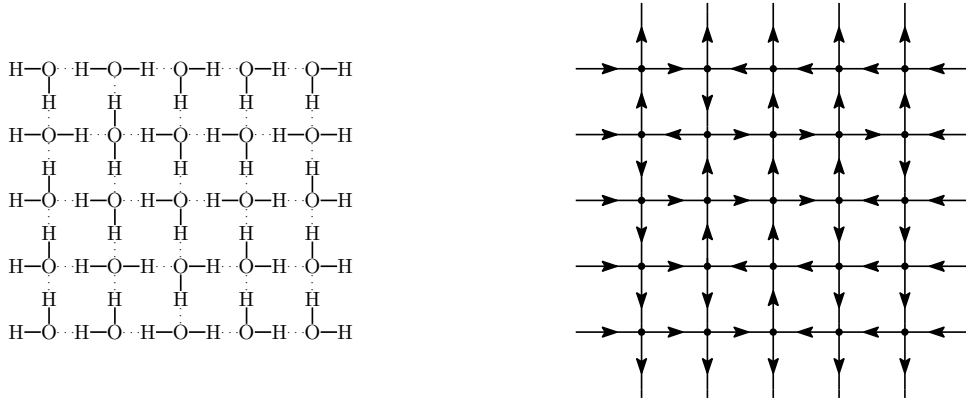
FIGURE 1.1. Left: a square-ice configuration in which the lines indicate the covalent bonds and the dotted lines the hydrogen bonds. Right: the six-vertex configuration corresponding to the square-ice configuration on the left side.

representation of the square-ice model, there must be one of the six configurations displayed in Figure 1.2 around each vertex. This is why the graphical representation of the square-ice model is called the **six-vertex** model.

To the vertices in a six-vertex configuration weights can be assigned dependent on the orientations of the four adjacent edges as is indicated in Figure 1.2. Physically, the weights cohere with the energies of the configurations at each vertex. Two-dimensional ice-crystals correspond to taking all weights equal to 1. Additionally to two-dimensional ice-crystals, the six vertex model may represent other crystal arrangements. For instance 2-dimensional potassium dihydrogen phosphate crystals correspond to taking $a_1 = a_2 = 1$ and $b_1 = b_2 = c_1 = c_2 > 1$, see ([**27**]).
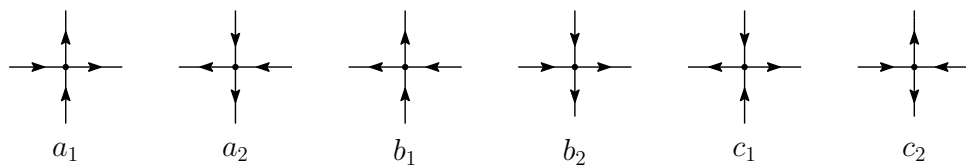


FIGURE 1.2. The six configurations around a vertex in the six-vertex model.

From now on, six-vertex configurations will be considered on $n \times n$-squares. The underlying graph of such configurations is the graph $G_n$ whose vertex set is $[n] \times [n]$, where $[n] = \{1, 2, \ldots, n\}$. Furthermore, any two vertices that are spaced at distance 1 are adjacent in $G_n$ and $4n$ external edges are attached to the vertices on the boundary as follows: external edges that are attached to vertices with $x$-coordinate 1 or $n$ are horizontal, while external edges that are attached to vertices with $y$-coordinate 1 or $n$ are vertical. A **six-vertex configuration of size** $n$ henceforth refers to a six-vertex configuration on $G_n$. Figure 1.1 displays an example. Six-vertex configurations of finite size may be studied with both restricted and unrestricted boundary conditions. Here, they shall obey the **domain wall boundary condition** (abbreviated DWBC) that was

introduced by Korepin in [13], whereby the horizontal external edges point inwards and the vertical external edges point outwards. The configuration in Figure 1.1 satisfies the DWBC.
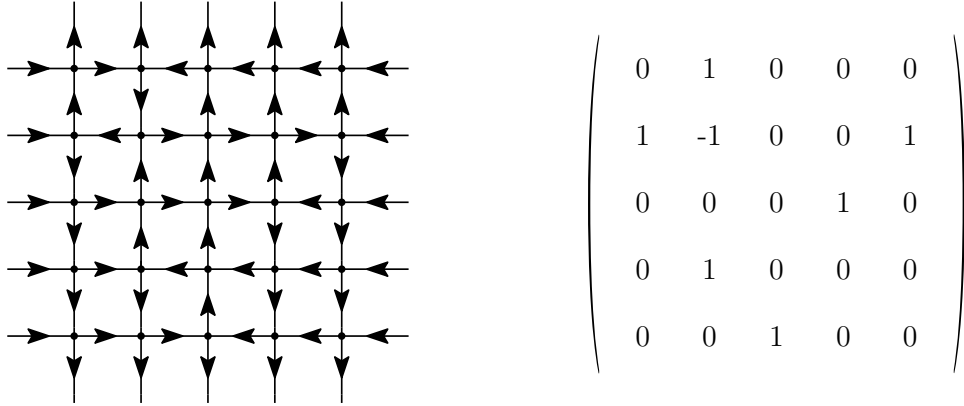


$$\begin{pmatrix} 0 & 1 & 0 & 0 & 0 \\ 1 & -1 & 0 & 0 & 1 \\ 0 & 0 & 0 & 1 & 0 \\ 0 & 1 & 0 & 0 & 0 \\ 0 & 0 & 1 & 0 & 0 \end{pmatrix}$$

FIGURE 1.3. The six-vertex configuration with DWBC from Figure 1.1 and its corresponding $5 \times 5$ ASM.

Six-vertex configurations are not only important in statistical mechanics but also in combinatorics. This comes from the fact that six-vertex configurations with DWBC are in one-to-one correspondence with **alternating sign matrices** (abbreviated ASMs). The latter are matrices with entries 1, $-1$ and 0 such that the non-zero elements in each row and column alternate in sign and sum up to 1. An example is given in Figure 1.3. ASMs came up in the study of $\lambda$-determinants by Mills, Robbins and Rumsey in 1982, see [16]. Since then many links have been discovered between ASMs and other fields of interest in combinatorics, including (amongst others) *descending plane partitions*, *totally symmetric self-complementary plane partitions* and *domino tilings*.

The number of alternating sign matrices of size $n$, denoted $A_n$, is given by the following nice formula:

$$(1.1) \qquad\qquad A_n = \prod_{k=0}^{n-1} \frac{(3k+1)!}{(n+k)!}$$

This formula was conjectured by Mills, Robbins and Rumsey ([17]) in 1983. Great efforts were made to prove it in the years following, and in the end it was Zeilberger ([31]) who found the first proof. He proposed it in 1992 and thereafter it took the referees a further three years to verify his argument. In 1995 Kuperberg ([14]) gave a simpler proof of (1.1) that exploited the connection between ASMs and the six-vertex model. It relied on the *Yang-Baxter equation* for the six vertex model. The correspondence between ASMs and six-vertex configurations has played a key role in proofs of identities for ASMs ever since. Most recently, it has been used by Behrend, Fischer and Konvalinka

to prove enumeration results for *diagonally and antidiagonally symmetric* ASMs of odd order, see [**4**].

**1.1.2. Fully packed loop configurations.** In 1996 Batchelor, Blöte, Nienhuis and Yung ([**3**]) were the first to investigate **fully packed loops** on the square lattice (abbreviated FPLs), which are subgraphs $f$ of the square grid such that each vertex is incident to precisely two edges of $f$. An FPL is of size $n$ if it is a subgraph of the graph $G_n$. In the following, we limit ourselves to FPLs satisfying the domain wall boundary conditions (without mentioning this explicitly again). An FPL fulfils the **domain wall boundary conditions** if along the border every other external edge belongs to the FPL, starting with the topmost on the left side. Beginning at this edge the $2n$ external edges belonging to the FPL are numbered counter-clockwise. An example of an FPL is displayed in Figure 1.4.
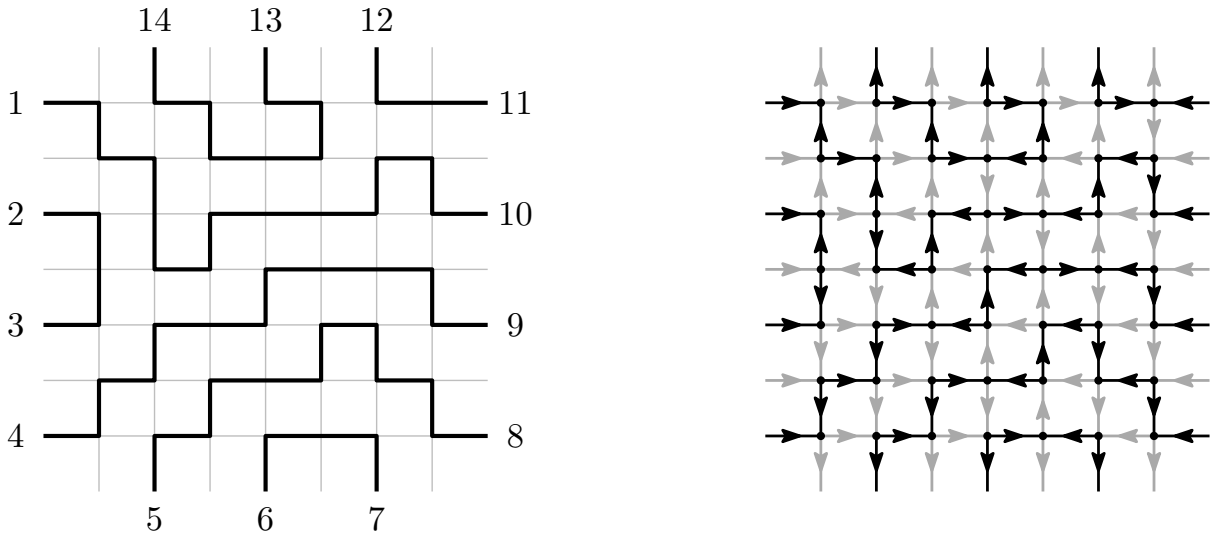


FIGURE 1.4. An FPL of size 7 together with its corresponding six-vertex configuration.

FPLs of size $n$ are in one-to-one correspondence with six-vertex configurations of size $n$ satisfying the DWBC and thus with ASMs of size $n$. The correspondence between FPLs and six-vertex configurations satisfying the DWBC is indicated by the example in Figure 1.4. In contrast to ASMs and six-vertex configurations, FPLs offer a refined study with respect to the connectivity of the occupied external edges (these connections are encoded as a link pattern). A **link pattern** $\pi$ of size $2n$ is defined as a partition of $[2n] = \{1, 2, \ldots, 2n\}$ into $n$ blocks of size 2 that are pairwise non-crossing, that is, there are no integers $i < j < k < \ell$ such that $\{i, k\}$ and $\{j, \ell\}$ are both in $\pi$. In the following, link patterns are represented by non-crossing arches between $2n$ aligned points. The link pattern associated with the FPL in Figure 1.4 is depicted in Figure 1.5.

Studying FPLs with respect to their link patterns has yielded much fruit. Let $A_\pi$ denote the number of FLPs corresponding to a prescribed link pattern $\pi$. In 2000
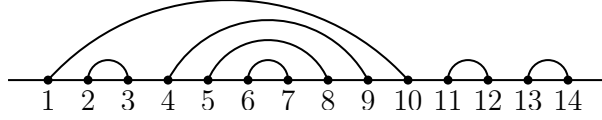
FIGURE 1.5. The link pattern $\{\{1,10\},\{2,3\},\{4,9\},\{5,8\},\{6,7\},\{11,12\},\{13,14\}\}$.

Wieland ([**30**]) proved the rotational invariance of the numbers $A_\pi$. That is, for all link patterns $\pi$,

$$A_{\mathrm{r}(\pi)} = A_\pi \tag{1.2}$$

where $\mathrm{r}(\pi) = \{\{i+1\,(\mathrm{mod}\,2n), j+1\,(\mathrm{mod}\,2n)\} : \{i,j\} \in \pi\}$. (Sometimes link patterns are represented by non-crossing arches between $2n$ points drawn equidistantly on a circle. Using this representation, r is simply a rotation, hence the term rotational invariance.) A short time later Razumov and Stroganov ([**25**]) conjectured that the coordinates of the ground state vector in the XXY spin chain model are given by the numbers $A_\pi$. Their conjecture excited the enumerative study of FPLs corresponding to a fixed link pattern. Various beautiful conjectures and identities for the numbers $A_\pi$ have arisen from that study. Worth mentioning is for instance Zuber ([**35**]) who contributed many nice conjectures, two of which were proved by Caselli, Krattenthaler, Lass and Nadeau ([**10**]). Cantini and Sportiello ([**9**]) proved the conjecture by Razumov and Stroganov in 2010, thereby widening the range of influence of the numbers $A_\pi$ significantly. The assertion of the Razumov-Stroganov-Cantini-Sportiello theorem and a sketch of its consequences can be found in Section 1.2.

**1.1.3. Triangular fully packed loop configurations.** Triangular fully packed loop configurations (abbreviated TFPLs) are the central objects of this thesis. Crucial in their development were FPLs corresponding to link patterns with a large number of nested arches. A link pattern $\pi$ of size $n$ is said to possess $m$ **nested arches** if there exists an $i \in [2n]$ such that $\{i-k+1\,(\mathrm{mod}\,2n), i+k\,(\mathrm{mod}\,2n)\} \in \pi$ for all $1 \le k \le m$. An example of a link pattern that exhibits nested arches is depicted in Figure 1.6. Due to Wieland's result it suffices to consider the case $i = 2n - m - 1$ in connection with the study of the numbers $A_\pi$. Hence, denote with $(\pi)_m$ the link pattern of size $n$ that comprises a link pattern $\pi$ of size $n - m$ on $[2(n-m)]$ and $m$ nested arches.
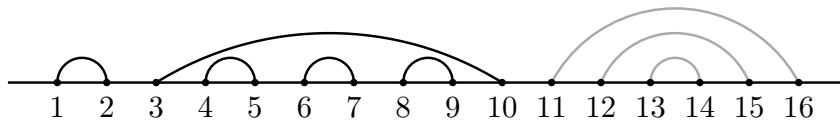


FIGURE 1.6. A link pattern of size 8 with three nested arches. The link pattern on [10] here is $\pi = \{\{1,2\},\{3,10\},\{4,5\},\{6,7\},\{8,9\}\}$.

Zuber ([**35**]) conjectured that $A_{(\pi)_m}$ is polynomial in $m$. An important observation in the proof of this conjecture by Caselli et al. ([**10**]) is that FPLs corresponding to a link pattern with a large number of nested arches admit a decomposition, in which TFPLs naturally arise, see Figure 1.7 for an example. The vertices of a TFPL that lie on the left and on the right boundary are of degree 0 or 1 as indicated in Figure 1.7. The degrees of the vertices along the left and right boundary are encoded by *Dyck-words* $u$ and $v$, each of which corresponds to a side of the TFPL (see Figure 1.8 for an example). In the following, the number of TFPLs corresponding to fixed words $u$ and $v$ and the link pattern $\pi$ is denoted by $t_{u,v}^{\mathbf{w}(\pi)}$. In the interest of convenience, $\pi$ is encoded by a Dyck-word, denoted $\mathbf{w}(\pi)$.
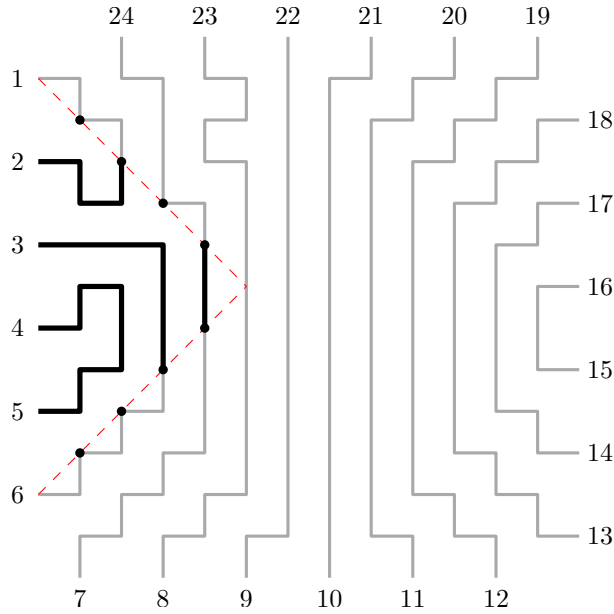


FIGURE 1.7. An FPL of size 12 that corresponds to a link pattern possessing nine nested arches. The TFPL that is contained in that FPL is indicated in black.

It was proved in [**10, 19, 29**] that for all integers $n > m \geq 0$ and link patterns $\pi$ of size $n$ the following holds:

$$(1.3) \qquad A_{(\pi)_m} = \sum_{u,v \in \mathcal{D}_{n-m}} P_{\lambda(u)}(n-m) t_{u,v}^{\mathbf{w}(\pi)} P_{\lambda(v)'}(m - 2(n-m) + 1).$$

The sum in (1.3) runs through the Dyck-words of length $2(n-m)$. Furthermore, $\lambda(\omega)$ denotes the Young-diagram associated to the Dyck-word $\omega$ as explained in Section 2.1. Finally, $P_\lambda(n) = \prod_{x \in \lambda} \frac{c(x)+n}{h(x)}$ where the product runs through the cells $x$ of the Young-diagram $\lambda$, $c(x)$ denotes the *content* of $x$ and $h(x)$ the *hook length* of $x$. (That is, $c(x) = j_x - i_x$ and $h(x) = |\{x' \in \lambda : i_{x'} \geq i_x \text{ and } j_{x'} = j_x\}| + |\{x' \in \lambda : i_{x'} = i_x \text{ and } j_{x'} > j_x\}|$

when $i_x$ (*resp.* $j_x$) denotes the index of the row (*resp.* column) of the cell $x$). For positive $n$ by $P_\lambda(n)$ semi-standard Young tableaux of shape $\lambda$ with entries at most $n$ are counted (Stanley's **hook-content formula** ([**28**, Theorem 15.3])).
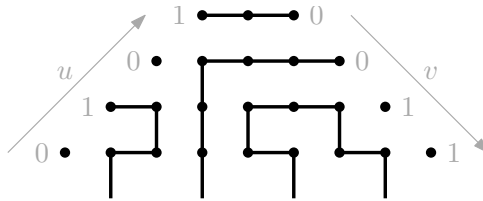


FIGURE 1.8. The TFPL from Figure 1.7 with the words $u$ and $v$ indicated.

At the time at which the identity (1.3) was found, the conjecture by Razumov and Stroganov had not been proved. Since the expression in (1.3) offered a new interpretation of the numbers $A_\pi$, the attention of those who were interested in proving the Razumov-Stroganov-conjecture was drawn to TFPLs. Zinn-Justin indeed conjectured a formula for the numbers $t_{u,v}^{\mathbf{w}(\pi)}$ from which the Razumov-Stroganov-conjecture would follow, see [**34**]. His conjecture remains unproven to this day. Nonetheless, a special case was proved by Nadeau ([**20**]), namely that $t_{u,v}^{\mathbf{w}(\pi)}$ is given by the *Littlewood-Richardson coefficient* $c_{\lambda(u),\lambda(v)}^{\lambda(\mathbf{w}(\pi))}$ if $\lambda(\mathbf{w}(\pi))$ has as many cells as $\lambda(u)$ and $\lambda(v)$ have together. In symbols,

$$(1.4) \qquad t_{u,v}^{\mathbf{w}(\pi)} = c_{\lambda(u),\lambda(v)}^{\lambda(\mathbf{w}(\pi))}.$$

Although the Razumov-Stroganov-conjecture has been proved the study of TFPLs is still worthwhile. Enumeration formulas for TFPLs, on the one hand, provide a deeper understanding of the enumeration of FPLs corresponding to fixed link patterns due to the identity (1.3) and thus may help to prove open conjectures. On the other hand, TFPLs offer fascinating combinatorics. The first such already occurred in the study of FPLs corresponding to link patterns $\pi \cup m$, see [**29**] and [**19**]. Thereafter many more were found including the aforementioned enumeration result by Nadeau. Particularly worth mentioning in this regard is the work by Fischer and Nadeau in [**11**].

## 1.2. The many appearances of the numbers $A_\pi$

As sources for this section I mainly used an article by Romik ([**26**]) and a book by Zinn-Justin ([**33**]).

**1.2.1. XXZ spin chains.** The model that we consider in this subsection is a 1-dimensional chain of $L$ sites with a *spin-$\frac{1}{2}$ particle* on each site. Other than in more complicated quantum mechanical models, the spin of a spin-$\frac{1}{2}$ particle can be expressed

as a linear combination of two *eigenspinors* (or *eigenstates*) with coefficients in $\mathbb{C}$. Traditionally, the eigenspinors are labelled spin up and spin down. Hence, set $|\uparrow\rangle = \left(\begin{smallmatrix} 1 \\ 0 \end{smallmatrix}\right) \in \mathbb{C}^2$ and $|\downarrow\rangle = \left(\begin{smallmatrix} 0 \\ 1 \end{smallmatrix}\right) \in \mathbb{C}^2$.

Since every spin can be identified with a 2-dimensional complex vector the *quantum-mechanical spin operators* can be represented by $2 \times 2$-matrices with complex entries. The $2 \times 2$-matrices that represent the quantum-mechanical spin operators for spin-$\frac{1}{2}$ particle are the **Pauli spin-$\frac{1}{2}$ matrices**, that is, the matrices

$$(1.5) \qquad \sigma^x = \begin{pmatrix} 0 & 1 \\ 1 & 0 \end{pmatrix}, \qquad \sigma^y = \begin{pmatrix} 0 & -i \\ i & 0 \end{pmatrix}, \qquad \sigma^z = \begin{pmatrix} 1 & 0 \\ 0 & -1 \end{pmatrix}.$$

The matrices that we will actually need for our purposes are the following:

$$(1.6) \qquad \sigma^+ = \frac{1}{2}(\sigma^x + i\sigma^y) = \begin{pmatrix} 0 & 1 \\ 0 & 0 \end{pmatrix}, \qquad \sigma^- = \frac{1}{2}(\sigma^x - i\sigma^y) = \begin{pmatrix} 0 & 0 \\ 1 & 0 \end{pmatrix}.$$

EXAMPLE 1.1. It holds that $\sigma^+ \cdot |\uparrow\rangle = \mathbf{0}$, $\sigma^+ \cdot |\downarrow\rangle = |\uparrow\rangle$, $\sigma^- \cdot |\uparrow\rangle = |\downarrow\rangle$, $\sigma^- \cdot |\downarrow\rangle = \mathbf{0}$, $\sigma^z \cdot |\uparrow\rangle = |\uparrow\rangle$ and $\sigma^z \cdot |\downarrow\rangle = -|\downarrow\rangle$.

An XXZ spin chain exhibits $L$ spin-$\frac{1}{2}$ particles, hence a state of the XXZ spin chain model consists of $L$ spins $s_1, s_2, \ldots, s_L$. It is encoded by the tensor $s_1 \otimes s_2 \otimes \cdots \otimes s_L$, so that the tensor product made up of $L$ copies of $\mathbb{C}^2$ forms the **space of spins** for the XXZ spin chain model. The matrices $\sigma^+$, $\sigma^-$ and $\sigma^z$ act on the space of spins as follows: for $\ell = 1, \ldots, L-1$ set

$$(1.7) \qquad \sigma_\ell^\pm = \underbrace{\mathrm{id}_{\mathbb{C}^2} \otimes \cdots \otimes \mathrm{id}_{\mathbb{C}^2}}_{\ell\text{-}1} \otimes \sigma^\pm \otimes \mathrm{id}_{\mathbb{C}^2} \otimes \cdots \otimes \mathrm{id}_{\mathbb{C}^2},$$

$$(1.8) \qquad \sigma_\ell^z = \underbrace{\mathrm{id}_{\mathbb{C}^2} \otimes \cdots \otimes \mathrm{id}_{\mathbb{C}^2}}_{\ell\text{-}1} \otimes \sigma^z \otimes \mathrm{id}_{\mathbb{C}^2} \otimes \cdots \otimes \mathrm{id}_{\mathbb{C}^2}.$$

The **Hamiltonian** with *anisotropy parameter* $\Delta$ (which is set $-1/2$ in the following) for this model is defined as

$$(1.9) \qquad \mathrm{H}_{XXZ}^L = \sum_{\ell=1}^{L} \left( \sigma_\ell^+ \sigma_{\ell+1}^- + \sigma_\ell^- \sigma_{\ell+1}^+ + \frac{\Delta}{2} \sigma_\ell^z \sigma_{\ell+1}^z \right)$$

where $\sigma_{L+1}^z = \sigma_1^z$ (**periodic boundary condition**) and $\sigma_{L+1}^\pm = q^{\pm 2}\sigma_1^\pm$ (**twisted boundary conditions**) for $q = e^{\frac{\pi i}{3}}$. As a remark, if $\Delta = 1$ then the Hamiltonian in (1.9) is the Hamiltonian of the *XXX spin chain* model.

EXAMPLE 1.2.

$$H^2_{XXZ}(|\uparrow\rangle \otimes |\downarrow\rangle) = \sigma^+ \cdot |\uparrow\rangle \otimes \sigma^- \cdot |\downarrow\rangle + \sigma^- \cdot |\uparrow\rangle \otimes \sigma^+ \cdot |\downarrow\rangle + \frac{\Delta}{2}\sigma^z \cdot |\uparrow\rangle \otimes \sigma^z \cdot |\downarrow\rangle$$

$$+ q^{-2}\sigma^- \cdot |\uparrow\rangle \otimes \sigma^+ \cdot |\downarrow\rangle + q^2\sigma^+ \cdot |\uparrow\rangle \otimes \sigma^- \cdot |\downarrow\rangle + \frac{\Delta}{2}\sigma^z \cdot |\uparrow\rangle \otimes \sigma^z \cdot |\downarrow\rangle$$

$$= (1 + q^{-2})|\downarrow\rangle \otimes |\uparrow\rangle - \Delta|\uparrow\rangle \otimes |\downarrow\rangle$$

In statistical mechanics, one is interested in the **ground states**, that is, the lowest-energy states, of a model. It was shown in [**1**] that the ground state energy in the XXZ spin chain model with twisted periodic boundary conditions equals

$$(1.10) \qquad\qquad E_0 = \frac{3L}{4}.$$

The ground states $|\Psi\rangle$ with energy $E_0$ are precisely the eigenvectors of the Hamiltonian with eigenvalue $E_0$, that is,

$$(1.11) \qquad\qquad H^L_{XXZ}|\Psi\rangle = \frac{3L}{4}|\Psi\rangle.$$

Razumov and Stroganov put forth an astonishing conjecture on the coordinates of the ground state vector for the XXZ spin chain model with twisted periodic boundary conditions and with even $L$ in 2004, see [**25**]. Their conjectured coordinates involve the numbers of FPLs with a given link pattern. In 2011 Cantini and Sportiello proved the conjecture, see [**9**]. To understand their theorem it is necessary to relate link patterns to XXZ spin chains.

To each link pattern $\pi$ of size $2n$, an element of the space of spins of dimension $2n$ can be assigned as follows: first, orient the arches of $\pi$ and generate the set $\mathfrak{O}(\pi)$ of all orientations of $\pi$. Thereafter, assign the weight $\omega(\overrightarrow{\pi}) = \mathrm{LR}(\overrightarrow{\pi}) - \mathrm{RL}(\overrightarrow{\pi})$ to each $\overrightarrow{\pi} \in \mathfrak{O}(\pi)$ where $\mathrm{LR}(\overrightarrow{\pi})$ denotes the number of arches in $\overrightarrow{\pi}$ that are oriented from left to right and $\mathrm{RL}(\overrightarrow{\pi})$ the number of the arches in $\overrightarrow{\pi}$ that are oriented from right to left. Finally, map each $\overrightarrow{\pi} \in \mathfrak{O}(\pi)$ to a $2n$-fold tensor product $|\overrightarrow{\pi}\rangle = s_1 \otimes \cdots \otimes s_{2n}$ made up of eigenspinors $s_1, \ldots, s_{2n}$ such that $s_i = |\uparrow\rangle$ whenever the out-degree of $i$ is 1 in $\overrightarrow{\pi}$ and $s_i = |\downarrow\rangle$ whenever the in-degree of $i$ is 1 in $\overrightarrow{\pi}$. The element of the space of spins of dimension $2n$ assigned to $\pi$ is then

$$(1.12) \qquad\qquad |\pi\rangle = \sum_{\overrightarrow{\pi} \in \mathfrak{O}(\pi)} q^{\frac{\omega(\overrightarrow{\pi})}{2}}|\overrightarrow{\pi}\rangle,$$

where $q = e^{\frac{\pi i}{3}}$.

EXAMPLE 1.3.

$$\left|\overset{\frown}{\underset{1\ \ 2\ \ 3}{\smile}}\ \overset{}{\underset{4\ \ 5\ \ 6}{\smile}}\right\rangle = q^{\frac{3}{2}}\left|\underset{1\ \ 2\ \ 3\ \ 4\ \ 5\ \ 6}{}\right\rangle + q^{\frac{1}{2}}\left|\underset{1\ \ 2\ \ 3\ \ 4\ \ 5\ \ 6}{}\right\rangle + q^{\frac{1}{2}}\left|\underset{1\ \ 2\ \ 3\ \ 4\ \ 5\ \ 6}{}\right\rangle$$

$$+ q^{\frac{1}{2}}\left|\underset{1\ \ 2\ \ 3\ \ 4\ \ 5\ \ 6}{}\right\rangle + q^{-\frac{1}{2}}\left|\underset{1\ \ 2\ \ 3\ \ 4\ \ 5\ \ 6}{}\right\rangle + q^{-\frac{1}{2}}\left|\underset{1\ \ 2\ \ 3\ \ 4\ \ 5\ \ 6}{}\right\rangle$$

$$+ q^{-\frac{1}{2}}\left|\underset{1\ \ 2\ \ 3\ \ 4\ \ 5\ \ 6}{}\right\rangle + q^{-\frac{3}{2}}\left|\underset{1\ \ 2\ \ 3\ \ 4\ \ 5\ \ 6}{}\right\rangle$$

$$= q^{\frac{3}{2}}|\uparrow\rangle \otimes |\uparrow\rangle \otimes |\downarrow\rangle \otimes |\downarrow\rangle \otimes |\uparrow\rangle \otimes |\downarrow\rangle + q^{\frac{1}{2}}|\uparrow\rangle \otimes |\downarrow\rangle \otimes |\uparrow\rangle \otimes |\downarrow\rangle \otimes |\uparrow\rangle \otimes |\downarrow\rangle$$

$$+ q^{\frac{1}{2}}|\downarrow\rangle \otimes |\uparrow\rangle \otimes |\downarrow\rangle \otimes |\uparrow\rangle \otimes |\uparrow\rangle \otimes |\downarrow\rangle + q^{\frac{1}{2}}|\uparrow\rangle \otimes |\uparrow\rangle \otimes |\downarrow\rangle \otimes |\downarrow\rangle \otimes |\downarrow\rangle \otimes |\uparrow\rangle$$

$$+ q^{-\frac{1}{2}}|\uparrow\rangle \otimes |\downarrow\rangle \otimes |\uparrow\rangle \otimes |\downarrow\rangle \otimes |\downarrow\rangle \otimes |\uparrow\rangle + q^{-\frac{1}{2}}|\downarrow\rangle \otimes |\uparrow\rangle \otimes |\downarrow\rangle \otimes |\uparrow\rangle \otimes |\downarrow\rangle \otimes |\uparrow\rangle$$

$$+ q^{-\frac{1}{2}}|\downarrow\rangle \otimes |\downarrow\rangle \otimes |\uparrow\rangle \otimes |\uparrow\rangle \otimes |\uparrow\rangle \otimes |\downarrow\rangle + q^{-\frac{3}{2}}|\downarrow\rangle \otimes |\downarrow\rangle \otimes |\uparrow\rangle \otimes |\uparrow\rangle \otimes |\downarrow\rangle \otimes |\uparrow\rangle$$

EXAMPLE 1.4.

$$\left|\underset{1\ \ 2}{\frown}\ \underset{3\ \ 4}{\frown}\ \underset{5\ \ 6}{\frown}\right\rangle = q^{\frac{3}{2}}|\uparrow\rangle \otimes |\downarrow\rangle \otimes |\uparrow\rangle \otimes |\downarrow\rangle \otimes |\uparrow\rangle \otimes |\downarrow\rangle + q^{\frac{1}{2}}|\uparrow\rangle \otimes |\downarrow\rangle \otimes |\uparrow\rangle \otimes |\downarrow\rangle \otimes |\downarrow\rangle \otimes |\uparrow\rangle$$

$$+ q^{\frac{1}{2}}|\uparrow\rangle \otimes |\downarrow\rangle \otimes |\downarrow\rangle \otimes |\uparrow\rangle \otimes |\uparrow\rangle \otimes |\downarrow\rangle + q^{\frac{1}{2}}|\downarrow\rangle \otimes |\uparrow\rangle \otimes |\uparrow\rangle \otimes |\downarrow\rangle \otimes |\uparrow\rangle \otimes |\downarrow\rangle$$

$$+ q^{-\frac{1}{2}}|\downarrow\rangle \otimes |\uparrow\rangle \otimes |\downarrow\rangle \otimes |\uparrow\rangle \otimes |\uparrow\rangle \otimes |\downarrow\rangle + q^{-\frac{1}{2}}|\downarrow\rangle \otimes |\uparrow\rangle \otimes |\uparrow\rangle \otimes |\downarrow\rangle \otimes |\downarrow\rangle \otimes |\uparrow\rangle$$

$$+ q^{-\frac{1}{2}}|\uparrow\rangle \otimes |\downarrow\rangle \otimes |\downarrow\rangle \otimes |\uparrow\rangle \otimes |\downarrow\rangle \otimes |\uparrow\rangle + q^{-\frac{3}{2}}|\downarrow\rangle \otimes |\downarrow\rangle \otimes |\uparrow\rangle \otimes |\uparrow\rangle \otimes |\downarrow\rangle \otimes |\uparrow\rangle.$$

In the following, denote by $\mathcal{LP}(n)$ the set of link patterns of size $n$. Furthermore, let $\mathbb{C}^{\mathcal{LP}(n)}$ be the complex vector space with basis $\mathcal{LP}(n)$ (that is, the space of linear combinations of link patterns of size $2n$ with coefficients in $\mathbb{C}$). Then the previous map naturally extends to an injective map from $\mathbb{C}^{\mathcal{LP}(n)}$ to $(\mathbb{C}^2)^{\otimes 2n}$. Thus, we can set

$$(1.13) \qquad\qquad |s_n\rangle = \sum_{\pi \in \mathcal{LP}(n)} A_\pi |\pi\rangle \in (\mathbb{C}^2)^{\otimes L}.$$

Razumov and Stroganov conjectured that $|s_n\rangle$ is a ground state of the XXZ spin chain model with twisted periodic boundary conditions and anisotropy parameter $\Delta = -\frac{1}{2}$, which was proved by Cantini and Sportiello.

THEOREM 1.5 (**Cantini-Sportiello-Razumov-Stroganov theorem** ([**25, 9**])).

$$(1.14) \qquad\qquad H_{XXZ}^{2n}|s_n\rangle = \frac{3n}{2}|s_n\rangle.$$

Finally, the Hamiltonian can be rewritten in terms of the following operators on the space of spins $(\mathbb{C}^2)^{\otimes L}$: for $\ell = 1, \ldots, L$ set

$$(1.15) \qquad e_\ell = \sigma_\ell^+ \sigma_{\ell+1}^- + \sigma_\ell^- \sigma_{\ell+1}^+ + \frac{\Delta}{2}(\sigma_\ell^z \sigma_{\ell+1}^z - \mathrm{id}_{(\mathbb{C}^2)^{\otimes L}}) - \frac{i\sqrt{3}}{4}(\sigma_{\ell+1}^z - \sigma_\ell^z)$$

EXAMPLE 1.6. $e_1(|\uparrow\rangle \otimes |\downarrow\rangle) = |\downarrow\rangle \otimes |\uparrow\rangle + q|\uparrow\rangle \otimes |\downarrow\rangle$, $e_1(|\downarrow\rangle \otimes |\uparrow\rangle) = |\uparrow\rangle \otimes |\downarrow\rangle + q^{-1}|\downarrow\rangle \otimes |\uparrow\rangle$, $e_1(|\uparrow\rangle \otimes |\uparrow\rangle) = e_1(|\downarrow\rangle \otimes |\downarrow\rangle) = \mathbf{0}$, $e_2(|\uparrow\rangle \otimes |\downarrow\rangle) = q^{-2}|\downarrow\rangle \otimes |\uparrow\rangle + q|\uparrow\rangle \otimes |\downarrow\rangle$, $e_2(|\downarrow\rangle \otimes |\uparrow\rangle) = q^2|\uparrow\rangle \otimes |\downarrow\rangle + q^{-1}|\downarrow\rangle \otimes |\uparrow\rangle$, $e_2(|\uparrow\rangle \otimes |\uparrow\rangle) = e_2(|\downarrow\rangle \otimes |\downarrow\rangle) = \mathbf{0}$

The operators $e_1, \ldots, e_{L-1}$ satisfy the following relations (the **Jones relations**):

$$(1.16) \qquad e_i^2 = e_i, \qquad\qquad e_i e_{i\pm 1} e_i = e_i, \qquad\qquad e_i e_j = e_j e_i \text{ if } |j - i| > 1.$$

This is noteworthy because the generators of the *Temperley-Lieb algebra* of size $L$ with parameter $\tau = 1$ fulfil these relations too. Thus the action of $e_1, \ldots, e_{L-1}$ on the space of spins is a representation of the Temperley-Lieb algebra. Furthermore, it is easy to check that

$$(1.17) \qquad\qquad \mathrm{H}_{XXZ}^L = \sum_{\ell=1}^L \left(e_\ell + \frac{\Delta}{2}\,\mathrm{id}_{(\mathbb{C}^2)^{\otimes L}}\right).$$

The assertion of the Cantini-Sportiello-Razumov-Stroganov theorem is thus equivalent to the following identity:

$$(1.18) \qquad\qquad \sum_{\ell=1}^{2n} e_\ell |s_n\rangle = 2n|s_n\rangle.$$

The operator $\sum_{\ell=1}^L e_\ell$ often is referred to as the **Temperley-Lieb Hamiltonian**. Besides the aforementioned representation the Temperley-Lieb algebra exhibits a representation on the set of link patterns, which will be the content of the next subsection. The denotation of the representation on link patterns will the same as the denotation of the representation on $\mathbb{C}^{\otimes L}$. That is due to the following relation between the two representations:

$$(1.19) \qquad\qquad e_\ell(|\pi\rangle) = |e_\ell(\pi)\rangle$$

for $\ell = 1, \ldots, L - 1$.

EXAMPLE 1.7. A short computation shows that



**1.2.2. Temperley-Lieb random walk or Temperley-Lieb stochastic process.** It has already been mentioned in the previous subsection that the **Temperley-Lieb operators** $e_1, \ldots, e_{2n-1}$ can be applied to link patterns of size $2n$. Given a link pattern

$\pi \in \mathcal{LP}(n)$ for $\ell = 1, \ldots, 2n - 1$ the link pattern $e_\ell(\pi)$ is determined as follows: first, subtract the blocks that contain $\ell$ or $\ell + 1$ from $\pi$; then add the block $\{\ell, \ell + 1\}$ and the block made up of the elements of $[2n] \backslash \{\ell, \ell + 1\}$ that are in a block with $\ell$ or $\ell + 1$ in $\pi$.

EXAMPLE 1.8.

(1.20)
$$e_1 \left( \overset{}{\underset{1 \; 2 \; 3 \; 4 \; 5 \; 6}{\frown}} \right) = \overset{}{\underset{1 \; 2 \quad 3 \quad 4 \quad 5 \quad 6}{\frown}}$$

A nice graphical representation of the action of $e_\ell$ may be obtained by associating the operators $e_\ell$ for $\ell = 1, \ldots, 2n - 1$ with the following diagrams:

(1.21)
$$e_\ell \qquad \longleftrightarrow \qquad \overset{}{\underset{1 \quad 2 \quad\; \ell-1 \;\; \ell \;\; \ell+1 \; \ell+2 \quad\; 2n-1 \; 2n}{\Big| \; \Big| \; \cdots \; \Big| \; \smile \; \Big| \; \cdots \; \Big| \; \Big|}}$$

In order to obtain the link pattern $e_\ell(\pi)$, first the diagram corresponding to $e_\ell$ is placed below $\pi$ such that the top vertices in the diagram and the vertices in $\pi$ coincide. Now, the bottom vertices in the diagram of $e_\ell$ are pairwise connected by arcs. Thus, the link pattern $e_\ell(\pi)$ is the link pattern of size $2n$ in which the same pairs of vertices are connected. The graphical representation for the example in Example 1.8 is depicted in Figure 1.9.
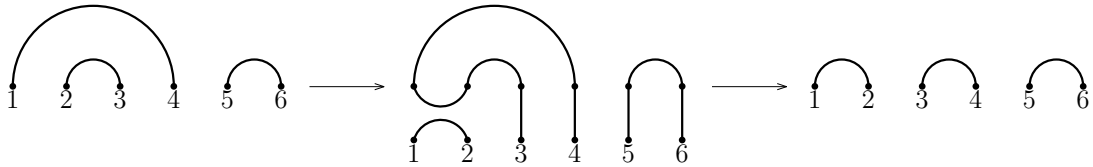


FIGURE 1.9. An example for the graphical representation of the action of the Temperley-Lieb operator $e_1$ on link patterns.

For our purpose, it is necessary to have an operator $e_{2n}$. Hence, the definition of $e_{2n}$ shall be the same as the definition of $e_\ell$ for $\ell = 1, \ldots, 2n - 1$ with the sole exception that the integers are considered modulo $2n$. An example is given in Figure 1.10. The Temperley-Lieb operators $e_1, e_2, \ldots, e_{2n}$ now indeed satisfy (1.19).
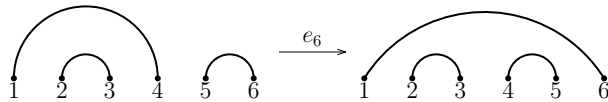


FIGURE 1.10. The operator $e_6$ applied to a link pattern of size 6.

A **Temperley-Lieb random walk** or **Temperley-Lieb stochastic process** ([**23**]) is defined as a sequence $(\pi_m)_{m \geq 0}$ of link patterns of size $2n$, beginning with an initial link pattern $\pi_0$, where each link pattern $\pi_{m+1}$ is obtained from $\pi_m$ by choosing $\ell$ from $\{1, 2, \ldots, 2n\}$ uniformly at random and setting $\pi_{m+1} = e_\ell(\pi)$. It is easy to see that

Temperley-Lieb random walks are stationary Markov chains. Thus the transition probability distribution can be represented by a **transition matrix**. The entries of the transition matrix $T_n$ are $t_{\pi,\pi'} = Pr(\pi_{m+1} = \pi' \,|\, \pi_m = \pi)$ (that is, the probability that $\pi_{m+1} = \pi'$ under the condition that $\pi_m = \pi$). Since $\ell \in \{1, 2, \ldots, 2n\}$ is chosen uniformly randomly it holds that

$$(1.22) \qquad\qquad t_{\pi,\pi'} = \frac{1}{2n} |\{1 \leq \ell \leq 2n : e_\ell(\pi) = \pi'\}|$$

for all link patterns $\pi$ and $\pi'$ of size $2n$. This is why the stationary distribution $\mu_n = (\mu_\pi)_{\pi \in \mathcal{LP}(n)}$ of the Temperley-Lieb random walk must satisfy

$$(1.23) \qquad\qquad \mu_\pi = \frac{1}{2n} \sum_{\ell=1}^{2n} \sum_{\substack{\pi' \in \mathcal{LP}(n): \\ e_\ell(\pi') = \pi}} \mu_{\pi'}.$$

It will be shown next that the Cantini-Sportiello-Razumov-Stroganov theorem implies the following expression for $\mu_\pi$ in terms of numbers of FPLs:

$$(1.24) \qquad\qquad \mu_\pi = \frac{A_\pi}{A_n}.$$

To see that (1.24) follows from Theorem 1.5 it suffices to revisit the identity (1.18):

$$\sum_{\pi \in \mathcal{LP}(n)} 2n A_\pi |\pi\rangle = 2n |s_n\rangle = \sum_{\ell=1}^{2n} e_\ell |s_n\rangle = \sum_{\pi' \in \mathcal{LP}(n)} A_{\pi'} \sum_{\ell=1}^{2n} e_\ell |\pi'\rangle = \sum_{\pi' \in \mathcal{LP}(n)} A_{\pi'} \sum_{\ell=1}^{2n} |e_\ell(\pi')\rangle$$

$$(1.25) \qquad\qquad = \sum_{\pi \in \mathcal{LP}(n)} \sum_{\ell=1}^{2n} \sum_{\substack{\pi' \in \mathcal{LP}(n): \\ e_\ell(\pi') = \pi}} \mu_{\pi'} A_{\pi'} |\pi\rangle.$$

Comparing the coefficients in (1.25) shows that $A_\pi$ satisfies the identity (1.23). In conclusion, $\mu_\pi = \frac{A_\pi}{A_n}$ because the stationary distribution must be normalized, that is, it must satisfy $\sum_{\pi \in \mathcal{LP}(n)} \mu_\pi = 1$.

**1.2.3. The dense $\mathcal{O}(1)$ loop model.** In this subsection we consider another model in which the probability vector $(\frac{A_\pi}{A_n})_{\pi \in \mathcal{LP}(n)}$ occurs: the dense $\mathcal{O}(1)$ loop model of statistical mechanics with periodic boundary conditions. Its states are random tilings of $[0, L] \times [0, \infty)$ for an $L > 0$ with the following two **plaquettes**:

$$(1.26) \qquad\qquad \text{} \qquad \text{}$$

Each plaquette is uniformly randomly chosen. Furthermore, we superimpose periodic boundary conditions on $[0, L] \times [0, \infty)$, that is, we identify $(0, k)$ and $(L, k)$ for each $k \geq 0$. Figure 1.11 displays a section of a dense $\mathcal{O}(1)$ loop on $[0, 8] \times [0, \infty)$ with periodic boundary conditions.
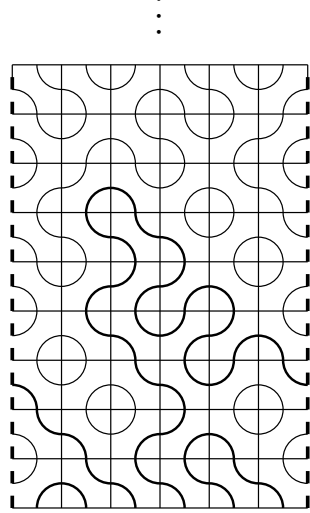
$$\vdots$$



FIGURE 1.11. A section of a dense $\mathcal{O}(1)$ loop on the strip $[0, 6] \times [0, \infty)$ with periodic boundary conditions.

A dense $\mathcal{O}(1)$ loop on the strip $[0, 2n] \times [0, \infty)$ subject to periodic boundary conditions may be assigned a link pattern $\Pi_*^{(n)}$ as follows: for each $i = 0, \ldots, 2n - 1$ follow the path starting in $(\frac{2i+1}{2}, 0)$ until it reaches a vertex $(\Pi_*^{(n)}(i), 0)$. Now, set $\Pi_*^{(n)} = \{\{i, \Pi_*^{(n)}(i)\} : 1 \leq i \leq 2n - 1\}$. The dense $\mathcal{O}(1)$ loop in Figure 1.11 has link pattern $\{\{1, 2\}, \{3, 4\}, \{5, 6\}\}$. The link pattern $\Pi_*^{(n)}$ is often referred to as the **connectivity pattern**. For a link pattern $\pi \in \mathcal{LP}(n)$ denote by

$$(1.27) \qquad \mu_\pi = Pr(\Pi_*^{(n)} = \pi)$$

the probability that the connectivity pattern of a dense $\mathcal{O}(1)$ loop on the strip $[0, 2n] \times [0, \infty)$ with periodic boundary conditions is $\pi$. The probability vector $\mu_n = (\mu_\pi)_{\pi \in \mathcal{LP}(n)}$ satisfies the following:

THEOREM 1.9 ([**18, 26**]). *Let $e_1, \ldots, e_{2n}$ be the Temperley-Lieb operators. Furthermore, let $H_n$ be the square matrix with rows and columns indexed by link patterns of size $2n$ and with entries $(H_n)_{\pi, \pi'} = 2n - |\{1 \leq \ell \leq 2n : e_\ell(\pi) = \pi'\}|$. Then*

$$(1.28) \qquad H_n \mu_n = \boldsymbol{0}.$$

Thus if we set $M_n = \mathrm{id}_{\mathbb{C}\mathcal{LP}(n)} - \frac{1}{2n} H_n$ then $M_n \mu_n = \mu_n$. From the Cantini-Sportiello-Razumov-Stroganov-theorem it follows that

$$\tag{1.29} \mu_\pi = \frac{A_\pi}{A_n}.$$

## 1.3. Structure of the thesis

**1.3.1. Chapter 2.** In this chapter, the combinatorial objects that are consistently needed throughout this thesis are summarised. Furthermore, the previous work on TFPLs by Fischer and Nadeau ([**19**], [**20**], [**11**]) is outlined. That is because it forms the basis for this thesis.

**1.3.2. Chapter 3.** This chapter contains the definition of Wieland drift as the natural adoption of Wieland gyration – a map on FPLs invented by Wieland [**30**] in order to prove the rotational invariance of the numbers $A_\pi$ – to TFPLs. Furthermore, a detailed study of some of its properties is given.

**1.3.3. Chapter 4.** In this chapter, an expression for the number of TFPLs of excess 2 in terms of TFPLs that are stable under the application of Wieland drift is proved. It generalises previous enumerative results by Fischer and Nadeau for TFPLs of excess 0 or 1. (The excess of a TFPL must be a non-negative integer.)

**1.3.4. Chapter 5.** In this chapter, hexagonal fully packed loop configurations are introduced as a generalisation of TFPLs. In addition the results for TFPLs by Fischer and Nadeau are generalised to hexagonal fully packed loop configurations.

# Preliminaries

In this chapter, the terms and definitions that are consistently needed in the thesis are summarised. The first part recaps elementary combinatorial objects, statistics on these objects and properties of these objects. In the second part, triangular fully packed loop configurations are introduced together with the concepts and terms that are crucial for the thesis. Furthermore, the parts of the work by Fischer and Nadeau on triangular fully packed loop configurations ([**19**], [**20**], [**11**]) that are needed for the thesis are outlined.

## 2.1. Words and Young diagrams

Throughout the thesis, a **word** $\omega$ of length $N$ is defined as a finite sequence $\omega = \omega_1 \omega_2 \cdots \omega_N$ where $\omega_i \in \{0, 1\}$ for all $1 \leq i \leq N$. Furthermore, the following notations are used:

- The number of occurrences of $i$ in a word $\omega$ is denoted $|\omega|_i$ for $i = 0, 1$;
- Two words $\omega, \sigma$ of length $N$ is said to satisfy $\omega \leq \sigma$ if $|\omega_1 \cdots \omega_n|_1 \leq |\sigma_1 \cdots \sigma_n|_1$ for all $1 \leq n \leq N$;
- The number of inversions of $\omega$, that is, pairs $1 \leq i < j \leq N$ such that $\omega_i = 1$ and $\omega_j = 0$, is denoted $\mathrm{d}(\omega)$;
- Given a word $\omega = \omega_1 \omega_2 \cdots \omega_N$ the word $\overline{\omega_1} \cdots \overline{\omega_n}$ in which $\overline{0} = 1$ and $\overline{1} = 0$ is denoted by $\overline{\omega}$, the word $\omega_N \omega_{N-1} \cdots \omega_1$ is denoted $\overleftarrow{\omega}$ and the word $\overline{\overleftarrow{\omega}}$ is denoted $\omega^*$.

For instance, $\overline{0010101} = 1101010$, $\overleftarrow{0010101} = 1010100$ and $0010101^* = 0101011$.

DEFINITION 2.1.     (1) *A **Young diagram** is a finite collection of boxes arranged in left-justified rows, with the row lengths weakly decreasing.*
  (2) *Two Young diagrams $\mu$ and $\lambda$ are said to satisfy $\mu \subseteq \lambda$ if $\lambda$ contains $\mu$ set-theoretically. The set-theoretic difference of two Young diagrams $\mu$ and $\lambda$ that satisfy $\mu \subseteq \lambda$ is said to be the **skew diagram** $\lambda/\mu$.*
  (3) *The number of boxes a Young diagram $\lambda$ (resp. skew diagram $\lambda/\mu$) is made up of is denoted by $|\lambda|$ (resp. $|\lambda/\mu|$).*
  (4) *The conjugate of a Young diagram $\lambda$ is defined as the Young diagram obtained by reflecting $\lambda$ along its main diagonal.*

Throughout the thesis, with a word $\omega$ a Young diagram $\lambda(\omega)$ will be associated as follows: to a given word $\omega$ a path on the square lattice is constructed by drawing a $(0, 1)$-step if $\omega_i = 0$ and a $(1, 0)$-step if $\omega_i = 1$ for $i$ from 1 to $n$. Additionally, a vertical line

FIGURE 2.1. A Young diagram and a skew diagram.

through the paths starting point and a horizontal line through its ending point are drawn. Then the region enclosed by the lattice path and the two lines is a Young diagram which shall be the image of $\omega$ under $\lambda$. In Figure 2.2, examples of words and their corresponding Young diagrams are given.
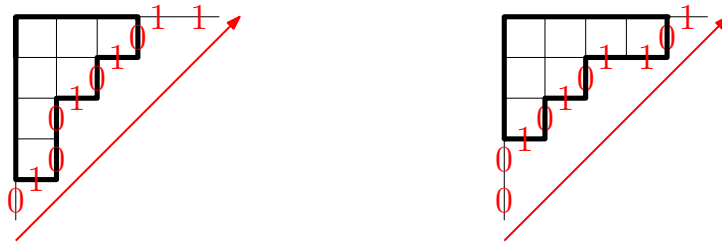


FIGURE 2.2. The Young diagram $\lambda(0100101011)$ and the Young diagram $\lambda(0100101011^*)$.

For two words $\omega$ and $\sigma$ of length $N$ it holds $\omega \leq \sigma$ if and only if $\lambda(\omega) \subseteq \lambda(\sigma)$. Furthermore, $|\lambda(\omega)| = \mathrm{d}(\omega)$ and $\lambda(\omega^*)$ coincides with the conjugate of $\lambda(\omega)$.

The following two skew shapes will play an important role in the thesis:

DEFINITION 2.2. *A skew diagram is said to be a **horizontal strip** (resp. a **vertical strip**) if each of its columns (resp. rows) contains at most one box. Throughout the thesis, if the skew diagram of skew shape $\lambda(\sigma)/\lambda(\omega)$ is a horizontal strip (resp. a vertical strip) it will be written $\omega \xrightarrow{\mathrm{h}} \sigma$ (resp. $\omega \xrightarrow{\mathrm{v}} \sigma$).*
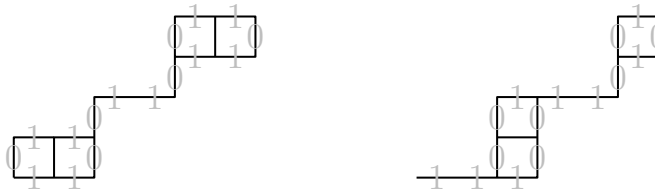


FIGURE 2.3. A horizontal and a vertical strip.

For two words $\omega$ and $\sigma$ of length $N$ satisfying $\omega \leq \sigma$ the skew diagram of skew shape $\lambda(\sigma)/\lambda(\omega)$ is a horizontal strip (*resp.* a vertical strip) if and only if the following holds:

if $\omega_i$ is the $j$-th one (*resp.* zero) in $\omega$ then $\sigma_{i-1}$ or $\sigma_i$ (*resp.* $\sigma_i$ or $\sigma_{i+1}$) is the $j$-th one (*resp.* zero) in $\sigma$ for each $j \in \{1, \ldots, |\omega|_1\}$ (*resp.* for each $j \in \{1, 2, \ldots, |\omega|_0\}$).

DEFINITION 2.3. *Let $\lambda$ and $\mu$ be two Young diagrams such that $\lambda$ contains $\mu$.*

(1) *A **Young tableau** of skew shape $\lambda/\mu$ is a filling of the boxes of the skew diagram of skew shape $\lambda/\mu$ with positive integers. Recording the occurrences of each number appears in a Young tableau gives a sequence that is denoted the **content** of the tableau.*

(2) *A Young tableau is said to be **semi-standard** if the entries in each row are non-decreasing and the entries in each column are (strictly) increasing.*
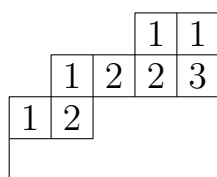


FIGURE 2.4. A semi-standard Young tableau of skew shape $\lambda(011011100)/\lambda(001011011)$.

Throughout the thesis, semi-standard Young tableaux $T$ of skew shape $\lambda/\mu$ with entries smaller than or equal to $m$ are associated with a sequences of Young diagrams

$$\mu = \tau_0 \subseteq \tau_1 \subseteq \cdots \subseteq \tau_{m-1} \subseteq \tau_m = \lambda$$

such that $\tau_i/\tau_{i-1}$ is a horizontal strip for all $1 \leq i \leq m$ by letting $\tau_i$ be the Young diagram that satisfies $\tau_i \supseteq \mu$ and that $\tau_i \supseteq \mu$ consists of the cells of $\lambda/\mu$ that have entry at most $i$ in $T$ for all $1 \leq i \leq m$. For instance, the semi-standard Young tableau of skew shape $\lambda(011011100)/\lambda(001011011)$ in Figure 2.4 corresponds to the sequence

$$\lambda(001011011) \xrightarrow{\text{h}} \lambda(010101110) \xrightarrow{\text{h}} \lambda(011011010) \xrightarrow{\text{h}} \lambda(011011100).$$

## 2.2. Triangular fully packed loop configurations

**2.2.1. Triangular fully packed loop configurations.** To give the definition of triangular fully packed loop configurations the following graph is needed:

DEFINITION 2.4. *Let $N$ be a positive integer. The graph $G^N$ is defined as the induced subgraph of the square grid made up of $N$ consecutive centred rows of $3, 5, \ldots, 2N+1$ vertices from top to bottom together with $2N+1$ vertical external edges incident to the $2N+1$ bottom vertices.*

In Figure 2.5, the graph $G^7$ is depicted. From now on, the vertices of $G^N$ are partitioned into **odd** and **even** vertices in a chessboard manner such that the leftmost vertex
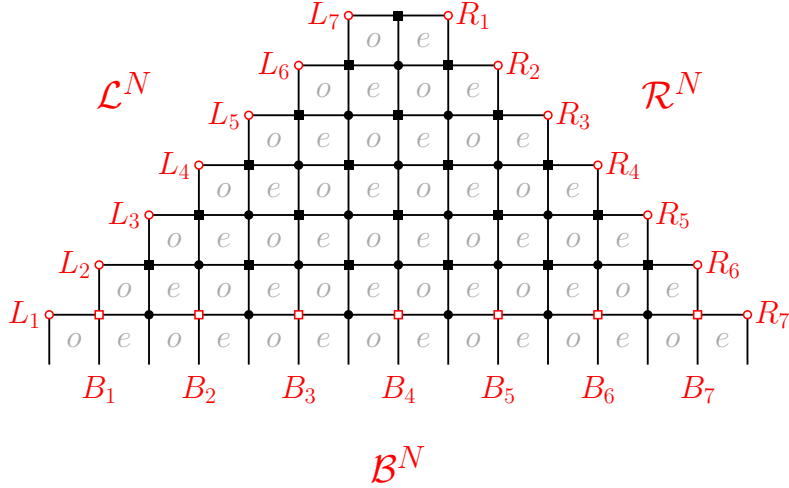
FIGURE 2.5. The graph $G^7$.

of the top row in $G^N$ is odd. In the figures, odd vertices are represented by circles and even vertices by squares. There are vertices of $G^N$ that play a special role (indicated in red in Figure 2.5): let $\mathcal{L}^N = \{L_1, L_2, \ldots, L_N\}$ (*resp.* $\mathcal{R}^N = \{R_1, R_2, \ldots, R_N\}$) be the set made up of the vertices, that are leftmost (*resp.* rightmost) in each of the $N$ rows of $G^N$, and let $\mathcal{B}^N = \{B_1, B_2, \ldots, B_N\}$ be the set made up of the even vertices of the bottom row of $G^N$. All vertices are numbered from left to right. Furthermore, the $N(N+1)$ unit squares of $G^N$ including external unit squares that have three surrounding edges only are said to be the **cells of** $G^N$. From now on, they are partitioned into **odd** and **even** cells in a chessboard manner such that the top left cell of $G^N$ is odd.

DEFINITION 2.5. *Let $N$ be a positive integer. A **triangular fully packed loop configuration** (abbreviated TFPL) of size $N$ is a subgraph $f$ of $G^N$ such that:*

(1) *precisely the external edges that are incident to vertices in $\mathcal{B}^N$ are occupied by $f$;*

(2) *the $2N$ vertices in $\mathcal{L}^N \cup \mathcal{R}^N$ have degree $0$ or $1$;*

(3) *all other vertices of $G^N$ have degree $2$ in $f$;*

(4) *a path in $f$ neither connects two vertices of $\mathcal{L}^N$ nor two vertices of $\mathcal{R}^N$.*

An example of a TFPL is given in Figure 2.6. A **cell of** $f$ is a cell of $G^N$ together with those of its surrounding edges that are occupied by $f$.

DEFINITION 2.6. *Let $f$ be a TFPL of size $N$. A triple $(u, v; w)$ of words of length $N$ is assigned to $f$ as follows: for $i = 1, \ldots, N$*

(1) *set $u_i = 1$, if the vertex $L_i \in \mathcal{L}^N$ has degree $1$, and $u_i = 0$, otherwise;*

(2) *set $v_i = 0$, if the vertex $R_i \in \mathcal{R}^N$ has degree $1$, and $v_i = 1$, otherwise;*

(3) *set $w_i = 1$, if in $f$ the vertex $B_i \in \mathcal{B}^N$ is connected with a vertex in $\mathcal{L}^N$ or with a vertex $B_h$ for an $h < i$, and $w_i = 0$, otherwise.*

*The triple $(u, v; w)$ is said to be the **boundary** of $f$. Furthermore, the set of TFPLs with boundary $(u, v; w)$ is denoted $T_{u,v}^w$ and its cardinality $t_{u,v}^w$.*
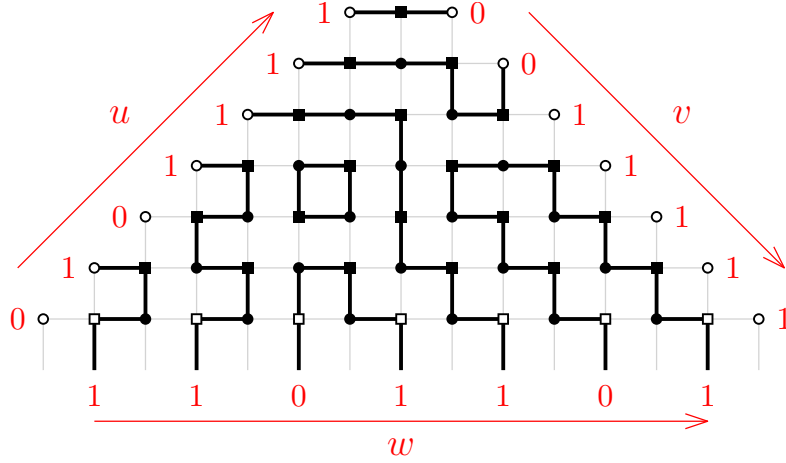
FIGURE 2.6. A TFPL of size 7. Its boundary is $(0101111, 0011111; 1101101)$.

In [**10**], [**29**] and [**11**] it was proved that the boundary of a TFPL must necessarily satisfy the following conditions:

THEOREM 2.7 ([**10, 29, 11**]). *If $t_{u,v}^w > 0$, then*

(1) $|u|_1 = |v|_1 = |w|_1$ *and* $|u|_0 = |v|_0 = |w|_0$;

(2) $u \leq w$ *and* $v \leq w$;

(3) $\mathrm{d}(u) + \mathrm{d}(v) \leq \mathrm{d}(w)$.

In terms of diagrams, (2) means $\lambda(u) \subseteq \lambda(w)$ and $\lambda(v) \subseteq \lambda(w)$, while (3) means $|\lambda(u)| + |\lambda(v)| \leq |\lambda(w)|$. A new proof of the third condition is given in Chapter 3.

DEFINITION 2.8 ([**11**]). *Let $u, v, w$ be words of length $N$. The **excess** of $u, v, w$ is defined as*

$$\mathrm{exc}(u, v; w) = \mathrm{d}(w) - \mathrm{d}(u) - \mathrm{d}(v).$$

*If $\mathrm{exc}(u, v; w) = k$ then a TFPL with boundary $(u, v; w)$ is said to be of excess $k$.*

**2.2.2. Oriented Triangular fully packed loop configurations.** The definitions of both TFPLs and their boundaries contain global conditions (Definition 2.5(4) and Definition 2.6(3)). Those can be omitted when adding an orientation to each edge of a TFPL.

DEFINITION 2.9. *An **oriented TFPL** of size $N$ is a TFPL of size $N$ together with an orientation of its edges such that the edges attached to $\mathcal{L}^N$ are outgoing, the edges attached to $\mathcal{R}^N$ are incoming and all other vertices of $G^N$ are incident to an incoming and an outgoing edge.*

An example of an oriented TFPL of size 7 is depicted in Figure 2.7. In the definition of the underlying TFPL of an oriented TFPL condition (4) can be omitted. That is
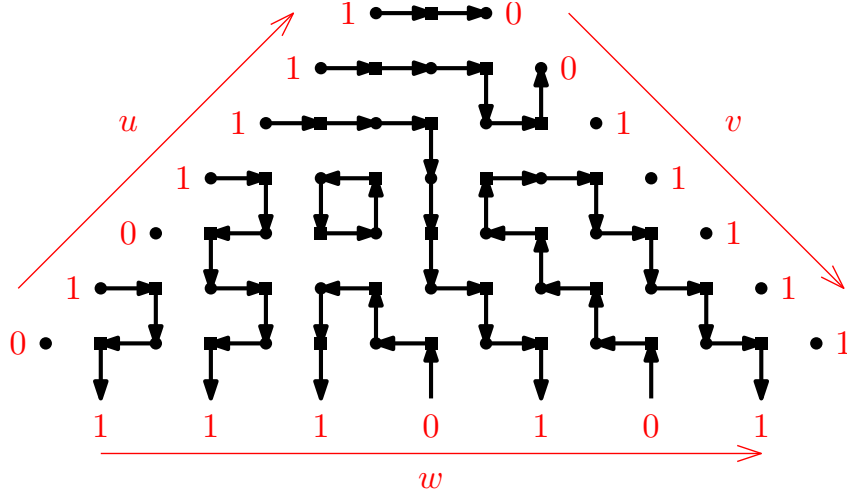
FIGURE 2.7. An oriented TFPL of size 7.

because the required orientations of the edges attached to vertices of the left and right boundary prevent paths from returning to the respective boundary.

DEFINITION 2.10. *An oriented TFPL $f$ has boundary $(u, v; w)$ if the following hold:*

(1) *If $L_i \in \mathcal{L}^N$ has out-degree 1 in $f$, then $u_i = 1$. Otherwise, $u_i = 0$.*
(2) *If $R_i \in \mathcal{R}^N$ has in-degree 1 in $f$, then $v_i = 0$. Otherwise, $v_i = 1$.*
(3) *If the external edge attached to the vertex $B_i \in \mathcal{B}^N$ is outgoing in $f$, then $w_i = 1$. Otherwise, $w_i = 0$.*

*The set of all oriented TFPLs with boundary $(u, v; w)$ is denoted $\overrightarrow{T}^w_{u,v}$ and its cardinality $\overrightarrow{t}^w_{u,v}$.*

While $u$ and $v$ coincide with the respective boundary word in the underlying ordinary TFPL this is not the case for $w$. Instead of the connectivity of the paths, $w$ encodes the local orientation of the edges. Only in the case when in an oriented TFPL all paths between two vertices $B_i$ and $B_j$ of $\mathcal{B}^N$ are oriented from $B_i$ to $B_j$, if $i < j$, the boundary word $w$ coincides with the respective boundary word of the underlying TFPL. This shows that for each TFPL with boundary $(u, v; w)$ there exists an oriented TFPL with boundary $(u, v; w)$ underlying this TFPL:

DEFINITION 2.11. *The **canonical orientation** of a TFPL is defined as the orientation of the edges of the TFPL that satisfies the conditions in Definition 2.9 and in addition that each path between two vertices $B_i, B_j \in \mathcal{B}^N$ is oriented from $B_i$ to $B_j$, if $i < j$, and that all closed paths are oriented clockwise.*

The previous observations imply that

(2.1) $$t^w_{u,v} \leq \overrightarrow{t}^w_{u,v}.$$

It was proved in [**11**] that also the boundary of an oriented TFPL must satisfy the conditions (1), (2) and (3) in Theorem 2.7. What sets oriented TFPLs apart from ordinary

TFPLs is that the excess of an oriented TFPL admits the following interpretation in terms of numbers of occurrences of certain local configurations:

THEOREM 2.12 ([**11**, Theorem 4.3]). *Let $f$ be an oriented TFPL with boundary $(u, v; w)$. Then*

$$(2.2) \qquad \mathrm{exc}(u, v; w) = \begin{smallmatrix}\end{smallmatrix} + \begin{smallmatrix}\end{smallmatrix} + \begin{smallmatrix}\end{smallmatrix} + \begin{smallmatrix}\end{smallmatrix} + \begin{smallmatrix}\end{smallmatrix} + \begin{smallmatrix}\end{smallmatrix} + \begin{smallmatrix}\end{smallmatrix} + \begin{smallmatrix}\end{smallmatrix}$$

*where by* $\begin{smallmatrix}\end{smallmatrix}$, $\begin{smallmatrix}\end{smallmatrix}$, *etc. the numbers of occurrences of the local configurations* $\begin{smallmatrix}\end{smallmatrix}$, $\begin{smallmatrix}\end{smallmatrix}$, *etc. in* $f$ *are denoted.*

Obviously, Theorem 2.12 implies that $\mathrm{d}(u) + \mathrm{d}(v) \leq \mathrm{d}(w)$, whenever $(u, v; w)$ is the boundary of an oriented TFPL.

**2.2.3. Blue-red path tangles.** In this subsection an alternative representation of oriented TFPLs will be introduced, namely blue-red path tangles. They came up in [**11**] and will be crucial for several proofs in the thesis. Throughout this subsection, let $u, v, w$ be words of length $N$ such that $|u|_0 = |v|_0 = |w|_0$, $|u|_1 = |v|_1 = |w|_1$, $u \leq w$, $v \leq w$ and $\mathrm{d}(u) + \mathrm{d}(v) \leq \mathrm{d}(w)$. Furthermore, set $N_0 = |u|_0$ and $N_1 = |u|_1$.

A blue-red path tangle is made up of an $N_0$-tuple of non-intersecting **blue** lattice paths and an $N_1$-tuple of non-intersecting **red** lattice paths. The blue lattice paths use steps $(-1, 1)$, $(-1, -1)$ and $(-2, 0)$, while the red lattice paths use steps $(1, 1)$, $(1, -1)$ and $(2, 0)$. Furthermore, neither a blue nor a red lattice path goes below the $x$-axis.

For each $k = 1, \ldots, N_0$ and $\ell = 1, \ldots, N_1$, let $i_k$ (*resp.* $i'_\ell$) be the index of the $k$-th zero (*resp.* $\ell$-th one) in $w$ and $j_k$ (*resp.* $j'_\ell$) be the index of the $k$-th zero in $u$ (*resp.* $\ell$-th one in $v$). Then the starting point $D_k$ (*resp.* $D'_\ell$) of the $k$-th blue path (*resp.* $\ell$-th red path) is defined as the vertex midway between the $i_k$-th (*resp.* $i'_\ell$-th) even vertex on the bottom row of $G^N$ and the odd vertex to its left (*resp.* right). The ending point $E_k$ (*resp.* $E'_\ell$) of the $k$-th blue path (*resp.* $\ell$-th red path), on the other hand, is defined as the vertex midway between $L_{j_k}$ (*resp.* $R_{j'_\ell}$) and the even vertex to it right (*resp.* left). An example is displayed in Figure 2.8.

In the following, the set of $N_0$-tuples $(P_1, P_2, \ldots, P_{N_0})$ of non-intersecting blue lattice paths, where $P_k$ is a path from $D_k$ to $E_k$, is denoted by $\mathcal{P}(u, w)$ and the set of $N_1$-tuples of non-intersecting red paths $(P'_1, P'_2, \ldots, P'_{N_1})$, where $P'_\ell$ is a path from $D'_\ell$ to $E'_\ell$, is denoted by $\mathcal{P}'(v, w)$.

THEOREM 2.13 ([**11**, Theorem 4.1]). *The set $\overrightarrow{T}^w_{u,v}$ is in bijection with the set of pairs $(B, R) \in \mathcal{P}(u, w) \times \mathcal{P}'(v, w)$ that satisfy the two following conditions:*

(1) *no diagonal step of $R$ crosses a diagonal step of $B$;*

(2) *each middle point of a horizontal step in $B$ (resp. $R$) is used by a step in $R$ (resp. $B$).*
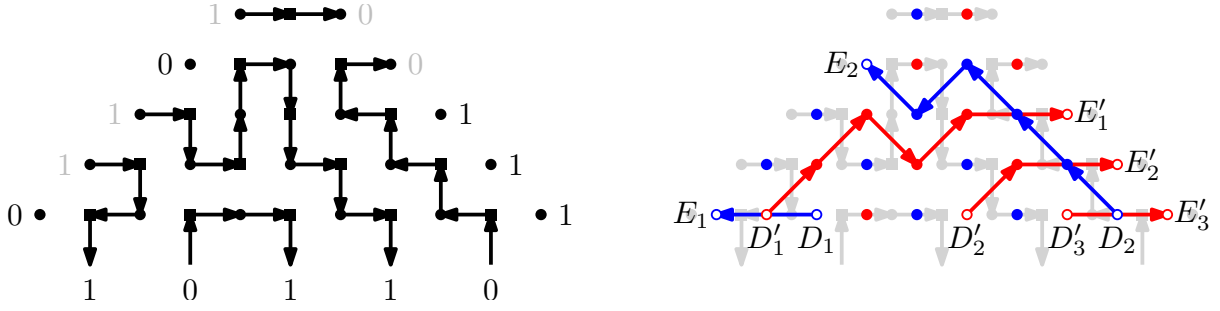
FIGURE 2.8. An oriented TFPL with boundary $(01101, 00111; 10110)$ and its corresponding blue-red path tangle with boundary $(01101, 00111; 10110)$.

*The set of such configurations is denoted by* $\mathrm{BlueRed}(u, v; w)$ *and a configuration in* $\mathrm{BlueRed}(u, v; w)$ *is said to be a **blue-red path tangle with boundary** $(u, v; w)$.*
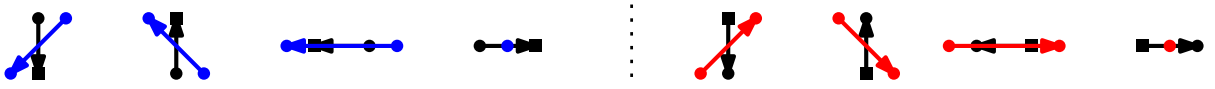


FIGURE 2.9. From oriented TFPLs to blue-red path tangles.

PROOF. Here the bijection given in [**11**] is repeated: let $f$ be an oriented TFPL of size $N$ and with boundary $(u, v; w)$. As a start blue vertices are inserted in the middle of each horizontal edge of $G^N$ that has an odd vertex to its left and red vertices are inserted in the middle of each horizontal edge of $G^N$ that has an even vertex to its left. Next, blue edges are inserted as indicated in the left part of Figure 2.9 and red edges are inserted as indicated in the right part of Figure 2.9. Then the blue vertices together with the blue edges give rise to an $N_0$–tuple of non-intersecting paths $B = (P_1, P_2, \ldots, P_{N_0})$ in $\mathcal{P}(u, w)$ and the red vertices together with the red edges give rise to an $N_1$–tuple of non-intersecting paths $R = (P'_1, P'_2, \ldots, P'_{N_1})$ in $\mathcal{P}'(v, w)$. The condition that no diagonal step of $R$ crosses a diagonal step of $B$ is equivalent to that there is a unique orientation of each vertical edge in $f$. On the other hand, the condition that each middle point of a horizontal step in $B$ (*resp.* $R$) is used by a step in $R$ (*resp.* $B$) is equivalent to that each even vertex in $f$ must be incident to an outgoing (*resp.* incoming) edge. Thus, $(B, R) \in \mathrm{BlueRed}(u, v; w)$. $\square$

**2.2.4. Enumeration of TFPLs of excess $0$ or $1$.** From Theorem 2.7 it follows that $t^w_{u,v} = 0$ unless $\mathrm{exc}(u, v; w) \geq 0$. For both oriented and ordinary TFPLs of excess 0 and 1 enumeration results are known. In this subsection, those for ordinary TFPLs are recapped.

DEFINITION 2.14. *A **Littlewood-Richardson tableau** is a semi-standard Young tableau with the additional property that the sequence obtained by concatenating its reversed rows is a **lattice permutation**, that is, in every initial part of the sequence any*

*number $i$ occurs at least as often as the number $i + 1$. The **Littlewood-Richardson coefficient** $c^\lambda_{\nu,\mu}$ is defined as the number of skew shape $\nu/\lambda$ with content $\mu$.*

Littlewood-Richardson coefficients appear in many areas of mathematics including representation theory and algebraic geometry. Their first appearance though Littlewood-Richardson coefficients made in algebraic combinatorics as the structure constants for the product in the ring of symmetric functions with respect to the basis of Schur functions. From now on, write $c^w_{u,v}$ for the the Littlewood-Richardson coefficient $c^{\lambda(w)}_{\lambda(u),\lambda(v)}$.

THEOREM 2.15 ([**20**, **11**]). *Let $u, v$ and $w$ be words such that $\mathrm{exc}(u, v; w) = 0$. Then*

$$(2.3) \qquad\qquad t^w_{u,v} = c^w_{u,v}.$$

This was first proved by Nadeau for Dyck words in [**20**]. Later, he and Fischer proved the general case in [**11**], thereby establishing TFPLs as a generalised model of Littlewood-Richardson coefficients. In the same article, they proved an expression for $t^w_{u,v}$ in terms of Littlewood-Richardson coefficients for words $u$, $v$ and $w$ with $\mathrm{exc}(u, v; w) = 1$.

DEFINITION 2.16. *Let $\omega$ and $\omega^+$ be words such that $\omega = \omega_L 01 \omega_R$ and $\omega^+ = \omega_L 10 \omega_R$ for appropriate words $\omega_L$ and $\omega_R$. Then set $L_i(\omega, \omega^+) = |\omega_L|_i$ and $R_i(\omega, \omega^+) = |\omega_R|_i$. Furthermore, set $L(\omega, \omega^+) = L_0(\omega, \omega^+) + L_1(\omega, \omega^+) + 1$.*

In the following, write $\omega \to \omega^+$ if $\omega = \omega_L 01 \omega_R$ and $\omega^+ = \omega_L 10 \omega_R$ for appropriate words $\omega_L$ and $\omega_R$. Observe that $\omega \to \omega^+$ is equivalent to $|\omega|_i = |\omega^+|_i$ for $i = 0, 1$, $\omega \le \omega^+$ and $\mathrm{d}(\omega^+) = \mathrm{d}(\omega) + 1$.

THEOREM 2.17 ([**11**]). *Let $u$, $v$ and $w$ be words such that $\mathrm{exc}(u, v; w) = 1$. Then*

$$(2.4) \qquad t^w_{u,v} = \sum_{u^+ : u \to u^+} |u|_1 c^w_{u^+,v} + \sum_{v^+ : v \to v^+} L(v, v^+) c^w_{u,v^+} - \sum_{w^- : w^- \to w} L_1(w^-, w) c^{w^-}_{u,v}.$$

The proof of Theorem 2.17 in [**11**] was split into two steps. In the first step, they proved that the number of TFPLs with boundary $(u, v; w)$ that contain the edge $\lceil$ is given by

$$(2.5) \qquad \sum_{u^+ : u \to u^+} (R_1(u, u^+) + 1) c^w_{u^+,v} + \sum_{v^+ : v \to v^+} (L_0(v, v^+) + 1) c^w_{u,v^+}.$$

Thereto they developed moves that ultimately transform TFPLs of excess 1 that contain the edge $\lceil$ into TFPLs of excess 0. In the second step, they proved that the number of TFPLs with boundary $(u, v; w)$ that do not contain the edge $\lceil$ equals

$$\text{(2.6)} \qquad \sum_{u^+ : u \to u^+} L_1(u, u^+) c^w_{u^+, v} + \sum_{v^+ : v \to v^+} L_1(v, v^+) c^w_{u, v^+} - \sum_{w^- : w^- \to w} L_1(w^-, w) c^{w^-}_{u, v}.$$

# Wieland drift

In 2000, Wieland [**30**] invented the operation on FPLs that bears his name. The *Wieland gyration* was used to prove the rotational invariance of the numbers $A_\pi$ of FPLs corresponding to a given link pattern $\pi$. It was later heavily used by Cantini and Sportiello [**9**] to prove the Razumov-Stroganov conjecture. It also came up in connection with TFPLs already in [**19**] following work of [**29**].

The main contribution of this chapter is the explicit definition of Wieland drift for TFPLs together with a detailed study of some of its properties. Everything presented in this chapter is joint work with Fischer and Nadeau and was published in [**8**]. This chapter is divided as follows. Section 3.1 contains the definition of Wieland drift on TFPLs, which is based on Wieland's original definition. Furthermore, its first properties – culminating in Theorem 3.7 – are given. We can then state the theorems about stability of TFPLs, namely Theorems 3.10 and 3.11, which are proved in Section 3.2. Finally, Section 3.3 contains applications of Wieland drift to enumerative questions concerning TFPLs.

## 3.1. Wieland drift for TFPLs

In this section the definitions of left- and right-Wieland drift for TFPLs are given and some first properties are derived. The starting point is the definition of Wieland gyration for FPLs. In that which follows FPLs of size $n$ are considered subgraphs of $G_n$ that occupy every other external edge. Furthermore, the cells of $G_n$ are partitioned into odd and even cells in a chessboard manner such that by convention the leftmost cell of the top row of $G_n$ is odd.
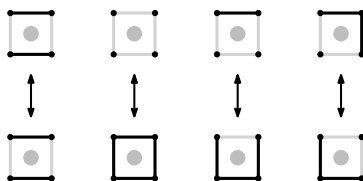


FIGURE 3.1. Up to rotation, the action of W on the active cells of an FPL.

Wieland gyration is composed of local operations on all **active** cells of an FPL: the active cells of an FPL can be chosen to be either all its odd or all its even cells. Now, let $F$ be an FPL and $c$ be an active cell of $F$. Then two cases must be distinguished:

- If $c$ contains precisely two edges of $F$ on opposite sides Wieland gyration W leaves $c$ invariant.

• Otherwise, the effect of W on $c$ is that edges and non-edges of $F$ are exchanged.

In Figure 3.1, the action of W on active cells is illustrated. The result of applying W to each active cell of $F$ is said to be the image of $F$ under Wieland gyration and is denoted by $W(F)$. In Figure 3.2, an FPL and its the image under Wieland gyration with the odd cells being active is pictured.
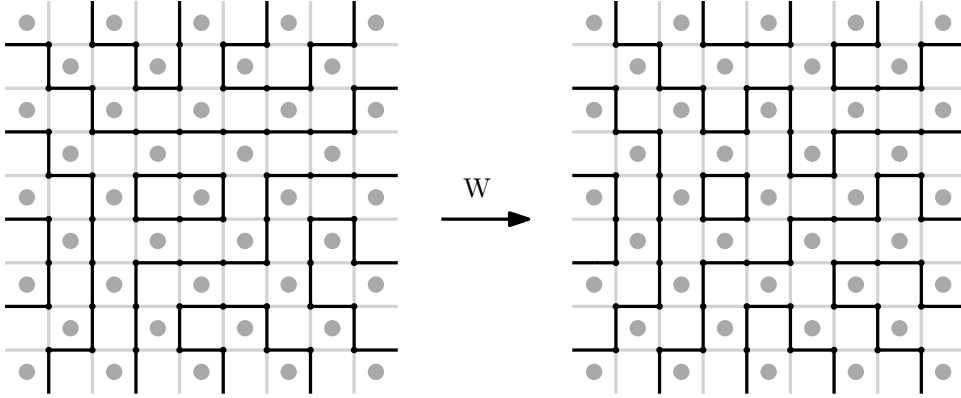


FIGURE 3.2. An FPL and its image under Wieland gyration with the odd cells being active.

Wieland drift as it will be defined for TFPLs is based on the operation W. As active cells of a TFPL can be chosen either all its odd cells or all its even cells. Choosing all odd cells as active cells will lead to what will be defined as left-Wieland drift, while choosing all even cells as active cells will lead to what will be defined as right-Wieland drift.

DEFINITION 3.1. *Let $f$ be a TFPL with left boundary word $u$, and let $u^-$ be a word such that $u^- \xrightarrow{h} u$. The **image of $f$ under left-Wieland drift with respect to** $u^-$ is determined as follows:*

(1) *Insert a vertex $L'_i$ to the left of $L_i$ for $1 \leq i \leq N$. Then run through the occurrences of one in $u^-$: Let $\{i_1 < i_2 < \ldots < i_{N_1}\} = \{i|u_i^- = 1\}$.*

   (a) *If $u_{i_j}$ is the $j$-th one in $u$, add a horizontal edge between $L'_{i_j}$ and $L_{i_j}$.*

   (b) *If $u_{i_j-1}$ is the $j$-th one in $u$, add a vertical edge between $L'_{i_j}$ and $L_{i_j-1}$.*

(2) *Apply Wieland gyration to each odd cell of $f$ .*

(3) *Delete all vertices in $\mathcal{R}^N$ and their incident edges.*

*After shifting the whole construction one unit to the right, one obtains the desired image* $\mathrm{WL}_{u^-}(f)$. *In the case $u^- = u$, it will be simply written $\mathrm{WL}(f)$ and spoken of the **image of $f$ under left-Wieland drift**.*

In Figure 3.3 a TFPL with its odd cells marked by grey dots and its image under left-Wieland drift with respect to 0011111 are depicted. Note that $0011111 \xrightarrow{h} 0101111$. What is more, the right boundary 0101111 of the image of the TFPL under $\mathrm{WL}_{0011111}$ and the right boundary 0011111 of the preimage satisfy that $0011111 \xrightarrow{v} 0101111$. This turns out to hold in general:
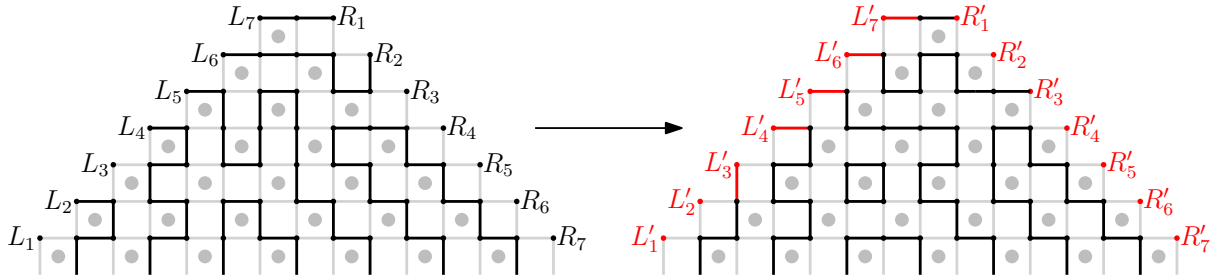
FIGURE 3.3. A TFPL with boundary $(0101111, 0011111; 1101101)$ and its image under left-Wieland drift with respect to $0011111$.

PROPOSITION 3.2. *Let $f$ be a TFPL with boundary $(u, v; w)$ and let $u^-$ be a word satisfying $u^- \xrightarrow{\text{h}} u$. Then $\mathrm{WL}_{u^-}(f)$ is a TFPL with boundary $(u^-, v^+; w)$ where $v^+$ is a word satisfying $v \xrightarrow{\text{v}} v^+$.*

PROOF. First, it has to be checked that $\mathrm{WL}_{u^-}(f)$ indeed is a TFPL, that is, the four conditions in Definition 2.5 must be satisfied. To begin with, the vertices in $\mathcal{L}^N$ have degree 0 or 1 in $\mathrm{WL}_{u^-}(f)$ by construction. On the other hand, for the degree of $R_i$ to be 2 in $\mathrm{WL}_{u^-}(f)$, the vertex to the left of $R_i$ would need to be adjacent to both $R_{i-1}$ and $R_i$ in $f$, which is excluded since no path in $f$ joins two vertices in $\mathcal{R}^N$ by Definition 2.5(4). Thus, the vertices in $\mathcal{R}^N$ have degree 0 or 1 in $\mathrm{WL}_{u^-}(f)$. All other vertices have degree 2 in $\mathrm{WL}_{u^-}(f)$ since they simply come from the application of W to cells of $f$. For the fourth condition observe that Wieland gyration preserves the connectivity of path endpoints in each active cell. Thus, a path in $\mathrm{WL}_{u^-}(f)$ cannot join two vertices in $\mathcal{L}^N$ by construction. On the other hand, if a path in $\mathrm{WL}_{u^-}(f)$ joined two vertices of $\mathcal{R}^N$, say $R_i$ and $R_j$, then a path in $f$ would have to join the vertex to the left of $R_i$ and the vertex to the left of $R_j$. Since $R_i$ and $R_j$ are of degree 1 in $\mathrm{WL}_{u^-}(f)$ both the vertex to the left of $R_i$ and the vertex to the left of $R_j$ would have to be adjacent to a vertex of $\mathcal{R}^N$ in $f$. In summary, if a path in $\mathrm{WL}_{u^-}(f)$ joined two vertices in $\mathcal{R}^N$ then there would exist a path in $f$ that joins two vertices in $\mathcal{R}^N$, which is excluded by Definition 2.5(4). Therefore, no path in $\mathrm{WL}_{u^-}(f)$ joins two vertices in $\mathcal{R}^N$.

It remains to check the assertion on the boundary. The left boundary of $\mathrm{WL}_{u^-}(f)$ is $u^-$ by construction. The right boundary $v^+$ of $\mathrm{WL}_{u^-}(f)$ satisfies $v \xrightarrow{\text{v}} v^+$ by Proposition 3.4 below and the characterisation of pairs $\sigma, \sigma^+$ of words satisfying $\sigma \xrightarrow{\text{v}} \sigma^+$ in the first section of Chapter 2.

Finally, the bottom boundary of $\mathrm{WL}_{u^-}(f)$ is $w$ because Wieland gyration preserves the connectivity of path endpoints in each active cell. $\square$

The lemma below treats the effects of left-Wieland drift along the right boundary of a TFPL.

LEMMA 3.3. *Let $f, u^-, v^+$ be as in Proposition 3.2. Then $v^+ \neq v$ if and only if there exists a vertex in $\mathcal{R}^N$, which is incident to a vertical edge of $f$.*

PROOF. Denote by $x_s$ the vertex to the left of $R_s$ for all $1 \leq s \leq N$.

Let $f$ be a TFPL with a vertex $R_j$ incident to a vertical edge and pick $j$ minimal. Then $x_j$ is necessarily adjacent to both the vertex to its left and to the vertex below, which is why $R_j$ is of degree 0 in $\mathrm{WL}_{u^-}(f)$. Since $R_j$ is of degree 1 in $f$ this shows $v \neq v^+$.

Conversely, suppose that $v^+ \neq v$. Then by Proposition 3.2 it must hold $v < v^+$ and therefore $v_j = 0$ and $v_j^+ = 1$ for a $j \in \{1, 2, \ldots, N-1\}$. Thus, $R_j$ is of degree 0 in $\mathrm{WL}_{u^-}(f)$ and $x_j$ is adjacent to the vertex to its left and to the vertex below in $f$. Since $R_j$ is of degree 1 in $f$, it is necessarily incident to a vertical edge. $\qquad\square$

As a byproduct of the previous proof, one can in fact precisely describe the right boundary $v^+$ as follows:

PROPOSITION 3.4. *Conserve the hypotheses of Lemma 3.3. For each $i$ such that $R_i$ is adjacent to a horizontal edge (resp. a vertical edge) then $v_i^+ = 0$ (resp. $v_{i+1}^+ = 0$). All other values $v_j^+$'s are equal to 1.*

**Right-Wieland drift.** Right-Wieland drift depends on a word $v^-$ satisfying $v^- \xrightarrow{\mathrm{v}} v$, which encodes what happens along the right boundary of a TFPL with boundary $(u, v; w)$, and is denoted by $\mathrm{WR}_{v^-}$ respectively $\mathrm{WR}$, if $v^- = v$. It is defined in an obvious way as the symmetric version of left Wieland-drift and shall simply be illustrated by the example in Figure 3.4.
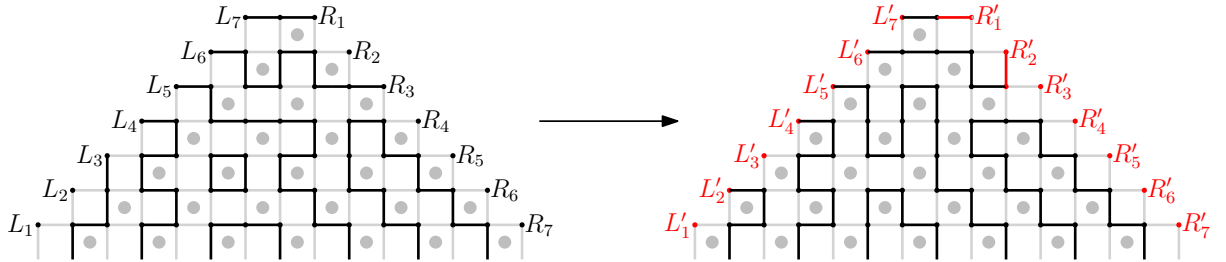


FIGURE 3.4. A TFPL and its image under right-Wieland drift with respect to 0011111.

There are immediate symmetrical versions of Propositions 3.2 and 3.4 for right-Wieland drift that we record:

PROPOSITION 3.5. *The image of a TFPL with boundary $(u, v; w)$ under right-Wieland drift with respect to $v^-$ is a TFPL with boundary $(u^+, v^-; w)$ where $u^+$ is a word satisfying $u \xrightarrow{\mathrm{h}} u^+$.*

PROPOSITION 3.6. *Keep the notations of the previous proposition. For each index $i$ such that $L_i$ is incident to a horizontal edge (resp. a vertical edge), there holds $u_i^+ = 1$ (resp. $u_{i-1}^+ = 1$). All other values $u_j^+$'s are equal to 0.*

Given a TFPL with right boundary $v$, the effect of left-Wieland drift along the right boundary of the TFPL is inverted by right-Wieland drift with respect to $v$. On the other

hand, given a TFPL with left boundary $u$ the effect of right-Wieland drift along the left boundary is inverted by left-Wieland drift with respect to $u$. Since Wieland gyration is an involution on each cell, it follows:

THEOREM 3.7 (**B.**, **Fischer**, **Nadeau**, [8]).     (1) *Let $f$ be a TFPL with boundary $(u^+, v; w)$ and $u$ be a word such that $u \xrightarrow{\text{h}} u^+$. Then*

$$\text{WR}_v(\text{WL}_u(f)) = f.$$

(2) *Let $f$ be a TFPL with boundary $(u, v^+; w)$ and $v$ be a word such that $v \xrightarrow{\text{v}} v^+$. Then*

$$\text{WL}_u(\text{WR}_v(f)) = f.$$

REMARK 3.8. It is perhaps useful to point out that $\text{WR}(\text{WL}(f)) \neq f$ in general. Indeed by Lemma 3.3 equality holds precisely when all vertices $R_i$ of degree one are incident to horizontal edges.

In Section 3.2, the behaviour of TFPLs under iterated applications of WL will be studied. An example of a TFPL to which left-Wieland drift is repeatedly applied is depicted in Figure 3.5: one checks that the last TFPL in the sequence is invariant by left-Wieland drift.

DEFINITION 3.9. *A TFPL is said to be **stable** if it is invariant under the application of left-Wieland drift.*
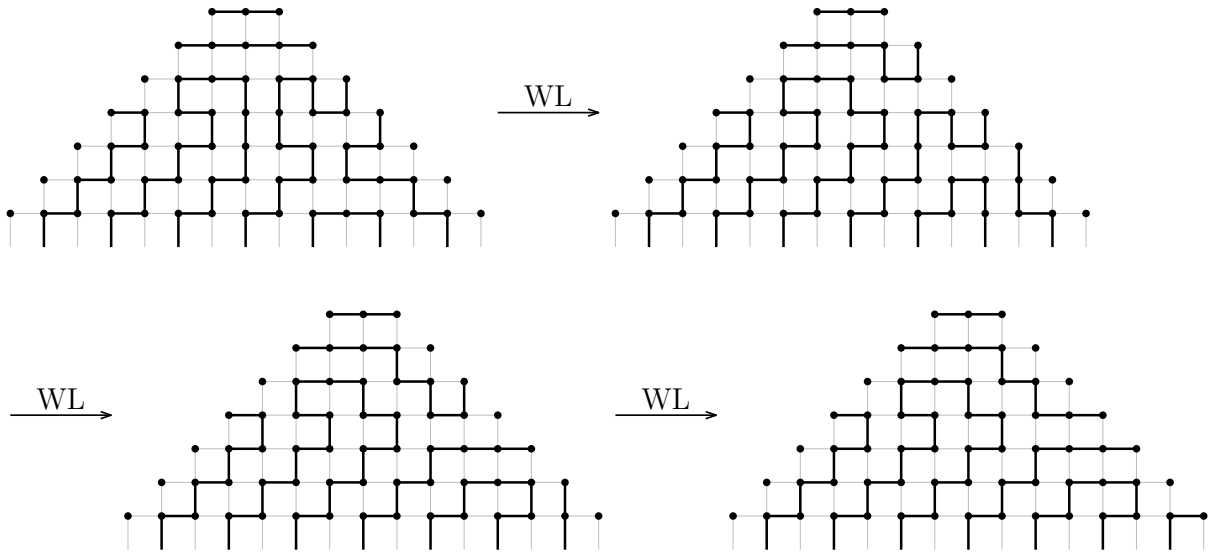


FIGURE 3.5. A TFPL to which left-Wieland drift is repeatedly applied.

Given a TFPL $f$, the sequence $(\text{WL}^m(f))_{m \geq 0}$ is eventually periodic since there are only finitely many TFPLs of a fixed size. The length of this period is in fact always 1.

THEOREM 3.10 (**B.**, **Fischer**, **Nadeau**, [**8**]). *Let $f$ be a TFPL of size $N$. Then* $\mathrm{WL}^{2N-1}(f)$ *is stable, so that the following holds for all $m \geq 2N - 1$ :*

$$\mathrm{WL}^m(f) = \mathrm{WL}^{2N-1}(f).$$

*The same holds for right-Wieland drift.*

In order to prove Theorem 3.10, it is necessary to characterise TFPLs that are invariant under left-Wieland drift. Note that a TFPL is invariant under left-Wieland drift if and only if it is invariant under right-Wieland drift by Theorem 3.7.

## 3.2. Stable TFPLs

From now on the vertices of $G^N$ will be considered partitioned into odd and even vertices as specified in Section 2.2. In this section, it will be proved that stable TFPLs can be characterised as follows:

THEOREM 3.11 (**B.**, **Fischer**, **Nadeau**, [**8**]). *A TFPL is stable if and only if it contains no edge of the form* ⌡.

DEFINITION 3.12. *The edge* ⌡ *is called a **drifter**.*

The number of drifters that a TFPL can contain is bounded by the excess of the TFPL:

PROPOSITION 3.13. *A TFPL of excess $k$ contains at most $k$ drifters.*

PROOF. If a TFPL of excess $k$ is oriented canonically then the so-obtained oriented TFPL again is of excess $k$. Thus, the assertion immediately follows from Theorem 2.12. □

Theorem 3.11 and Proposition 3.13 give rise to the following class of stable TFPLs:

COROLLARY 3.14. *If a TFPL is of excess $0$, then it is stable.*

In the following, the possible cells of a TFPL play an important role in the proofs. For convenience, notations for the 16 odd and 16 even cells of a TFPL are fixed. In Figure 3.6 the chosen notation can be seen.

**3.2.1. Characterisation of stable TFPLs.** To prove Theorem 3.11, we will begin by showing that a TFPL containing a drifter is not stable.

PROPOSITION 3.15. *Let $f$ be a TFPL that contains a drifter. Then $\mathrm{WL}(f) \neq f$.*
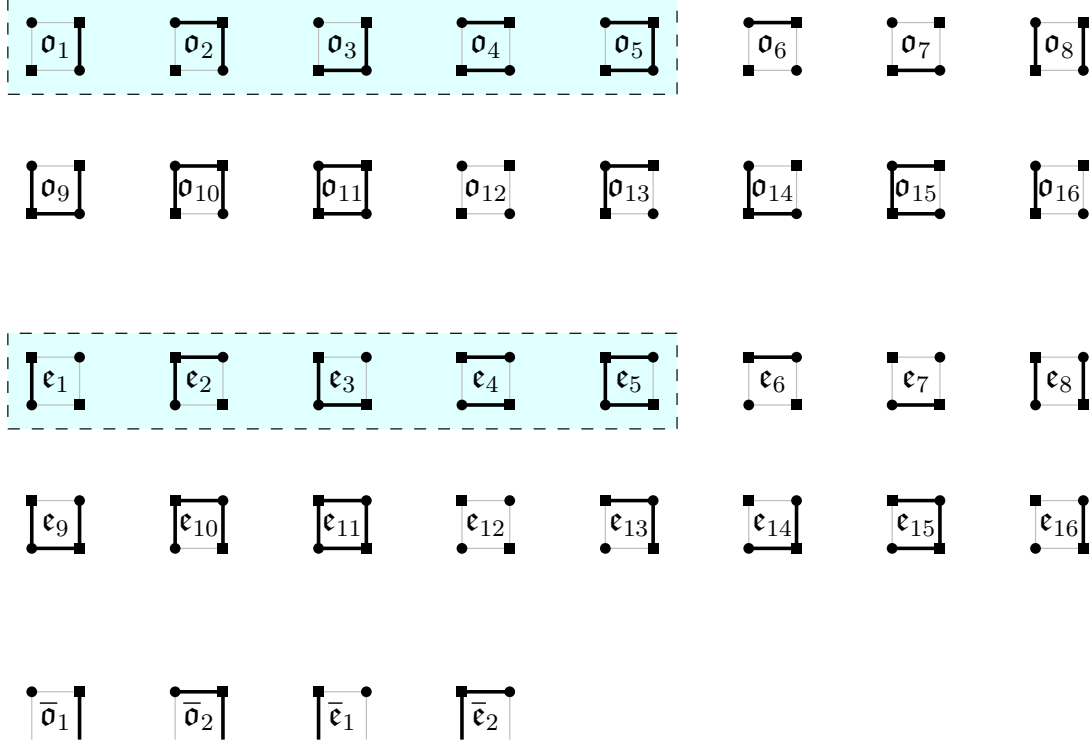
FIGURE 3.6. The notations for the 16 odd and 16 even internal cells of a TFPL, with emphasis on the subsets $\mathfrak{O} = \{\mathfrak{o}_1, \mathfrak{o}_2, \mathfrak{o}_3, \mathfrak{o}_4, \mathfrak{o}_5\}$ and $\mathfrak{E} = \{\mathfrak{e}_1, \mathfrak{e}_2, \mathfrak{e}_3, \mathfrak{e}_4, \mathfrak{e}_5\}$. Furthermore, the notations for the 2 odd and 2 even external cells of a TFPL.

PROOF. If $f$ contains a drifter incident to a vertex in $\mathcal{R}^N$, then by Lemma 3.3 the right boundaries of $f$ and $\mathrm{WL}(f)$ are different, so that necessarily $\mathrm{WL}(f) \neq f$.

Hence, assume that no vertex in $\mathcal{R}^N$ is incident to a drifter. Let $\iota$ be a drifter in $f$ with maximal $x$-coordinate and consider the odd cell $o$ in $f$ that contains $\iota$. Furthermore, let $x$ be the top right vertex of $o$ and $y$ be the bottom right vertex of $o$. By the choice of $\iota$ the vertices $x$ and $y$ are not incident to a drifter in $f$.
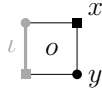


Therefore, $o \in \{\mathfrak{o}_8, \mathfrak{o}_9, \mathfrak{o}_{10}, \mathfrak{o}_{11}, \mathfrak{o}_{15}\}$. If $o$ is of the form $\mathfrak{o}_8$ or $\mathfrak{o}_{15}$, the vertex to the right of $x$ is incident to a drifter in $\mathrm{WL}(f)$. In that case, $\mathrm{WL}(f) \neq f$ because the vertex to the right of $x$ in $f$ is not incident to a drifter by assumption. If $o$ is of the form $\mathfrak{o}_9$, $\mathfrak{o}_{10}$ or $\mathfrak{o}_{11}$, the vertices $x$ and $y$ are not adjacent in $\mathrm{WL}(f)$. Thus, $\mathrm{WL}(f) \neq f$ because $x$ and $y$ are adjacent in $f$. $\qquad \square$

To prove that a TFPL without a drifter is indeed stable, we need to determine the types of cells that may occur. Define $\mathfrak{O} = \{\mathfrak{o}_1, \mathfrak{o}_2, \mathfrak{o}_3, \mathfrak{o}_4, \mathfrak{o}_5\}$ and $\mathfrak{E} = \{\mathfrak{e}_1, \mathfrak{e}_2, \mathfrak{e}_3, \mathfrak{e}_4, \mathfrak{e}_5\}$.

LEMMA 3.16. *If $f$ is a TFPL without drifters, then all interior odd cells belong to $\mathfrak{O}$ while all of its interior even cells belong to $\mathfrak{E}$.*

PROOF. Let $f$ be a TFPL without a drifter, and $o$ be one of its interior odd cells. Since $o$ has no drifter, it can only belong to $\mathfrak{O}$ or have one of the types $\mathfrak{o}_6, \mathfrak{o}_7$ or $\mathfrak{o}_{12}$. But in types $\mathfrak{o}_6$ (*resp.* $\mathfrak{o}_7$) or $\mathfrak{o}_{12}$, there would exist an interior cell below (*resp.* above) $o$ that contains a drifter, which is excluded.

The case of even cells is entirely analogous. □

Furthermore, in a TFPL with no drifter each odd cell has a uniquely determined even cell to its right.

LEMMA 3.17. *Let $f$ be a TFPL without drifters, $o$ an odd cell of $f$ and $e$ the even cell of $f$ to the right of $o$. If $o$ and $e$ are interior, then they can only occur as part of one of the following pairs:*
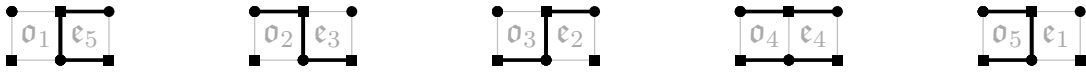


*On the other hand, if $o$ and $e$ contain an external edge, then $o$ and $e$ can only occur as part of one of the following pairs:*



PROOF. Here, only the case when $o$ is an interior odd cell and $o = \mathfrak{o}_1$ is considered, the other cases being similar. Obviously, the cell $e$ cannot equal $\mathfrak{e}_4$. But it cannot equal $\mathfrak{e}_1, \mathfrak{e}_2$ or $\mathfrak{e}_3$ either, since otherwise one of the right vertices of $o$ would be be incident to a drifter. The only remaining possibility is that $e$ is of type $\mathfrak{e}_5$ by Lemma 3.16. □

The proof of Theorem 3.11 now can be completed by showing that a TFPL without drifters is invariant under left-Wieland drift.

PROPOSITION 3.18. *If $f$ is a TFPL without drifters, then $\mathrm{WL}(f) = f$.*

PROOF. Let $o$ be an odd cell of $f$ and $e$ be the even cell to its right. By Lemma 3.17, $e$ is uniquely determined by $o$. The crucial observation is that $e$ coincides with the image of $o$ under Wieland gyration. Thus, each even cell of $f$ and its corresponding even cell of $\mathrm{WL}(f)$ coincide. By definition all edges and non-edges of $f$ incident to a vertex in $\mathcal{L}^N$ are preserved by left-Wieland drift. In summary, $\mathrm{WL}(f) = f$. □

**3.2.2. TFPLs are eventually stable under Wieland drift.** In this subsection, we will prove Theorem 3.10. The idea of the proof is the following: when applying left-Wieland drift to a TFPL, the drifters of the TFPL are globally moved to the right. Thus, after a finite number of applications of left-Wieland drift, all drifters eventually disappear through the right boundary. As a consequence of Theorem 3.11 a stable TFPL is then obtained.

In a TFPL of size $N$, there are $2N + 1$ columns of vertices which we label from left to right from 1 to $2N + 1$.

PROPOSITION 3.19. *Let $f$ be a TFPL of size $N$ that contains a drifter in the $n$-th column but no drifter in the columns $1, \ldots, n-1$ to its left. Then $\mathrm{WL}(f)$ contains no drifter in any of the columns $1, \ldots, n$.*

PROOF. First of all, notice that by the definition of left-Wieland drift, no vertex of $\mathcal{L}^N$ is incident to a drifter in $\mathrm{WL}(f)$. By definition of WL, the occurrence of a drifter in an even cell $e$ of $\mathrm{WL}(f)$ depends solely on the odd cell to the left of the even cell $e$ in $f$. By hypothesis, no odd cell of $f$ occurring to the left of the $(n-1)$-st column has a vertex incident to a drifter. It follows from the proof of Lemma 3.16 that all these odd cells belong to $\mathfrak{O}$. This entails that all even cells of $\mathrm{WL}(f)$ to the left of the $n$-th column belong to $\mathfrak{E}$, and thus do not contain a drifter. Since these even cells cover all vertical edges in the columns $1, \ldots, n$, the proof is complete. $\qquad\square$

PROOF OF THEOREM 3.10. By induction on the result of Proposition 3.19, we know that the configuration $\mathrm{WL}^{2N+1-n}(f)$ contains no drifter, and thus is stable under WL by Theorem 3.11, that is,

$$(3.1) \qquad\qquad \mathrm{WL}^m(f) = \mathrm{WL}^{2N+1-n}(f)$$

for all $m \geq 2N+1-n$. Since the first column of vertices of a TFPL consists only of the vertex $L_1$, we have $n \geq 2$, which proves the theorem. $\qquad\square$

## 3.3. Applications of Wieland drift on TFPLs

**3.3.1. Some linear relations.** The following was conjectured for Dyck words in [**29**] and proved in [**19**] using Wieland gyration on FPLs.

PROPOSITION 3.20. *Let $u$, $v$ and $w$ be words. Then*

$$\sum_{u^+ : u \xrightarrow{\mathrm{h}} u^+} t^w_{u^+,v} = \sum_{v^+ : v \xrightarrow{\mathrm{v}} v^+} t^w_{u,v^+}.$$

PROOF. Indeed the function $\mathrm{WL}_u(\cdot)$ acts on all TFPLs with boundary $(u^+, v; w)$, while $\mathrm{WR}_v(\cdot)$ acts on TFPLs with boundary $(u, v^-; w)$. By Theorem 3.7, these functions are inverses of one another, and the result is obtained by taking cardinalities. $\qquad\square$

**3.3.2. The inequality in Theorem 2.7.** This states that $|\lambda(u)| + |\lambda(v)| \leq |\lambda(w)|$ always holds for the boundaries $(u, v; w)$ of TFPLs. It was given in [**29**, Lemma 3.7] in the Dyck word case. Later, another proof in connection with oriented TFPLs was given in [**11**]. For the exact result in [**11**] see Theorem 2.12.

Now an independent proof based on the properties of Wieland drift will be given; the idea for this proof comes from the original one by Thapper, which can be seen as relying on Wieland gyration on FPLs in an indirect way.

PROOF OF THEOREM 2.7(3). Let $f$ be a TFPL with boundary $(u, v; w)$. The proof is done by induction on $|\lambda(u)|$. In the case when $|\lambda(u)| = 0$ it has to be shown that $|\lambda(v)| \leq |\lambda(w)|$; the latter immediately follows from Theorem 2.7(2).

Assume now $|\lambda(u)| \geq 1$. By removing a corner of $\lambda(u)$, there exists a Young diagram $\lambda(u^-) \subseteq \lambda(u)$ with one cell less than $\lambda(u)$. In particular $\lambda(u)/\lambda(u^-)$ is a horizontal strip.

It first will be proved that there exists an $i > 0$ such that $\mathrm{WL}^i_{u^-}(f)$ has right boundary $v^+ \neq v$. Assume the contrary, that is, the right boundary of $\mathrm{WL}^i_{u^-}(f)$ is $v$ for all $i > 0$. Since there is only a finite number of TFPLs with boundary $(u^-, v; w)$, there exist integers $i_0, p > 0$ such that

$$\mathrm{WL}^{i_0+p}_{u^-}(f) = \mathrm{WL}^{i_0}_{u^-}(f).$$

By applying $\mathrm{WR}^{i_0}_v$ to both sides of the identity and by Theorem 3.7 it follows that $\mathrm{WL}^p_{u^-}(f) = f$. But these configurations have left boundaries $u, u^-$ respectively, which contradicts the assumption $u^- \neq u$.

Hence, let $i$ be a positive integer such that $\mathrm{WL}^i_{u^-}(f)$ has boundary $(u^-, v^+; w)$ where $v^+ \neq v$. By Proposition 3.2 it holds $\lambda(v) \subsetneq \lambda(v^+)$. Applying the induction hypothesis to $\mathrm{WL}^i_{u^-}(f)$ completes the proof:

$$|\lambda(u)| + |\lambda(v)| = |\lambda(u^-)| + 1 + |\lambda(v)| \leq |\lambda(u^-)| + |\lambda(v^+)| \leq |\lambda(w)|.$$

$\square$

## 3.4. Outlook

One of the most intriguing properties of Wieland drift is that it is eventually periodic with period 1. This property now offers to relate TFPLs to stable TFPLs by use of Wieland drift, thereby establishing an approach to the enumeration of TFPLs. (Note that below the number of stable TFPLs with boundary $(u, v; w)$ is denoted by $s^w_{u,v}$.)

The enumeration results for TFPLs that we have seen up to this point are, on the one hand, that $t^w_{u,v}$ coincides with the Littlewood-Richardson coefficient $c^w_{u,v}$ if $\mathrm{exc}(u, v; w) = 0$ (Theorem 2.15) and, on the other hand, a linear expression in terms of Littlewood-Richardson coefficients for $t^w_{u,v}$ if $\mathrm{exc}(u, v; w) = 1$ (Theorem 2.17). Given that TFPLs of excess 0 are necessarily stable (Corollary 3.14) we may construe the first result as the consequence of the two identities $t^w_{u,v} = s^w_{u,v}$ and $s^w_{u,v} = c^w_{u,v}$ (if $\mathrm{exc}(u, v; w) = 0$). The second result just as well can be seen as the consequence of an expression for $t^w_{u,v}$ in terms of numbers of stable TFPLs and an expression for the number of stable TFPLs in terms of Littlewood-Richardson coefficients as per particulars given below.

It is mentioned in Section 2.2.4 that the proof of the result for TFPLs of excess 1 in [11] treats TFPLs that exhibit the edge ⬒ and those that do not separately. This edge is our drifter, meaning that in retrospective the numbers of both instable and stable TFPLs of excess 1 are expressed in terms of Littlewood-Richardson coefficients in [11]. (The precise formulations can be found in (2.5) and (2.6) respectively.) Since for words $u^+$, $v^+$ and

$w^-$ with $\mathrm{exc}(u^+, v^+; w^-) = 0$ the Littlewood-Richardson coefficient $c_{u^+,v^+}^{w^+}$ coincides with the number of stable TFPLs with boundary $(u^+, v^+; w^-)$ the expression for the number of instable TFPLs with boundary $(u, v; w)$ in (2.5) is actually an expression in terms of numbers of stable TFPLs. To be more precise, (2.5) is equivalent to

$$(3.2) \qquad t_{u,v}^w - s_{u,v}^w = \sum_{u^+: u \to u^+} (R_1(u, u^+) + 1)s_{u^+,v}^w + \sum_{v^+: v \to v^+} (L_0(v, v^+) + 1)s_{u,v^+}^w$$

where $u \to u^+$ means that $u = u_L 01 u_R$ and $u^+ = u_L 10 u_R$ for appropriate words $u_L$ and $u_R$, $R_i(u, u^+) = |u_L|_i$ and $L_i(u, u^+) = |u_R|_i$ for $i = 0, 1$. Furthermore, (2.6) is equivalent to

$$(3.3) \quad s_{u,v}^w = \sum_{u^+: u \to u^+} L_1(u, u^+)c_{u^+,v}^w + \sum_{v^+: v \to v^+} L_1(v, v^+)c_{u,v^+}^w - \sum_{w^-: w^- \to w} L_1(w^-, w)c_{u,v}^{w^-}.$$

To prove the expression in (2.5) for the number of instable TFPLs with boundary $(u, v; w)$ the authors in [11] invented transformations that ultimately transform instable TFPLs of excess 1 into TFPLs of excess 0 and counted how many instable TFPLs with boundary $(u, v; w)$ are transformed into the same TFPL of excess 0. These transformations turn out to be essentially equivalent to a simple application of Wieland drift. Instable TFPLs thus may be related to stable TFPLs through Wieland drift in a way that generalises the way set forth for instable TFPLs of excess 1 in [11], in order to at best find an expression for $t_{u,v}^w$ in terms of numbers of stable TFPLs. In a parallel line of research stable TFPLs should be studied and enumerated. It might be possible to express $s_{u,v}^w$ in terms of Littlewood-Richardson coefficients.

# Triangular fully packed loop configurations of excess 2

The main contribution of this chapter is a linear expression for $t_{u,v}^w$ in terms of numbers of stable TFPLs for any words $u$, $v$ and $w$ with $\text{exc}(u, v; w) = 2$. This linear expression generalises the expression for the excess-1-case in (3.2). To give the exact formulation of the main result of this chapter further notation is needed.

DEFINITION 4.1. *Let $u$ and $u^+$ be two $01$-words of the same length that satisfy $|u|_1 = |u^+|_1 = N_1$ and $\lambda(u) \subseteq \lambda(u^+)$. Then denote by $g_{u,u^+}$ the number of semi-standard Young tableaux of skew shape $\lambda(u^+)/\lambda(u)$ with entries in the $i$-th column – when counted from the left – restricted to $1, 2, \ldots, N_1 - i + 1$.*
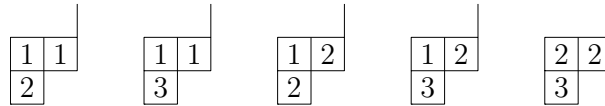


FIGURE 4.1. The semi-standard Young tableaux that contribute to $g_{001101,101001}$.

For instance $g_{001101,101001} = 5$. From now on, denote the set of stable TFPLs with boundary $(u^+, v^+; w)$ with $S_{u^+,v^+}^w$ and its cardinality with $s_{u^+,v^+}^w$.

THEOREM 4.2. *Let $u, v, w$ be words of the same length such that $|u|_1 = |v|_1 = |w|_1$ and $\text{exc}(u, v; w) = 2$. Then*

$$(4.1) \qquad t_{u,v}^w = \sum_{u^+ \geq u, v^+ \geq v} g_{u,u^+} \; g_{v^*,(v^+)^*} \; s_{u^+,v^+}^w.$$

By Theorem 2.7 $s_{u^+,v^+}^w = 0$ unless $|u^+|_1 = |v^+|_1 = |w|_1$ and $\text{d}(u^+) + \text{d}(v^+) \leq \text{d}(w)$. The sum in (4.1) is finite since it is restricted to words $u^+$ and $v^+$ that satisfy $|u^+|_1 = |v^+|_1 = |w|_1$ and $\text{d}(u^+) + \text{d}(v^+) \leq \text{d}(w)$. Furthermore, if $\text{exc}(u, v; w) = 0$ then

$$(4.2) \qquad t_{u,v}^w = s_{u,v}^w$$

by Corollary 3.14. For words $u$, $v$ and $w$ with $\text{exc}(u, v; w) = 1$ Fischer and Nadeau proved an expression for $t_{u,v}^w$ in terms of Littlewood-Richardson coefficients, see (2.5). This expression now can be written as follows:

$$(4.3) \qquad t_{u,v}^{w} = s_{u,v}^{w} + \sum_{u^+ \geq u} g_{u,u^+}\ s_{u^+,v}^{w} + \sum_{v^+ \geq v} g_{v^*,(v^+)^*}\ s_{u,v^+}^{w}.$$

Thus, the linear expression stated in Theorem 4.2 generalises the already existing enumeration results for TFPLs with boundary $(u, v; w)$ where $\mathrm{exc}(u, v; w) = 0, 1$.

This chapter is structured as follows. In Section 4.1 the effect of Wieland drift on TFPLs of excess 2 will be studied in detail. We already know from the previous chapter that Wieland drift changes a TFPL solely near the drifters. The main contribution of the first section will be the definition of (five) transformations around drifters – so-called *moves* – that suffice to describe the effect of Wieland drift on TFPLs of excess 2, see Proposition 4.3. In Section 4.2, we will study the numbers of times left- (*resp.* right-) Wieland drift has to be applied to TFPLs until a from the outset fixed drifter is incident to a vertex of the right (*resp.* left) boundary. This study will culminate in Corollary 4.11, which will be crucial for the proof of Theorem 4.2 that is the content of Section 4.3.

The work presented in this chapter was presented as a poster at the 27th International Conference on Formal Power Series and Algebraic Combinatorics in 2015 ([**6**]). Furthermore, it has recently been accepted to be published by The Electronic Journal of Combinatorics ([**7**]).

### 4.1. An alternative description of Wieland drift for TFPLs of excess 2

The main contribution of this section is a description of the effect of Wieland drift on TFPLs of excess at most 2 as a composition of moves. In Figure 4.2, the moves that form the basis for that description are depicted. Recall that a TFPL of excess 2 contains at most 2 drifters, which is why there occur at most two drifters in every move. Furthermore, if the move $M_4$ is applicable to a TFPL of excess 2 then no other moves are applicable to that TFPL by Theorem 2.12.
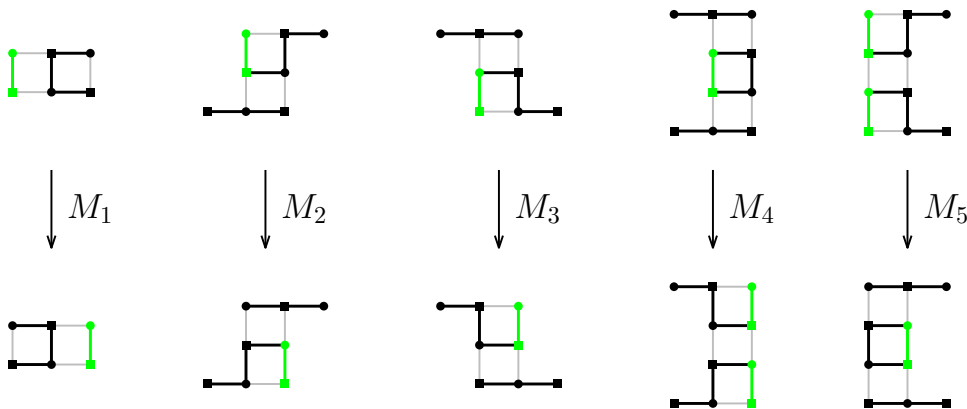


FIGURE 4.2. The moves that describe the effect of left-Wieland drift on instable TFPLs of excess 2.

PROPOSITION 4.3. *Let $f$ be an instable TFPL with boundary $(u, v; w)$ such that* $\mathrm{exc}(u, v; w) \leq 2$. *Furthermore, let $u^-$ be a word that satisfies $u^- \stackrel{\mathrm{h}}{\longrightarrow} u$. Then the image of $f$ under left-Wieland drift with respect to $u^-$ is determined as follows:*

(1) *if $R_i$ in $\mathcal{R}^N$ is incident to a drifter delete that drifter and add a horizontal edge incident to $R_{i+1}$ for $i = 1, 2, \ldots, N-1$;*

(2) *perform $M_4$ or $M_5$ if possible; otherwise, run through the columns of $G^N$ from right to left, that is, for $j = 2N+1, 2N, \ldots, 1$:*

   (a) *if there is precisely one drifter in the $j$-th column of $G^N$, apply $M_1$, $M_2$ or $M_3$ to it;*

   (b) *if there are two drifters in the $j$-th column of $G^N$, apply $M_1$, $M_2$ or $M_3$ to each of the drifters in the following order: if the odd cell that contains the upper drifter is the cell $\mathfrak{o}_9$, that is, $\boxed{\phantom{x}}$, move the lower drifter first. Otherwise, move the upper drifter first.*

(3) *run through the occurrences of one in $u^-$: let $\{i_1 < \cdots < i_{N_1}\} = \{i : u_i^- = 1\}$. If $u_{i_j - 1}$ is the $j$-th one in $u$ delete the horizontal edge incident to $L_{i_j - 1}$ and add a vertical edge incident to $L_{i_j}$ for $j = 1, 2, \ldots, N_1$.*

In Figure 4.3 a TFPL of excess 2 with two drifters and its image under left-Wieland drift are depicted. The two drifters in the original TFPL have the same $x$-coordinate and the odd cell that contains the upper drifter is of the form $\mathfrak{o}_9$. Thus, by left-Wieland drift the move $M_1$ is applied to the lower drifter before the move $M_2$ is applied to the other drifter. The rest of the TFPL is preserved.
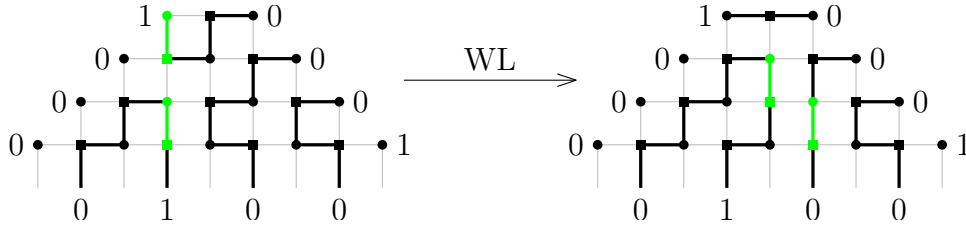


FIGURE 4.3. A TFPL of excess 2 with two drifters and its image under left-Wieland drift.

In the proof of Proposition 4.3 the effect of left-Wieland drift will be checked cell by cell. From the set of cells that can occur in a TFPL of excess at most 2 the following cells can be excluded:

LEMMA 4.4. *In a TFPL of excess at most 2, none of the following cells can occur:*
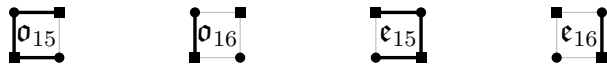


Since the proofs in this section work by studying the cells of a TFPL it is convenient to fix notations for all the odd and even cells that can occur in a TFPL. These notations are chosen as in the previous chapter, see Figure 3.6.

PROOF. Let $f$ be a TFPL and $\overrightarrow{f}$ its canonical orientation. First, suppose that $f$ contains a cell $c$ of the form $\mathfrak{o}_{15}$. Then $c$ must exhibit two configurations in $\overrightarrow{f}$ that contribute to the excess, see Theorem 2.12. On the other hand, the right vertex of the horizontal edge in $c$ which is oriented from right to left in $\overrightarrow{f}$ either is adjacent to the vertex to its right or is incident to a drifter. Thus, $\overrightarrow{f}$ exhibits yet another configuration that contributes to the excess. The excess of $f$ thus must be at least 3. For the same reason, a TFPL of excess at most 2 cannot contain the third cell in the list.

Now, suppose that a cell $c$ in $f$ is of the form $\mathfrak{o}_{16}$. Then both the top and the bottom rightmost vertex in $c$ have to be incident to a drifter. Therefore, $f$ contains at least three drifters and therefore has to be of excess at least 3. By the same argument, the fourth cell in the list cannot occur in a TFPL of excess at most 2. $\qquad\square$

In the following, it will be convenient to distinguish between the cells of a TFPL and the cells of its image under left-Wieland drift. To this end, given a cell $c$ of $G^N$ it is written $c$ when it is referred to the cell $c$ of the TFPL and $c'$ when it is referred to the cell $c$ of the image of the TFPL under WL. When the cells of a TFPL and of its image under left-Wieland drift are compared it has to be kept in mind that in the last step of left-Wieland drift the whole configuration is shifted one unit to the right. For that reason, for each odd cell $o$ of a TFPL and the even cell $e$ to the right of $o$ the following holds when **disregarding** the distinction between odd and even vertices:

$$(4.4) \qquad\qquad\qquad e' = \mathrm{W}(o)$$

To begin with, in the image of a TFPL under WL all edges incident to a vertex in $\mathcal{L}^N$ must be horizontal by definition. This is why it suffices to determine the effect of WL on the even cells of a TFPL. The following lemma gives conditions under which even cells are preserved under WL. Its proof is analogous to the proof of Lemma 3.17 and therefore omitted.

LEMMA 4.5. *Let $f$ be a TFPL. Furthermore, let $o$ be an odd cell of $f$ and $e$ the even cell to the right of $o$ such that no vertex of $o$ and $e$ is incident to a drifter. If $o$ and $e$ are interior cells, then they can only occur as part of one of the following pairs:*



*On the other hand, if $o$ and $e$ contain an external edge, then $o$ and $e$ can only occur as part of one of the following pairs:*



*In particular, $e' = e$.*

Due to Lemma 4.5 it remains to determine the effect of WL on even cells $e$ such that a vertex in $e$ or in the odd cell $o$ to the left of $e$ is incident to a drifter. Now, each drifter that is not incident to a vertex in $\mathcal{L}^N \cup \mathcal{R}^N$ brings about four such even cells, see Figure 4.4. These even cells and the odd cells to their left shall in the following be denoted as indicated in Figure 4.4. Finally, a drifter that is incident to a vertex in $\mathcal{L}^N$ (resp. $\mathcal{R}^N$) solely entails the cells $o_r$, $e_r$, $o_b$ and $e_b$ (resp. $o_l$, $e_l$, $o_b$ and $e_b$).
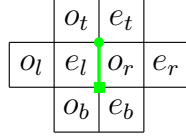


FIGURE 4.4. A drifter and its surrounding cells.

The next lemma addresses the effect of left-Wieland drift on the cells $e_t$, $e_l$ and $e_b$.

LEMMA 4.6. *Let $f$ be an instable TFPL of excess at most 2, $o$ an odd cell of $f$ and $e$ the even cell to the right of $o$. If $o$ does not contain a drifter, a vertex of $e$ is incident to a drifter and $o \notin \{\mathfrak{o}_6, \mathfrak{o}_7, \mathfrak{o}_{12}\}$, then $e'$ and $e$ coincide with the following sole exceptions:*

  (1) *if in $e$ there is a drifter, then in $e'$ there is none,*
  (2) *if the top left vertex of $e$ is incident to a drifter, then there is no horizontal edge between the two top vertices of $e$ but there is one between the two top vertices of $e'$,*
  (3) *if the bottom left vertex of $e$ is incident to a drifter, then there is no horizontal edge between the two bottom vertices of $e$ but there is one between the two bottom vertices of $e'$.*

PROOF. If $o$ and $e$ are external cells such that a vertex of $e$ is incident to a drifter, then $o = \overline{\mathfrak{o}}_1$, $e = \overline{\mathfrak{e}}_1$ and $e' = \overline{\mathfrak{e}}_2$. In that case, $e'$ and $e$ coincide with the sole exception that there is no horizontal edge between the two top vertices of $e$ whereas there is one between the two top vertices of $e'$. Suppose that $o$ and $e$ are internal cells such that $o$ does not contain a drifter, a vertex of $e$ is incident to a drifter and $o$ is not in $\{\mathfrak{o}_6, \mathfrak{o}_7, \mathfrak{o}_{12}\}$. Then $(o, e)$ can only occur as part of one of the following pairs:
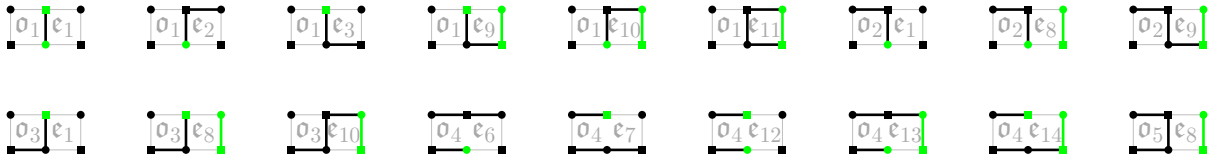




Now, $e' = \mathfrak{e}_5$ if $o = \mathfrak{o}_1$, $e' = \mathfrak{e}_3$ if $o = \mathfrak{o}_2$, $e' = \mathfrak{e}_2$ if $o = \mathfrak{o}_3$, $e' = \mathfrak{e}_4$ if $o = \mathfrak{o}_4$ and $e' = \mathfrak{e}_1$ if $o = \mathfrak{o}_5$. It can easily be checked that in any case $e'$ and $e$ satisfy the assertions. $\square$

Proposition 4.3 now is proved separately for instable TFPLs of excess at most 2 that contain precisely one drifter and for those that contain two drifters.

PROOF OF PROPOSITION 4.3(ONE DRIFTER). Let $f$ be an instable TFPL of excess at most 2 that contains precisely one drifter $\mathfrak{d}$. First, the case when $\mathfrak{d}$ is incident to a vertex $R_i$ in $\mathcal{R}^N$ is considered. In that case the cells $o_l$, $e_l$, $o_b$ and $e_b$ exist. Furthermore, both $o_l$ and $o_b$ do not contain a drifter and are not in $\{\mathfrak{o}_6, \mathfrak{o}_7, \mathfrak{o}_{12}\}$ because in $f$ there is only one drifter. Thus, by Lemma 4.6 on the one hand $e'_l$ and $e_l$ coincide with the sole exception that in $e'_l$ there is no drifter whereas in $e_l$ there is one and on the other hand $e'_b$ and $e_b$ coincide with the sole exception that in $e'_b$ the two top vertices are adjacent whereas in $e_b$ they are not. By Lemma 4.5 the effect of left-Wieland drift on $f$ is that the drifter incident to $R_i$ is replaced by a horizontal edge incident to $R_{i+1}$ while the rest of $f$ is preserved.

It remains to consider the case when $\mathfrak{d}$ is not incident to a vertex in $\mathcal{R}^N$. In that case the cells $o_r$, $e_r$, $o_b$ and $e_b$ of $f$ have to exist. Since $f$ contains precisely one drifter $o_r \in \{\mathfrak{o}_8, \mathfrak{o}_9, \mathfrak{o}_{10}, \mathfrak{o}_{11}\}$ by Lemma 4.4. It will be proceeded by treating each of the four possible cases for $o_r$ separately.

First, the case when $o_r = \mathfrak{o}_8$ is regarded. In that case, $e_r = \mathfrak{e}_5$ because $f$ contains precisely one drifter. Furthermore, $\mathrm{W}(\mathfrak{o}_8) = \mathfrak{o}_8$ and therefore $e'_r = \mathfrak{e}_8$. On the other hand, $e'_b$ and $e_b$ coincide with the sole exception that the two top vertices in $e'_b$ are adjacent whereas in $e_b$ they are not by Lemma 4.6. If the cells $o_t$, $e_t$, $o_l$ and $e_l$ exist, then both $o_t$ and $o_l$ cannot be in $\{\mathfrak{o}_6, \mathfrak{o}_7, \mathfrak{o}_{12}\}$ and for that reason $e'_t$ and $e_t$ coincide with the sole exception that the two bottom vertices in $e'_t$ are adjacent whereas in $e_t$ they are not and $e'_l$ and $e_l$ coincide with the sole exception that in $e'_l$ there is no drifter whereas in $e_l$ there is one by Lemma 4.6. By Lemma 4.5, the effect of left-Wieland drift on $f$ is that the move $M_1$ is applied to $\mathfrak{d}$ while the rest of $f$ is preserved.

Next, the case when $o_r = \mathfrak{o}_9$ is considered. In that case, $e_r = \mathfrak{e}_2$, $o_b = \mathfrak{o}_7$ and $e_b = \mathfrak{e}_4$. Furthermore, $\mathrm{W}(\mathfrak{o}_9) = \mathfrak{o}_6$ that is $e'_r = \mathfrak{e}_6$ and $\mathrm{W}(\mathfrak{o}_7) = \mathfrak{o}_{10}$ that is $e'_b = \mathfrak{e}_{10}$. If the cells $o_l$, $e_l$, $o_t$ and $e_t$ exist, then neither $o_t$ nor $o_l$ is in $\{\mathfrak{o}_6, \mathfrak{o}_7, \mathfrak{o}_{12}\}$. By Lemma 4.6 and Lemma 4.5 the effect of left-Wieland drift on $f$ is that the move $M_2$ is applied to $\mathfrak{d}$ while the rest of $f$ is preserved.

Next, the case when $o_r = \mathfrak{o}_{10}$ is regarded. In that case, $o_t$, $e_t$, $o_l$ and $e_l$ exist. Furthermore, $e_r = \mathfrak{e}_3$, $o_t = \mathfrak{o}_6$ and $e_t = \mathfrak{e}_4$. Therefore, $e'_r = \mathfrak{e}_7$ and $e'_t = \mathfrak{e}_9$. Since neither $o_b$ nor $o_l$ is in $\{\mathfrak{o}_6, \mathfrak{o}_7, \mathfrak{o}_{12}\}$ by Lemma 4.6 and Lemma 4.5 the effect of left-Wieland drift on $f$ is that the move $M_3$ is applied to $\mathfrak{d}$ while the rest of $f$ is preserved.

Finally, the case when $o_r = \mathfrak{o}_{11}$ is checked. In that case $o_t$, $e_t$, $o_l$ and $e_l$ exist. Furthermore, $e_r = \mathfrak{e}_1$, $o_b = \mathfrak{o}_7$, $e_b = \mathfrak{e}_4$, $o_l = \mathfrak{o}_5$, $e_l = \mathfrak{e}_8$, $o_t = \mathfrak{o}_6$ and $e_t = \mathfrak{e}_4$. Therefore, $e'_r = \mathfrak{e}_{12}$, $e'_b = \mathfrak{e}_{10}$, $e'_l = \mathfrak{e}_1$ and $e'_t = \mathfrak{e}_9$. By Lemma 4.5 the effect of left-Wieland drift on $f$ is that the move $M_4$ is applied to $\mathfrak{d}$ while the rest of $f$ is preserved. $\qquad\square$

The proof of Proposition 4.3 for instable TFPLs $f$ of excess 2 that contain two drifters is split into the following three parts: (1) all drifters in $f$ are incident to vertices in $\mathcal{R}^N$;

(2) one drifter in $f$ is incident to a vertex in $\mathcal{R}^N$ and the other is not; (3) no drifter in $f$ is incident to a vertex in $\mathcal{R}^N$.

PROOF OF PROPOSITION 4.3(TWO DRIFTERS (1)). Let $f$ be a TFPL of excess 2 that contains two drifters. If in $f$ all drifters are incident to a vertex in $\mathcal{R}^N$ then for each drifter in $f$ the cells $o_l$ and $o_b$ do not exhibit a drifter and are not of the form $\mathfrak{o}_6$, $\mathfrak{o}_7$ or $\mathfrak{o}_{12}$. Therefore, by Lemma 4.6 and Lemma 4.5 the effect of WL on $f$ is that each drifter is replaced by a horizontal edge such that if a drifter is incident to $R_i$ in $f$ the respective horizontal edge in $\mathrm{WL}(f)$ is incident to $R_{i+1}$, while the rest of $f$ remains unchanged. $\square$

PROOF OF PROPOSITION 4.3(TWO DRIFTERS (2)). Let $f$ be a TFPL of excess 2 that contains two drifters $\mathfrak{d}$ and $\mathfrak{d}^*$ whereof $\mathfrak{d}$ is incident to a vertex $R_i$ in $\mathcal{R}^N$ and $\mathfrak{d}^*$ is not incident to a vertex in $\mathcal{R}^N$. Note that $f$ contains neither a cell of type $\mathfrak{o}_{11}$ nor of type $\mathfrak{e}_{11}$. That is because when adding the canonical orientation to $f$ such a cell would give rise to two local configurations that contribute to the excess which would imply that $f$ is of excess greater than 2. As a start, suppose that no vertex of $o_l$ and $o_b$ is incident to $\mathfrak{d}^*$. In that case $e_l'$ and $e_l$ coincide with the sole exception that in $e_l'$ there is no drifter and $e_b'$ and $e_b$ coincide with the sole exception that in $e_b'$ the two top vertices are adjacent whereas in $e_b$ they are not by Lemma 4.6. On the other hand, since $\mathfrak{d}^*$ is not incident to a vertex in $\mathcal{R}^N$ the cells $o_r^*$, $e_r^*$, $o_b^*$ and $e_b^*$ exist. Furthermore, no vertex of $o_r^*$, $e_r^*$, $o_b^*$ and $e_b^*$ is incident to $\mathfrak{d}$. If the cells $o_l^*$, $e_l^*$, $o_t^*$ and $e_t^*$ exist then also no vertex of these cells is incident to $\mathfrak{d}$. For those reasons, by analogous arguments as in the proof of Proposition 4.3(1) the effect of left-Wieland drift on $f$ is that $\mathfrak{d}$ is replaced by a horizontal edge incident to $R_{i+1}$ before a unique move of $\{M_1, M_2, M_3\}$ is applied to $\mathfrak{d}^*$. The rest of $f$ is preserved by left-Wieland drift.

Now, if the bottom right vertex of $o_b$ is incident to $\mathfrak{d}^*$, then $o_r^* \in \{\mathfrak{o}_8, \mathfrak{o}_9, \mathfrak{o}_{10}\}$. If $o_r^* = \mathfrak{o}_8$, then $e_r^* = \mathfrak{e}_5$. Furthermore, $o_l$, $o_b$, $o_l^*$ and $o_b^*$ do not contain a drifter and are not in $\{\mathfrak{o}_6, \mathfrak{o}_7, \mathfrak{o}_{12}\}$. Thus, the effect of left-Wieland drift is that $\mathfrak{d}$ is replaced by a horizontal edge incident to $R_{i+1}$ before the move $M_1$ is applied to $\mathfrak{d}^*$ while the rest of $f$ is preserved. If $o_r^* = \mathfrak{o}_9$, then $e_r^* = \mathfrak{e}_2$, $o_b^* = \mathfrak{o}_7$ and $e_b^* = \mathfrak{e}_4$. Additionally, $o_l$, $o_b$ and $o_l$ do not contain a drifter and are not in $\{\mathfrak{o}_6, \mathfrak{o}_7, \mathfrak{o}_{12}\}$. Therefore, the effect of left-Wieland drift is that $\mathfrak{d}$ is replaced by a horizontal edge incident to $R_{i+1}$ before the move $M_2$ is applied to $\mathfrak{d}^*$ while the rest of $f$ is preserved. Finally, if $o_r^* = \mathfrak{o}_{10}$, then $e_r^* = \mathfrak{e}_3$, $o_b = \mathfrak{o}_6$ and $e_b = \mathfrak{e}_7$. Furthermore, $o_l$, $o_l^*$ and $o_b^*$ do not contain a drifter and are not in $\{\mathfrak{o}_6, \mathfrak{o}_7, \mathfrak{o}_{12}\}$. For those reasons, the effect of left-Wieland drift is that $\mathfrak{d}$ is replaced by a horizontal edge incident to $R_{i+1}$ before the move $M_3$ is applied to $\mathfrak{d}^*$ while the rest of $f$ is preserved.

Next, if $o_l$ contains $\mathfrak{d}^*$, then $o_l = \mathfrak{o}_{10}$, $e_l = \mathfrak{e}_9$, $o_t^* = \mathfrak{o}_6$, $e_t^* = \mathfrak{e}_4$, $o_b = \mathfrak{o}_4$, $e_b = \mathfrak{e}_7$ and $o_b^* \notin \{\mathfrak{o}_6, \mathfrak{o}_7, \mathfrak{o}_{12}\}$. Therefore, $e_l' = \mathfrak{e}_7$, $e_t' = \mathfrak{e}_9$, $e_b' = \mathfrak{e}_4$ and by Lemma 4.6 the cells $e_b^{*\prime}$ and $e_b^*$ coincide with the sole exception that in $e_b^{*\prime}$ there is an edge between the two top vertices whereas in $e_b^*$ there is none. For those reasons, the effect of left-Wieland drift

on $f$ is that $\mathfrak{d}$ is replaced by a horizontal edge incident to $R_{i+1}$ before the move $M_3$ is applied to $\mathfrak{d}^*$ while the rest of $f$ is preserved.

Finally, if $o_b$ contains $\mathfrak{d}^*$, then $o_b \in \{\mathfrak{o}_8, \mathfrak{o}_9\}$. If $o_b = \mathfrak{o}_8$, then $e_b = \mathfrak{e}_3$. Furthermore, none of the cells $o_l$, $o_l^*$ and $o_b^*$ is in $\{\mathfrak{o}_6, \mathfrak{o}_7, \mathfrak{o}_{12}\}$. Thus, the effect of left-Wieland drift on $f$ is that $\mathfrak{d}$ is replaced by a horizontal edge incident to $R_{i+1}$ before the move $M_1$ is applied to $\mathfrak{d}^*$ while the rest of $f$ is preserved. On the other hand, if $o_b = \mathfrak{o}_9$, then $e_b = \mathfrak{e}_1$, $o_b^* = \mathfrak{o}_7$ and $e_b^* = \mathfrak{e}_4$. Additionally, $o_l$ and $o_l^*$ do not contain a drifter and are not in $\{\mathfrak{o}_6, \mathfrak{o}_7, \mathfrak{o}_{12}\}$. Therefore, the effect of left-Wieland drift on $f$ is that $\mathfrak{d}$ is replaced by a horizontal edge incident to $R_{i+1}$ before the move $M_2$ is applied to $\mathfrak{d}^*$ while the rest of $f$ is preserved. $\quad\square$

PROOF OF PROPOSITION 4.3(TWO DRIFTERS (3)). Let $f$ be a TFPL of excess 2 that contains two drifters whereof none is incident to a vertex in $\mathcal{R}^N$. In that case the cells $o_r$, $e_r$, $o_b$, $e_b$ and the cells $o_r^*$, $e_r^*$, $o_b^*$, $e_b^*$ exist. Furthermore, both $o_r$ and $o_r^*$ have to be in $\{\mathfrak{o}_8, \mathfrak{o}_9, \mathfrak{o}_{10}, \mathfrak{o}_{13}, \mathfrak{o}_{14}\}$. It is started with the case when no vertex of the cells $o_r$, $e_r$, $o_b$, $e_b$ is incident to $\mathfrak{d}^*$ and no vertex of the cells $o_r^*$, $e_r^*$, $o_b^*$, $e_b^*$ is incident to $\mathfrak{d}$. This implies that if the cells $o_l$, $e_l$, $o_t$ and $e_t$ exist then none of their vertices is incident to $\mathfrak{d}^*$ and if the cells $o_l^*$, $e_l^*$, $o_t^*$ and $e_t^*$ exist then none of their vertices is incident to $\mathfrak{d}$. Therefore, by the same arguments as in the proof of Proposition 4.3(1) the effect of left-Wieland drift on $f$ is that simultaneously to each of the two drifters $\mathfrak{d}$ and $\mathfrak{d}^*$ a unique move in $\{M_1, M_2, M_3\}$ is applied while the rest of $f$ is conserved. Since the moves can be performed simultaneously they can be performed in the order stated in Proposition 4.3(2).

It remains to study the case when a vertex of $o_r$, $e_r$, $o_b$ or $e_b$ is incident to $\mathfrak{d}^*$ or a vertex of $o_r^*$, $e_r^*$, $o_b^*$ or $e_b^*$ is incident to $\mathfrak{d}$. Hence, without loss of generality assume that a vertex of the cells $o_r$, $e_r$, $o_b$, $e_b$ that is not the top right vertex of $o_r$ is incident to the drifter $\mathfrak{d}^*$. Then $o_r$ does not equal $\mathfrak{o}_{14}$ and $o_r^*$ does not equal $\mathfrak{o}_{13}$.

As a start, the case when the bottom right vertex of $o_b$ is incident to $\mathfrak{d}^*$ is considered. In that case $\mathfrak{d}$ and $\mathfrak{d}^*$ have the same $x$-coordinate and $\mathfrak{d}$ has the larger $y$-coordinates than $\mathfrak{d}^*$. If the cells $o_t$, $e_t$, $o_l$ and $e_l$ exist then $o_t$ neither equals $\mathfrak{o}_7$ nor $\mathfrak{o}_{12}$. Furthermore, if $o_t = \mathfrak{o}_6$ then $e_t = \mathfrak{e}_4$, $o_r = \mathfrak{o}_{10}$ and $e_r = \mathfrak{e}_3$. Thus, $e_t' = \mathfrak{e}_9$ and $e_r' = \mathfrak{e}_7$. On the other hand, if $o_t$ does not equal $\mathfrak{o}_6$ then $e_t'$ and $e_t$ coincide with the sole exception that in $e_t'$ there is a horizontal edge between its two bottom vertices whereas in $e_t$ there is none by Lemma 4.6. Since neither $o_l$ nor $o_l^*$ equals $\mathfrak{o}_6$, $\mathfrak{o}_7$ or $\mathfrak{o}_{12}$ the cells $e_l'$ and $e_l$ (*resp.* $e_l^{*\prime}$ and $e_l^*$) coincide with the sole exception that in $e_l'$ (*resp.* $e_l^{*\prime}$) there is no drifter by Lemma 4.6. Finally, $o_b^*$ does neither equal $\mathfrak{o}_6$ nor $\mathfrak{o}_{12}$ and if it equals $\mathfrak{o}_7$ then $e_b^* = \mathfrak{e}_4$, $o_r^* = \mathfrak{o}_9$, $e_r^* = \mathfrak{e}_2$, $e_b^{*\prime} = \mathfrak{e}_{10}$ and $e_r^{*\prime} = \mathfrak{e}_3$. $\omega \to \omega^+$ By Lemma 4.5, it remains to study the cells $o_r$, $e_r$, $o_b$, $e_b$, $o_r^*$, $e_r^*$, $e_r'$, $e_b'$ and $e_r^{*\prime}$. A list of all possible configurations in the cells $o_r$, $e_r$, $o_b$, $e_b$, $o_r^*$, $e_r^*$, $e_r'$, $e_b'$ and $e_r^{*\prime}$ is given in Table 1.

In summary, left-Wieland drift has the following effect:

- The move $M_5$ is applied if $o_r = \mathfrak{o}_9$ and $o_r^* = \mathfrak{o}_{10}$.

| $o_r$ | $\mathfrak{o}_8$ | $\mathfrak{o}_8$ | $\mathfrak{o}_8$ | $\mathfrak{o}_8$ | $\mathfrak{o}_8$ | $\mathfrak{o}_9$ | $\mathfrak{o}_9$ | $\mathfrak{o}_9$ | $\mathfrak{o}_{10}$ | $\mathfrak{o}_{10}$ | $\mathfrak{o}_{10}$ | $\mathfrak{o}_{10}$ |
|---|---|---|---|---|---|---|---|---|---|---|---|---|
| $e_r$ | $\mathfrak{e}_5$ | $\mathfrak{e}_5$ | $\mathfrak{e}_5$ | $\mathfrak{e}_5$ | $\mathfrak{e}_5$ | $\mathfrak{e}_2$ | $\mathfrak{e}_2$ | $\mathfrak{e}_2$ | $\mathfrak{e}_3$ | $\mathfrak{e}_3$ | $\mathfrak{e}_3$ | $\mathfrak{e}_3$ |
| $o_r^*$ | $\mathfrak{o}_8$ | $\mathfrak{o}_8$ | $\mathfrak{o}_9$ | $\mathfrak{o}_9$ | $\mathfrak{o}_{10}$ | $\mathfrak{o}_8$ | $\mathfrak{o}_9$ | $\mathfrak{o}_{10}$ | $\mathfrak{o}_8$ | $\mathfrak{o}_8$ | $\mathfrak{o}_9$ | $\mathfrak{o}_{10}$ |
| $e_r^*$ | $\mathfrak{e}_5$ | $\mathfrak{e}_5$ | $\mathfrak{e}_2$ | $\mathfrak{e}_2$ | $\mathfrak{e}_3$ | $\mathfrak{e}_5$ | $\mathfrak{e}_2$ | $\mathfrak{e}_3$ | $\mathfrak{e}_5$ | $\mathfrak{e}_5$ | $\mathfrak{e}_2$ | $\mathfrak{e}_3$ |
| $o_b$ | $\mathfrak{o}_1$ | $\mathfrak{o}_4$ | $\mathfrak{o}_1$ | $\mathfrak{o}_4$ | $\mathfrak{o}_6$ | $\mathfrak{o}_7$ | $\mathfrak{o}_7$ | $\mathfrak{o}_{12}$ | $\mathfrak{o}_1$ | $\mathfrak{o}_4$ | $\mathfrak{o}_4$ | $\mathfrak{o}_6$ |
| $e_b$ | $\mathfrak{e}_1$ | $\mathfrak{e}_{12}$ | $\mathfrak{e}_1$ | $\mathfrak{e}_{12}$ | $\mathfrak{e}_7$ | $\mathfrak{e}_6$ | $\mathfrak{e}_6$ | $\mathfrak{e}_4$ | $\mathfrak{e}_1$ | $\mathfrak{e}_{12}$ | $\mathfrak{e}_{12}$ | $\mathfrak{e}_7$ |
| $e_r'$ | $\mathfrak{e}_8$ | $\mathfrak{e}_8$ | $\mathfrak{e}_8$ | $\mathfrak{e}_8$ | $\mathfrak{e}_8$ | $\mathfrak{e}_6$ | $\mathfrak{e}_6$ | $\mathfrak{e}_6$ | $\mathfrak{e}_7$ | $\mathfrak{e}_7$ | $\mathfrak{e}_7$ | $\mathfrak{e}_7$ |
| $e_r^{*\prime}$ | $\mathfrak{e}_8$ | $\mathfrak{e}_8$ | $\mathfrak{e}_6$ | $\mathfrak{e}_6$ | $\mathfrak{e}_7$ | $\mathfrak{e}_8$ | $\mathfrak{e}_6$ | $\mathfrak{e}_7$ | $\mathfrak{e}_8$ | $\mathfrak{e}_8$ | $\mathfrak{e}_6$ | $\mathfrak{e}_7$ |
| $e_b'$ | $\mathfrak{e}_{15}$ | $\mathfrak{e}_4$ | $\mathfrak{e}_{15}$ | $\mathfrak{e}_4$ | $\mathfrak{e}_9$ | $\mathfrak{e}_{10}$ | $\mathfrak{e}_{10}$ | $\mathfrak{e}_{11}$ | $\mathfrak{e}_{15}$ | $\mathfrak{e}_4$ | $\mathfrak{e}_4$ | $\mathfrak{e}_9$ |

TABLE 1. The cells $o_r, e_r, o_r^*, e_r^*, o_b$ and $e_b$ of $f$ and the cells $e_r', e_r^{*\prime}$ and $e_b'$ of WL($f$) in the case when $\mathfrak{d}^*$ is incident to the bottom right vertex of $o_b$ in $f$.

- The move $M_1/M_2$ is applied to $\mathfrak{d}^*$ before the move $M_2$ is applied to $\mathfrak{d}$ if $o_r = \mathfrak{o}_9$ and $o_r^* = \mathfrak{o}_8/\mathfrak{o}_9$.
- The move $M_1$ is applied to $\mathfrak{d}$ before the move $M_1/M_2/M_3$ is applied to $\mathfrak{d}^*$ if $o_r = \mathfrak{o}_8$ and $o_r^* = \mathfrak{o}_8/\mathfrak{o}_9/\mathfrak{o}_{10}$.
- The move $M_3$ is applied to $\mathfrak{d}$ before the move $M_1/M_2/M_3$ is applied to $\mathfrak{d}^*$ if $o_r = \mathfrak{o}_{10}$ and $o_r^* = \mathfrak{o}_8/\mathfrak{o}_9/\mathfrak{o}_{10}$.

In all cases the rest of $f$ is preserved by left-Wieland drift.

Next, the case when the drifter $\mathfrak{d}^*$ is contained in $e_r$ is studied. In that case the $x$-coordinate of $\mathfrak{d}^*$ is larger than the one of $\mathfrak{d}$. Note that $(o_r, e_r) \in \{(\mathfrak{o}_9, \mathfrak{e}_{10}), (\mathfrak{o}_{10}, \mathfrak{e}_9)\}$ since $f$ contains neither of the cells $\mathfrak{o}_{11}$ and $\mathfrak{e}_{11}$. Now, if $o_r = \mathfrak{o}_9$ then $o_b = \mathfrak{o}_7$, $e_b = \mathfrak{e}_4$, $o_t^* = \mathfrak{o}_4$, $e_t^* = \mathfrak{e}_6$ and $(o_r^*, e_r^*) \in \{(\mathfrak{o}_8, \mathfrak{e}_5), (\mathfrak{o}_9, \mathfrak{e}_2)\}$. Furthermore, if $o_r^* = \mathfrak{o}_9$ then $o_b^* = \mathfrak{o}_7$ and $e_b^* = \mathfrak{e}_4$. Thus, $e_r' = \mathfrak{e}_6$, $e_b' = \mathfrak{e}_{10}$, $e_t^{*\prime} = \mathfrak{e}_4$ and if $o_r^* = \mathfrak{o}_9$ then $e_r^{*\prime} = \mathfrak{e}_6$ and $e_b^{*\prime} = \mathfrak{e}_{10}$. On the other hand, if $o_r = \mathfrak{o}_{10}$ then $o_t = \mathfrak{o}_6$, $e_t = \mathfrak{e}_4$, $o_b^* = \mathfrak{o}_4$, $e_b^* = \mathfrak{e}_7$ and $(o_r^*, e_r^*) \in \{(\mathfrak{o}_8, \mathfrak{e}_5), (\mathfrak{o}_{10}, \mathfrak{e}_3)\}$. Furthermore, if $o_r^* = \mathfrak{o}_{10}$ then $o_t^* = \mathfrak{o}_6$ and $e_t^* = \mathfrak{e}_4$. Thus, $e_r' = \mathfrak{e}_7$, $e_t' = \mathfrak{e}_9$ and $e_b^{*\prime} = \mathfrak{e}_4$ and if $o_r^* = \mathfrak{o}_{10}$ then $e_r^{*\prime} = \mathfrak{e}_7$ and $e_t^{*\prime} = \mathfrak{e}_9$. By Lemma 4.5 and Lemma 4.6 the effect of left-Wieland drift is the following:

- The move $M_1/M_2$ is applied to $\mathfrak{d}^*$ before the move $M_2$ is applied to $\mathfrak{d}$ if $o_r = \mathfrak{o}_9$ and $o_r^* = \mathfrak{o}_8/\mathfrak{o}_9$.
- The move $M_1/M_3$ is applied to $\mathfrak{d}^*$ before the move $M_3$ is applied to $\mathfrak{d}$ if $o_r = \mathfrak{o}_{10}$ and $o_r^* = \mathfrak{o}_8/\mathfrak{o}_{10}$.

In both cases the rest of $f$ is preserved by left-Wieland drift.

Next, the case when $\mathfrak{d}^*$ is contained in $e_b$ is regarded. In that case the $x$-coordinate of $\mathfrak{d}^*$ is larger than the one of $\mathfrak{d}$. The cells $o_l$ and $o_b$ are both not contained in $\{\mathfrak{o}_6, \mathfrak{o}_7, \mathfrak{o}_{12}\}$. For instance, it is not possible that $o_b$ equals $\mathfrak{o}_7$ because then $e_b$ would have to equal $e_{15}$ or the bottom right vertex of $o_b$ would be incident to a drifter. As a start, if $o_t$ exists then it cannot be in $\{\mathfrak{o}_7, \mathfrak{o}_{12}\}$. Furthermore, if $o_t = \mathfrak{o}_6$ then $e_t = \mathfrak{e}_4$, $o_r = \mathfrak{o}_{10}$, $e_r = \mathfrak{e}_3$, $e_t' = \mathfrak{e}_9$ and $e_r' = \mathfrak{e}_7$. On the other hand, $o_b^*$ cannot be in $\{\mathfrak{o}_6, \mathfrak{o}_{12}\}$. Furthermore, if $o_b^* = \mathfrak{o}_7$ then

$e_b^* = \mathfrak{e}_4$, $o_r^* = \mathfrak{o}_9$, $e_r^* = \mathfrak{e}_2$, $e_b^{*'} = \mathfrak{e}_{10}$ and $e_r^{*'} = \mathfrak{e}_6$. To determine the effect of left-Wieland drift on $f$ it remains to study the cells $o_r^*$, $e_r^*$, $o_r$, $e_r$, $e_r^{*'}$ and $e_r'$. In Table 2 all possible configurations in these cells are listed.

| $o_r^*$ | $\mathfrak{o}_8$ | $\mathfrak{o}_8$ | $\mathfrak{o}_9$ | $\mathfrak{o}_9$ | $\mathfrak{o}_{10}$ |
|---|---|---|---|---|---|
| $e_r^*$ | $\mathfrak{e}_5$ | $\mathfrak{e}_5$ | $\mathfrak{e}_2$ | $\mathfrak{e}_2$ | $\mathfrak{e}_3$ |
| $o_r$ | $\mathfrak{o}_8$ | $\mathfrak{o}_{10}$ | $\mathfrak{o}_8$ | $\mathfrak{o}_{10}$ | $\mathfrak{o}_{13}$ |
| $e_r$ | $\mathfrak{e}_2$ | $\mathfrak{e}_1$ | $\mathfrak{e}_2$ | $\mathfrak{e}_1$ | $\mathfrak{e}_4$ |
| $e_r^{*'}$ | $\mathfrak{e}_8$ | $\mathfrak{e}_8$ | $\mathfrak{e}_6$ | $\mathfrak{e}_6$ | $\mathfrak{e}_7$ |
| $e_r'$ | $\mathfrak{e}_8$ | $\mathfrak{e}_7$ | $\mathfrak{e}_8$ | $\mathfrak{e}_7$ | $\mathfrak{e}_{14}$ |

TABLE 2. The cells $o_r^*$, $e_r^*$, $o_r$ and $e_r$ of $f$ and the cells $e_r^{*'}$ and $e_r'$ of WL($f$) in the case when $\mathfrak{d}^*$ is contained in $e_b$.

In summary, the effect of left-Wieland drift on $f$ is the following:
- The move $M_1$ is applied to $\mathfrak{d}^*$ before the move $M_1/M_3$ is applied to $\mathfrak{d}$ if $o_r^* = \mathfrak{o}_8$ and $o_r = \mathfrak{o}_8/\mathfrak{o}_{10}$.
- The move $M_2$ is applied to $\mathfrak{d}^*$ before the move $M_1/M_3$ is applied to $\mathfrak{d}$ if $o_r^* = \mathfrak{o}_9$ and $o_r = \mathfrak{o}_8/\mathfrak{o}_{10}$.
- The move $M_3$ is applied to $\mathfrak{d}^*$ before it also is applied to $\mathfrak{d}$ if $o_r^* = \mathfrak{o}_{10}$ and $o_r = \mathfrak{o}_{13}$.

In all cases the rest of $f$ is preserved by left-Wieland drift.

The last case that is to be considered is the case when $\mathfrak{d}^*$ is contained in $o_b$. In that case the $x$-coordinate of $\mathfrak{d}$ is larger than the one of $\mathfrak{d}^*$. Furthermore, the cells $o_l$ and $o_l^*$ are not contained in $\{\mathfrak{o}_6, \mathfrak{o}_7, \mathfrak{o}_12\}$, if $o_t$ exists then it cannot be in $\{\mathfrak{o}_7, \mathfrak{o}_{12}\}$ and $o_b^*$ cannot be in $\{\mathfrak{o}_6, \mathfrak{o}_{12}\}$. On the other hand, if $o_t = \mathfrak{o}_6$ then $e_t = \mathfrak{e}_4$, $o_r = \mathfrak{o}_{10}$, $e_r = \mathfrak{e}_3$, $e_t' = \mathfrak{e}_9$ and $e_r' = \mathfrak{e}_7$ and if $o_b^* = \mathfrak{o}_7$ then $e_b^* = \mathfrak{e}_4$, $o_r^* = \mathfrak{o}_9$, $e_r^* = \mathfrak{e}_2$, $e_b^{*'} = \mathfrak{e}_{10}$ and $e_r^{*'} = \mathfrak{e}_6$. To determine the effect of left-Wieland drift on $f$ it remains to study the cells $o_r^*$, $e_r^*$, $o_r$, $e_r$, $e_r^{*'}$ and $e_r'$. In Table 3 all possible configurations in these cells are listed.

| $o_r$ | $\mathfrak{o}_8$ | $\mathfrak{o}_8$ | $\mathfrak{o}_9$ | $\mathfrak{o}_{10}$ | $\mathfrak{o}_{10}$ |
|---|---|---|---|---|---|
| $e_r$ | $\mathfrak{e}_5$ | $\mathfrak{e}_5$ | $\mathfrak{e}_2$ | $\mathfrak{e}_3$ | $\mathfrak{e}_3$ |
| $o_b$ | $\mathfrak{o}_8$ | $\mathfrak{o}_9$ | $\mathfrak{o}_{14}$ | $\mathfrak{o}_8$ | $\mathfrak{o}_9$ |
| $e_b$ | $\mathfrak{e}_3$ | $\mathfrak{e}_1$ | $\mathfrak{e}_4$ | $\mathfrak{e}_3$ | $\mathfrak{e}_1$ |
| $e_r'$ | $\mathfrak{e}_8$ | $\mathfrak{e}_8$ | $\mathfrak{e}_6$ | $\mathfrak{e}_7$ | $\mathfrak{e}_7$ |
| $e_b'$ | $\mathfrak{e}_8$ | $\mathfrak{e}_6$ | $\mathfrak{e}_3$ | $\mathfrak{e}_8$ | $\mathfrak{e}_6$ |

TABLE 3. The cells $o_r$, $e_r$, $o_b$ and $e_b$ of $f$ and the cells $e_r'$ and $e_b'$ of WL($f$) in the case when $\mathfrak{d}^*$ is contained in $o_b$.

By Lemma 4.5 and Lemma 4.6 the effect of left-Wieland drift on $f$ is the following:
- The move $M_1$ is applied to $\mathfrak{d}$ before the move $M_1/M_2$ is applied to $\mathfrak{d}^*$ if $o_r = \mathfrak{o}_8$ and $o_b = \mathfrak{o}_8/\mathfrak{o}_9$.

60

- The move $M_2$ is first applied to $\mathfrak{d}$ and then to $\mathfrak{d}^*$ if $o_r = \mathfrak{o}_9$ and $o_b = \mathfrak{o}_{14}$.
- The move $M_3$ is applied to $\mathfrak{d}$ before the move $M_1/M_2$ is applied to $\mathfrak{d}^*$ if $o_r = \mathfrak{o}_{10}$ and $o_b = \mathfrak{o}_8/\mathfrak{o}_9$.

$\square$

The description of the effect of right-Wieland drift on an instable TFPL of excess at most 2 follows from the description of the effect of left-Wieland drift on an instable TFPL of excess at most 2 by vertical symmetry.

PROPOSITION 4.7. *Let $f$ be an instable TFPL with boundary $(u, v; w)$ such that* $\mathrm{exc}(u, v; w) \leq 2$. *Furthermore, let $v^-$ be a word so that $v^- \xrightarrow{\mathrm{v}} v$. Then the image of $f$ under right-Wieland drift with respect to $v^-$ is determined as follows:*

(1) *if $L_i$ in $\mathcal{L}^N$ is incident to a drifter delete that drifter and add a horizontal edge incident to $L_{i-1}$ for $i = 2, 3, \ldots, N$; denote the so-obtained TFPL by $f'$;*

(2) *perform $M_4^{-1}$ or $M_5^{-1}$ if possible; otherwise, run through the columns of $G^N$ from left to right, that is, for $j = 1, 2, \ldots, 2N + 1$:*

(3) *if there is precisely one drifter in the $j$-th column of $G^N$, apply $M_1^{-1}$, $M_2^{-1}$ or $M_3^{-1}$ to it;*

(4) *if there are two drifters in the $j$-th column of $G^N$, apply $M_1^{-1}$, $M_2^{-1}$ or $M_3^{-1}$ to each of the drifters in the following order: if the even cell that contains the lower drifter is not of the form $\mathfrak{o}_{10}$ (see Figure 3.6) move the lower drifter first; otherwise, move the upper drifter first;*

(5) *run through the occurrences of zero in $v^-$: let $\{i_1 < \cdots < i_{N_0}\} = \{i : v_i^- = 0\}$. If $v_{i_j+1}$ is the $j$-th zero in $v$ delete the horizontal edge incident to $R_{i_j+1}$ and add a vertical edge incident to $R_{i_j}$ for $j = 1, 2, \ldots, N_0$.*

## 4.2. The path of a drifter under Wieland drift for TFPLs of excess $2$

The focus of this section is on studying how many iterations of left- (*resp.* right-) Wieland drift are needed until a drifter in an instable TFPL of excess 2 is incident to a vertex in $\mathcal{R}^N$ (*resp.* $\mathcal{L}^N$). For this purpose, it is necessary to specify which drifter in the image of a TFPL under left- (*resp.* right-) Wieland drift is assigned to which drifter in the initial TFPL. To begin with, in both the preimage and the image of each of the moves $M_1$, $M_2$ and $M_3$ (*resp.* $M_1^{-1}$, $M_2^{-1}$ and $M_3^{-1}$) there is precisely one drifter. Thus, from now on, the drifter in the image is assigned to the drifter in the preimage for each of these moves.

In contrast to the moves $M_1$, $M_2$ and $M_3$ (*resp.* $M_1^{-1}$, $M_2^{-1}$ and $M_3^{-1}$) the preimage and the image of both $M_4$ and $M_5$ (*resp.* $M_4^{-1}$ and $M_5^{-1}$) do not exhibit the same number of drifters. Hence, fix a drifter in the image of $M_4$ (*resp.* $M_5^{-1}$) that is from now on assigned to the drifter in the preimage of $M_4$ (*resp.* $M_5^{-1}$). Reversely, if to a drifter the move $M_5$ (*resp.* $M_4^{-1}$) is applied then the drifter in the image of the move $M_5$ (*resp.*

$M_4^{-1}$) is assigned to this drifter. Figure 4.5 displays an example for the case when the upper drifter in the image of the move $M_4$ is assigned to the drifter in the preimage of the move $M_4$.
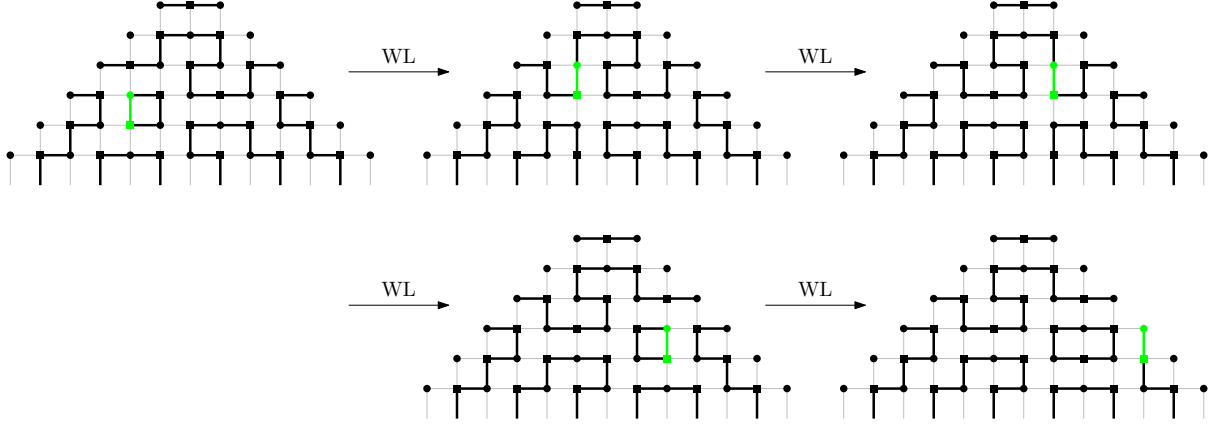


FIGURE 4.5. A TFPL of excess 2 and its instable images under left-Wieland drift. In each of the images the drifter that is assigned to the drifter in the initial TFPL is indicated in green if, say, the upper drifter in the image of the move $M_4$ is assigned to the drifter in the preimage of the move $M_4$.

Now, let $f$ be an instable TFPL of excess 2 and $\mathfrak{d}_0$ a drifter in $f$. Furthermore, denote with $\mathfrak{d}(\ell)$ (*resp.* $\mathfrak{d}(-r)$) the drifter in $\mathrm{WL}^\ell(f)$ (*resp.* $\mathrm{WR}^r(f)$) that is assigned to $\mathfrak{d}_0$ and with $L_f(\mathfrak{d})$ (*resp.* $R_f(\mathfrak{d})$) the unique non-negative integer such that $\mathfrak{d}(L_f(\mathfrak{d}))$ (*resp.* $\mathfrak{d}(R_f(\mathfrak{d}))$) is incident to a vertex in $\mathcal{R}^N$ (*resp.* $\mathcal{L}^N$). (The latter exist due to Proposition 4.3 *resp.* Proposition 4.7.) Thus, $\mathfrak{d}$ can be understood as a map on $[-R_f(\mathfrak{d}), L_f(\mathfrak{d})]$ that assigns to $\ell \in [0; L_f(\mathfrak{d})]$ a drifter in $\mathrm{WL}^\ell(f)$ and to $-r \in [-R_f(\mathfrak{d}); -1]$ a drifter in $\mathrm{WR}^r(f)$. (Note that $\mathfrak{d}(0) = \mathfrak{d}_0$.)

DEFINITION 4.8 ($\mathrm{Path}_f(\mathfrak{d}), \mathrm{Left}_f(\mathfrak{d}), \mathrm{Right}_f(\mathfrak{d}), \mathrm{HeightL}_f(\mathfrak{d}), \mathrm{HeightR}_f(\mathfrak{d})$). *Define the* ***path*** *of* $\mathfrak{d}$ *as the sequence*

$$\mathrm{Path}_f(\mathfrak{d}) = \left( \mathrm{WR}^{R_f(\mathfrak{d})}(f), \ldots, \mathrm{WR}(f), f, \mathrm{WL}(f), \ldots, \mathrm{WL}^{L_f(\mathfrak{d})}(f) \right).$$

*Furthermore, set* $\mathrm{Left}_f(\mathfrak{d}) = \mathrm{WL}^{L_f(\mathfrak{d})}(f)$ *and* $\mathrm{WR}^{R_f(\mathfrak{d})}(f) = \mathrm{Right}_f(\mathfrak{d})$. *Finally, set* $\mathrm{HeightL}_f(\mathfrak{d})$ *the positive integer* $h$ *such that* $\mathfrak{d}(L_f(\mathfrak{d}))$ *is incident to* $R_{N-h}$ *in* $\mathrm{Left}_f(\mathfrak{d})$ *and* $\mathrm{HeigthR}(\mathfrak{d})$ *the positive integer* $h'$ *such that* $\mathfrak{d}(R_f(\mathfrak{d}))$ *is incident to* $L_{h'+1}$ *in* $\mathrm{Right}_f(\mathfrak{d})$.

Observe that $|\mathrm{Path}_f(\mathfrak{d})| = L_f(\mathfrak{d}) + R_f(\mathfrak{d}) + 1$. In Figure 4.2 an example for the path of a drifter is displayed. Now, for $i = 1, 2, 3, 4, 5$ set

$$\#M_i(\mathfrak{d}) = |\{0 \le r < R_f(\mathfrak{d}) : \text{ by WR the move } M_i^{-1} \text{ is applied to } \mathfrak{d}(r) \text{ in } \mathrm{WR}^r(f)\}|$$
$$+ |\{0 \le \ell < L_f(\mathfrak{d}) : \text{ by WL the move } M_i \text{ is applied to } \mathfrak{d}(\ell) \text{ in } \mathrm{WL}^\ell(f)\}|.$$

Thus, $|\mathrm{Path}_f(\mathfrak{d})| = \#M_1(\mathfrak{d}) + \#M_2(\mathfrak{d}) + \#M_3(\mathfrak{d}) + \#M_4(\mathfrak{d}) + \#M_5(\mathfrak{d}) + 1$ and in summary

$$(4.5) \qquad L_f(\mathfrak{d}) + R_f(\mathfrak{d}) = \sum_{i=1}^{5} \#M_i(\mathfrak{d}).$$

DEFINITION 4.9 $(R_i(u^{R_f(\mathfrak{d})}), L_i(v^{L_f(\mathfrak{d})}))$. *Let $u^{R_f(\mathfrak{d})}$ be the left boundary of $\mathrm{WR}^{R_f(\mathfrak{d})}(f)$ and $v^{L_f(\mathfrak{d})}$ the right boundary of $\mathrm{WL}^{L_f(\mathfrak{d})}(f)$. Then $R_i(u^{R_f(\mathfrak{d})})$ denotes the number of occurrences of $i$ among the last $(N - 1 - \mathrm{HeightR}_f(\mathfrak{d}))$ letters of $u^{R_f(\mathfrak{d})}$ and $L_i(v^{L_f(\mathfrak{d})})$ denotes the number of occurrences of $i$ among the first $(N - 1 - \mathrm{HeightL}_f(\mathfrak{d}))$ letters of $v^{L_f(\mathfrak{d})}$ for $i = 0, 1$.*

PROPOSITION 4.10. *Let $u^{R_f(\mathfrak{d})}$ be the left boundary of $\mathrm{WR}^{R_f(\mathfrak{d})}(f)$ and $v^{L_f(\mathfrak{d})}$ the right boundary of $\mathrm{WL}^{L_f(\mathfrak{d})}(f)$. Then*

$$(4.6) \qquad \sum_{i=1}^{5} \#M_i(\mathfrak{d}) = R_1(u^{R_f(\mathfrak{d})}) + L_0(v^{L_f(\mathfrak{d})}) + 1.$$

COROLLARY 4.11. *Let $u^{R_f(\mathfrak{d})}$ be the left boundary of $\mathrm{WR}^{R_f(\mathfrak{d})}(f)$ and $v^{L_f(\mathfrak{d})}$ the right boundary of $\mathrm{WL}^{L_f(\mathfrak{d})}(f)$. Then*

$$(4.7) \qquad L_f(\mathfrak{d}) + R_f(\mathfrak{d}) = R_1(u^{R_f(\mathfrak{d})}) + L_0(v^{L_f(\mathfrak{d})}) + 1.$$
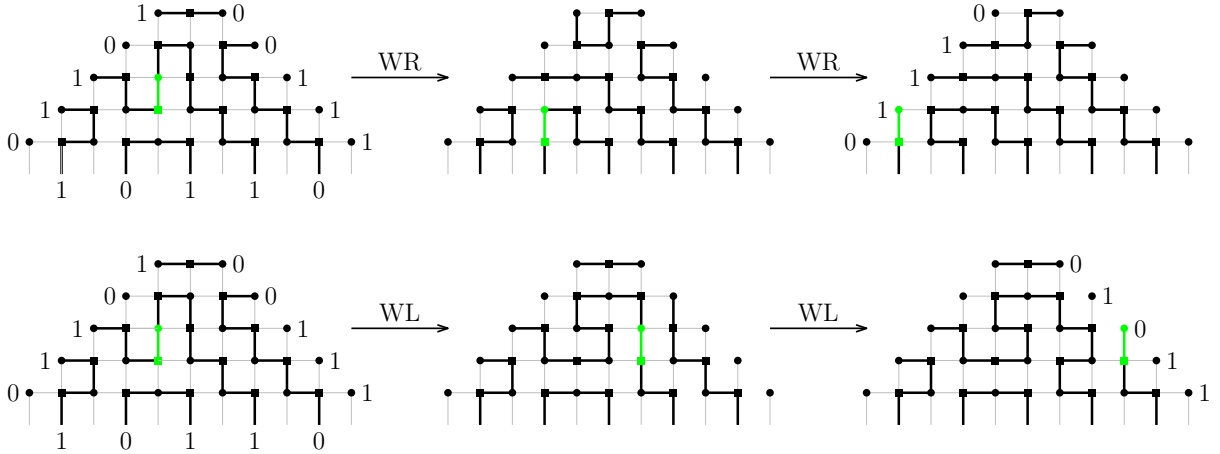


FIGURE 4.6. A TFPL with boundary $(01101, 00111; 10110)$ and the path of the drifter that is indicated in green.

The proof of Proposition 4.10 is the objective of the rest of this section. It requires to consider TFPLs of excess 2 together with the canonical orientation of their edges. In doing so, the moves by which the effect of Wieland drift is described in Proposition 4.3 translate into the moves depicted in Figure 4.7. It follows from Theorem 2.12 that the move $M_1$ has the four oriented counterparts $\overrightarrow{M}_{1,1}$, $\overrightarrow{M}_{1,2}$, $\overrightarrow{M}_{1,3}$ and $\overrightarrow{M}_{1,4}$, the move $M_2$ the three oriented counterparts $\overrightarrow{M}_{2,1}$, $\overrightarrow{M}_{2,2}$, $\overrightarrow{M}_{2,3}$ and the move $M_3$ the three oriented

counterparts $\overrightarrow{M}_{3,1}$, $\overrightarrow{M}_{3,2}$ and $\overrightarrow{M}_{3,3}$. Furthermore, both $M_4$ and $M_5$ have only one oriented counterpart, namely $\overrightarrow{M}_4$ and $\overrightarrow{M}_5$ respectively.

REMARK 4.12. The moves $\overrightarrow{M}_{1,1}$, $\overrightarrow{M}_{1,2}$, $\overrightarrow{M}_{1,3}$, $\overrightarrow{M}_{1,4}$, $\overrightarrow{M}_{2,1}$ and $\overrightarrow{M}_{3,1}$ coincide with the moves $BB$, $BR$, $RR$, $RB$, $B$ and $R$ respectively invented in [**11**] for oriented TFPLs of excess 1.
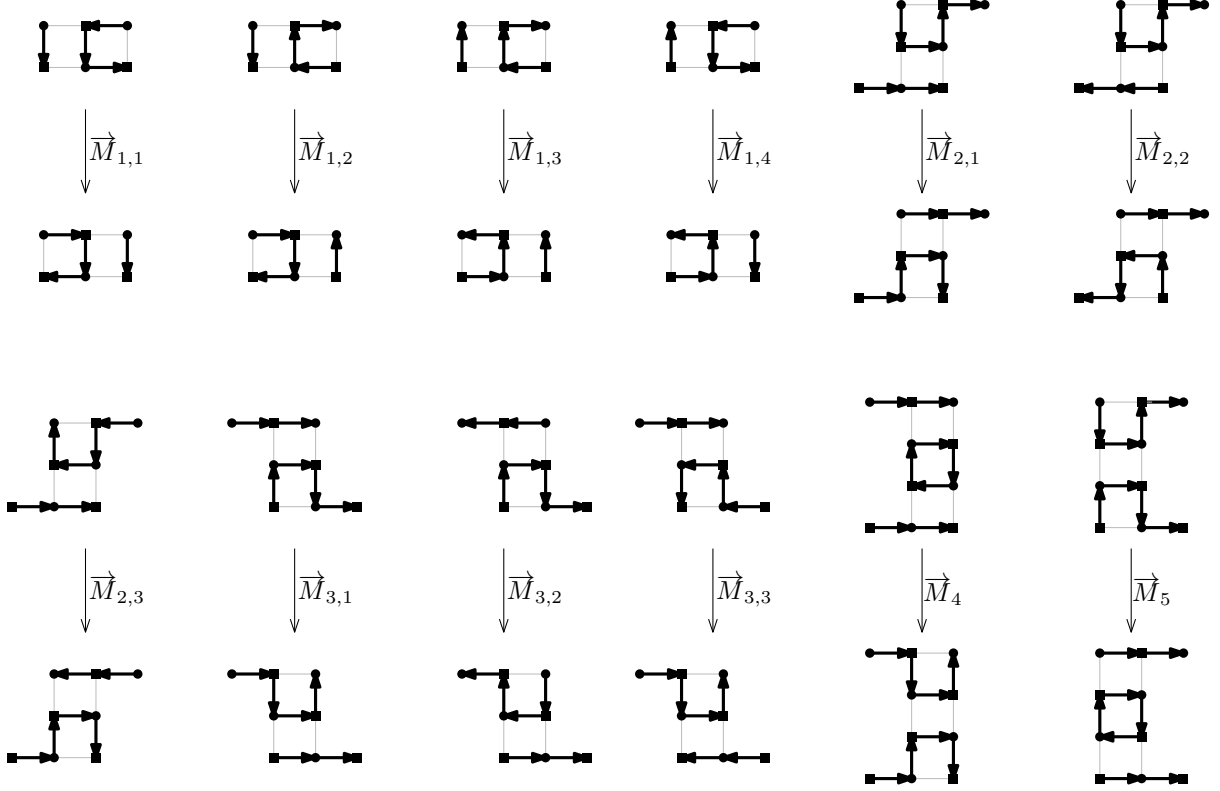


FIGURE 4.7. The moves describing the effect of Wieland drift on TFPLs of excess 2 that are equipped with the canonical orientation.

The following lemmas are immediate consequences of Proposition 4.3 and Proposition 4.7. They describe the effect of left- and right-Wieland drift respectively on $\overrightarrow{f}$, that is, $f$ together with its canonical orientation, in terms of the moves in Figure 4.7.

LEMMA 4.13. *If not all drifters in $f$ are incident to vertices in $\mathcal{R}^N$, the effect of left-Wieland drift on $f$ translates into the following effect on $\overrightarrow{f}$:*

(1) *If in $\overrightarrow{f}$ there is precisely one drifter then by left-Wieland drift a unique move in $\{\overrightarrow{M}_{1,1}, \overrightarrow{M}_{1,2}, \overrightarrow{M}_{1,3}, \overrightarrow{M}_{1,4}, \overrightarrow{M}_{2,1}, \overrightarrow{M}_{2,2}, \overrightarrow{M}_{2,3}, \overrightarrow{M}_{3,1}, \overrightarrow{M}_{3,2}, \overrightarrow{M}_{3,3}, \overrightarrow{M}_4\}$ is performed while the rest of $\overrightarrow{f}$ remains unchanged.*

(2) *If in $\overrightarrow{f}$ there are two drifters and none of those drifters is incident to a vertex in $\mathcal{R}^N$ then by left-Wieland drift either $\overrightarrow{M}_5$ is performed or to each drifter a unique move in $\{\overrightarrow{M}_{1,1}, \overrightarrow{M}_{1,2}, \overrightarrow{M}_{1,3}, \overrightarrow{M}_{1,4}, \overrightarrow{M}_{2,1}, \overrightarrow{M}_{3,1}\}$ is applied in the same order as in Proposition 4.3. The rest of $\overrightarrow{f}$ remains unchanged.*

(3) If in $\overrightarrow{f}$ there are two drifters whereof one is incident to a vertex in $\mathcal{R}^N$ then by left-Wieland drift the drifter incident to a vertex $R_i$ in $\mathcal{R}^N$ is replaced by a horizontal edge incident to $R_{i+1}$ before to the remaining drifter a unique move in $\{\overrightarrow{M}_{1,1}, \overrightarrow{M}_{1,2}, \overrightarrow{M}_{1,3}, \overrightarrow{M}_{1,4}, \overrightarrow{M}_{2,1}, \overrightarrow{M}_{3,1}\}$ is applied. The rest of $\overrightarrow{f}$ remains unchanged by left-Wieland drift.

Recall that when in $f$ all drifters are incident to vertices in $\mathcal{R}^N$ then by left-Wieland drift these drifters are simply replaced by horizontal edges.

LEMMA 4.14. *If not all drifters in $f$ are incident to a vertex in $\mathcal{L}^N$, the effect of right-Wieland drift on $f$ translates into the following effect on $\overrightarrow{f}$ :*

(1) *If in $\overrightarrow{f}$ there is precisely one drifter then by right-Wieland drift $\overrightarrow{M}_{1,1}^{-1}$, $\overrightarrow{M}_{1,2}^{-1}$, $\overrightarrow{M}_{1,3}^{-1}$, $\overrightarrow{M}_{1,4}^{-1}$, $\overrightarrow{M}_{2,1}^{-1}$, $\overrightarrow{M}_{2,2}^{-1}$, $\overrightarrow{M}_{2,3}^{-1}$, $\overrightarrow{M}_{3,1}^{-1}$, $\overrightarrow{M}_{3,2}^{-1}$, $\overrightarrow{M}_{3,3}^{-1}$ or $\overrightarrow{M}_5^{-1}$ is performed while the rest of $\overrightarrow{f}$ remains unchanged.*

(2) *If in $\overrightarrow{f}$ there are two drifters and none of those drifters is incident to a vertex in $\mathcal{L}^N$ then by right-Wieland drift either $\overrightarrow{M}_4^{-1}$ is performed or to each drifter in $\overrightarrow{f}$ a unique move in $\{\overrightarrow{M}_{1,1}^{-1}, \overrightarrow{M}_{1,2}^{-1}, \overrightarrow{M}_{1,3}^{-1}, \overrightarrow{M}_{1,4}^{-1}, \overrightarrow{M}_{2,1}^{-1}, \overrightarrow{M}_{3,1}^{-1}\}$ is applied in the same order as in Proposition 4.7. The rest of $\overrightarrow{f}$ remains unchanged.*

(3) *If in $\overrightarrow{f}$ there are two drifters whereof one is incident to a vertex in $\mathcal{L}^N$ then by right-Wieland drift the drifter incident to a vertex $L_j$ in $\mathcal{L}^N$ is replaced by a horizontal edge incident to $L_{j-1}$ before a unique move in $\{\overrightarrow{M}_{1,1}^{-1}, \overrightarrow{M}_{1,2}^{-1}, \overrightarrow{M}_{1,3}^{-1}, \overrightarrow{M}_{1,4}^{-1}, \overrightarrow{M}_{2,1}^{-1}, \overrightarrow{M}_{3,1}^{-1}\}$ is applied to the remaining drifter. The rest of $\overrightarrow{f}$ remains unchanged by right-Wieland drift.*

In the following, set

$$\#\overrightarrow{M}_{i,j}(\mathfrak{o}) = |\{0 \le r < R_f(\mathfrak{o}) : \text{ by WR the move } \overrightarrow{M}_{i,j}^{-1} \text{ is applied to } \mathfrak{o}(r) \text{ in } \text{WR}^r(\overrightarrow{f})\}|$$
$$+ |\{0 \le \ell < L_f(\mathfrak{o}) : \text{ by WL the move } \overrightarrow{M}_{i,j} \text{ is applied to } \mathfrak{o}(\ell) \text{ in } \text{WL}^\ell(\overrightarrow{f})\}|.$$

for $(i,j) \in \{(1,1),(1,2),(1,3),(1,4),(2,1),(2,2),(2,3),(3,1),(3,2),(3,3)\}$. For the moves $\overrightarrow{M}_4^{-1}$ and $\overrightarrow{M}_5$ it needs to be distinguished which of the two drifters in the respective image is chosen. Hence, for $i = 4, 5$ set

$$\#\overrightarrow{M}_i(\mathfrak{o}) = |\{0 \le r < R_f(\mathfrak{o}) : \text{ by WR the move } \overrightarrow{M}_i^{-1} \text{ is applied to } \mathfrak{o}(r) \text{ in } \text{WR}^r(\overrightarrow{f})\}|$$
$$+ |\{0 \le \ell < L_f(\mathfrak{o}) : \text{ by WL the move } \overrightarrow{M}_i \text{ is applied to } \mathfrak{o}(\ell) \text{ in } \text{WL}^\ell(\overrightarrow{f})\}|.$$

and indicate by a $t$ or $b$ whether in the respective image the top or the bottom drifter is associated with $\mathfrak{o}$ in $f$. In that way, one obtains the notations $\#\overrightarrow{M}_i^b(\mathfrak{o})$ and $\#\overrightarrow{M}_i^t(\mathfrak{o})$ respectively for $i = 4, 5$.

LEMMA 4.15. *Let $u^{R_f(\mathfrak{o})}$ be the left boundary of $\text{WR}^{R_f(\mathfrak{o})}(f)$ and $v^{L_f(\mathfrak{o})}$ the right boundary of $\text{WL}^{L_f(\mathfrak{o})}(f)$. Then we have:*

(1) $\sum_{i=1}^{4} \#\overrightarrow{M}_{1,i}(\mathfrak{o}) + \sum_{j=1}^{3} \#\overrightarrow{M}_{3,j}(\mathfrak{o}) + \#\overrightarrow{M}_4^t(\mathfrak{o}) + \#\overrightarrow{M}_5^b(\mathfrak{o}) = N - \mathrm{HeightR}_f(\mathfrak{o})$,

(2) $\sum_{i=1}^{4} \#\overrightarrow{M}_{1,i}(\mathfrak{o}) + \sum_{j=1}^{3} \#\overrightarrow{M}_{2,j}(\mathfrak{o}) + \#\overrightarrow{M}_4^b(\mathfrak{o}) + \#\overrightarrow{M}_5^t(\mathfrak{o}) = N - \mathrm{HeightL}_f(\mathfrak{o})$,

(3) $\#\overrightarrow{M}_{1,1}(\mathfrak{o}) + \#\overrightarrow{M}_{1,4}(\mathfrak{o}) + \#\overrightarrow{M}_{2,3}(\mathfrak{o}) - \#\overrightarrow{M}_{3,3}(\mathfrak{o}) + \#\overrightarrow{M}_4^b(\mathfrak{o}) = L_1(v^{L_f(\mathfrak{o})})$,

(4) $\#\overrightarrow{M}_{1,2}(\mathfrak{o}) + \#\overrightarrow{M}_{1,3}(\mathfrak{o}) - \#\overrightarrow{M}_{2,3}(\mathfrak{o}) + \#\overrightarrow{M}_{3,3}(\mathfrak{o}) - \#\overrightarrow{M}_4^b(\mathfrak{o}) = R_0(u^{R_f(\mathfrak{o})}) + 1$.

The identities in Lemma 4.15 generalise the identities stated in Proposition 6.11 and Proposition 6.12 in [**11**] for $\#BB$, $\#BR$, $\#RR$, $\#RB$, $\#B$ and $\#R$. The proof of Lemma 4.15 is given in terms of blue-red path tangles and uses analogous arguments as the proofs of Proposition 6.11 and Proposition 6.12 in [**11**].
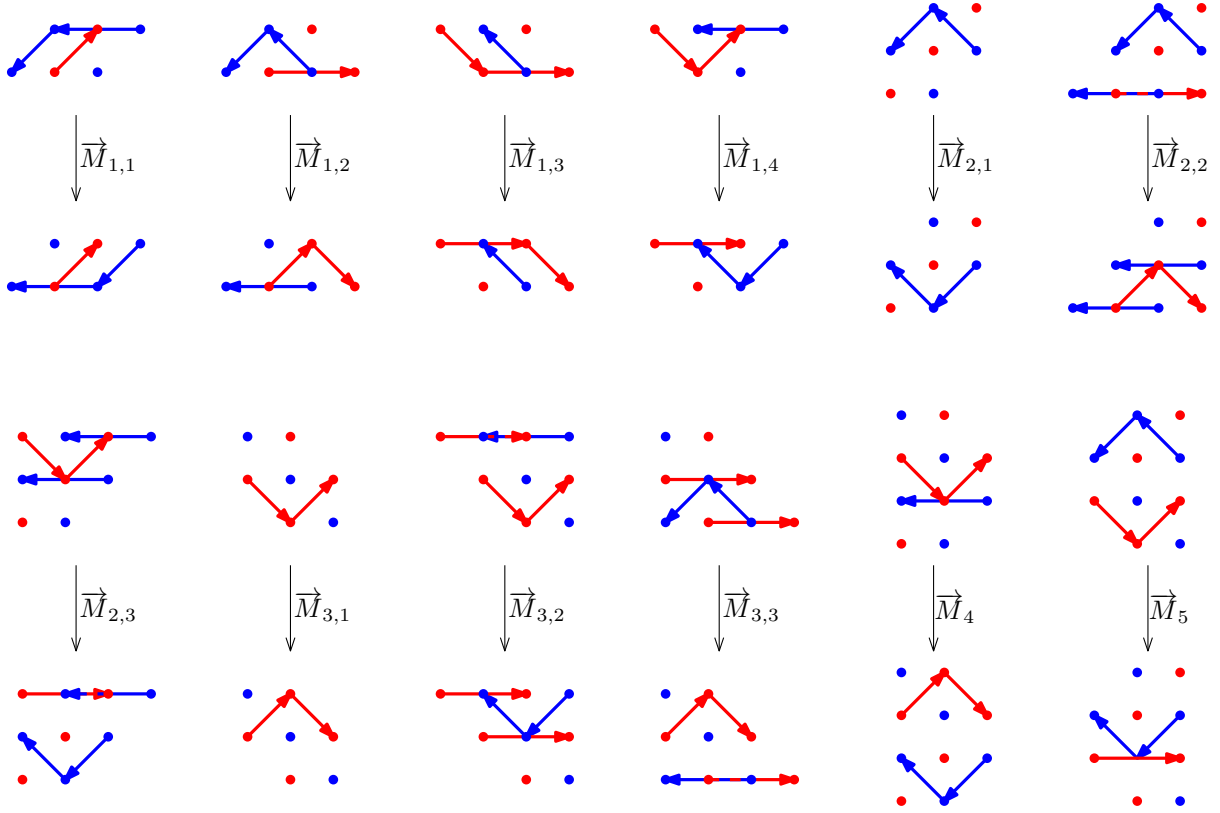


FIGURE 4.8. The moves in terms of blue-red path tangles that describe the effect of Wieland drift on canonically oriented TFPLs of excess 2.

PROOF. For the first identity, observe that the set of odd vertices in $G^N$ is decomposed of $N + 1$ sets such that in each such set the odd vertices are aligned with slope $-\sqrt{2}$. These sets are denoted the \-diagonals of $G^N$ in the following. For instance, $\mathcal{R}^N$ is a \-diagonal of $G^N$. It can be seen from Figure 4.2 that if a move $M_1$ or $M_3$ is applicable to $\mathfrak{o}(\ell)$ in $\mathrm{WL}^\ell(f)$, then the odd vertex incident to $\mathfrak{o}(\ell+1)$ in $\mathrm{WL}^{\ell+1}(f)$ lies on a \-diagonal to the right of the one on which the odd vertex incident to $\mathfrak{o}(\ell)$ lies. The same is true if $M_4$ or $M_5$ is applicable to $\mathfrak{o}(\ell)$ and $\mathfrak{o}(\ell+1)$ is chosen to be the top drifter in the image of $M_4$ respectively $\mathfrak{o}(\ell)$ is the bottom drifter in the preimage of the move $M_5$. In all the

other cases the odd vertices incident to $\mathfrak{d}(\ell)$ and $\mathfrak{d}(\ell+1)$ lie on the same \-diagonal of $G^N$. The first identity now follows since the odd vertex incident to $\mathfrak{d}(R_f(\mathfrak{d}))$ in $\text{Right}_f(\mathfrak{d})$ (*resp.* $\mathfrak{d}(L_f(\mathfrak{d}))$ in $\text{Left}_f(\mathfrak{d})$) lies on the $\text{HeightR}_f(\mathfrak{d})$-th (*resp.* $N+1$-st) \-diagonal of $G^N$ when counted from the left.

The second identity can be shown using analogous arguments as for the first identity. Instead into \-diagonals the odd vertices in $G^N$ are to be decomposed into sets such that the odd vertices in each set are aligned with slope $\sqrt{2}$.

For the third identity, observe that in the blue-red path tangle corresponding to $\text{WR}^{R_f(\mathfrak{d})}(\overrightarrow{f})$ the drifter $\mathfrak{d}(R_f(\mathfrak{d}))$ correspond to a blue $(-1,-1)$-step, while $\mathfrak{d}(L_f(\mathfrak{d}))$ is a red $(1,-1)$-step in the blue-red path tangle corresponding to $\text{WL}^{L_f(\mathfrak{d})}(\overrightarrow{f})$. Furthermore, in the blue-red path tangle corresponding to $\text{WL}^{L_f(\mathfrak{d})}$ there are $L_1(v^{L_f(\mathfrak{d})})$ many red paths that intersect the right boundary above the red path on which $\mathfrak{d}(L_f(\mathfrak{d}))(\overrightarrow{f})$ lies. Thus, when running through $r \in \{-R_f(\mathfrak{d}), \ldots, -1, 0\}$ and $\ell \in \{1, \ldots, L_f(\mathfrak{d})\}$ in increasing order, $\mathfrak{d}$ must overcome $L_1(v^{L_f(\mathfrak{d})})$ red paths. On the other hand, a red path is overcome precisely by the moves $\overrightarrow{M}_{1,1}$, $\overrightarrow{M}_{1,4}$, $\overrightarrow{M}_{2,3}$ or $\overrightarrow{M}_4^b$ as it can be seen in Figure 4.8. That is because by the moves $\overrightarrow{M}_{2,3}$ or $\overrightarrow{M}_4^b$ the drifter is transformed from a red into a blue down step that lies in the area below the red path. On the other hand, the move $\overrightarrow{M}_{3,3}$ is the only move by which the drifter is transformed from a blue down step is into a red down step that lies in the area above the blue path. For that reason, $\#\overrightarrow{M}_{3,3}(\mathfrak{d})$ must be subtracted. Finally, by no move is a blue down step moved from the area below a red path into the area above the very same red path.

The last identity follows by analogous arguments as the third. Instead of the red paths blue paths need to be considered. $\qquad\square$

PROOF OF PROPOSITION 4.10. By subtracting (4) from (1) in Lemma 4.15 one obtains

$$R_1(u^{R_f(\mathfrak{d})}) = \sum_{j \in \{1,4\}} \#\overrightarrow{M}_{1,j}(\mathfrak{d}) + \#\overrightarrow{M}_{2,3}(\mathfrak{d}) + \sum_{j \in \{1,2\}} \#\overrightarrow{M}_{3,j}(\mathfrak{d}) + \#\overrightarrow{M}_4^b(\mathfrak{d}) + \#\overrightarrow{M}_4^t(\mathfrak{d}) + \#\overrightarrow{M}_5^b(\mathfrak{d}).$$

On the other hand, by subtracting (3) from (2) in Lemma 4.15 one obtains

$$L_0(v^{L_f(\mathfrak{d})}) + 1 = \sum_{j \in \{2,3\}} \#\overrightarrow{M}_{1,j}(\mathfrak{d}) + \sum_{j \in \{1,2\}} \#\overrightarrow{M}_{2,j}(\mathfrak{d}) + \#\overrightarrow{M}_{3,3}(\mathfrak{d}) + \#\overrightarrow{M}_5^t(\mathfrak{d}).$$

Summing these two identities gives the assertion. $\qquad\square$

## 4.3. Proof of Theorem 4.2

In this section, Theorem 4.2 is proved bijectively. The following consequence of Proposition 4.10 plays a decisive role in this respect: let $f$ be an instable TFPL of excess 2 and $\mathfrak{d}$ a drifter in $f$. Then it holds either

$$(4.8) \qquad L_f(\mathfrak{d}) \leq L_0(v^{L_f(\mathfrak{d})}) \text{ and } R_f(\mathfrak{d}) > R_1(u^{R_f(\mathfrak{d})})$$

or

$$(4.9) \qquad L_f(\mathfrak{d}) > L_0(v^{L_f(\mathfrak{d})}) \text{ and } R_f(\mathfrak{d}) \leq R_1(u^{R_f(\mathfrak{d})}).$$

Recall that it is fixed which drifter in the image of the move $M_4$ (*resp.* $M_5^{-1}$) is assigned to the drifter in the preimage of the move $M_4$ (*resp.* $M_5^{-1}$). Nevertheless, whether a drifter $\mathfrak{d}$ in a TFPL of excess 2 satisfies either (4.8) or (4.9) does not depend on the choice of the drifters. This follows from the lemma below.

LEMMA 4.16. *If $f$ exhibits the preimage of the move $M_4$ (resp. $M_5^{-1}$) then in $\mathrm{WR}^r(f)$ (resp. $\mathrm{WL}^\ell(f)$) there is precisely one drifter for all $0 \leq r \leq R_f(\mathfrak{d})$ (resp. $0 \leq \ell \leq L_f(\mathfrak{d})$).*

PROOF. Let $f$ be a TFPL of excess 2 that exhibits the preimage of the move $M_4$ and $\overrightarrow{f}$ its canonical orientation. Then by Theorem 2.12 the loop in the preimage of the move $M_4$ in $f$ gives rise to two configurations that contribute to the excess. The drifter in the preimage of $\overrightarrow{M}_4$ is thus the sole drifter in $\overrightarrow{f}$. It is now easy to check that by right-Wieland drift either $\overrightarrow{M}_{1,2}^{-1}$ or $\overrightarrow{M}_{1,3}^{-1}$ is applied to the drifter in $f$. By Proposition 4.7 therefore the vertices of a drifter in $\overrightarrow{\mathrm{WR}^r(f)}$ have $y$-coordinate smaller than the $y$-coordinate of the vertices of the drifter in $f$ for all $r > 0$. In consequence, the even vertex that is incident to the drifter in $f$ is the centre of two succeeding $(-1,0)$-steps – a configuration that contributes to the excess – in $\overrightarrow{\mathrm{WR}^r(f)}$ for all $r > 0$. Thus, in $\overrightarrow{\mathrm{WR}^r(f)}$ there is precisely one configuration other than these two succeeding $(-1,0)$-steps that contributes to the excess for $0 < r \leq R(f)$. This configuration must be a drifter by Proposition 4.7, which concludes the proof.

The proof of the second assertion follows from the previous by symmetry. $\square$

Let $f$ be a TFPL with boundary $(u, v; w)$ where $\mathrm{exc}(u, v; w) = 2$. Furthermore, let $L(f) = \max\{\ell \geq 0 : \mathrm{WL}^\ell(f) \text{ is instable}\}$ and $\mathrm{Left}(f) = \mathrm{WL}^{L(f)+1}(f)$ *resp.* $R(f) = \max\{r \geq 0 : \mathrm{WR}^r(f) \text{ is instable}\}$ and $\mathrm{Right}(f) = \mathrm{WR}^{R(f)+1}(f)$. Then a triple $(S(f), g(f), T(f))$ in $\bigcup_{u^+ \geq u, \, v^+ \geq v} G_{u,u^+} \times S^w_{u^+,v^+} \times G_{v^*,(v^+)^*}$ is assigned to $f$ as follows:

(1) if $f$ is stable, set $g(f) = f$, $S(f)$ the empty semi-standard Young tableau of skew shape $\lambda(u)/\lambda(u)$ and $T(f)$ the empty semi-standard Young tableau of skew shape $\lambda(v^*)/\lambda(v^*)$.

(2) if $R_f(\mathfrak{d}) \leq R_1(u^{R_f(\mathfrak{d})})$ holds for each drifter $\mathfrak{d}$ in $f$, set $g(f)$ the stable TFPL $\mathrm{Right}(f)$ and $u^+$ the left boundary of $g(f)$. Then $u^+ > u$. Set furthermore $S(f)$

the semi-standard Young tableau of skew shape $\lambda(u^+)/\lambda(u)$ corresponding to the sequence

$$u = u^0 \xrightarrow{\ \mathrm{h}\ } u^1 \xrightarrow{\ \mathrm{h}\ } \cdots \xrightarrow{\ \mathrm{h}\ } u^{R(f)} \xrightarrow{\ \mathrm{h}\ } u^{R(f)+1} = u^+,$$

where $u^r$ is the left boundary of $\mathrm{WR}^r(f)$ for each $0 \le r \le R(f) + 1$, and $T(f)$ the empty semi-standard Young tableau of skew shape $\lambda(v^*)/\lambda(v^*)$.

(3) if $L_f(\mathfrak{d}) \le L_0(v^{L_f(\mathfrak{d})})$ holds for each drifter $\mathfrak{d}$ in $f$, set $g(f)$ the stable TFPL $\mathrm{Left}(f)$ and $v^+$ the right boundary of $g(f)$. Then $v^+ > v$. Set furthermore $S(f)$ the empty semi-standard Young tableau of skew shape $\lambda(u)/\lambda(u)$ and $T(f)$ the semi-standard Young tableau of skew shape $\lambda((v^+)^*)/\lambda(v^*)$ corresponding to the sequence

$$v^* = (v^0)^* \xrightarrow{\ \mathrm{h}\ } (v^1)^* \xrightarrow{\ \mathrm{h}\ } \cdots \xrightarrow{\ \mathrm{h}\ } (v^{L(f)})^* \xrightarrow{\ \mathrm{h}\ } (v^{L(f)+1})^* = (v^+)^*,$$

where $v^\ell$ is the right boundary of $\mathrm{WL}^\ell(f)$ for each $0 \le \ell \le L(f) + 1$.

(4) if there are two drifters $\mathfrak{d}_\mathfrak{r}$ and $\mathfrak{d}_\mathfrak{l}$ in $f$ that satisfy $R_f(\mathfrak{d}_\mathfrak{r}) \le R_1(u^{R_f(\mathfrak{d}_\mathfrak{r})})$ and $L_f(\mathfrak{d}_\mathfrak{l}) \le L_0(v^{L_f(\mathfrak{d}_\mathfrak{l})})$, then set $g(f)$ the TFPL that is obtained from $f$ as follows: move $\mathfrak{d}_\mathfrak{l}$ to the right boundary using the moves $M_1$, $M_2$, $M_3$ and replace it by a horizontal edge; thereafter, move $\mathfrak{d}_\mathfrak{r}$ to the left boundary using the moves $M_1^{-1}$, $M_2^{-1}$, $M_3^{-1}$ and replace it by a horizontal edge. Observe that $g(f)$ indeed is stable. In the following, let $u^+$ be the left and $v^+$ the right boundary of $g(f)$. Then $u^+ > u$, $|\lambda(u^+)/\lambda(u)| = 1$, $v^+ > v$ and $|\lambda((v^+)^*)/\lambda(v^*)| = 1$. Finally, set $S(f)$ the semi-standard Young tableau of skew shape $\lambda(u^+)/\lambda(u)$ with entry $R_f(\mathfrak{d}_\mathfrak{r})+1$ and $T(f)$ is the semi-standard Young tableau of skew shape $\lambda((v^+)^*)/\lambda(v^*)$ with entry $L_f(\mathfrak{d}_\mathfrak{l}) + 1$.

In Figure 4.9, a TFPL of excess 2 and the triple $(S, g, T)$ associated with it are depicted.
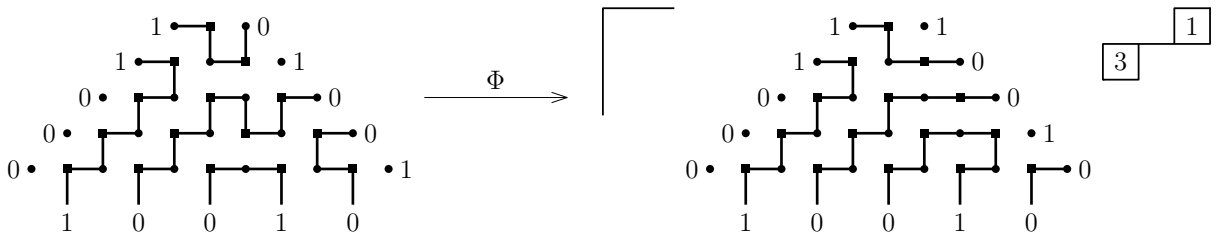


FIGURE 4.9. An instable TFPL with boundary $(00011, 01001; 10010)$ and the triple $(S, g, T)$ it is associated with.

THEOREM 4.17. *Let $u, v, w$ be words of the same length such that $|u|_1 = |v|_1 = |w|_1$ and $\exc(u, v; w) = 2$. Furthermore, set $N_1 = |u|_1$. Then the map*

$$\Phi : T_{u,v}^w \longrightarrow \bigcup_{\substack{u^+ \geq u,\, v^+ \geq v:\\ |u^+|_1 = |v^+|_1 = N_1}} G_{u,u^+} \times S_{u^+,v^+}^w \times G_{v^*,(v^+)^*}$$

$$f \longmapsto (S(f), g(f), T(f))$$

*is a bijection.*

REMARK 4.18. The assertion of Theorem 4.2 immediately follows from Theorem 4.17.

PROPOSITION 4.19. *Let $f$ be an instable TFPL of excess $2$ that contains two drifters $\mathfrak{d}_{\mathfrak{r}}$ and $\mathfrak{d}_{\mathfrak{l}}$ such that $R_f(\mathfrak{d}_{\mathfrak{r}}) \leq R_1(u^{R_f(\mathfrak{d}_{\mathfrak{r}})})$ and $L_f(\mathfrak{d}_{\mathfrak{l}}) \leq L_0(v^{L_f(\mathfrak{d}_{\mathfrak{l}})})$. Then $\mathfrak{d}_{\mathfrak{r}}$ can be moved to the left boundary by the moves $M_1^{-1}$, $M_2^{-1}$ and $M_3^{-1}$ and $\mathfrak{d}_{\mathfrak{l}}$ can be moved to the right boundary by the moves $M_1$, $M_2$ and $M_3$.*

The proof of Proposition 4.19 is based on the following two lemmas. To begin with, note that two drifters $\mathfrak{d}$ and $\mathfrak{d}^*$ in a TFPL $f$ of excess 2 that contains the preimage of the move $M_5$ (*resp.* $M_4^{-1}$) must satisfy $L_f(\mathfrak{d}) = L_f(\mathfrak{d}^*)$ (*resp.* $R_f(\mathfrak{d}) = R_f(\mathfrak{d}^*)$). Therefore, a TFPL that contains the preimage of the move $M_5$ (*resp.* $M_4^{-1}$) does not fulfil the preconditions of Proposition 4.19 by Corollary 4.11.

LEMMA 4.20. *Let $f$ be a TFPL of excess $2$ that contains two drifters $\mathfrak{d}$ and $\mathfrak{d}^*$, whereof $\mathfrak{d}$ is not incident to a vertex in $\mathcal{R}^N$. Furthermore, $f$ shall not exhibit the preimage of the move $M_5$. Then, if none of the moves $M_1$, $M_2$ or $M_3$ can be applied to $\mathfrak{d}$, $\mathfrak{d}$ is prevented from being moved by $\mathfrak{d}^*$ by way of one of the following **blockades**:*
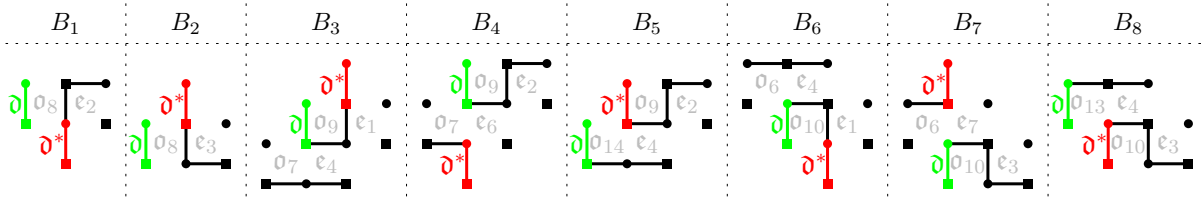


PROOF. Since $\mathfrak{d}$ is not incident to a vertex in $\mathcal{R}^N$ it is contained in an odd cell $o$ of $f$. Furthermore, $o \in \{\mathfrak{o}_8, \mathfrak{o}_9, \mathfrak{o}_{10}, \mathfrak{o}_{13}, \mathfrak{o}_{14}\}$ because $f$ cannot contain the odd cell $\mathfrak{o}_{11}$ and two drifters at the same time by Theorem 2.12. Here, only the case when $o = \mathfrak{o}_8$ is considered. In that case, for the even cell $e$ to the right of $o$ it holds $e \in \{\mathfrak{e}_2, \mathfrak{e}_3, \mathfrak{e}_5\}$. The case $e = \mathfrak{e}_5$ is impossible since by assumption the move $M_1$ cannot be applied to $\mathfrak{d}$. Thus, $e = \mathfrak{e}_2$ or $e = \mathfrak{e}_3$ which give rise to the blockades $B_1$ and $B_2$ respectively. $\qquad\square$

LEMMA 4.21. *Let the assumptions be the same as in Lemma 4.20. Then*

$$L_f(\mathfrak{d}) - L_f(\mathfrak{d}^*) = L_0(v^{L_f(\mathfrak{d})}) - L_0(v^{L_f(\mathfrak{d}^*)}) + 1.$$

The crucial idea for the proof of Lemma 4.21 is to consider TFPLs of excess at most 2 together with their canonical orientation and then represent them in terms of blue-red path tangles. By doing so the blockades in Lemma 4.20 translate into the blockades depicted in Figure 4.10 and Figure 4.11.
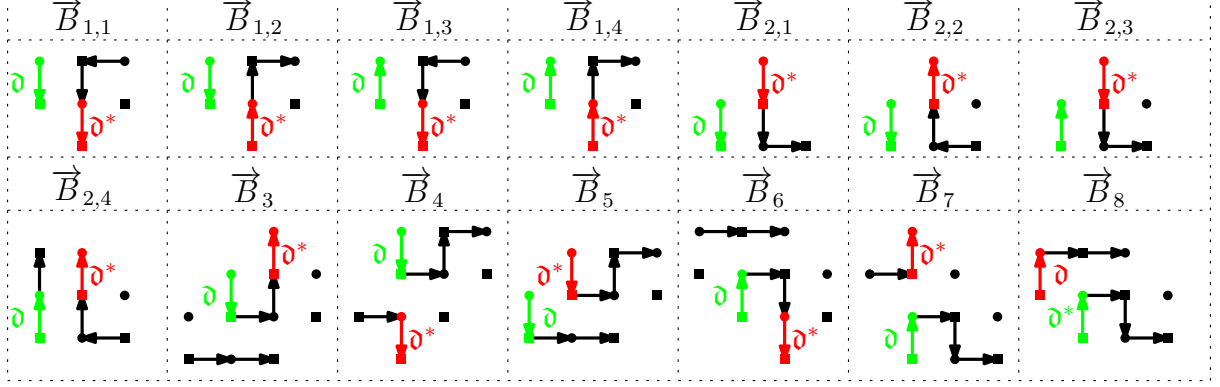


FIGURE 4.10. The blockades of Lemma 4.20 in a TFPL of excess 2 that is equipped with the canonical orientation.

PROOF. In the following, set

$$\#\overrightarrow{ML}_{i,j}(\mathfrak{d}) = |\{0 \leq \ell < L_f(\mathfrak{d}) : \overrightarrow{M}_{i,j} \text{ is applied by WL to } \mathfrak{d}(\ell) \text{ in } \text{WL}^{\ell}(\overrightarrow{f})\}|.$$

for $(i,j) \in \{(1,1),(1,2),(1,3),(1,4),(2,1),(2,2),(2,3),(3,1),(3,2),(3,3)\}$. The numbers $\#\overrightarrow{ML}_4^b(\mathfrak{d})$, $\#\overrightarrow{ML}_4^t(\mathfrak{d})$, $\#\overrightarrow{ML}_5^b(\mathfrak{d})$ and $\#\overrightarrow{ML}_5^t(\mathfrak{d})$ are defined analogously. Furthermore, fix the following notations:

$$\mathrm{D}_{NW}(\mathfrak{d},\mathfrak{d}^*) = \sum_{i=1}^{4}(\#\overrightarrow{ML}_{1,i}(\mathfrak{d}) - \#\overrightarrow{ML}_{1,i}(\mathfrak{d}^*)) + \sum_{j=1}^{3}(\#\overrightarrow{ML}_{3,j}(\mathfrak{d}) - \#\overrightarrow{ML}_{3,j}(\mathfrak{d}^*))$$

$$+ \#\overrightarrow{ML}_4^t(\mathfrak{d}) - \#\overrightarrow{ML}_4^t(\mathfrak{d}^*) + \#\overrightarrow{ML}_5^b(\mathfrak{d}) - \#\overrightarrow{ML}_5^b(\mathfrak{d}^*);$$

$$\mathrm{D}_{NE}(\mathfrak{d},\mathfrak{d}^*) = \sum_{i=1}^{4}(\#\overrightarrow{ML}_{1,i}(\mathfrak{d}^*) - \#\overrightarrow{ML}_{1,i}(\mathfrak{d})) + \sum_{j=1}^{3}(\#\overrightarrow{ML}_{2,j}(\mathfrak{d}^*) - \#\overrightarrow{ML}_{2,j}(\mathfrak{d}))$$

$$+ \mathrm{HeightL}_f(\mathfrak{d}^*) - \mathrm{HeightL}_f(\mathfrak{d}) + \#\overrightarrow{ML}_4^b(\mathfrak{d}^*) - \#\overrightarrow{ML}_4^b(\mathfrak{d}) + \#\overrightarrow{ML}_5^t(\mathfrak{d}^*) - \#\overrightarrow{ML}_5^t(\mathfrak{d});$$

$$\mathrm{Red}(\mathfrak{d},\mathfrak{d}^*) = \sum_{j\in\{1,4\}}(\#\overrightarrow{ML}_{1,j}(\mathfrak{d}^*) - \#\overrightarrow{ML}_{1,j}(\mathfrak{d})) + \#\overrightarrow{ML}_{2,3}(\mathfrak{d}^*) - \#\overrightarrow{ML}_{2,3}(\mathfrak{d})$$

$$- \#\overrightarrow{ML}_{3,3}(\mathfrak{d}^*) + \#\overrightarrow{ML}_{3,3}(\mathfrak{d}) + \#\overrightarrow{ML}_4^b(\mathfrak{d}^*) - \#\overrightarrow{ML}_4^b(\mathfrak{d}) + L_1(v^{L_f(\mathfrak{d})}) - L_1(v^{L_f(\mathfrak{d}^*)});$$

$$\mathrm{Blue}(\mathfrak{d},\mathfrak{d}^*) = \#\overrightarrow{ML}_{1,2}(\mathfrak{d}) + \#\overrightarrow{ML}_{1,3}(\mathfrak{d}) - \#\overrightarrow{ML}_{2,3}(\mathfrak{d}) + \#\overrightarrow{ML}_{3,3}(\mathfrak{d}) - \#\overrightarrow{ML}_4^b(\mathfrak{d})$$

$$- \#\overrightarrow{ML}_{1,2}(\mathfrak{d}^*) - \#\overrightarrow{ML}_{1,3}(\mathfrak{d}^*) + \#\overrightarrow{ML}_{2,3}(\mathfrak{d}^*) - \#\overrightarrow{ML}_{3,3}(\mathfrak{d}^*) + \#\overrightarrow{ML}_4^b(\mathfrak{d}^*).$$

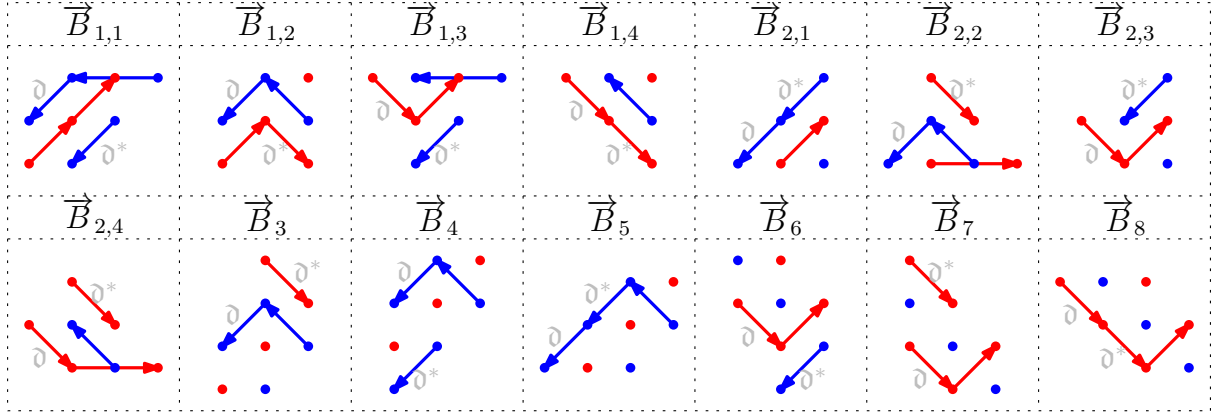FIGURE 4.11. The blockades of Figure 4.10 in terms of blue-red path tangles.

An easy computation shows that $D_{NW}(\mathfrak{d}, \mathfrak{d}^*) - \mathrm{Blue}(\mathfrak{d}, \mathfrak{d}^*) - D_{NE}(\mathfrak{d}, \mathfrak{d}^*) + \mathrm{Red}(\mathfrak{d}, \mathfrak{d}^*)$ equals $L_f(\mathfrak{d}) - L_f(\mathfrak{d}^*) - L_0(v^{L_f(\mathfrak{d})}) + L_0(v^{L_f(\mathfrak{d}^*)})$. To conclude the proof of Lemma 4.21 it will be shown that $D_{NW}(\mathfrak{d}, \mathfrak{d}^*) - \mathrm{Blue}(\mathfrak{d}, \mathfrak{d}^*) - D_{NE}(\mathfrak{d}, \mathfrak{d}^*) + \mathrm{Red}(\mathfrak{d}, \mathfrak{d}^*)$ equals 1. For that purpose, alternative interpretations of the integers $D_{NW}(\mathfrak{d}, \mathfrak{d}^*)$, $D_{NE}(\mathfrak{d}, \mathfrak{d}^*)$, $\mathrm{Red}(\mathfrak{d}, \mathfrak{d}^*)$ and $\mathrm{Blue}(\mathfrak{d}, \mathfrak{d}^*)$ will be derived by analogous arguments as in the proof of Lemma 4.15.

To begin with, decompose $G^N$ into \-diagonals as in the proof of Lemma 4.15. Furthermore, a \-diagonal – denoted $\mathsf{d}_r$ – is said to lie to the right of another \-diagonal – denoted $\mathsf{d}_l$ – if the odd vertex with the smallest $y$-coordinate in $\mathsf{d}_r$ has a larger $x$-coordinate than the odd vertex with the smallest $y$-coordinate in $\mathsf{d}_l$. Now, suppose that the odd vertex incident to $\mathfrak{d}$ is part of the $i(\mathfrak{d})$-th \-diagonal in $f$ and the odd vertex incident to $\mathfrak{d}^*$ is part of the $i(\mathfrak{d}^*)$-th \-diagonal in $f$ when counted from the left. Then $D_{NW}(\mathfrak{d}, \mathfrak{d}^*) = i(\mathfrak{d}^*) - i(\mathfrak{d})$ by the same arguments as in the proof of Lemma 4.15(1).

Next, decompose the odd vertices in $G^N$ into $N + 1$ sets such that in each set the odd vertices are aligned with slope $\sqrt{2}$. These sets are said to be the /-diagonals of $G^N$. Furthermore, a /-diagonal $\mathsf{d}_r$ is said to lie to the right of another /-diagonal $\mathsf{d}_l$ in $G^N$ if the odd vertex with the smallest $y$-coordinate in $\mathsf{d}_r$ has a larger $x$-coordinate than the odd vertex with the smallest $y$-coordinate in $\mathsf{d}_l$. Suppose that the odd vertex incident to $\mathfrak{d}$ is part of the $j(\mathfrak{d})$-th \-diagonal in $f$ and the odd vertex incident to $\mathfrak{d}^*$ is part of the $j(\mathfrak{d}^*)$-th \-diagonal in $f$ when counted from the left. Then $D_{NE}(\mathfrak{d}, \mathfrak{d}^*) = j(\mathfrak{d}) - j(\mathfrak{d}^*)$ by the same arguments as in the proof of Lemma 4.15(2).

From now on, consider the blue-red path tangle associated with $\mathrm{WL}^\ell(\overrightarrow{f})$ for all $0 \leq \ell \leq L_f(\mathfrak{d})$. Then $\mathrm{Red}(\mathfrak{d}, \mathfrak{d}^*)$ equals the difference of the number of red paths $\mathfrak{d}$ "jumps over" in the process of moving to the left boundary by repeatedly applying right-Wieland drift and the number of red paths $\mathfrak{d}^*$ "jumps over" in the process of moving to the left boundary by the iterated application of right-Wieland drift by the same arguments as in the proof of Lemma 4.15(3). To be more precise, a blue down step "jumps over" a red path by the application of WR if before the application of WR it is in the area below the red path and after the application it is in the area above the red path. On the other

hand, a red down step "jumps over" a red path if after the application of WR it is a blue down step that lies in the area above the red path.

Finally, $\mathrm{Blue}(\mathfrak{d}, \mathfrak{d}^*)$ is the difference of the number of blue paths $\mathfrak{d}$ "jumps over" in the process of moving to the right boundary by repeatedly applying left-Wieland drift and the number of blue paths $\mathfrak{d}^*$ "jumps over" in the process of moving to the right boundary by the iterated application of left-Wieland drift by the same arguments as in the proof of Lemma 4.15(4). To be more precise, a red down step "jumps over" a blue path by the application of WL if before the application of WL it lies in the area below the blue path and after the application it is in the area above the blue path. On the other hand, a blue down step "jumps over" a blue path if after the application of WL it is a red down step that lies in the area above the red path.

Thus, $\mathrm{D}_{NW}(\mathfrak{d}, \mathfrak{d}^*)$, $\mathrm{D}_{NE}(\mathfrak{d}, \mathfrak{d}^*)$, $\mathrm{Red}(\mathfrak{d}, \mathfrak{d}^*)$ and $\mathrm{Blue}(\mathfrak{d}, \mathfrak{d}^*)$ can be computed separately for each blockade by looking at Figure 4.10 and Figure 4.11, which is done in Table 4.

|  | $\vec{B}_{1,1}$ | $\vec{B}_{1,2}$ | $\vec{B}_{1,3}$ | $\vec{B}_{1,4}$ | $\vec{B}_{2,1}$ | $\vec{B}_{2,2}$ | $\vec{B}_{2,3}$ | $\vec{B}_{2,4}$ | $\vec{B}_3$ | $\vec{B}_4$ | $\vec{B}_5$ | $\vec{B}_6$ | $\vec{B}_7$ | $\vec{B}_8$ |
|---|---|---|---|---|---|---|---|---|---|---|---|---|---|---|
| $\mathrm{D}_{NW}$ | 0 | 0 | 0 | 0 | 1 | 1 | 1 | 1 | 1 | $-1$ | 1 | 0 | 1 | 0 |
| $\mathrm{D}_{NE}$ | $-1$ | $-1$ | $-1$ | $-1$ | 0 | 0 | 0 | 0 | 0 | $-1$ | 0 | $-1$ | 1 | $-1$ |
| Red | $-1$ | 0 | $-1$ | 0 | 0 | 1 | 0 | 1 | 1 | 0 | 0 | $-1$ | 1 | 0 |
| Blue | $-1$ | 0 | $-1$ | 0 | 0 | 1 | 0 | 1 | 1 | $-1$ | 0 | $-1$ | 0 | 0 |

TABLE 4. The numbers $\mathrm{D}_{NW}(\mathfrak{d}, \mathfrak{d}^*)$, $\mathrm{D}_{NE}(\mathfrak{d}, \mathfrak{d}^*)$, $\mathrm{Red}(\mathfrak{d}, \mathfrak{d}^*)$ and $\mathrm{Blue}(\mathfrak{d}, \mathfrak{d}^*)$ computed separately for each type of blockade.

In summary, it follows that

$$\mathrm{D}_{NW}(\mathfrak{d}, \mathfrak{d}^*) - \mathrm{Blue}(\mathfrak{d}, \mathfrak{d}^*) - \mathrm{D}_{NE}(\mathfrak{d}, \mathfrak{d}^*) + \mathrm{Red}(\mathfrak{d}, \mathfrak{d}^*) = 1.$$

Therefore, $L_f(\mathfrak{d}) - L_f(\mathfrak{d}^*) - L_0(v^{L_f(\mathfrak{d})}) + L_0(v^{L_f(\mathfrak{d}^*)}) = 1.$ $\qquad\square$

Proposition 4.19 follows immediately from Lemma 4.21.

PROOF OF PROPOSITION 4.19. Let $f$ be an instable TFPL of excess 2 that contains two drifters $\mathfrak{d}_{\mathfrak{l}}$ and $\mathfrak{d}_{\mathfrak{r}}$ such that $R_f(\mathfrak{d}_{\mathfrak{r}}) \leq R_1(u^{R_f(\mathfrak{d}_{\mathfrak{r}})})$ and $L_f(\mathfrak{d}_{\mathfrak{l}}) \leq L_0(v^{L_f(\mathfrak{d}_{\mathfrak{l}})})$. Without loss of generality, suppose that $\mathfrak{d}_{\mathfrak{l}}$ cannot be moved to the right boundary using the moves $M_1$, $M_2$ and $M_3$. Then, by Lemma 4.21

$$L_f(\mathfrak{d}_{\mathfrak{l}}) \geq L_f(\mathfrak{d}_{\mathfrak{r}}) + L_0(v^{L_f(\mathfrak{d}_{\mathfrak{l}})}) - L_0(v^{L_f(\mathfrak{d}_{\mathfrak{r}})}) + 1.$$

Thus, $L_f(\mathfrak{d}_{\mathfrak{l}}) > L_0(v^{L_f(\mathfrak{d}_{\mathfrak{l}})})$ and equivalently $R_f(\mathfrak{d}_{\mathfrak{r}}) > R_1(u^{R_f(\mathfrak{d}_{\mathfrak{r}})}) + 1$. That is a contradiction. Therefore, $\mathfrak{d}_{\mathfrak{l}}$ can be moved to the right boundary using the moves $M_1$, $M_2$ and $M_3$.

By vertical symmetry, $\mathfrak{d}_{\mathfrak{r}}$ can be moved to the left boundary by the moves $M_1^{-1}$, $M_2^{-1}$ or $M_3^{-1}$. $\qquad\square$

In Figure 4.12, the instable TFPL of excess 2 of Figure 4.2 and the triple $(S, g, T)$ associated with it are depicted.
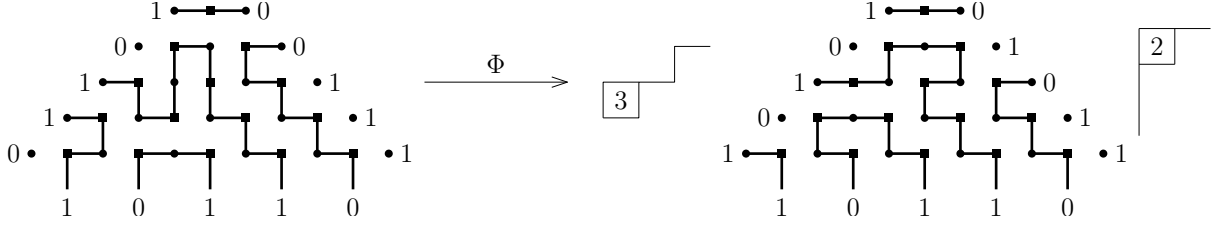
FIGURE 4.12. The instable TFPL of Figure 4.2 and the triple $(S, g, T)$ it is associated with.

PROOF OF THEOREM 4.17. Let $u, v, w$ be words of length $N$ satisfying that $|u|_1 = |v|_1 = |w|_1 = N_1$ and $\mathrm{exc}(u, v; w) \leq 2$. Furthermore, let $f \in T_{u,v}^w$ be instable and denote by $(S, g, T)$ the image of $f$ under $\Phi$. As a start, $S$ is an element of $G_{u,u^+}$ for the following reason: let $c$ be a cell of the Young diagram of skew shape $\lambda(u^+)/\lambda(u)$ then its entry in $S$ has to be $R_f(\mathfrak{d}) + 1$ for a drifter $\mathfrak{d}$ in $f$ and it has to hold $R_f(\mathfrak{d}) \leq R_1(u^{R_f(\mathfrak{d})})$ by the definition of $\Phi$. Now, if $c$ is part of the $i$-th column in $\lambda(u^+)/\lambda(u)$ then $R_1(u^{R_f(\mathfrak{d})}) = N_1 - i$ and therefore the entry of $c$ in $S$ is at most $N_1 - i + 1$. By analogous arguments it follows that $T \in G_{v^*,(v^+)^*}$.

It remains to show that $\Phi$ is a bijection. This will be done by giving the inverse map: let $u^+ \geq u$, $v^+ \geq v$, $S \in G_{u,u^+}$, $g \in S_{u^+,v^+}^w$ and $T \in G_{v^*,(v^+)^*}$ and consider the sequences

$$\lambda(u) = \lambda(u^0) \subseteq \lambda(u^1) \subseteq \cdots \subseteq \lambda(u^{R+1}) = \lambda(u^+)$$

corresponding to $S$ where $R + 1$ is the largest entry of $S$ and

$$\lambda(v^*) = \lambda((v^0)^*) \subseteq \lambda((v^1)^*) \subseteq \cdots \subseteq \lambda((v^{L+1})^*) = \lambda((v^+)^*)$$

corresponding to $T$ where $L + 1$ is the largest entry of $T$. Then associate $(S, g, T)$ with a TFPL $\Psi(S, g, T)$ in $T_{u,v}^w$ as follows:

(1) if $u^+ > u$ and $v^+ = v$, set $\Psi(S, g, T) = (\mathrm{WL}_{u^0} \circ \mathrm{WL}_{u^1} \circ \cdots \circ \mathrm{WL}_{u^{R-1}} \circ \mathrm{WL}_{u^R})(g)$.

(2) if $u^+ = u$ and $v^+ > v$, set $\Psi(S, g, T) = (\mathrm{WR}_{v^0} \circ \mathrm{WR}_{v^1} \circ \cdots \circ \mathrm{WR}_{v^{L-1}} \circ \mathrm{WR}_{v^L})(g)$.

(3) if $u^+ > u$ and $v^+ > v$, set $\Psi(S, g, T)$ the TFPL obtained from $g$ as follows: since $u^+ > u$ and $v^+ > v$ the skew shapes $\lambda(u^+)/\lambda(u)$ and $\lambda((v^+)^*)/\lambda(v^*)$ both consist of precisely one cell. In the following, suppose that the cell in $\lambda(u^+)/\lambda(u)$ (*resp.* in $\lambda((v^+)^*)/\lambda(v^*)$) is part of the $j$-th (*resp.* $j'$-th) column when counted from the left. To begin with, insert two drifters in $g$ as follows: a drifter $\mathfrak{d}_{\mathfrak{r}}$ incident to $L_{i_j+1}$ is inserted while the horizontal edge incident to $L_{i_j}$ is deleted if $i_j$ is the index of the $j$-th one in $u^+$ and a drifter $\mathfrak{d}_{\mathfrak{l}}$ incident to $R_{i_{|v|_0-j'+1}-1}$ is inserted while the horizontal edge incident to $R_{i_{|v|_0-j'+1}}$ is deleted if $i_{|v|_0-j'+1}$ the index of the $|v|_0 - j + 1'$-st zero in $v^+$. Thereafter, $\mathfrak{d}_{\mathfrak{r}}$ is moved $R$ times by the moves $M_1$, $M_2$ and $M_3$ and $\mathfrak{d}_{\mathfrak{l}}$ is moved $L$ times by the moves $M_1^{-1}$, $M_2^{-1}$ and $M_3^{-1}$. The so-obtained TFPL shall be the image of $(S, g, T)$ under $\Psi$.

(4) If $u^+ = u$ and $v^+ = v$, then $\Psi(S, g, T) = g$.

It is easy to check that $\Psi$ is the inverse map of $\Phi$. $\qquad\square$

## 4.4. Outlook

In this chapter, an expression for the numbers of TFPLs of excess 2 in terms of stable TFPLs has been established, which generalises the expressions in Theorem 2.15 and Theorem 2.17 for TFPLs of excess 0 and 1 respectively. The logical next step is to check whether this expression is valid for TFPLs of excess greater than 2. The answer turns out to be no. Already for TFPLs of excess 3 there are counterexamples, one of which is given below.

EXAMPLE 4.22. It is easy to check that $t^{1010}_{0011,0011} = s^{1010}_{0011,0011} + 17$. Figure 4.19 at the end of this section shows all instable TFPLs with boundary $(0011, 0011; 1010)$. On the other hand, computing the right side in (4.1) for $u = v = 0011$ and $w = 1010$ gives $s^{1010}_{0011,0011} + 18$.

In the following, it is outlined at which point the methods used to prove Theorem 4.2 fail for TFPLs of excess 3. Furthermore, a modification of the expression (4.1) is conjectured for the excess-3-case. It adds weights to TFPLs dependent on the occurrences of the cells $\mathfrak{o}_{15}$ and $\mathfrak{o}_{16}$. An interesting question for future studies is whether this modification is true in the general case.

To begin with, the effect of left- and right-Wieland drift on TFPLs of excess 3 as the composition of moves will be conjectured. The moves that are additionally needed for this purpose are displayed in Figure 4.13. From Theorem 2.12 it follows that a TFPL of excess 3 that contains the preimage of one of the new moves there cannot be another drifter. Thus, in the course of the application of WL to such a TFPL no other move but the respective new move is performed. The analogous is true for WR.
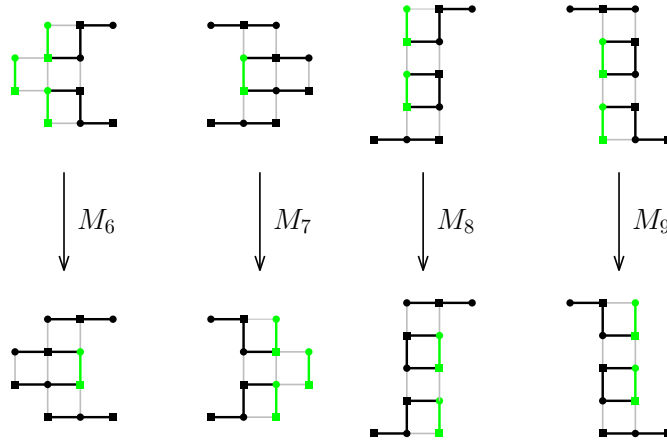


FIGURE 4.13. The new moves that are needed to describe the effect of WL on TFPLs of excess 3.

CONJECTURE 1. Let $u$, $v$ and $w$ be words such that $\mathrm{exc}(u, v; w) = 3$ and $f \in T^w_{u,v}$ instable. Furthermore, let $u^-$ be a word such that $u^- \xrightarrow{\mathrm{h}} u$. Then the image of $f$ under left-Wieland drift with respect to $u^-$ is determined as follows:

(1) *if $R_i \in \mathcal{R}^N$ is incident to a drifter delete that drifter and add a horizontal edge incident to $R_{i+1}$ for $i = 1, 2, \ldots, N-1$;*

(2) *perform the move $M_6$, $M_7$, $M_8$ or $M_9$ if possible; otherwise, run through the columns of $G^N$ from right to left, that is, for $j = 2N+1, \ldots, 1$:*

    (a) *if there is precisely one drifter on the $j$-th column of $G^N$, apply the move $M_1$, $M_2$, $M_3$ or $M_4$ to it;*

    (b) *if there are precisely two drifters $\mathfrak{d}_b$ and $\mathfrak{d}_t$ on the $j$-th column of $G^N$, either apply the move $M_5$ to them or apply $M_1$, $M_2$ or $M_3$ to each of them in the following order: move $\mathfrak{d}_b$ first, if $\mathfrak{d}_t$ lies above $\mathfrak{d}_b$ and the odd cell that contains $\mathfrak{d}_t$ is $\mathfrak{o}_9$; otherwise, move $\mathfrak{d}_t$ first.*

    (c) *if there are three drifters on the $j$-th column of $G^N$ then either apply $M_5$ to two of them and thereafter apply $M_1$, $M_2$ or $M_3$ to the other drifter or apply $M_1$, $M_2$ or $M_3$ to each of them in the order determined by the following: for each two drifters $\mathfrak{d}_b$ and $\mathfrak{d}_t$ in-between which there is no other drifter move $\mathfrak{d}_b$ before $\mathfrak{d}_t$, if $\mathfrak{d}_t$ lies above $\mathfrak{d}_b$ and the odd cell that contains $\mathfrak{d}_t$ is $\mathfrak{o}_9$, and otherwise move $\mathfrak{d}_t$ before $\mathfrak{d}_b$.*

(3) *run through the occurrences of one in $u^-$, that is, for $j = 1, \ldots, |u^-|_1$ delete the horizontal edge incident to $L_{i_j - 1}$ and add a vertical edge incident to $L_{i_j}$, where $i_j$ is the index of the $j$-th one in $u^-$.*
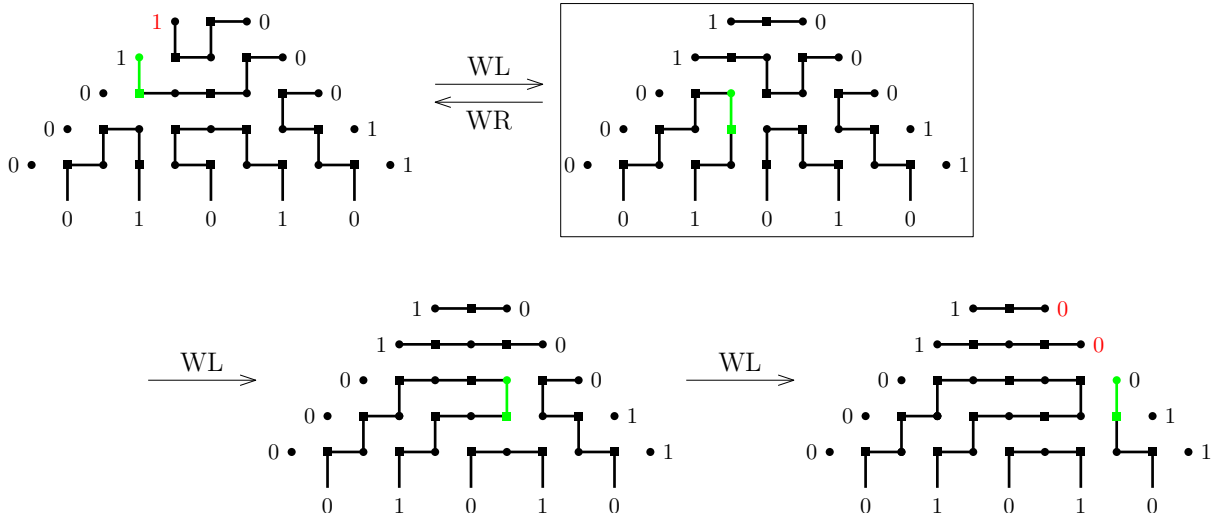


FIGURE 4.14. A TFPL with boundary $(00011, 00011; 01010)$ and its images under left-Wieland drift that have excess 3.

In Figure 4.14 a TFPL of excess 3 and its images under WL of excess 3 are depicted. Conjecture 1 together with Theorem 3.7 would immediately yield an alternative description of the effect of WR on TFPLs of excess 3. Furthermore, Conjecture 1 would allow to define $L(f)$, $R(f)$, $L_f(\mathfrak{d})$, $R_f(\mathfrak{d})$, $\mathrm{Path}_f(\mathfrak{d})$, $(u^r)_{r=0}^{R(f)+1}$, $R_1(u^{R_f(\mathfrak{d})})$, $(v^\ell)_{\ell=0}^{L(f)+1}$ and $L_0(v^{L_f(\mathfrak{d})})$ for TFPLs $f$ of excess 3.

The essential property in the excess-2-case is that $L_f(\mathfrak{d}) + R_f(\mathfrak{d}) = R_1(u^{R_f(\mathfrak{d})}) + L_0(v^{L_f(\mathfrak{d})})+1$ holds for each drifter $\mathfrak{d}$ in a TFPL $f$ of excess 2. When regarding the framed TFPL in Figure 4.14 then for the drifter $\mathfrak{d}$ that is indicated in green it holds $L_f(\mathfrak{d}) = 2 = L_0(v^{L_f(\mathfrak{d})})$ and $R_f(\mathfrak{d}) = 1 = R_1(u^{R_f(\mathfrak{d})})$. Thus, $L_f(\mathfrak{d}) + R_f(\mathfrak{d}) = R_1(u^{R_f(\mathfrak{d})}) + L_0(v^{L_f(\mathfrak{d})})$ in that example, which disagrees with the excess-2-case. For this reason, it is expedient to investigate the quantity $L_f(\mathfrak{d}) + R_f(\mathfrak{d})$ for drifters $\mathfrak{d}$ in TFPLs $f$ of excess 3.

For this purpose, it is helpful to regard the effect of the new moves on individual drifters. In doing so, one immediately sees that in the preimage of the move $M_6$ there are three drifters while in its image there is one and that in the preimage of the move $M_7$ there is one drifter while in its image there are three. For the purpose of studying the effect of left-Wieland drift on a particular drifter encode with $M_{6,b}$, $M_{6,c}$ and $M_{6,t}$ whether the bottommost, central or topmost drifter in the preimage of the move $M_6$ is regarded before the three drifters merge. Furthermore, a drifter in the image of the move $M_7$ that shall be regarded from that point forward needs to be chosen. Encode with $M_{7,b}$, $M_{7,c}$ and $M_{7,t}$ whether the bottommost, the central or the topmost drifter in the image of the move $M_7$ is chosen. Finally, in the preimages and images of both $M_8$ and $M_9$ there are two drifters. In the following, for both moves identify the topmost (*resp.* bottommost) drifter in the preimage with the topmost (*resp.* bottommost) drifter in the image. Furthermore, encode with $M_{8,b}$ *resp.* $M_{9,b}$ and $M_{8,t}$ *resp.* $M_{9,t}$ whether the bottommost or the topmost drifter is considered.

The basic idea in the proof of the equality $L_f(\mathfrak{d})+R_f(\mathfrak{d}) = R_1(u^{R_f(\mathfrak{d})}+L_0(v^{L_f(\mathfrak{d})})+1$ in the excess-2-case was to give linear relations in the numbers $\#M_1(\mathfrak{d})$, $\#M_2(\mathfrak{d})$, $\#M_3(\mathfrak{d})$, $\#M_{4,b}(\mathfrak{d})$, $\#M_{4,t}(\mathfrak{d})$, $\#M_{5,b}(\mathfrak{d})$ and $\#M_{5,t}(\mathfrak{d})$. Thus, the same should be tried in the excess-3-case. For that purpose, for any move $M$ set

$$
\begin{aligned}
\#M(\mathfrak{d}) = &\,|\{0 \leq r \leq R_f(\mathfrak{d}) - 1 : \text{ by WR the move } M^{-1} \text{ is applied to } \mathfrak{d} \text{ in WR}^r(f)\}| \\
&+ |\{0 \leq \ell \leq L_f(\mathfrak{d}) - 1 : \text{ by WL the move } M \text{ is applied to } \mathfrak{d} \text{ in WL}^\ell(f)\}|.
\end{aligned}
$$

Thus, $|\operatorname{Path}_f(\mathfrak{d})| = \sum_{i=1}^{3} \#M_i(\mathfrak{d}) + \sum_{j=4}^{9}(\#M_{j,b}(\mathfrak{d}) + \#M_{j,t}(\mathfrak{d})) + \sum_{i=6}^{7} \#M_{i,c}(\mathfrak{d})$ and in summary

$$
L_f(\mathfrak{d}) + R_f(\mathfrak{d}) = \sum_{i=1}^{3} \#M_i(\mathfrak{d}) + \sum_{j=4}^{9}(\#M_{j,b}(\mathfrak{d}) + \#M_{j,t}(\mathfrak{d})) + \sum_{i=6}^{7} \#M_{i,c}(\mathfrak{d}).
$$

Using the same ideas as in the excess-2-case would give the following:

CONJECTURE 2. *Let $u$, $v$ and $w$ be words that satisfy $\mathrm{exc}(u,v;w) = 3$. Furthermore, let $f \in T_{u,v}^w$ instable and $\mathfrak{d}$ a drifter in $f$. Then*

$$R_1(u^{R_f(\mathfrak{d})}) + L_0(v^{L_f(\mathfrak{d})}) + 1 = \sum_{i=1}^{3} \#M_i(\mathfrak{d}) + \sum_{j=4}^{9}(\#M_{j,b}(\mathfrak{d}) + \#M_{j,t}(\mathfrak{d})) + 2\sum_{i=6}^{7} \#M_{i,c}(\mathfrak{d}).$$

*In particular, $L_f(\mathfrak{d}) + R_f(\mathfrak{d}) \in \{R_1(u^{R_f(\mathfrak{d})}) + L_0(v^{L_f(\mathfrak{d})}), R_1(u^{R_f(\mathfrak{d})}) + L_0(v^{L_f(\mathfrak{d})}) + 1\}$.*

Conjecture 2 would imply that a drifter $\mathfrak{d}$ in a TFPL of excess 3 satisfies one of the following:

(4.10) $\qquad\qquad\qquad L_f(\mathfrak{d}) \leq L_0(v^{L_f(\mathfrak{d})})$ and $R_f(\mathfrak{d}) > R_1(u^{R_f(\mathfrak{d})})$;

(4.11) $\qquad\qquad\qquad L_f(\mathfrak{d}) > L_0(v^{L_f(\mathfrak{d})})$ and $R_f(\mathfrak{d}) \leq R_1(u^{R_f(\mathfrak{d})})$;

(4.12) $\qquad\qquad\qquad L_f(\mathfrak{d}) = L_0(v^{L_f(\mathfrak{d})})$ and $R_f(\mathfrak{d}) = R_1(u^{R_f(\mathfrak{d})})$.

To TFPLs $f$ of excess 3 in which no drifter $\mathfrak{d}$ satisfies $L_f(\mathfrak{d}) = L_0(v^{L_f(\mathfrak{d})})$ and $R_1(u^{R_f(\mathfrak{d})})$ at the same time, triples $(S(f), g(f), T(f)) \in G_{u,u^+} \times S_{u^+,v^+}^w \times G_{v^*,(v^+)^*}$ for appropriate words $u^+ \geq u$ and $v^+ \geq v$ may be assigned analogous as in the excess-2-case. Thus, solely TFPLs $f$ of excess 3 that contain a drifter $\mathfrak{d}$ that satisfies $L_f(\mathfrak{d}) = L_0(v^{L_f(\mathfrak{d})})$ and $R_f(\mathfrak{d}) = R_1(u^{R_f(\mathfrak{d})})$ will be considered in the following. It will turn out that some of these TFPLs are counted twice and some once by the right side in (4.1).

To begin with, observe that in a TFPL of excess 3 the preimage of the move $M_6$ (*resp.* $M_7$) must be part of the left (*resp.* right) configuration in Figure 4.15 by Theorem 2.12. Since in both configurations in Figure 4.15 the connectivity of the vertices of degree 1 is the same the following holds:

REMARK 4.23. Let $u$, $v$ and $w$ be words such that $\mathrm{exc}(u,v;w) = 3$. Then TFPLs with boundary $(u,v;w)$ that contain the preimage of the move $M_6$ are in one-to-one correspondence with TFPLs with boundary $(u,v;w)$ that contain the preimage of the move $M_7$.
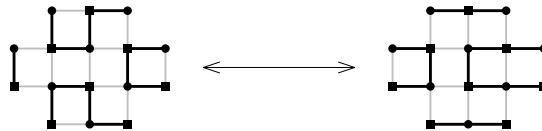


FIGURE 4.15. The correspondence between TFPLs of excess 3 that contain the preimage of the move $M_6$ and those that contain the preimage of the move $M_7$.

In the following, let $f \in T_{u,v}^w$ such that (4.12) holds for a drifter $\mathfrak{d}$ in $f$. Then either $\mathrm{WL}^\ell(f)$ for an $\ell \geq 0$ or $\mathrm{WR}^r(f)$ for an $r > 0$ contains the preimage of the move $M_6$ or $M_7$.
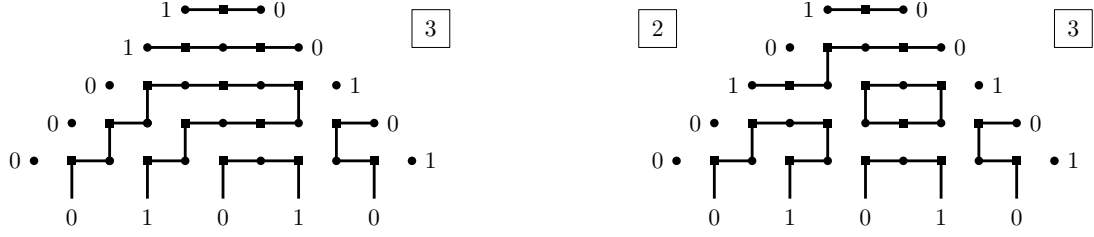
FIGURE 4.16. The two triples that give the framed TFPL in Figure 4.14.

To begin with, if $\text{WL}^\ell(f)$ contains the preimage of the move $M_6$ for an $\ell \geq 0$ then $f$ may be associated with two triples by moving all drifters to the right boundary or by moving $\mathfrak{d}$ to the left boundary and the remaining drifters to the right boundary and deleting them there. For instance, the framed TFPL in Figure 4.14 can be associated with the two triples depicted in Figure 4.16.

On the other hand, $\text{WL}^\ell(f)$ corresponds to a TFPL $f' \in T_{u,v}^w$ that contains the preimage of the move $M_7$ by Remark 4.23. Furthermore, the drifter $\mathfrak{d}'$ satisfies (4.12) in $\text{WR}^{\ell+1}(f')$. This is why $\text{WR}^{\ell+1}(f')$ can be associated with a triple in $\bigcup_{u^+,v^+} G_{u,u^+} \times S_{u^+,v^+}^w \times G_{v^*,(v^+)^*}$ by moving $\mathfrak{d}'$ to the left boundary and deleting it there. Figure 4.17 displays the TFPL that corresponds to the framed TFPL in Figure 4.14 by Remark 4.23. In addition, it depicts the triple in $\bigcup_{u^+,v^+} G_{00101,u^+} \times S_{u^+,v^+}^0 1010 \times G_{00011^*,(v^+)^*}$ that is associated with that TFPL.
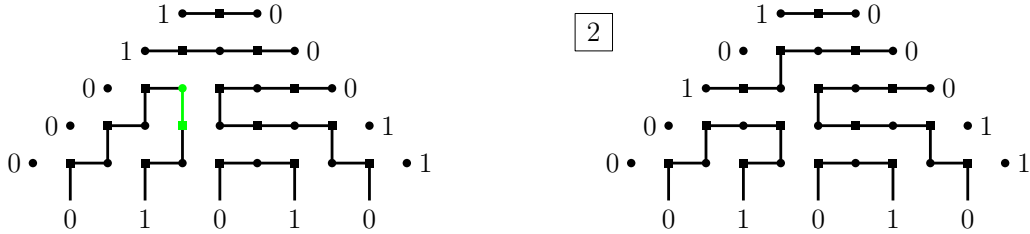


FIGURE 4.17. The TFPL corresponding to the framed TFPL in Figure 4.14 and the triple that is associated with it.

Finally, in $\text{WL}(f')$ the topmost drifter $\mathfrak{d}_t$ in the image of the move $M_7$ must fulfil $R_{\text{WL}(f')}(\mathfrak{d}_t) = R_1(u^{R_{\text{WL}(f')}(\mathfrak{d}_t)}) + \ell + 2$ and therefore $L_{\text{WL}(f')}(\mathfrak{d}_t) = L_0(v^{L_{\text{WL}(f')}(\mathfrak{d}_t)}) - \ell - 1$ by Conjecture 2. In summary,

$$L_{\text{WR}^{\ell+1}(f')}(\mathfrak{d}_t) = \ell + 2 + L_0(v^{L_{\text{WR}^{\ell+1}(f')}(\mathfrak{d}_t)}) - \ell - 1 = L_0(v^{L_{\text{WR}^{\ell+1}(f')}(\mathfrak{d}_t)}) + 1.$$

Thus, if $\mathfrak{d}'$ in $\text{WR}^{\ell+1}(f')$ was moved to the right boundary the entry of the cell corresponding to $\mathfrak{d}_t$ would have to be $L_0(v^{L_{\text{WR}^{\ell+1}(f')}(\mathfrak{d}_t)}) + 2$, which is permitted. This is why $\text{WR}^{\ell+1}(f')$ is associated with only one triple in $\bigcup_{u^+,v^+} G_{u,u^+} \times S_{u^+,v^+}^w \times G_{v^*,(v^+)^*}$. In summary, $f$ and $\text{WR}^{\ell+1}(f')$ may in total be associated with <u>three</u> triples in $\bigcup_{u^+,v^+} G_{u,u^+} \times S_{u^+,v^+}^w \times G_{v^*,(v^+)^*}$.

By vertical symmetry it follows that if $\text{WR}^r(f)$ contains the preimage of the move $M_6$ for an $r > 1$ then $f$ is associated with only one triple in $\bigcup_{u^+,v^+} G_{u,u^+} \times S^w_{u^+,v^+} \times G_{v^*,(v^+)^*}$. Furthermore, $\text{WR}^r(f)$ corresponds to a TFPL $f'$ in $T^w_{u,v}$ that contains the preimage of the move $M_7$ by Remark 4.23. Thus, $\text{WL}^{r-1}(f')$ contains a drifter $\mathfrak{d}'$ that satisfies (4.12) and is associated with two triples in $\bigcup_{u^+,v^+} G_{u,u^+} \times S^w_{u^+,v^+} \times G_{v^*,(v^+)^*}$. For those reasons, $f$ and $\text{WL}^{r-1}(f')$ may in total be associated with <u>three</u> triples in $\bigcup_{u^+,v^+} G_{u,u^+} \times S^w_{u^+,v^+} \times G_{v^*,(v^+)^*}$.

Finally, if $\text{WR}(f)$ contains the preimage of the move $M_6$ then it is easy to check that $f$ is associated with only one triple in $\bigcup_{u^+,v^+} G_{u,u^+} \times S^w_{u^+,v^+} \times G_{v^*,(v^+)^*}$. Furthermore, the same is true for the TFPL $\text{WL}(f')$ where $f'$ is the TFPL corresponding to $\text{WR}(f)$ due to Remark 4.23. However, the existence of $f$ is equivalent to the existence of a triple in $\bigcup_{u^+,v^+} G_{u,u^+} \times S^w_{u^+,v^+} \times G_{v^*,(v^+)^*}$ that cannot be assigned a TFPL of excess 3 by $\Psi$. The stable TFPL of that triple is obtained from $f$ by performing the transformation



and thereafter moving the leftmost (*resp.* rightmost) drifter to the left (*resp.* right) boundary. Furthermore, the tableau $T$ is the tableau of skew shape $\lambda(u^{R_f(\mathfrak{d})})/\lambda(u)$ with entry $R_1(u^{R_f(\mathfrak{d})})+1$ and the tableau $S$ is the tableau of skew shape $\lambda(v^{L_f(\mathfrak{d})})^*/\lambda(v)^*$ with entry $L_0(v^{L_f(\mathfrak{d})})+1$. For instance, the triple in Figure 4.18 is such a triple. Furthermore, the TFPL with boundary $(0011, 0011; 1010)$ that entails the existence of that triple is depicted in Figure 4.18. In summary, $f$ and $\text{WL}(f')$ are in total associated with three triples in $\bigcup_{u^+,v^+} G_{u,u^+} \times S^w_{u^+,v^+} \times G_{v^*,(v^+)^*}$.



FIGURE 4.18. Left: the TFPL with boundary $(0011, 0011; 1010)$ that contains a drifter that satisfies (4.12) and whose image under WR contains the preimage of the move $M_6$; right: the triple to which a TFPL with boundary $(0011, 0011; 1010)$ cannot be assigned by $\Phi$.

Analogous observations can be made if $\text{WL}^\ell(f)$ for an $\ell \geq 0$ or $\text{WR}^r(f)$ for an $r > 0$ contains the preimage of the $M_7$. Thus, the following weighted enumeration of TFPLs seems natural:

DEFINITION 4.24. *Let $f$ be a TFPL. Then denote the number of occurrences of the cells $\mathfrak{o}_{15}$ (that is, the cell* ⬜ *) in $f$ by $\mathfrak{o}_{15}(f)$. Furthermore, set*

$$t^w_{u,v}(q) = \sum_{f \in T^w_{u,v}} q^{\mathfrak{o}_{15}(f)}.$$

CONJECTURE 3. *Let $u$, $v$ and $w$ be words of length $N$ such that $|u|_1 = |v|_1 = |w|_1$ and $\mathrm{exc}(u,v;w) = 3$. Furthermore, set $N_1 = |u|_1$. Then*

$$(4.13) \qquad t^w_{u,v}(2) = \sum_{\substack{u^+,v^+ : u^+ \geq u,\, v^+ \geq v \\ |u^+|_1 = |v^+|_1 = N_1}} g_{u,u^+}\, g_{v^*,(v^+)^*}\, s^w_{u^+,v^+}.$$

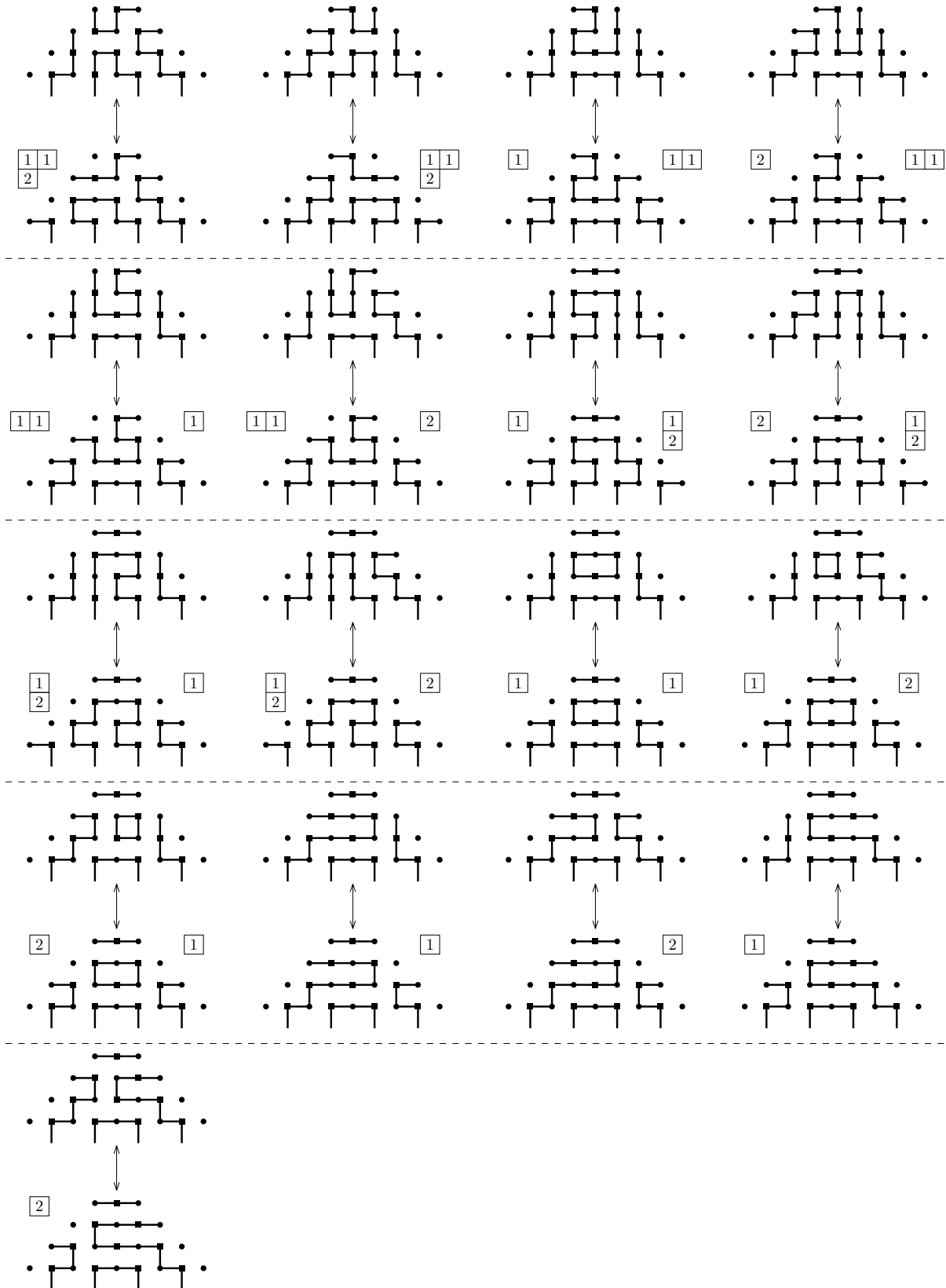Observe that (4.13) is true for $u = 0011$, $v = 0011$ and $w = 1010$.

FIGURE 4.19. The instable TFPLs with boundary $(0011, 0011; 1010)$.

# Hexagonal fully packed loop configurations

In this chapter we introduce fully packed loop configurations of hexagonal shape (HF-PLs) as the generalisation of triangular fully packed loop configurations. The first main result of this chapter establishes necessary conditions for the boundary $(\mathsf{l_T}, \mathsf{t}, \mathsf{r_T}; \mathsf{l_B}, \mathsf{b}, \mathsf{r_B})$ of an HFPL. The inequality $\mathrm{d}(\mathsf{r_B}) + \mathrm{d}(\mathsf{b}) + \mathrm{d}(\mathsf{l_B}) \geq \mathrm{d}(\mathsf{l_T}) + \mathrm{d}(\mathsf{t}) + \mathrm{d}(\mathsf{r_T}) + |\mathsf{l_T}|_1 |\mathsf{t}|_0 + |\mathsf{t}|_1 |\mathsf{r_T}|_0 + |\mathsf{r_B}|_0 |\mathsf{l_B}|_1$ is an example of one such condition (here $|\cdot|_i$ denotes the number of occurrences of $i$ and $\mathrm{d}(\cdot)$ denotes the number of inversions). It is the content of Theorem 5.11.

The other main results of this chapters are expressions in terms of Littlewood-Richardson coefficients for the numbers of HFPLs with boundary $(\mathsf{l_T}, \mathsf{t}, \mathsf{r_T}; \mathsf{l_B}, \mathsf{b}, \mathsf{r_B})$ such that $\mathrm{d}(\mathsf{r_B}) + \mathrm{d}(\mathsf{b}) + \mathrm{d}(\mathsf{l_B}) - \mathrm{d}(\mathsf{l_T}) - \mathrm{d}(\mathsf{t}) - \mathrm{d}(\mathsf{r_T}) - |\mathsf{l_T}|_1 |\mathsf{t}|_0 - |\mathsf{t}|_1 |\mathsf{r_T}|_0 - |\mathsf{r_B}|_0 |\mathsf{l_B}|_1 = 0, 1$. They can be found in Theorem 5.35 and Theorem 5.49.

The content of this chapter was published in [**5**].

## 5.1. Hexagonal fully packed loop configurations

In this section the main objects of this thesis are introduced, namely hexagonal FPLs. From now on, let $K, L, M$ and $N$ be non-negative integers such that $K \leq M + N$ and $N \leq K + L$. Furthermore, let

$$\mathsf{H}^{K,L,M,N} = \{(x,y) \in \mathbb{R}^2 : y \leq x, y \leq K - 1, y \leq -x + 2(K+L),$$
$$y \geq -x - 1, y \geq -M - N + K, y \geq x - 2(M+L) - 1\}.$$

DEFINITION 5.1. *The graph $H^{K,L,M,N}$ is defined as the induced subgraph of the square grid with vertex set $\mathsf{H}^{K,L,M,N} \cap \mathbb{Z}^2$.*
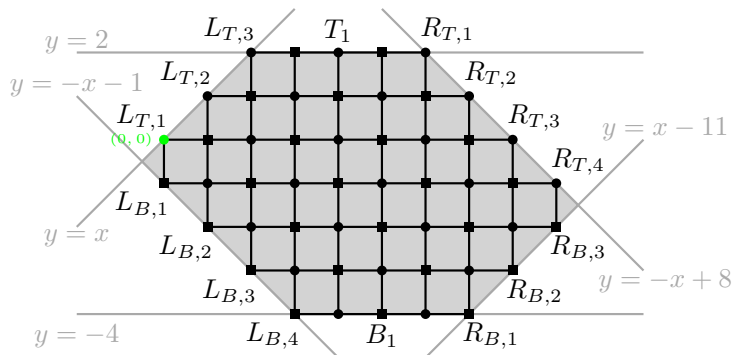


FIGURE 5.1. The graph $H^{3,1,4,3}$.

In Figure 5.1, the graph $H^{3,1,4,3}$ is depicted. From now on, the vertices of $H^{K,L,M,N}$ are partitioned into *odd* and *even* vertices in a chessboard manner such that the vertices which lie on the lines $y = x$ and $y = -x + 2(K + L)$ are odd and those which lie on the lines $y = -x - 1$ and $y = x - 2(M + L) - 1$ are even. In the pictures, odd vertices are illustrated by circles and even vertices by squares. Some vertices of $H^{K,L,M,N}$ are of special interest:

$\mathcal{L}_T = \{L_{T,1}, \ldots, L_{T,K}\}$: the leftmost vertices of the $K$ topmost rows;

$\mathcal{R}_T = \{R_{T,1}, \ldots, R_{T,M}\}$: the rightmost vertices of the $M$ topmost rows;

$\mathcal{T} = \{T_1, \ldots, T_L\}$: the odd vertices of the top row that are not in $\mathcal{L}_T \cup \mathcal{R}_T$;

$\mathcal{L}_B = \{L_{B,1}, \ldots, L_{B,M+N-K}\}$: the leftmost vertices of the $M + N - K$ lowermost rows;

$\mathcal{R}_B = \{R_{B,1}, \ldots, R_{B,N}\}$: the rightmost vertices of the $N$ lowermost rows;

$\mathcal{B} = \{B_1, \ldots, B_{K+L-N}\}$: the even vertices of the bottom row that are not in $\mathcal{L}_B \cup \mathcal{R}_B$.

All vertices are numbered from left to right.

### 5.1.1. Hexagonal fully packed loop configurations.

DEFINITION 5.2. *A **hexagonal fully packed loop configuration** (HFPL) of size $(K, L, M, N)$ is a subgraph $f$ of $H^{K,L,M,N}$ which satisfies the following conditions:*

(1) *the vertices in $\mathcal{L}_B \cup \mathcal{L}_T \cup \mathcal{R}_B \cup \mathcal{R}_T$ are of degree 0 or 1;*

(2) *the vertices in $\mathcal{T} \cup \mathcal{B}$ are of degree 1;*

(3) *all other vertices of $H^{K,L,M,N}$ are of degree 2;*

(4) *a path in $f$ neither joins two vertices in $\mathcal{L}_B \cup \mathcal{L}_T$ nor two vertices in $\mathcal{R}_B \cup \mathcal{R}_T$.*
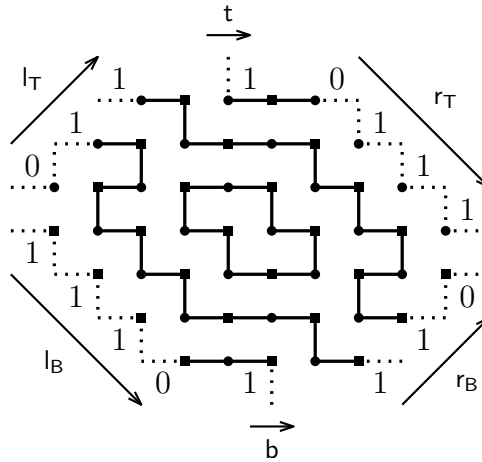


FIGURE 5.2. A hexagonal fully packed loop configuration of size $(3, 1, 4, 3)$.

REMARK 5.3. TFPLs of size $n$ appear as a subset of HFPLs when considered HFPLs of size $(n, 0, n, 0)$.

An example of an HFPL is given in Figure 5.2. Later, local configurations around each vertex of an HFPL are considered. It then will be necessary that each vertex of an HFPL is of degree 2. To achieve that, external edges along each boundary of an HFPL are attached as follows: given an HFPL $f$ to each vertex in $\mathcal{B} \cup \mathcal{T}$ a vertical external edge is attached, to each vertex in $\mathcal{L}_B \cup \mathcal{L}_T \cup \mathcal{R}_B \cup \mathcal{R}_T$ of degree 1 a horizontal external edges is attached and to each vertex in $\mathcal{L}_B \cup \mathcal{L}_T \cup \mathcal{R}_B \cup \mathcal{R}_T$ of degree 0 both a horizontal and a vertical edge are attached. The HFPL $f$ with the external edges attached will be denoted by $\overline{f}$. In the figures, the external edges will be represented by dotted lines.

In an HFPL non-closed paths have their extremities in $\mathcal{L}_T \cup \mathcal{T} \cup \mathcal{R}_T \cup \mathcal{R}_B \cup \mathcal{B} \cup \mathcal{L}_B$. In the following, HFPLs will be considered according to a sextuple $(\mathsf{l_T}, \mathsf{t}, \mathsf{r_T}; \mathsf{l_B}, \mathsf{b}, \mathsf{r_B})$ of words. This sextuple, on the one hand, encodes whether a vertex in $\mathcal{L}_B \cup \mathcal{L}_T \cup \mathcal{R}_B \cup \mathcal{R}_T$ is of degree 0 or 1. On the other hand, for vertices in $\mathcal{B} \cup \mathcal{T}$ it encodes with which other vertex on the boundary it is connected.

DEFINITION 5.4. *To each HFPL $f$ of size $(K, L, M, N)$ is assigned a sextuple of words $(\mathsf{l_T}, \mathsf{t}, \mathsf{r_T}; \mathsf{l_B}, \mathsf{b}, \mathsf{r_B})$ of lengths $(K, L, M; M + N - K, K + L - N, N)$ respectively in the following way:*

   ($\mathsf{l_T}$) *if the vertex $L_{T,i} \in \mathcal{L}_T$ is of degree 1, set $(\mathsf{l_T})_i = 1$, otherwise, set $(\mathsf{l_T})_i = 0$;*
   ($\mathsf{t}$) *if the vertex $T_i \in \mathcal{T}$ is connected with a vertex in $\mathcal{L}_T \cup \mathcal{L}_B \cup \mathcal{B}$ or a vertex $T_h$ in $\mathcal{T}$ for an $h < i$, set $\mathsf{t}_i = 0$, otherwise, set $\mathsf{t}_i = 1$;*
   ($\mathsf{r_T}$) *if the vertex $R_{T,i} \in \mathcal{R}_T$ is of degree 1, set $(\mathsf{r_T})_i = 0$, otherwise, set $(\mathsf{r_T})_i = 1$;*
   ($\mathsf{l_B}$) *if the vertex $L_{B,i} \in \mathcal{L}_B$ is of degree 1, set $(\mathsf{l_B})_i = 0$, otherwise, set $(\mathsf{l_B})_i = 1$;*
   ($\mathsf{b}$) *if the vertex $B_i \in \mathcal{B}$ is connected with a vertex in $\mathcal{R}_T \cup \mathcal{R}_B \cup \mathcal{T}$ or a vertex $B_j$ in $\mathcal{B}$ for a $j > i$, set $\mathsf{b}_i = 0$, otherwise, set $\mathsf{b}_i = 1$;*
   ($\mathsf{r_B}$) *if the vertex $R_{B,i} \in \mathcal{R}_B$ is of degree 1, set $(\mathsf{r_B})_i = 1$, otherwise, set $(\mathsf{r_B})_i = 0$.*

*The HFPL $f$ then is said to have **boundary** $(\mathsf{l_T}, \mathsf{t}, \mathsf{r_T}; \mathsf{l_B}, \mathsf{b}, \mathsf{r_B})$. Furthermore, the set of HFPLs with boundary $(\mathsf{l_T}, \mathsf{t}, \mathsf{r_T}; \mathsf{l_B}, \mathsf{b}, \mathsf{r_B})$ is denoted by $H_{\mathsf{l_B}, \mathsf{b}, \mathsf{r_B}}^{\mathsf{l_T}, \mathsf{t}, \mathsf{r_T}}$ and its cardinality by $h_{\mathsf{l_B}, \mathsf{b}, \mathsf{r_B}}^{\mathsf{l_T}, \mathsf{t}, \mathsf{r_T}}$.*

REMARK 5.5. A TFPL with boundary $(u, v; w)$ when considered an HFPL of size $(n, 0, n, 0)$ has boundary $(u, \varepsilon, v; \varepsilon, w, \varepsilon)$ where $\varepsilon$ denotes the empty word.

The HFPL depicted in Figure 5.2 has boundary $(011, 1, 0111; 1110, 1, 110)$. As from now, to an HFPL of size $(K, L, M, N)$ a pair of extended link patterns $(\pi_b, \pi_t)$ (where $\pi_b$ is an extended link pattern on $\{1, \ldots, K + L - N\}$ and $\pi_t$ an extended link pattern on $\{1, \ldots, L\}$) is assigned as follows:

   ($\pi_b$) for all $B_i, B_j \in \mathcal{B}$ which are linked by a path in $f$ let $\{i, j\} \in \pi_b$; for all $B_\ell \in \mathcal{B}$ which are connected with a vertex in $\mathcal{L}_B \cup \mathcal{L}_T$ let $\ell$ be a left point of $\pi_b$; for all $B_r \in \mathcal{B}$ which are connected with a vertex in $\mathcal{T} \cup \mathcal{R}_T \cup \mathcal{R}_B$ let $r$ be a right point of $\pi_b$.

($\pi_t$) for all $T_i, T_j \in \mathcal{T}$ which are linked by a path in $f$ let $\{i, j\} \in \pi_t$; for all $T_\ell \in \mathcal{T}$ which are connected with a vertex in $\mathcal{L}_B \cup \mathcal{L}_T \cup \mathcal{B}$ let $\ell$ be a left point of $\pi_t$; for all $T_r$ which are connected with a vertex in $\mathcal{R}_T \cup \mathcal{R}_B$ let $r$ be a right point of $\pi_t$.

In Figure 5.3 an example of an HFPL and its associated pair of extended link patterns is given. For any HFPL in $H_{l_B,b,r_B}^{l_T,t,r_T}$ with extended link patterns $\pi_b$ and $\pi_t$, it holds $\mathbf{w}(\pi_b) = \mathsf{b}$ and $\mathbf{w}(\pi_t) = \bar{\mathsf{t}}$.
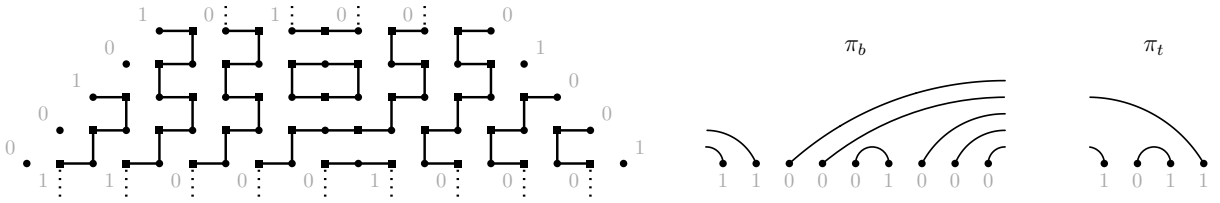


FIGURE 5.3. An HFPL of size $(5, 4, 5, 0)$ with boundary $(00101, 0100, 01001; \varepsilon, 110001000, \varepsilon)$ and its associated pair of extended link patterns.

### 5.1.2. Oriented hexagonal fully packed loop configurations.

The definition of HFPLs contains global conditions, as do the definitions of the top and the bottom boundary. These global conditions can be omitted when adding an orientation to each edge of an HFPL.

DEFINITION 5.6. *An **oriented HFPL** of size $(K, L, M, N)$ is an HFPL of the same size together with an orientation of each edge such that each vertex of degree $2$ is incident to an incoming and an outgoing edge, each edge attached to a vertex in $\mathcal{L}_T \cup \mathcal{L}_B$ is outgoing and each edge attached to a vertex in $\mathcal{R}_T \cup \mathcal{R}_B$ is incoming.*

REMARK 5.7. Oriented TFPLs of size $n$ appear as subsets of oriented HFPLs when considered oriented HFPLs of size $(n, 0, n, 0)$.

In Figure 5.4, an example of an oriented HFPL is given. The condition that in an oriented HFPL edges attached to a vertex in $\mathcal{L}_T \cup \mathcal{L}_B$ (*resp.* $\mathcal{R}_T \cup \mathcal{R}_B$) are outgoing (*resp.* incoming) guarantees that in the underlying HFPL a path does not connect two vertices in $\mathcal{L}_T \cup \mathcal{L}_B$ (*resp.* $\mathcal{R}_T \cup \mathcal{R}_B$). This is why in the definition of the underlying HFPL of an oriented HFPL the fourth condition can be omitted.

DEFINITION 5.8. *To each oriented HFPL its **boundary** $(l_T, t, r_T; l_B, b, r_B)$ is assigned as follows:*

($l_T$) *if $L_{T,i} \in \mathcal{L}_T$ has out-degree 1, then $(l_T)_i = 1$, otherwise, $(l_T)_i = 0$;*

(t) *if $T_i \in \mathcal{T}$ has in-degree 1, then $t_i = 0$, otherwise, $t_i = 1$;*

($r_T$) *if $R_{T,i} \in \mathcal{R}_T$ has in-degree 1, then $(r_T)_i = 0$, otherwise, $(r_T)_i = 1$;*

($r_B$) *if $R_{B,i} \in \mathcal{R}_B$ has in-degree 1, then $(r_B)_i = 1$, otherwise, $(r_B)_i = 0$;*

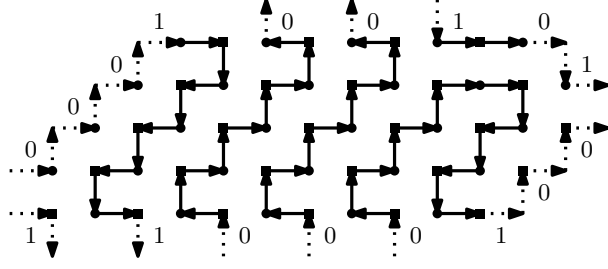(b) *if $B_i \in \mathcal{B}$ has in-degree 1, then $b_i = 1$, otherwise, $b_i = 0$;*

FIGURE 5.4. An oriented HFPL of size $(4, 3, 2, 3)$.

($\mathsf{l_B}$) *if $L_{B,i} \in \mathcal{L}_B$ has out-degree 1, then $(\mathsf{l_B})_i = 0$, otherwise, $(\mathsf{l_B})_i = 1$.*
*The set of oriented HFPLs with boundary $(\mathsf{l_T}, \mathsf{t}, \mathsf{r_T}; \mathsf{l_B}, \mathsf{b}, \mathsf{r_B})$ is denoted by $\overrightarrow{H}_{\mathsf{l_B}, \mathsf{b}, \mathsf{r_B}}^{\mathsf{l_T}, \mathsf{t}, \mathsf{r_T}}$ and its cardinality by $\overrightarrow{h}_{\mathsf{l_B}, \mathsf{b}, \mathsf{r_B}}^{\mathsf{l_T}, \mathsf{t}, \mathsf{r_T}}$.*

REMARK 5.9. An oriented TFPL with boundary $(u, v; w)$ when considered an oriented HFPL of size $(n, 0, n, 0)$ has boundary $(u, \varepsilon, v; \varepsilon, w, \varepsilon)$ where $\varepsilon$ denotes the empty word.

The oriented HFPL depicted in Figure 5.4 has boundary $(0001, 001, 01; 1, 1000, 100)$. For oriented HFPLs nice symmetries hold:

PROPOSITION 5.10.　　(1) *Vertical reflection together with the reorientation of all edges exchanges $\overrightarrow{H}_{\mathsf{l_B}, \mathsf{b}, \mathsf{r_B}}^{\mathsf{l_T}, \mathsf{t}, \mathsf{r_T}}$ and $\overrightarrow{H}_{\mathsf{r_B^*}, \mathsf{b^*}, \mathsf{l_B^*}}^{\mathsf{r_T^*}, \mathsf{t^*}, \mathsf{l_T^*}}$. Thus, $\overrightarrow{h}_{\mathsf{l_B}, \mathsf{b}, \mathsf{r_B}}^{\mathsf{l_T}, \mathsf{t}, \mathsf{r_T}} = \overrightarrow{h}_{\mathsf{r_B^*}, \mathsf{b^*}, \mathsf{l_B^*}}^{\mathsf{r_T^*}, \mathsf{t^*}, \mathsf{l_T^*}}$.*
(2) *Horizontal reflection exchanges $\overrightarrow{H}_{\mathsf{l_B}, \mathsf{b}, \mathsf{r_B}}^{\mathsf{l_T}, \mathsf{t}, \mathsf{r_T}}$ and $\overrightarrow{H}_{\overline{\mathsf{l_T}}, \overline{\mathsf{t}}, \overline{\mathsf{r_T}}}^{\overline{\mathsf{l_B}}, \overline{\mathsf{b}}, \overline{\mathsf{r_B}}}$. Thus, $\overrightarrow{h}_{\mathsf{l_B}, \mathsf{b}, \mathsf{r_B}}^{\mathsf{l_T}, \mathsf{t}, \mathsf{r_T}} = \overrightarrow{h}_{\overline{\mathsf{l_T}}, \overline{\mathsf{t}}, \overline{\mathsf{r_T}}}^{\overline{\mathsf{l_B}}, \overline{\mathsf{b}}, \overline{\mathsf{r_B}}}$.*

The first main result of this section contains necessary conditions for the boundary of an oriented HFPL and will be stated next:

THEOREM 5.11. *Let $(\mathsf{l_T}, \mathsf{t}, \mathsf{r_T}; \mathsf{l_B}, \mathsf{b}, \mathsf{r_B})$ be a sextuple of words of length $(K, L, M; M + N - K, K + L - N, N)$ respectively. Then $\overrightarrow{h}_{\mathsf{l_B}, \mathsf{b}, \mathsf{r_B}}^{\mathsf{l_T}, \mathsf{t}, \mathsf{r_T}} > 0$ implies:*
(1) $|\mathsf{l_T}|_0 + |\mathsf{t}|_0 = |\mathsf{r_B}|_0 + |\mathsf{b}|_0$ *and* $|\mathsf{t}|_1 + |\mathsf{r_T}|_1 = |\mathsf{b}|_1 + |\mathsf{l_B}|_1$;
(2) $\mathsf{l_T}\, \mathsf{t} \le \mathsf{b}\, \mathsf{r_B}$ *and* $\mathsf{t}\, \mathsf{r_T} \le \mathsf{l_B}\, \mathsf{b}$ *for the concatenations $\mathsf{l_T}\, \mathsf{t}$, $\mathsf{b}\, \mathsf{r_B}$, $\mathsf{t}\, \mathsf{r_T}$ and $\mathsf{l_B}\, \mathsf{b}$;*
(3) $\mathrm{d}(\mathsf{r_B}) + \mathrm{d}(\mathsf{b}) + \mathrm{d}(\mathsf{l_B}) \ge \mathrm{d}(\mathsf{l_T}) + \mathrm{d}(\mathsf{t}) + \mathrm{d}(\mathsf{r_T}) + |\mathsf{l_T}|_1 |\mathsf{t}|_0 + |\mathsf{t}|_1 |\mathsf{r_T}|_0 + |\mathsf{r_B}|_0 |\mathsf{l_B}|_1$.

In Section 5.4, a proof of Theorem 5.11 using a model bijective to oriented HFPLs will be given. Theorem 5.11 immediately implies necessary conditions for the boundary $(u, v; w)$ of an oriented TFPL when considering the oriented TFPL an oriented HFPL with boundary $(u, \varepsilon, v; \varepsilon, w, \varepsilon)$.

COROLLARY 5.12. *Let $u, v, w$ be words of length $N$. Then the existence of an oriented TFPL with boundary $(u, v; w)$ implies the following:*
(1) $|u|_0 = |v|_0 = |w|_0$;
(2) $u \le w$ *and* $v \le w$;
(3) $\mathrm{d}(u) + \mathrm{d}(v) \le \mathrm{d}(w)$.

There is a natural injection from $H_{l_B,b,r_B}^{l_T,t,r_T}$ to $\overrightarrow{H}_{l_B,b,r_B}^{l_T,t,r_T}$: given an HFPL in $H_{l_B,b,r_B}^{l_T,t,r_T}$, orient all its edges so that the conditions in Definition 5.6 are fulfilled; in addition, all closed paths shall be oriented clockwise, each path connecting two vertices $B_i, B_j$ in $\mathcal{B}$ shall be oriented from $B_i$ to $B_j$ if $i < j$, each path connecting two vertices $T_i, T_j$ in $\mathcal{T}$ shall be oriented from $T_i$ to $T_j$ if $i < j$ and each path connecting a vertex $B_i$ in $\mathcal{B}$ and a vertex $T_j$ in $\mathcal{T}$ shall be oriented from $B_i$ to $T_j$. Note that the chosen orientation ensures that b is indeed the bottom boundary word of the resulting oriented HFPL and t the top boundary word. Thus, it holds

$$(5.1) \qquad\qquad h_{l_B,b,r_B}^{l_T,t,r_T} \leq \overrightarrow{h}_{l_B,b,r_B}^{l_T,t,r_T}$$

for any $l_T, t, r_T, r_B, b, l_B$. Conversely, with each oriented HFPL a non-oriented HFPL can be associated by ignoring the orientation of the edges but this operation does not have to preserve the bottom and the top boundary words. In Section 5.3, the number $h_{l_B,b,r_B}^{l_T,t,r_T}$ will be deduced from a certain weighted enumeration of oriented HFPLs. From (5.1) the following corollary of Theorem 5.11 follows immediately:

COROLLARY 5.13. *The conclusions of Theorem 5.11 hold if* $h_{l_B,b,r_B}^{l_T,t,r_T} > 0$.

To each oriented HFPL a pair $(\overrightarrow{\pi_b}, \overrightarrow{\pi_t})$ of directed extended link patterns is assigned in the natural way. In Figure 5.5, an example of an oriented HFPL and its assigned pair of directed extended link patterns is given. Note that $\overrightarrow{\pi_b}$ has to be left-incoming and $\overrightarrow{\pi_t}$ has to be right-outgoing. Furthermore, for any oriented HFPL in $\overrightarrow{H}_{l_B,b,r_B}^{l_T,t,r_T}$ the source-sink-word of $\overrightarrow{\pi_b}$ equals b and the source-sink-word of $\overrightarrow{\pi_t}$ equals $\overline{t}$.
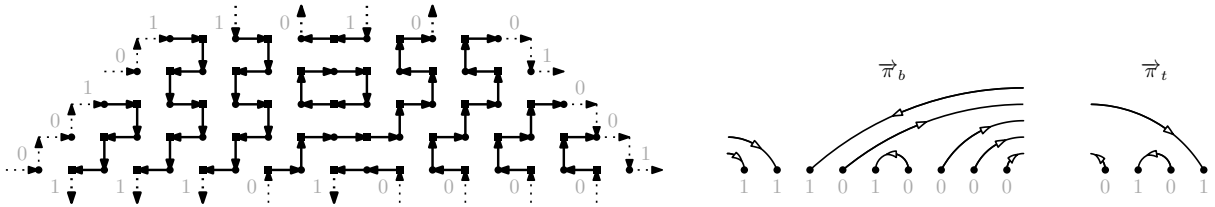


FIGURE 5.5. An oriented HFPL of size $(5, 4, 5, 0)$ together with its two corresponding oriented extended link patterns.

Later in this paper it will be needed that each vertex in an oriented HFPL is of degree 2. For that purpose, directed external edges are attached to an oriented HFPL $f$ as follows: first, external edges are attached to the underlying HFPL of $f$. Then an orientation is added to each external edge such that each vertex is incident to an incoming and an outgoing edge; furthermore, for vertices in $\mathcal{L}_T \cup \mathcal{L}_B$ that are incident to two external edges the horizontal edge shall be incoming and for vertices in in $\mathcal{R}_T \cup \mathcal{R}_B$ that are incident to two external edges the horizontal edge shall be outgoing. In the figures, the directed external edges are represented by dotted arrows.

## 5.2. Extended link patterns

A *link pattern* $\pi$ of size $2n$ is defined as a partition of $\{1, 2, \ldots, 2n\}$ into $n$ blocks of size 2 that are pairwise non-crossing that is there are no integers $i < j < k < l$ such that $\{i, k\}$ and $\{j, l\}$ are both in $\pi$. In the following, link patterns are represented by non-crossing arches between $2n$ aligned points. An example of a link pattern is given in Figure 5.6. It is a well known fact that link patterns of size $2n$ are in bijection with Dyck words of length $2n$: to a link pattern $\pi$ of size $2n$ the Dyck word $\omega$ of length $2n$ is assigned by setting $\omega_i = 0$ and $\omega_j = 1$ for each pair $\{i, j\}$ in $\pi$ with $i < j$. For example, the Dyck word corresponding to the link pattern depicted in Figure 5.6 is 001101000111. In this thesis, a more general notion of link patterns is needed.
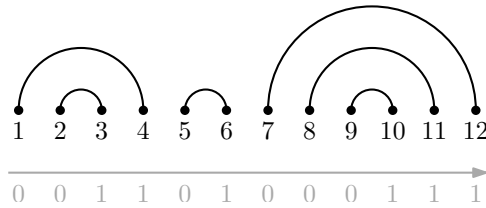


FIGURE 5.6. The link pattern $\{\{1, 4\}, \{2, 3\}, \{5, 6\}, \{7, 12\}, \{8, 11\}, \{9, 10\}\}$.

DEFINITION 5.14. *An **extended link pattern** $\pi$ on $\{1, \ldots, n\}$ is the data of integers*

$$1 \leq \ell_1 < \ell_2 < \cdots < \ell_i < r_1 < r_2 < \cdots < r_j \leq n$$

*together with a link pattern on each maximal interval of integers in $\{1, \ldots, n\}$ that does not contain any of the points $\ell_s$ or $r_t$. The integers $\ell_1, \ell_2, \ldots, \ell_i$ are said to be the **left points** of $\pi$ and the integers $r_1, r_2, \ldots, r_j$ are said to be the **right points** of $\pi$.*

In the figures, left and right points will be represented by attaching the extremity of an arch to the points $\ell_s$ and $r_t$ with the arch going left (*resp.* right) for a left point $\ell_s$ (*resp.* for a right point $r_t$). An example of an extended link pattern is given in Figure 5.7. To an extended link pattern $\pi$ with left points $\ell_1 < \ell_2 < \cdots < \ell_i$ and right points $r_1 < r_2 < \cdots < r_j$ a word $\omega = \mathbf{w}(\pi)$ is assigned as follows: as a start, set $\omega_{\ell_s} = 1$ for all $1 \leq s \leq i$ and $\omega_{r_t} = 0$ for all $1 \leq t \leq j$. Then associate each link pattern in $\pi$ with its corresponding Dyck word. For instance, the word assigned to the extended link pattern in Figure 5.7 is 1001101101010.

PROPOSITION 5.15. *The map $\mathbf{w}$ is a bijection from the set of extended link patterns on $\{1, \ldots, n\}$ to the set of words of length $n$.*

The proof of the previous proposition can be found in [**11**, Proposition 1.6]. In the course of this paper it will become necessary to consider *directed* extended link patterns that is extended link patterns together with an orientation of the arches. In the following, the number of arches in a directed link pattern $\overrightarrow{\pi}$ on $\{1, \ldots, n\}$ that connect two points
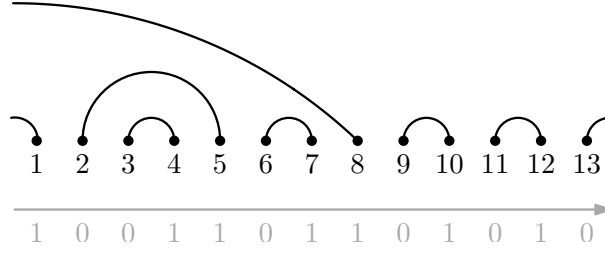
FIGURE 5.7. An extended link pattern with left points 1 and 8 and right point 13.

in $\{1, \ldots, n\}$ and are oriented from right to left is denoted by $RL(\overrightarrow{\pi})$. Furthermore, a point $i$ in a directed link pattern $\overrightarrow{\pi}$ on $\{1, \ldots, n\}$ is said to be a *source* if the arch attached to it is outgoing and a *sink* if the arch attached to it is incoming. To a directed extended link pattern $\overrightarrow{\pi}$ on $\{1, \ldots, n\}$ its *source-sink-word* $w = w_1 \cdots w_n$ is assigned as follows: for each $i$ from 1 to $n$ set $w_i = 0$ if $i$ is a source or $w_i = 1$ if $i$ is a sink. Finally, a directed extended link pattern is said to be *left-incoming* if all left points are sinks *resp. right-outgoing* if all right points are sources. An example of a right-outgoing directed extended link pattern is depicted in Figure 5.8. Its source-sink-word is 1010101010010.
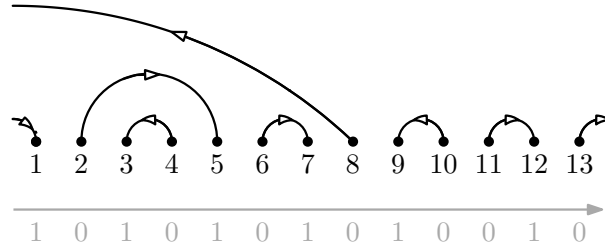


FIGURE 5.8. A directed extended link pattern with sources $2, 4, 6, 8, 10, 11, 13$ and sinks $1, 3, 5, 7, 9, 12$.

DEFINITION 5.16. (1) *A word $\omega'$ of size $n$ is* **feasible** *for a word $\omega$ of length $n$ if there exists a directed extended link pattern $\overrightarrow{\pi}$ with underlying extended link pattern $\mathbf{w}^{-1}(\omega')$ such that $\omega$ is the source-sink-word of $\overrightarrow{\pi}$. Such a $\overrightarrow{\pi}$ is unique and therefore one can define $g(\omega, \omega') = RL(\overrightarrow{\pi})$ for all words $\omega, \omega'$ such that $\omega'$ is feasible for $\omega$.*

(2) *A word $\omega'$ feasible for a word $\omega$ is said to be* **left-points-fixing** *if $\overrightarrow{\pi}$ is left-incoming resp.* **right-points-fixing** *if $\overrightarrow{\pi}$ is right-outgoing.*

For instance, the word 1001101101010 is feasible for 1010101010010; the latter is the source-sink word of the directed extended link pattern in Figure 5.8 and the former corresponds to the extended link pattern in Figure 5.7. Thus,

$$g(1010101010010, 1001101101010) = 2.$$

If a word $\omega'$ is left-points-fixing feasible for a word $\omega$, then $\omega_\ell = 1$ for each left point $\ell$ of $\overrightarrow{\pi}$. On the other hand, if $\omega'$ is right-points-fixing feasible for $\omega$, then $\omega_r = 0$ for each right point $r$ of $\overrightarrow{\pi}$.

## 5.3. Recovering HFPLs from oriented HFPLs

In this section the interplay between HFPLs and oriented HFPLs is studied. This is done by generalizing the study of the interplay between TFPLs and oriented TFPLs in [**11**].

**5.3.1. The weighted enumeration of oriented HFPLs.** The definition of the weight of an oriented HFPL is based on the following statistics on oriented HFPLs: for an oriented HFPL $f$ let $N^{\circlearrowright}(f)$ (*resp.* $N^{\circlearrowleft}(f)$) be the number of closed paths in $f$ that are oriented clockwise (*resp.* counter-clockwise) and set $RL_b(f) = RL(\overrightarrow{\pi_b})$ and $RL_t(f) = RL(\overrightarrow{\pi_t})$ where $\overrightarrow{\pi_b}$ and $\overrightarrow{\pi_t}$ are the two directed extended link patterns associated with $f$. Now, the weight of an oriented HFPL is defined as $q^{RL_b(f)-RL_t(f)+N^{\circlearrowright}(f)-N^{\circlearrowleft}(f)}$ which leads to the following weighted enumeration of oriented HFPLs:

$$(5.2) \qquad \overrightarrow{h}_{l_B,b,r_B}^{l_T,t,r_T}(q) = \sum_{f \in \overrightarrow{H}_{l_B,b,r_B}^{l_T,t,r_T}} q^{RL_b(f)-RL_t(f)} q^{N^{\circlearrowright}(f)-N^{\circlearrowleft}(f)}.$$

Next, an interpretation for the weight of an oriented HFPL in terms of numbers of occurrences of certain turns will be proved. To this end, a step is said to be of type $\mathbf{u}$ if it is a $(0,1)$-step, of type $\mathbf{d}$ if it is a $(0,-1)$-step, of type $\mathbf{r}$ if it is a $(1,0)$-step and of type $\mathbf{l}$ if it is a $(-1,0)$-step. Furthermore, a turn is said to be of type $\mathbf{dl}$ if it consists of a step of type $\mathbf{d}$ that is succeeded by a step of type $\mathbf{l}$. The types $\mathbf{ul}$, $\mathbf{lu}$, $\mathbf{ld}$, $\mathbf{dr}$, $\mathbf{ur}$, $\mathbf{ru}$ and $\mathbf{rd}$ of turns are defined analogously. In the following, set $R = \{\mathbf{dl}, \mathbf{lu}\}$ and $L = \{\mathbf{ld}, \mathbf{ul}\}$.
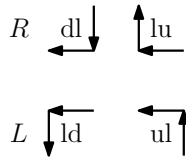


FIGURE 5.9. The four types of turns.

From now on, fix a turn $t_{\circlearrowleft} \in L$ and let $t_{\circlearrowright}$ be the turn in $R$ that is obtained by swapping the two steps in $t_{\circlearrowleft}$. The number of occurrences of turns of type $t_{\circlearrowleft}$ (*resp.* of type $t_{\circlearrowright}$) in an oriented subgraph $g$ of the square lattice $\mathbb{Z}^2$ shall be denoted by $t_{\circlearrowleft}(g)$ (*resp.* $t_{\circlearrowright}(g)$).

PROPOSITION 5.17. *Let $f$ be an oriented HFPL. Then*

$$t_{\circlearrowleft}(\overline{f}) - t_{\circlearrowright}(\overline{f}) = RL_b(f) - RL_t(f) + N^{\circlearrowright}(f) - N^{\circlearrowleft}(f).$$

PROOF. The proof of Proposition 5.17 is a generalisation of the proof of Proposition 2.4 in [11]. Essential for the proof is the following assertion that is given in [11, Corollary 2.3]: *for all directed closed self-avoiding paths $p$ on the square lattice, $t_{\circlearrowright}(p) - t_{\circlearrowleft}(p)$ equals -1 (resp. 1) if $p$ is oriented clockwise (resp. counter-clockwise).* Thus, it remains to evaluate $t_{\circlearrowright}(p) - t_{\circlearrowleft}(p)$ for the non-closed paths $p$ in $\overline{f}$. In the following, the external edges are considered part of the non-closed paths.

As a start, let $p$ be a non-closed path in $\overline{f}$ that connects two vertices in $\mathcal{T}$, see Figure 5.10 in a particular case. Then $p$ starts with a step of type **d** and ends with a step of type **u**. Now, $p$ is completed to a closed self-avoiding path $p'$ on the square lattice by adding a horizontal line above the configuration. If $p$ goes from $T_j$ to $T_i$ with $i < j$, then $p'$ is oriented clockwise and therefore $t_{\circlearrowright}(p') - t_{\circlearrowleft}(p') = -1$. Furthermore, the turns that appear in the exterior path are one turn of type **ur** and one of type **rd**. For that reason, $t_{\circlearrowright}(p') = t_{\circlearrowright}(p)$ and $t_{\circlearrowleft}(p') = t_{\circlearrowleft}(p)$. In summary, $-1 = t_{\circlearrowright}(p) - t_{\circlearrowleft}(p)$. On the other hand, if $p$ goes from $T_i$ to $T_j$ with $i < j$, then $p'$ is oriented counter-clockwise. Furthermore, the turns that occur in the exterior path are one turn of type **ul** and one of type **ld**. Therefore, $t_{\circlearrowleft}(p') = t_{\circlearrowleft}(p) + 1$ and $t_{\circlearrowright}(p') = t_{\circlearrowright}(p)$. In summary, $t_{\circlearrowright}(p) - t_{\circlearrowleft}(p) = 0$.
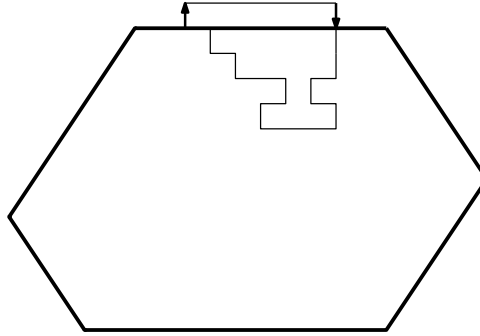


FIGURE 5.10. Closure of a path in an oriented HFPL.

Next, let $p$ be a non-closed path in $\overline{f}$ that connects a vertex in $\mathcal{B}$ and a vertex in $\mathcal{T}$. In that case, $p$ starts and ends either with a step of type **u** or with a step of type **d**. The non-closed path $p$ is completed to a closed self-avoiding path $p'$ on the square lattice by adding a path to the right of $\overline{f}$ with the least possible number of turns. If $p$ is oriented from the vertex in $\mathcal{B}$ to the vertex in $\mathcal{T}$, then $p'$ is oriented clockwise. Furthermore, the turns that appear in the exterior path are a turn of type **ur**, a turn of type **rd**, a turn of type **dl** and a turn of type **lu**. Thus, $t_{\circlearrowright}(p') = t_{\circlearrowright}(p)$ and $t_{\circlearrowleft}(p') = t_{\circlearrowleft}(p) + 1$. In summary, $t_{\circlearrowright}(p) - t_{\circlearrowleft}(p) = 0$. On the other hand if $p$ is oriented from the vertex in $\mathcal{T}$ to the vertex in $\mathcal{B}$, then $p'$ is oriented counter-clockwise and the turns that occur in the exterior path are a turn of type **dr**, a turn of type **ru**, a turn of type **ul** and a turn of type **ld**. Therefore, $t_{\circlearrowleft}(p') = t_{\circlearrowleft}(p) + 1$ and $t_{\circlearrowright}(p') = t_{\circlearrowright}(p)$. In summary, $t_{\circlearrowright}(p) - t_{\circlearrowleft}(p) = 0$.

Next, let $p$ be a non-closed path in $\overline{f}$ that goes from a vertex in $\mathcal{T}$ to a vertex in $\mathcal{R}_T \cup \mathcal{R}_B$. In that case $p$ starts with a step of type **d** and ends with a step of type **r**.

Now, $p$ is completed to a closed self-avoiding path $p'$ by adding a path above and to the right of $\overline{f}$ with the least possible number of turns. Then $p'$ is oriented counter-clockwise and the turns that occur in the exterior path are a turn of type $\mathbf{ru}$, a turn of type $\mathbf{ul}$ and a turn of type $\mathbf{ld}$. Therefore, $t_{\circlearrowleft}(p') = t_{\circlearrowleft}(p) + 1$ and $t_{\circlearrowright}(p') = t_{\circlearrowright}(p)$. In summary, $t_{\circlearrowleft}(p) - t_{\circlearrowright}(p) = 0$. The difference also vanishes if $p$ goes from a vertex in $\mathcal{T}$ to a vertex in $\mathcal{L}_B \cup \mathcal{L}_T$.

The remaining cases are covered by Proposition 2.4 in [**11**]. $\qquad\square$

Proposition 5.17 implies the following identity for the weighted enumeration of oriented HFPLs: let $t_{\circlearrowleft} \in L$ and $t_{\circlearrowright} \in R$ be the turn, that is obtained by swapping the two steps in $t_{\circlearrowleft}$. Then

$$\overrightarrow{h}^{\,l_T,t,r_T}_{l_B,b,r_B}(q) = \sum_{f \in \overrightarrow{H}^{\,l_T,t,r_T}_{l_B,b,r_B}} q^{t_{\circlearrowleft}(\overline{f}) - t_{\circlearrowright}(\overline{f})}.$$

**5.3.2. Deriving the number of ordinary HFPLs from the weighted enumeration of oriented HFPLs.** The goal of this subsection is to extract the number of HFPLs with boundary $(l_T, t, r_T; l_B, b, r_B)$ from the weighted enumeration of oriented HFPLs in (5.2). For that purpose, let $\overline{H}^{\,l_T,t,r_T}_{l_B,b,r_B}$ denote the subset of $\overrightarrow{H}^{\,l_T,t,r_T}_{l_B,b,r_B}$ that is made up of those oriented HFPLs whose associated directed link patterns $\overrightarrow{\pi_b}$ and $\overrightarrow{\pi_t}$ verify $RL(\overrightarrow{\pi_b}) = 0$ and $RL(\overrightarrow{\pi_t}) = 0$. Furthermore, let $\overline{h}^{\,l_T,t,r_T}_{l_B,b,r_B}(q)$ be the corresponding weighted enumeration, cf. (5.2). The following lemma relates $h^{l_T,t,r_T}_{l_B,b,r_B}$ to $\overline{h}^{\,l_T,t,r_T}_{l_B,b,r_B}(q)$:

LEMMA 5.18. *Let $\rho$ be a primitive sixth root of unity, so that $\rho$ satisfies $\rho + 1/\rho = 1$. Then*

$$\overline{h}^{\,l_T,t,r_T}_{l_B,b,r_B}(\rho) = h^{l_T,t,r_T}_{l_B,b,r_B}.$$

The proof of Lemma 5.18 is analogous to the proof of an analogous identity for TFPLs in [**11**, Proposition 2.5]. For that reason, the proof of Lemma 5.18 is omitted. Given an oriented HFPL $f$ in $\overrightarrow{H}^{\,l_T,t,r_T}_{l_B,b,r_B}$ consider the oriented HFPL $f'$ that is obtained from $f$ by orienting all paths in $f$ that connect two vertices in $\mathcal{B}$ or two vertices in $\mathcal{T}$ from left to right. The boundary of $f'$ then has to be $(l_T, t', r_T; l_B, b', r_B)$ for a word $b'$ that is left-points-fixing feasible for $b$ and a word $t'$ that is right-points-fixing feasible for $t$. Furthermore,

$$RL_b(f) - RL_t(f) + N^{\circlearrowleft}(f) - N^{\circlearrowright}(f) = g(b, b') - g(t, t') + N^{\circlearrowleft}(f') - N^{\circlearrowright}(f').$$

Therefore, the following holds:

$$(5.3) \qquad \overrightarrow{h}^{\,l_T,t,r_T}_{l_B,b,r_B}(q) = \sum_{\substack{t':\,t' \text{ right-points-fixing feasible for } t \\ b':\,b' \text{ left-points-fixing feasible for } b}} q^{-g(t,t')} q^{g(b,b')} \overline{h}^{\,r_B,b',l_B}_{l_T,t',r_T}(q).$$

In the following, the goal is to invert the relation in (5.3) in order to obtain an expression for the number of HFPLs in terms of the weighted enumeration with the help of Lemma 5.18.

DEFINITION 5.19.    (1) Let $M_b(n) = M$ be the square matrix of size $2^n$ which has rows and columns indexed by words of length $n$ and entry $M_{w,w'} = q^{g(w,w')}$ if $w'$ is left-points-fixing feasible for $w$ and entry $M_{w,w'} = 0$ otherwise.

(2) Let $M_t(n) = M$ be the square matrix of size $2^n$ which has rows and columns indexed by words of length $n$ and entry $M_{w,w'} = q^{-g(w,w')}$ if $w'$ is right-points-fixing feasible for $w$ and entry $M_{w,w'} = 0$ otherwise.

| | 000 | 001 | 010 | 100 | 011 | 101 | 110 | 111 |
|---|---|---|---|---|---|---|---|---|
| 000 | 1 | 0 | 0 | 0 | 0 | 0 | 0 | 0 |
| 001 | 1 | 1 | 0 | 0 | 0 | 0 | 0 | 0 |
| 010 | 1 | $q$ | 1 | 0 | 0 | 0 | 0 | 0 |
| 100 | 1 | 0 | $q$ | 1 | 0 | 0 | 0 | 0 |
| 011 | 1 | 0 | 1 | 0 | 1 | 0 | 0 | 0 |
| 101 | 1 | 1 | $q$ | 1 | $q$ | 1 | 0 | 0 |
| 110 | 1 | $q$ | 0 | 1 | 0 | $q$ | 1 | 0 |
| 111 | 1 | 0 | 0 | 1 | 0 | 0 | 1 | 1 |

| | 000 | 100 | 010 | 001 | 110 | 101 | 011 | 111 |
|---|---|---|---|---|---|---|---|---|
| 000 | 1 | 1 | 0 | 0 | 1 | 0 | 0 | 1 |
| 100 | 0 | 1 | $q^{-1}$ | 0 | 1 | 0 | $q^{-1}$ | 1 |
| 010 | 0 | 0 | 1 | $q^{-1}$ | 1 | $q^{-1}$ | 1 | 1 |
| 001 | 0 | 0 | 0 | 1 | 0 | 1 | 0 | 1 |
| 110 | 0 | 0 | 0 | 0 | 1 | $q^{-1}$ | 0 | 1 |
| 101 | 0 | 0 | 0 | 0 | 0 | 1 | $q^{-1}$ | 1 |
| 011 | 0 | 0 | 0 | 0 | 0 | 0 | 1 | 1 |
| 111 | 0 | 0 | 0 | 0 | 0 | 0 | 0 | 1 |

FIGURE 5.11. The matrices $M_b(3)$ (left) and $M_t(3)$ (right).

PROPOSITION 5.20. For any positive integer $n$ the matrices $M_b(n)$ and $M_t(n)$ are invertible.

PROOF. Throughout this proof, if $w'$ is feasible for $w$ let $\overrightarrow{\pi}$ be the unique directed extended link pattern with underlying extended link pattern $\mathbf{w}^{-1}(w')$ and source-sink word $w$.

It will first be proved that $M_b(n)$ is a lower triangular matrix with ones on the diagonal and therefore invertible. There are only ones on the diagonal of $M_b(n)$ because $q^{g(w,w)} = q^0 = 1$ for all words $w$ of length $n$. To show that $M_b(n)$ is lower triangular it is sufficient to find a linear order $\prec$ on the set of words of length $n$ that satisfies $w' \prec w$ whenever $w'$ is left-points-fixing feasible for $w$ and use it for the rows and columns of $M_b(n)$. First, note that if $w'$ is left-points-fixing feasible for $w$ and in $\overrightarrow{\pi}$ all right points are sinks then there exist ordered pairs $(i_1, j_1), (i_2, j_2), \ldots, (i_k, j_k)$ such that $w'_{i_s} = 0$, $w'_{j_s} = 1$, $w_{i_s} = 1$ and $w_{j_s} = 0$ for all $1 \leq s \leq k$ and $w_i = w'_i$ for all other indices. Thus, $|w'|_1 = |w|_1$ and $w' \leq w$ in that particular case. Now, given any two words $w$ and $w'$ of length $n$ such

that $w'$ is left-points-fixing feasible for $w$ then $|w|_1 - |w'|_1$ is the number of right points in $\overrightarrow{\pi}$ which are sinks. In particular, $|w|_1 \geq |w'|_1$. Hence, for to given words $w$ and $w'$ set $w' \preceq w$ if $|w'|_1 \leq |w|_1$ and in the case when $|w'|_1 = |w|_1$ if additionally $w' \leq w$. Then by $\preceq$ a partial order on the set of words of length $n$ is defined. Furthermore, for any two words $w$ and $w'$ of length $n$ such that $w'$ is left-points-fixing feasible for $w$ it follows $w' \preceq w$. Thus, for any linear order $\lhd$ on the set of words of length $n$ that extends $\preceq$ it holds that $w' \lhd w$ whenever $w'$ is left-points-fixing feasible for $w$.

The invertibility of $M_t(n)$ follows from the invertibility of $M_b(n)$ because they are related by rotation by $180°$ together with the inversion of the entries.

$\square$

COROLLARY 5.21. *Let* $\mathsf{l_T}$, $\mathsf{t}$, $\mathsf{r_T}$, $\mathsf{l_B}$, $\mathsf{b}$, $\mathsf{r_B}$) *be words of lengths* $K$, $L$, $M$, $M + N - K$, $K + L - N$, $N$ *respectively. Then*

$$\overline{h}^{\mathsf{l_T,t,r_T}}_{\mathsf{l_B,b,r_B}}(q) = \sum_{\mathsf{t',b'}} (M_b(K + L - N)^{-1})_{\mathsf{b,b'}} (M_t(L)^{-1})_{\mathsf{t,t'}} \overrightarrow{h}^{\mathsf{l_T,t',r_T}}_{\mathsf{l_B,b',r_B}}(q)$$

*and in particular*

$$h^{\mathsf{l_T,t,r_T}}_{\mathsf{l_B,b,r_B}} = \sum_{\mathsf{t',b'}} (M_b(K + L - N)^{-1})_{\mathsf{b,b'}} (M_t(L)^{-1})_{\mathsf{t,t'}} \overrightarrow{h}^{\mathsf{l_T,t',r_T}}_{\mathsf{l_B,b',r_B}}(\rho)$$

*where* $\rho$ *is a primitive sixth root of unity.*

## 5.4. Path tangles

In this section, hexagonal blue-red path tangles will be introduced which are in bijection with oriented HFPLs. Furthermore, proofs in terms of blue-red path tangles of the necessary conditions on the boundary of an oriented HFPL stated in Theorem 5.11 will be given.

**5.4.1. Path tangles.** For the definition of blue-red path tangles a new set of vertices is required: given non-negative integers $K$, $L$, $M$ and $N$ the vertices of a blue-red path tangle of size $(K, L, M, N)$ are the vertices in

$$V^{K,L,M,N} = \mathsf{H}^{K,L,M,N} \cap \{(x + \frac{1}{2}, y) : x,\, y \in \mathbb{Z}\}.$$

Note that $V^{K,L,M,N}$ is enclosed by the lines $y = x - \frac{1}{2}$, $y = K - 1$, $y = -x - \frac{1}{2} + 2(K + L)$, $y = -x - \frac{1}{2}$, $y = -M - N + K$ and $y = x - 2(M + L) - \frac{1}{2}$. An example is given in Figure 5.12. The vertices in $V^{K,L,M,N}$ are partitioned into *blue* and *red* vertices in a chessboard manner such that the vertices in $V^{K,L,M,N}$ that lie on the line $y = x - \frac{1}{2}$ or on the line $y = x - 2(M + L) - \frac{1}{2}$ are blue and the vertices that lie on the line $y = -x - \frac{1}{2}$ or on the line $y = -x - \frac{1}{2} + 2(K + L)$ are red. There are vertices in $V^{K,L,M,N}$ that play a special role:

- the $K + L$ blue vertices $\mathcal{E} = \{E_1, E_2, \ldots, E_{K+L}\}$ which lie on the line $y = x - \frac{1}{2}$ or on the line $y = K - 1$;
- the $K + L$ blue vertices $\mathcal{D} = \{D_1, D_2, \ldots, D_{K+L}\}$ which lie on the line $y = x - 2(M + L) - \frac{1}{2}$ or on the line $y = -M - N + K$;
- the $L + M$ red vertices $\mathcal{E}' = \{E_1', E_2', \ldots, E_{L+M}'\}$ which lie on the line $y = K - 1$ or on the line $y = -x - \frac{1}{2} + 2(K + L)$;
- the $L + M$ red vertices $\mathcal{D}' = \{D_1', D_2', \ldots, D_{L+M}'\}$ which lie on the line $y = -M - N + K$ or on the line $y = -x - \frac{1}{2}$.

All vertices are numbered from left to right.
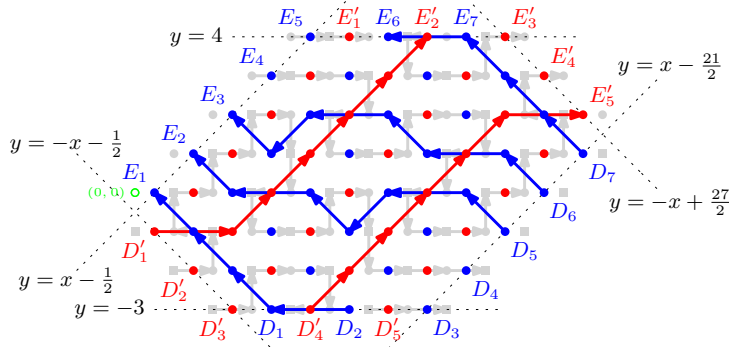


FIGURE 5.12. A hexagonal blue-red path tangle with boundary $(00011, 01, 001; 100, 10, 11000)$. The oriented HFPL it corresponds to is indicated in grey.

A *blue* path in a blue-red path tangle is defined to be a path that only uses steps $(-1, 1)$, $(-1, -1)$ and $(-2, 0)$, while a *red* path is defined to be a path that only uses steps $(1, 1)$, $(1, -1)$ and $(2, 0)$. From now on, the set of blue paths from $D_i$ to $E_j$ which never go below the line $y = -M - N + K$ and never above the line $y = K - 1$ is denoted by $\mathcal{P}(D_i, E_j)$ and the set of red paths from $D_{i'}'$ to $E_{j'}'$ which never go below the line $y = -M - N + K$ and never above the line $y = K - 1$ is denoted by $\mathcal{P}'(D_{i'}', E_{j'}')$.

Given a sextuple $(\mathsf{l_T}, \mathsf{t}, \mathsf{r_T}; \mathsf{l_B}, \mathsf{b}, \mathsf{r_B})$ of words of lengths $(K, L, M; M + N - K, K + L - N, N)$ respectively satisfying that

$$(5.4) \qquad |\mathsf{l_T}|_0 + |\mathsf{t}|_0 = |\mathsf{b}|_0 + |\mathsf{r_B}|_0 \qquad \text{and} \qquad |\mathsf{t}|_1 + |\mathsf{r_T}|_1 = |\mathsf{l_B}|_1 + |\mathsf{b}|_1.$$

denote the index of the $k$-th zero in the concatenation $\mathsf{b}\,\mathsf{r_B}$ (*resp.* by $j_k$) and the index of the $\ell$-th one in the concatenation $\mathsf{l_B}\,\mathsf{b}$ (*resp.* by $i_k$) by $i_\ell'$ (*resp.* by $j_\ell'$). Furthermore, denote the set of $(|\mathsf{l_T}|_0 + |\mathsf{t}|_0)$-tuples $(P_1, \ldots, P_{|\mathsf{l_T}|_0 + |\mathsf{t}|_0})$ of non-intersecting paths with $P_k \in \mathcal{P}(D_{i_k}, E_{j_k})$ by $\mathcal{P}(\mathsf{b}\,\mathsf{r_B}, \mathsf{l_T}\,\mathsf{t})$ and the set of $(|\mathsf{t}|_1 + |\mathsf{r_T}|_1)$-tuples $(P_1', \ldots, P_{|\mathsf{t}|_1 + |\mathsf{r_T}|_1}')$ of non-intersecting paths with $P_k' \in \mathcal{P}'(D_{i_k'}', E_{j_k'}')$ by $\mathcal{P}'(\mathsf{l_B}\,\mathsf{b}, \mathsf{t}\,\mathsf{r_T})$.

DEFINITION 5.22. *A pair* $(B, R) \in \mathcal{P}(\mathsf{b}\mathsf{r_B}, \mathsf{l_T}\mathsf{t}) \times \mathcal{P}'(\mathsf{l_B}\mathsf{b}, \mathsf{t}\mathsf{r_T})$ *is said to be a* **hexagonal blue-red path tangle with boundary** $(\mathsf{l_T}, \mathsf{t}, \mathsf{r_T}; \mathsf{l_B}, \mathsf{b}, \mathsf{r_B})$ *if it satisfies the following:*

(1) *no diagonal step of $R$ crosses a diagonal step of $B$;*

(2) *each middle point of a horizontal step of B (resp. of R) is used by a step in R (resp. B).*

*The set of blue-red path tangles with boundary* $(\mathsf{l_T}, \mathsf{t}, \mathsf{r_T}; \mathsf{l_B}, \mathsf{b}, \mathsf{r_B})$ *is denoted by* $\mathrm{BlueRed}(\mathsf{l_T}, \mathsf{t}, \mathsf{r_T}; \mathsf{l_B}, \mathsf{b}, \mathsf{r_B})$.

In Figure 5.12, a blue-red path tangle with boundary $(00011, 01, 001; 100, 10, 11000)$ is displayed. Hexagonal blue-red path tangles with boundary $(\mathsf{l_T}, \mathsf{t}, \mathsf{r_T}; \mathsf{l_B}, \mathsf{b}, \mathsf{r_B})$ encode oriented HFPLs with boundary $(\mathsf{l_T}, \mathsf{t}, \mathsf{r_T}; \mathsf{l_B}, \mathsf{b}, \mathsf{r_B})$: given an oriented HFPL $f \in \overrightarrow{H}_{\mathsf{l_B}, \mathsf{b}, \mathsf{r_B}}^{\mathsf{l_T}, \mathsf{t}, \mathsf{r_T}}$ blue vertices are added to $f$ in the middle of each horizontal line of $H^{K,L,M,N}$ having an odd left and an even right vertex and red vertices are added in the middle of each horizontal line of $H^{K,L,M,N}$ having an even left and an odd right vertex. Then blue and red arrows are added as indicated in Figure 5.13. After removing all vertices and edges
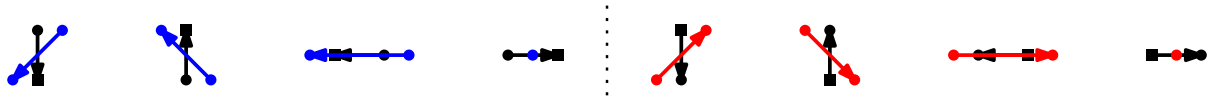


FIGURE 5.13. From oriented HFPLs to blue-red path tangles.

of $f$ a blue-red path tangle in $\mathrm{BlueRed}(\mathsf{l_T}, \mathsf{t}, \mathsf{r_T}; \mathsf{l_B}, \mathsf{b}, \mathsf{r_B})$ is obtained.

THEOREM 5.23. *Let* $(\mathsf{l_T}, \mathsf{t}, \mathsf{r_T}; \mathsf{l_B}, \mathsf{b}, \mathsf{r_B})$ *be a sextuple of words of lengths* $(K, L, M; M + N - K, K + L - N, N)$ *respectively. Then the map described above is a bijection between* $\overrightarrow{H}_{\mathsf{l_B}, \mathsf{b}, \mathsf{r_B}}^{\mathsf{l_T}, \mathsf{t}, \mathsf{r_T}}$ *and* $\mathrm{BlueRed}(\mathsf{l_T}, \mathsf{t}, \mathsf{r_T}; \mathsf{l_B}, \mathsf{b}, \mathsf{r_B})$.

In Figure 5.12, the oriented HFPL corresponding to the depicted blue-red path tangle is indicated in the same figure. The proof of Theorem 5.23 is omitted because its proof is analogous to the proof of Theorem 4.1 in [**11**]. From (5.4) and Theorem 5.23 the assertions of Theorem 5.11(1) follow immediately. Also the constraints on the boundary of an oriented HFPL stated in Theorem 5.11(2) now can be proved.

PROOF OF THEOREM 5.11(2). Let $f \in \overrightarrow{H}_{\mathsf{l_B}, \mathsf{b}, \mathsf{r_B}}^{\mathsf{l_T}, \mathsf{t}, \mathsf{r_T}}$ and $(B, R)$ its corresponding blue-red path tangle in $\mathrm{BlueRed}(\mathsf{l_T}, \mathsf{t}, \mathsf{r_T}; \mathsf{l_B}, \mathsf{b}, \mathsf{r_B})$. It will only be shown that $\mathsf{l_T}\,\mathsf{t} \leq \mathsf{b}\,\mathsf{r_B}$. To be more precise, it will be proved that $j_k \leq i_k$ for all $1 \leq k \leq |\mathsf{l_T}|_0 + |\mathsf{t}|_0$ which implies $\mathsf{l_T}\,\mathsf{t} \leq \mathsf{b}\,\mathsf{r_B}$. For that purpose, consider the $(|\mathsf{l_T}|_0 + |\mathsf{t}|_0)$-tuple $B = (P_1, \ldots, P_{|\mathsf{l_T}|_0 + |\mathsf{t}|_0})$
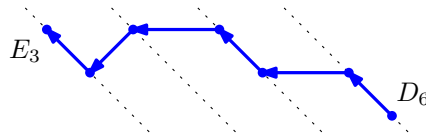


FIGURE 5.14. The path $P_3$ of the blue-red path tangle depicted in Figure 5.12.

of non-intersecting paths with $P_k \in \mathcal{P}(D_{i_k}, E_{j_k})$. Since for each $i = 1, \ldots, K + L$ the

vertices $D_i$ and $E_i$ both lie on the $i$-th Northwest-Southeast diagonal of blue vertices when counted from left the difference $i_k - j_k$ counts the $(-1, -1)$- and $(-2, 0)$-steps of $P_k$ for $k = 1, \ldots, |l_T|_0 + |t|_0$. This is why $i_k - j_k \geq 0$ for $k = 1, \ldots, |l_T|_0 + |t|_0$ which proves the assertion. $\qquad \square$

PROPOSITION 5.24. *For any oriented HFPL and blue-red path tangle with boundary* $(l_T, t, r_T; l_B, b, r_B)$ *respectively, the following two formulae hold:*

(1) $d(r_B) + d(b) + |r_B|_0 |b|_1 - d(l_T) - d(t) - |l_T|_1 |t|_0 = \blacksquare\!\!-\!\!\bullet \; + \; \big| = \bullet\!\!-\!\!\bullet \; + \; \diagup$ ;

(2) $d(b) + d(l_B) + |b|_0 |l_B|_1 - d(t) - d(r_T) - |t|_1 |r_T|_0 = \bullet\!\!-\!\!\blacksquare \; + \; \big| = \bullet\!\!-\!\!\blacktriangleright \; + \; \diagdown$ .

*Here,* $\blacksquare\!\!-\!\!\bullet$, *etc. denote the numbers of occurrences of the edge* $\blacksquare\!\!-\!\!\bullet$, *etc.*

PROOF. It follows from the proof of Theorem 5.11(2) that

$$\sum_{k=1}^{|l_T|_0 + |t|_0} (i_k - j_k) = \bullet\!\!-\!\!\bullet \; + \; \diagup .$$

On the other hand,

$$i_k - j_k = \# \text{ of } 1's \text{ among the first } i_k \text{ letters of } b\, r_B$$
$$- \# \text{ of } 1's \text{ among the first } j_k \text{ letters of } l_T\, t.$$

Thus,

$$\sum_{k=1}^{|l_T|_0 + |t|_0} (i_k - j_k) = d(b r_B) - d(l_T t) = d(r_B) + d(b) + |r_B|_0 |b|_1 - d(l_T) - d(t) - |l_T|_1 |t|_0,$$

which proves the first identity. The second identity follows analogously. $\qquad \square$

In the next subsection it will be necessary to regard blue-red path tangles together with *external* edges; given a path tangle $(B, R)$ to the vertices $E_{i_1}, \ldots, E_{i_{|l_T|_0 + |t|_0}}$ and $D_{j_1}, \ldots, D_{j_{|l_T|_0 + |t|_0}}$ $(-1, 1)$-steps are attached while to the vertices $E'_{i'_1}, \ldots, E'_{i'_{|t|_1 + |r_T|_1}}$ and $D'_{j'_1}, \ldots, D'_{j'_{|t|_1 + |r_T|_1}}$ $(1, 1)$-steps are attached. These external edges are consistent with the external edges attached to oriented HFPLs.

**5.4.2. The combinatorial interpretation of** $d(r_B) + d(b) + d(l_B) - d(l_T) - d(t) -$ $d(r_T) - |l_T|_1 |t|_0 - |t|_1 |r_T|_0 - |r_B|_0 |l_B|_1$. In this subsection, it will be shown that given an oriented HFPL in $\overline{H}_{l_B, b, r_B}^{l_T, t, r_T}$ by the quantity $d(r_B) + d(b) + d(l_B) - d(l_T) - d(t) - d(r_T) - |l_T|_1 |t|_0 -$ $|t|_1 |r_T|_0 - |r_B|_0 |l_B|_1$ the occurrences of certain local patterns are counted. Throughout this subsection, the numbers of occurrences of the local configurations $\blacksquare\!\!-\!\!\blacktriangleleft\!\!-\!\!\blacksquare$, etc. are denoted by $\blacksquare\!\!-\!\!\blacktriangleleft\!\!-\!\!\blacksquare$, etc.

For oriented TFPLs with boundary $(u, v; w)$ when considered HFPLs with boundary $(u, \varepsilon, v; \varepsilon, w, \varepsilon)$ Theorem 5.11 implies the following:

**COROLLARY 5.26.** *For any oriented TFPL with boundary $(u, v; w)$ the following holds:*

$$\mathrm{d}(w) - \mathrm{d}(u) - \mathrm{d}(v) = \;\blacksquare + \;\blacksquare + \;\blacksquare\!-\!\blacksquare + \;\blacksquare\!-\!\bullet + \;\blacksquare + \;\blacksquare + \;\blacksquare + \;\blacksquare \,.$$

The proof of Theorem 5.25 is done in terms of blue-red path tangles. To show (5.5), further identities for blue-red path tangles are needed.

**DEFINITION 5.27.** *In a blue-red path tangle a pair $(b, r)$ consisting of a blue path $b$ and a red path $r$ is said to be **intersecting** if $b$ and $r$ intersect at least once.*

The number of intersecting pairs of an element in $\mathrm{BlueRed}(\mathsf{l_T}, \mathsf{t}, \mathsf{r_T}; \mathsf{l_B}, \mathsf{b}, \mathsf{r_B})$, on the one hand, can be derived from $\mathsf{l_T}, \mathsf{t}, \mathsf{r_T}, \mathsf{l_B}, \mathsf{b}, \mathsf{r_B}$ and, on the other hand, can be expressed in terms of numbers of occurrences of certain local configurations.

**LEMMA 5.28.** *For any blue-red path tangle in $\mathrm{BlueRed}(\mathsf{l_T}, \mathsf{t}, \mathsf{r_T}; \mathsf{l_B}, \mathsf{b}, \mathsf{r_B})$ the number of its intersecting pairs equals*

$$(5.6) \qquad\qquad \mathrm{d}(\mathsf{b}) - \mathrm{d}(\mathsf{t}) + |\mathsf{b}|_0|\mathsf{l_B}|_1 + |\mathsf{r_B}|_0(|\mathsf{b}|_1 + |\mathsf{l_B}|_1).$$

**PROOF.** Let $(B, R)$ be a blue-red path-tangle with boundary $(\mathsf{l_T}, \mathsf{t}, \mathsf{r_T}; \mathsf{l_B}, \mathsf{b}, \mathsf{r_B})$ and $B = (P_1, \ldots, P_{|\mathsf{b}|_0 + |\mathsf{r_B}|_0})$ with $P_k \in \mathcal{P}(D_{i_k}, E_{j_k})$. The main idea of the proof is to compute the number of red paths that intersect with $P_k$ separately for each $k$ and then sum these numbers. In doing so the following three cases for $k$ are distinguished: $k \leq \min\{|\mathsf{b}|_0, |\mathsf{l_T}|_0\}$, $k > \max\{|\mathsf{b}|_0, |\mathsf{l_T}|_0\}$ and $\min\{|\mathsf{b}|_0, |\mathsf{l_T}|_0\} < k \leq \max\{|\mathsf{b}|_0, |\mathsf{l_T}|_0\}$.

In the first case, $i_k \leq K + L - N$ and $j_k \leq K$. Therefore, for each $k \leq \min\{|\mathsf{b}|_0, |\mathsf{l_T}|_0\}$ the number of red paths that intersect with $P_k$ is given by

$$|\mathsf{l_B}|_1 + \text{\# of 1's among the first } (i_k - 1) \text{ letters of } \mathsf{b}.$$

In the second case, $i_k > K + L - N$ and $j_k > K$. For that reason, for each $k > \max\{|\mathsf{b}|_0, |\mathsf{l_T}|_0\}$ the number of red paths that intersect with $P_k$ is given by

$$|\mathsf{b}|_1 + |\mathsf{l_B}|_1 - \text{\# of 1's among the first } (j_k - K - 1) \text{ letters of } \mathsf{t}.$$

In the last case, it is necessary to regard the cases $|b|_0 < |l_T|_0$ and $|l_T|_0 < |b|_0$ separately. If $|b|_0 < |l_T|_0$ then for each $|b|_0 < k \le |l_T|_0$ it holds $i_k > K + L - N$ and $j_k \le K$. For that reason, the number of red paths that intersect with $P_k$ is given by

$$|b|_1 + |l_B|_1.$$

On the other hand, if $|l_T|_0 < |b|_0$ then for each $|b|_0 < k \le |l_T|_0$ it holds $i_k \le K + L - N$ and $j_k > K$. For that reason, the number of red paths that intersect with $P_k$ is given by

$$|l_B|_1 + \# \text{ of 1's among the first } (i_k - 1) \text{ letters of } b - \# \text{ of 1's among the first}$$
$$(j_k - K - 1) \text{ letters of } t.$$

By summing the numbers of red paths that intersect with a path $P_k$ over all $k$ the assertion follows. $\qquad\square$

Expressing the number of intersecting pairs of a blue-red path tangle in terms of numbers of occurrences of local configurations gives the following identities:

LEMMA 5.29. *For any oriented HFPL and blue-red path tangle respectively that has boundary* $(l_T, t, r_T; l_B, b, r_B)$ *and is equipped with external edges one has the following:*

$$d(b) - d(t) + |b|_0 |l_B|_1 + |r_B|_0 (|b|_1 + |l_B|_1) = \ \text{[diagram]} + \text{[diagram]} - \text{[diagram]} - \text{[diagram]}$$

$$= \ \text{[diagram]} + \text{[diagram]} - \text{[diagram]} - \text{[diagram]}$$

$$d(b) - d(t) + |b|_0 |l_B|_1 + |r_B|_0 (|b|_1 + |l_B|_1) = \ \text{[diagram]} + \text{[diagram]} - \text{[diagram]} - \text{[diagram]}$$

$$= \ \text{[diagram]} + \text{[diagram]} - \text{[diagram]} - \text{[diagram]}$$

Lemma 5.29 generalises Lemma 4.7 in [**11**]. Its proof is omitted here because it is similar to the proof of Lemma 4.7 in [**11**]. Now, everything that is needed to prove Theorem 5.25 is provided.

PROOF OF THEOREM 5.25. Let $\overline{f} \in \overrightarrow{H}_{l_B, b, r_B}^{l_T, t, r_T}$ equipped with external edges. Then Proposition 5.24 implies the following identity for $\overline{f}$:

$$d(r_B) + d(b) + d(l_B) - d(l_T) - d(t) - d(r_T) - |l_T|_1 |t|_0 - |t|_1 |r_T|_0 - |r_B|_0 |l_B|_1$$
$$= \text{[diagram]} + \text{[diagram]} + \text{[diagram]} + \text{[diagram]} - (d(b) - d(t) + |b|_0 |l_B|_1 + |r_B|_0 (|l_B|_1 + |b|_1)).$$

It remains to consider the right side of the previous equation. The number ◄—■ + ■◄—● can be expressed in the following way:

$$◄—■ + ■◄—● = \frac{1}{2}(◄—■ + ◄—■) + \frac{1}{2}(■◄—● + ■◄—●)$$

$$= \frac{1}{2}\left( ⌐ + ◄—■◄—● + ⌐ + ⌐ + ■◄—◄—■ + ⌐ \right)$$

(5.7)
$$+ \frac{1}{2}\left( ⌐ + ■◄—●◄—■ + ⌐ + ⌐ + ◄—■◄—● + ⌐ \right).$$

By Lemma 5.29, the following identity holds for $\overline{f}$:

$$d(b) - d(t) + |b|_0 |l_B|_1 + |r_B|_0 (|b|_1 + |l_B|_1)$$

(5.8)
$$= \frac{1}{2}\left( ⌐ + ⌐ - ⌐ - ⌐ + ⌐ + ⌐ - ⌐ - ⌐ \right).$$

Finally, subtracting (5.8) from (5.7) proves (5.5) for oriented HFPLs with the external edges included. The external edges either are horizontal edges oriented from the left to the right vertex or vertical edges where the bottom vertex is odd and the top vertex is even. Since such oriented edges are not counted by the right side in (5.5) the identity in (5.5) stays true when the external edges in $\overline{f}$ are removed. □

## 5.5. Configurations of excess 0

In this section, ordinary and oriented HFPLs with boundary $(l_T, t, r_T; l_B, b, r_B)$ which satisfies that $d(r_B) + d(b) + d(l_B) - d(l_T) - d(t) - d(r_T) - |l_T|_1 |t|_0 - |t|_1 |r_T|_0 - |r_B|_0 |l_B|_1 = 0$ are considered; by Theorem 5.11(3) zero is the minimal value $d(r_B) + d(b) + d(l_B) - d(l_T) - d(t) - d(r_T) - |l_T|_1 |t|_0 - |t|_1 |r_T|_0 - |r_B|_0 |l_B|_1$ can assume for the boundary $(l_T, t, r_T; l_B, b, r_B)$ of an oriented HFPL.

DEFINITION 5.30. *Given a sextuple $(l_T, t, r_T; l_B, b, r_B)$ of words its **excess** is defined as*

$$\text{exc}(l_T, t, r_T; l_B, b, r_B) = d(r_B) + d(b) + d(l_B) - d(l_T) - d(t) - d(r_T) - |l_T|_1 |t|_0 - |t|_1 |r_T|_0 - |r_B|_0 |l_B|_1.$$

*In the case when $\text{exc}(l_T, t, r_T; l_B, b, r_B) = k$, both an ordinary and an oriented HFPL with boundary $(l_T, t, r_T; l_B, b, r_B)$ are said to be of excess $k$.*

In [**11**] the excess was defined for the boundary $(u, v; w)$ of TFPLs as the integer $d(w) - d(u) - d(v)$. The excess as it is defined in this paper is a generalisation of this excess. That is, because when considering TFPLs with boundary $(u, v; w)$ HFPLs with boundary $(u, \varepsilon, v; \varepsilon, w, \varepsilon)$ it holds that

$$\text{exc}(u, \varepsilon, v; \varepsilon, w, \varepsilon) = d(w) - d(u) - d(v).$$

The crucial objects in the approach to HFPLs of excess 0 set forth in this section are *hexagonal Knutson-Tao puzzles*; this is due to their one-to-one correspondence to HF-PLs of excess 0 and to the fact that the number of hexagonal Knutson-Tao puzzles with

boundary $(\mathsf{l_T}, \mathsf{t}, \mathsf{r_T}; \mathsf{l_B}, \mathsf{b}, \mathsf{r_B})$ is given by the Littlewood-Richardson coefficient in (5.9) below.

**5.5.1. Hexagonal Knutson-Tao puzzles.** In this subsection, hexagonal Knutson-Tao puzzles are defined and their enumeration by Littlewood-Richardson coefficients is proved.

DEFINITION 5.31 ([**12**]). *A **puzzle piece** is defined as one of the following equilateral plane figures with side length* 1 *and labelled edges:*
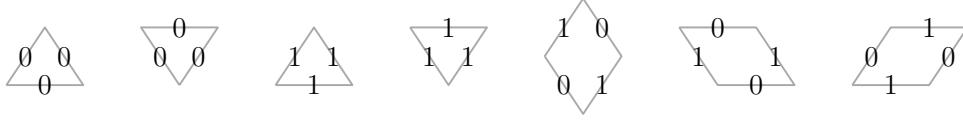


Below, the hexagon with vertices $(0,0)$, $(\frac{K}{2}, \frac{K\sqrt{3}}{2})$, $(\frac{K}{2} + L, \frac{K\sqrt{3}}{2})$, $(\frac{K+M}{2} + L, \frac{(K-M)\sqrt{3}}{2})$, $(\frac{K+M-N}{2} + L, \frac{(K-M-N)\sqrt{3}}{2})$ and $(\frac{M+N-K}{2}, \frac{(K-M-N)\sqrt{3}}{2})$ is denoted by $\mathcal{H}^{K,L,M,N}$. A decomposition $P$ of $\mathcal{H}^{K,L,M,N}$ into unit triangles and unit rhombi all edges labelled 0 or 1 such that each region is a puzzle piece is said to be a *hexagonal Knutson-Tao puzzle* of size $(K, L, M, N)$. Furthermore, a hexagonal Knutson-Tao puzzle is said to have boundary $(\mathsf{l_T}, \mathsf{t}, \mathsf{r_T}; \mathsf{l_B}, \mathsf{b}, \mathsf{r_B})$ if the labels of the top left, top, top right, bottom left, bottom and bottom right sides of $\mathcal{H}_{K,L,M,N}$ are given by $\mathsf{l_T}$, $\mathsf{t}$, $\mathsf{r_T}$, $\mathsf{l_B}$, $\mathsf{b}$ and $\mathsf{r_B}$ respectively, when read from left to right. In Figure 5.15, a hexagonal Knutson-Tao puzzle with boundary $(01, 010, 01; 1100, 0, 1100)$ is depicted.
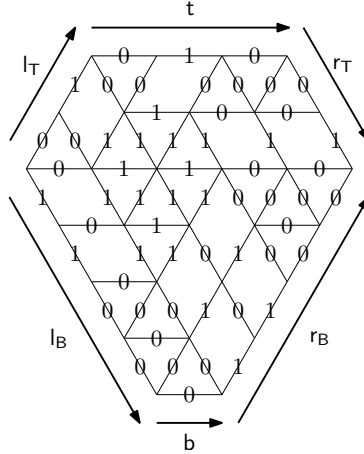


FIGURE 5.15. A hexagonal Knutson-Tao puzzle with boundary $(01, 010, 01; 1100, 0, 1100)$.

Recall from the introduction that by the map m to a 01-word $\omega$ of length $N$ the word of length $N$ where the first $|\omega|_0$ letters are zero and the last $|\omega|_1$ letters are 1 is assigned. For instance, $\mathsf{m}(010) = 001$.

PROPOSITION 5.32. *The number of hexagonal Knutson-Tao puzzles with boundary* $(\mathsf{l_T}, \mathsf{t}, \mathsf{r_T}; \mathsf{l_B}, \mathsf{b}, \mathsf{r_B})$ *is given by the Littlewood-Richardson coefficient*

(5.9)
$$c^{\mathsf{l_B}\, \mathsf{b}\, \mathsf{r_B}}_{\mathsf{m(l_B)}\, \mathsf{l_T}\, \mathsf{t}, \mathsf{m(t)} \mathsf{r_T}\, \mathsf{m(r_B)}}.$$

PROOF. From an enumeration result in [**12**] for triangular Knutson-Tao puzzles it follows that triangular Knutson-Tao puzzles with boundary $(m(l_B) \, l_T \, t, m(t) \, r_T \, m(r_B); l_B \, b \, r_B)$ are enumerated by the Littlewood-Richardson coefficient in (5.9). Therefore, to prove the assertion it suffices to associate each hexagonal Knutson-Tao puzzle with boundary $(l_T, t, r_T; l_B, b, r_B)$ in a bijective way with a triangular Knutson-Tao puzzle with boundary $(m(l_B) \, l_T \, t, m(t) \, r_T \, m(r_B); l_B \, b \, r_B)$. First, note that for a word $\omega$ there exist a unique triangular Knutson-Tao puzzle with boundary $(\omega, m(\omega); \omega)$ and a unique triangular Knutson-Tao puzzle with boundary $(m(\omega), \omega; \omega)$. From this it follows that for each hexagonal Knutson-Tao puzzle $P$ with boundary $(l_T, t, r_T; l_B, b, r_B)$ there exists a unique triangular Knutson-Tao puzzle with boundary $(m(l_B) \, l_T \, t, m(t) \, r_T \, m(r_B); l_B \, b \, r_B)$ that contains $P$. A particular case can be seen in Figure 5.16. Conversely, it can easily be checked that each triangular Knutson-Tao puzzle with boundary $(m(l_B) \, l_T \, t, m(t) \, r_T \, m(r_B); l_B \, b \, r_B)$ contains a hexagonal Knutson-Tao puzzle with boundary $(l_T, t, r_T; l_B, b, r_B)$. In summary, associating a hexagonal Knutson-Tao puzzle with boundary $(l_T, t, r_T; l_B, b, r_B)$ with the triangular Knutson-Tao puzzle with boundary $(m(l_B) \, l_T \, t, m(t) \, r_T \, m(r_B); l_B \, b \, r_B)$ that contains $P$ gives a bijective map. $\qquad \square$
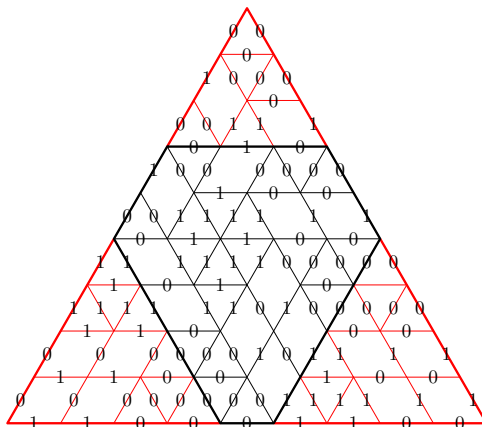


FIGURE 5.16. The triangular Knutson-Tao puzzle corresponding to the hexagonal one depicted in Figure 5.15.

**5.5.2. Configurations of excess 0.** In this subsection, oriented and ordinary HFPLs of excess 0 are regarded. By Theorem 5.25 oriented HFPLs of excess 0 have the following characterisation:

COROLLARY 5.33. *An oriented HFPL $f$ is of excess 0 if and only if none of the following four configurations occurs in $f$:*



The characterisation above and Theorem 5.11(3) imply the following properties of an oriented HFPL of excess 0:

PROPOSITION 5.34. *Oriented HFPLs of excess 0 have the following properties:*

(1) *they neither contain a path joining two vertices in $\mathcal{B}$ that is oriented from right to left nor a path joining two vertices in $\mathcal{T}$ that is oriented from right to left;*

(2) *their weight is 1;*

(3) *they do not contain closed paths.*

*In particular, $\overrightarrow{h}_{l_B,b,r_B}^{l_T,t,r_T}(q) = h_{l_B,b,r_B}^{l_T,t,r_T}$ if $\mathrm{exc}(l_T,t,r_T;l_B,b,r_B) = 0$.*

The previous proposition generalises Proposition 5.3 in [**11**] and Lemma 13 in [**20**].

PROOF. Let $l_T$, $t$, $r_T$, $l_B$, $b$ and $r_B$ be words with $\mathrm{exc}(l_T,t,r_T;l_B,b,r_B) = 0$. Furthermore, let $f \in \overrightarrow{H}_{l_B,b,r_B}^{l_T,t,r_T}$. If $f$ contained a path that joined two vertices in $\mathcal{B}$ or two vertices in $\mathcal{T}$ and was oriented from right to left then there would exist an oriented HFPL $f'$ with boundary $(l_T,t',r_T;l_B,b',r_B)$ such that $d(b') - d(t') < d(b) - d(t)$ ($f'$ is obtained from $f$ by reorienting the paths in $f$ which join two vertices in $\mathcal{B}$ or $\mathcal{T}$ and which are oriented from right to left). This is impossible by Theorem 5.25(3) because

$$(5.10) \qquad \mathrm{exc}(l_T,t',r_T;r_B,b',l_B) < \mathrm{exc}(l_T,t,r_T;l_B,b,r_B) = 0.$$

Thus, in $f$ there are no paths that join two vertices in $\mathcal{B}$ or $\mathcal{T}$ and that are oriented from right to left. The proofs of the second and the third proposition are analogous to the proofs of Proposition 5.3(2), (3) in [**11**]. This is why they are omitted. $\square$

In [**32**], [**20**] and in [**11**] it is shown that ordinary *resp.* oriented TFPLs of excess 0 are in bijection with (triangular) Knutson-Tao puzzles. The bijection given in [**11**] between oriented TFPLs and triangular Knutson-Tao puzzles naturally extends to a bijection between oriented HFPLs of excess 0 and hexagonal Knutson-Tao puzzles. It will not be stated in this paper but it will be indicated by an example; in Figure 5.17 the oriented HFPL of excess 0 corresponding to the hexagonal Knutson-Tao puzzle depicted in Figure 5.15 is displayed.

THEOREM 5.35. *Let $(l_T,t,r_T;l_B,b,r_B)$ be a sextuple of words of lengths $(K, L, M; M + N - K, K + L - N, N)$ respectively such that $\mathrm{exc}(l_T,t,r_T;l_B,b,r_B) = 0$. Then*

$$(5.11) \qquad \overrightarrow{h}_{l_B,b,r_B}^{l_T,t,r_T} = c_{m(l_B)\, l_T\, t,m(t)\, r_T\, m(r_B)}^{l_B\, b\, r_B}.$$

By Proposition 5.34 it holds $\overrightarrow{h}_{l_B,b,r_B}^{l_T,t,r_T} = h_{l_B,b,r_B}^{l_T,t,r_T}$ if $\mathrm{exc}(l_T,t,r_T;l_B,b,r_B) = 0$. Thus, from Theorem 5.35 one immediately obtains:

COROLLARY 5.36. *Let $(l_T,t,r_T;l_B,b,r_B)$ be as in Theorem 5.35. Then*

$$(5.12) \qquad h_{l_B,b,r_B}^{l_T,t,r_T} = c_{m(l_B)\, l_T\, t,m(t)\, r_T\, m(r_B)}^{l_B\, b\, r_B}.$$
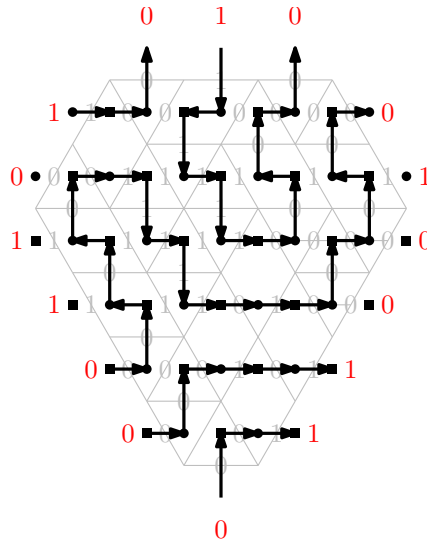
FIGURE 5.17. Except for scaling the oriented HFPL of excess 0 with boundary $(01, 010, 01; 1100, 0, 1100)$ that corresponds to the hexagonal Knutson-Tao puzzle with the same boundary depicted in Figure 5.15.

The following corollary is an immediate consequence of Theorem 5.35 and Corollary 5.36 for TFPLs and was first shown for the Dyck-word-case in [20] and later for the general case in [11].

COROLLARY 5.37. *Let $u, v, w$ be words of length $N$ such that $\mathrm{d}(w) - \mathrm{d}(u) - \mathrm{d}(v) = 0$. Then the number of both ordinary and oriented TFPLs with boundary $(u, v; w)$ is given by the Littlewood-Richardson coefficient $c_{u,v}^w$.*

## 5.6. Configurations of excess 1

The purpose of this section is to determine and examine both ordinary and oriented TFPLs of excess 1; the main result of this section will be an expression for the number of ordinary *resp.* oriented HFPLs of excess 1 in terms of Littlewood-Richardson coefficients.

**5.6.1. Configurations of excess 1.** It is started with the determination of oriented HFPLs of excess 1. By Theorem 5.25 they can be characterised as follows:

PROPOSITION 5.38. *An oriented HFPL is of excess 1 if and only if there is a local configuration among the first four in the list below that appears precisely once, whereas the other seven configurations in the list do not appear at all.*



*In terms of blue-red path tangles, a configuration is of excess 1 if and only if there is a local configuration among the first four in the list below that appears precisely once, whereas the other seven configurations in the list do not appear at all.*

By Proposition 5.38 configurations of excess 1 resemble configurations of excess 0 with the exception of one *defect*. This defect can be of four different types which from now on will be denoted as indicated in Figure 5.18. For hexagonal Knutson-Tao puzzles new puzzle pieces will be introduced in order to obtain puzzles that correspond to configurations of excess 1.

DEFINITION 5.39 ([**11**]). *A **hexagonal BD-puzzle** of size $(K, L, M, N)$ is a decomposition $P$ of $\mathcal{H}^{K,L,M,N}$ into unit triangles and unit rhombi all edges labelled 0 or 1 such that*

(1) *there is precisely one pair of adjacent /-edges (the **defect**) labelled as indicated in the first column of Figure 5.18,*

(2) *each region is a puzzle piece and*

(3) *whenever two puzzle pieces are adjacent their common edge has the same label in both puzzle pieces with the exception of the pair of adjacent edges that give rise to the defect.*

*A* hexagonal RD-puzzle *of size $(K, L, M, N)$ is defined analogously but with (1) replaced by*

(1') *there is precisely one pair of adjacent \-edges (the **defect**) labelled as indicated in the second column of Figure 5.18.*

*A **hexagonal DHD-puzzle** contains precisely one equilateral $\triangledown$-triangle of side length 2 with edges labelled as indicated in the third column of Figure 5.18 while a **hexagonal DHU-puzzle** contains precisely one equilateral $\triangle$-triangle of side length 2 with edges labelled as indicated in the fourth column of Figure 5.18.*



| | BD | RD | DHD | DHU |
|---|---|---|---|---|
| Oriented TFPL | | | | |
| Path tangle | | | | |
| Puzzle | | | | |

FIGURE 5.18. Supplementary configurations in the excess-1-case.

PROPOSITION 5.40. *Let* $l_T$, $t$, $r_T$, $l_B$, $b$ *and* $r_B$ *be words with* $exc(l_T, t, r_T; l_B, b, r_B) = 1$ *and* $X \in \{BD, RD, DHU, DHD\}$. *Then the oriented HFPLs of type $X$ with boundary* $(l_T, t, r_T; l_B, b, r_B)$ *are in one-to-one correspondence with the $X$-puzzles with boundary* $(l_T, t, r_T; l_B, b, r_B)$.

The proof of Proposition 5.40 is analogous to the proof of Proposition 6.5 in [**11**] and therefore is omitted. Examples of oriented HFPLs of excess 1 and their corresponding puzzles are given in Figure 5.19
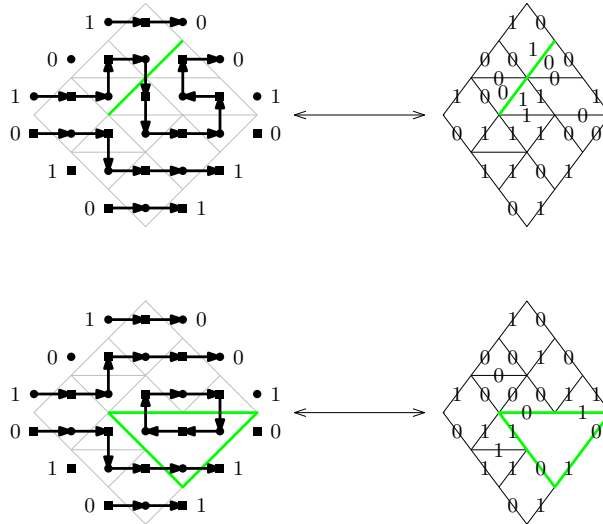


FIGURE 5.19. An oriented HFPL of excess 1 with a defect of type BD and its corresponding BD-puzzle and an oriented HFPL of excess 1 with a defect of type DHU and its corresponding DHU-puzzle.

PROPOSITION 5.41. *Let $f$ be an oriented HFPL of excess 1. Then the weight of $f$ is* 1 *if the defect is of type BD or RD, $q$ if the defect is of type DHD and $q^{-1}$ if the defect is of type DHU.*

The proof of Proposition 5.41 uses the interpretation of the weight of an oriented HFPL in terms of numbers of occurrences of certain turns; it is analogous to the proof of Proposition 6.3 in [**11**] and therefore is omitted.

**5.6.2. Moving a defect of type BD or RD.** In this subsection, oriented HFPLs of excess 1 where the defect is of type BD or RD are considered. To such oriented HFPLs certain *moves* will be applied for the purpose of obtaining an oriented HFPL of excess 0. These moves are the same as in [**11**, Section 6] for oriented TFPLs of excess 1 and are depicted in Figure 5.20. Their names are due to their representations in terms of blue-red path tangles.

LEMMA 5.42. *Let $f$ be an oriented HFPL of excess 1 where the defect is of type BD or RD.*
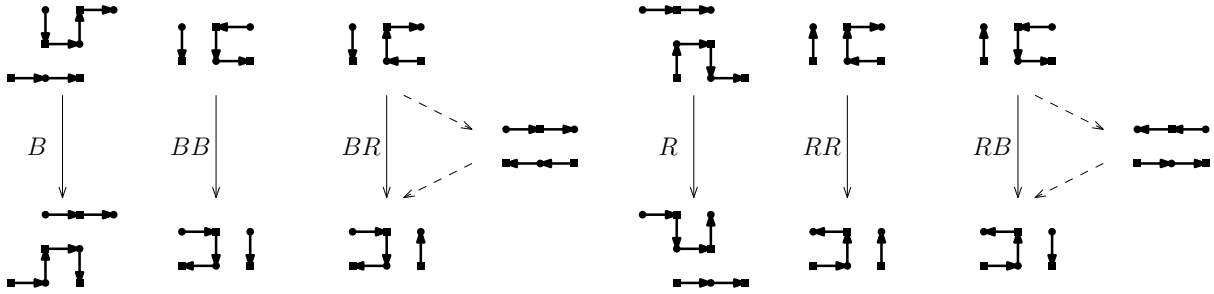
FIGURE 5.20. The rules for moving a defect of type BD or RD in an oriented HFPL of excess 1.

(1) *If the defect in $f$ is not incident to a vertex in $\mathcal{R}_T \cup \mathcal{R}_B$ then a unique move $B$, $BB$, $BR$, $R$, $RR$ or $RB$ can be applied to it. The oriented HFPL of excess 1 that is obtained from $f$ by applying this unique move is denoted by $\mathrm{MoveR}(f)$.*

(2) *If the defect in $f$ is not incident to a vertex in $\mathcal{L}_T \cup \mathcal{L}_B$ then a unique move $B^{-1}$, $BB^{-1}$, $BR^{-1}$, $R^{-1}$, $RR^{-1}$, $RB^{-1}$ can be applied to it. The oriented HFPL that is obtained from $f$ by applying this unique move is denoted by $\mathrm{MoveL}(f)$.*

The proof of Lemma 5.42 is analogous to the proof of Lemma 6.6 in [**11**] which states the analogous for oriented TFPLs. This is why it is omitted. By Lemma 5.42 any oriented HFPL of excess 1 where the defect is of type BD or RD can be transformed into a unique oriented HFPL of excess 1 where the defect is incident to a vertex in $\mathcal{R}_T \cup \mathcal{R}_B$ (*resp.* $\mathcal{L}_T \cup \mathcal{L}_B$) by the repeated application of MoveR (*resp.* MoveL). Figure 5.21 shows an oriented HFPL of excess 1 and its images under MoveR and MoveL.

It is described next how oriented HFPLs $f$ where the defect is incident to a vertex in $\mathcal{R}_T \cup \mathcal{R}_B$ or $\mathcal{L}_T \cup \mathcal{L}_B$ are associated with oriented HFPLs of excess 0. First, if the defect is incident to a vertex $R_{T,i}$ in $\mathcal{R}_T$ then the vertex $R_{T,i+1}$ has to be of degree 0. In that case, the oriented HFPL of excess 0 is obtained from $f$ by deleting the defect and by adding a horizontal edge incident to $R_{T,i+1}$. By that in $\mathsf{r}_T$ a zero and the one to its right are exchanged. If the defect is incident to a vertex $R_{B,j}$ in $\mathcal{R}_B$ then $R_{B,j-1}$ has to be of degree 0. In that case, the oriented HFPL of excess 0 is obtained from $f$ by deleting the defect and by adding a horizontal edge incident to $R_{B,j-1}$. In doing so a zero and the one to its left are exchanged in $\mathsf{r}_B$. On the other hand, if the defect in $f$ is incident to a vertex in $\mathcal{L}_T \cup \mathcal{L}_B$ an oriented HFPL of excess 0 is assigned to $f$ in the analogous way. For the changes in the boundary of an oriented HFPL of excess 1 caused by the deletion of a defect the following notation will be chosen:

DEFINITION 5.43. *Given two words $\omega$ and $\omega^+$ it is written $\omega \to \omega^+$ if $\omega = \omega_L 01 \omega_R$ and $\omega^+ = \omega_L 10 \omega_R$ for appropriate words $\omega_L$ and $\omega_R$.*

Conversely, given an oriented HFPL of excess 0 a defect may be introduced along the left or right boundary by reversing the previously described deletion process. If a defect is introduced along the left or right boundary of an oriented HFPL of excess 0 it can be
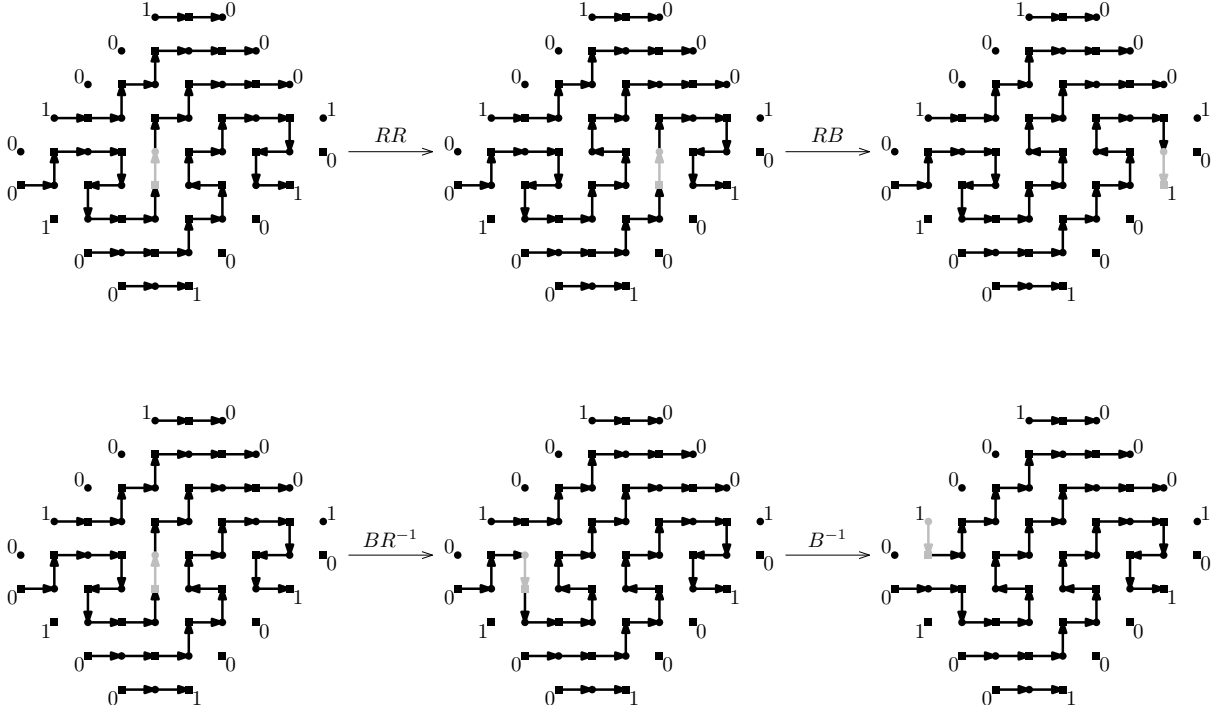
FIGURE 5.21. An oriented HFPL of excess 1 and its images under MoveR and under MoveL.

moved in a unique way to the opposite boundary by Lemma 5.42. For that reason, given a sextuple $(\mathsf{l_T}, \mathsf{t}, \mathsf{r_T}; \mathsf{l_B}, \mathsf{b}, \mathsf{r_B})$ of words such that $\mathrm{exc}(\mathsf{l_T}, \mathsf{t}, \mathsf{r_T}; \mathsf{l_B}, \mathsf{b}, \mathsf{r_B}) = 1$ it holds that

(5.13)
$$
\sum_{\mathsf{l_T^+} : \mathsf{l_T} \to \mathsf{l_T^+}} c^{\mathsf{l_B} \, \mathsf{b} \, \mathsf{r_B}}_{\mathrm{m}(\mathsf{l_B}) \, \mathsf{l_T^+} \, \mathsf{t}, \mathrm{m}(\mathsf{t}) \, \mathsf{r_T} \, \mathrm{m}(\mathsf{r_B})} + \sum_{\mathsf{l_B^-} : \mathsf{l_B^-} \to \mathsf{l_B}} c^{\mathsf{l_B^-} \, \mathsf{b} \, \mathsf{r_B}}_{\mathrm{m}(\mathsf{l_B^-}) \, \mathsf{l_T} \, \mathsf{t}, \mathrm{m}(\mathsf{t}) \, \mathsf{r_T} \, \mathrm{m}(\mathsf{r_B})}
$$
$$
= \sum_{\mathsf{r_T^+} : \mathsf{r_T} \to \mathsf{r_T^+}} c^{\mathsf{l_B} \, \mathsf{b} \, \mathsf{r_B}}_{\mathrm{m}(\mathsf{l_B}) \, \mathsf{l_T} \, \mathsf{t}, \mathrm{m}(\mathsf{t}) \, \mathsf{r_T^+} \, \mathrm{m}(\mathsf{r_B})} + \sum_{\mathsf{r_B^-} : \mathsf{r_B^-} \to \mathsf{r_B}} c^{\mathsf{l_B} \, \mathsf{b} \, \mathsf{r_B^-}}_{\mathrm{m}(\mathsf{l_B}) \, \mathsf{l_T} \, \mathsf{t}, \mathrm{m}(\mathsf{t}) \, \mathsf{r_T} \, \mathrm{m}(\mathsf{r_B^-})}.
$$

Figure 5.21 lists five different oriented HFPLs of excess 1. All of these oriented HFPLs are transformed into the same oriented HFPL of excess 1 by the repeated application of MoveR. In this oriented HFPL the defect is incident to a vertex in $\mathcal{R}_T \cup \mathcal{R}_B$. At the same time by the repeated application of MoveL the five oriented HFPLs in Figure 5.21 are transformed into the same oriented HFPL of excess 1. In this oriented HFPL the defect is incident to a vertex in $\mathcal{L}_T \cup \mathcal{L}_B$. Thus, all five oriented HFPLs in Figure 5.21 are associated with the same pair of oriented HFPLs of excess 0. This subsection will culminate in an expression for the number of oriented HFPLs with boundary $(\mathsf{l_T}, \mathsf{t}, \mathsf{r_T}; \mathsf{l_B}, \mathsf{b}, \mathsf{r_B})$ of excess 1 where the defect is of type BD or RD in terms of Littlewood-Richardson coefficients which will result from counting how many oriented HFPLs with boundary $(\mathsf{l_T}, \mathsf{t}, \mathsf{r_T}; \mathsf{l_B}, \mathsf{b}, \mathsf{r_B})$ and a defect of type BD or RD are associated with the same pair of oriented HFPLs of excess 0. The methods used to count these configurations resemble the methods developed in [11] for the study of oriented TFPLs of excess 1 with a defect of type BD or RD. They are

based on a detailed analysis of the moves displayed in Figure 5.20. More details can be found in Section 6.5 in [**11**]. To formulate the main result of this subsection the following notations are needed:

DEFINITION 5.44. *For two words* $\omega \to \omega^+$ *set* $L_i(\omega, \omega^+) = |\omega_L|_i$ *resp.* $R_i(\omega, \omega^+) = |\omega_R|_i$ *for* $i = 0, 1$ *and* $L(\omega, \omega^+) = L_0(\omega, \omega^+) + L_1(\omega, \omega^+) + 1$ *resp.* $R(\omega, \omega^+) = R_0(\omega, \omega^+) + R_1(\omega, \omega^+) + 1.$

PROPOSITION 5.45. *Let* $\mathsf{l_T}$, $\mathsf{t}$, $\mathsf{r_T}$, $\mathsf{r_B}$, $\mathsf{b}$ *and* $\mathsf{l_B}$ *be words with* $exc(\mathsf{l_T}, \mathsf{t}, \mathsf{r_T}; \mathsf{l_B}, \mathsf{b}, \mathsf{r_B}) = 1.$

(1) *The number of oriented HFPLs with boundary* $(\mathsf{l_T}, \mathsf{t}, \mathsf{r_T}; \mathsf{l_B}, \mathsf{b}, \mathsf{r_B})$ *to which one on the moves in* $\{BB, BR, R\}$ *can be applied is given by*

$$\sum_{\mathsf{l_T^+}: \mathsf{l_T} \to \mathsf{l_T^+}} (R_1(\mathsf{l_T}, \mathsf{l_T^+}) + |\mathsf{t}|_1 + 1) c^{\mathsf{l_B}\, \mathsf{b}\, \mathsf{r_B}}_{m(\mathsf{l_B})\, \mathsf{l_T^+}\, \mathsf{t}, m(\mathsf{t})\, \mathsf{r_T}\, m(\mathsf{r_B})} + \sum_{\mathsf{l_B^-}: \mathsf{l_B^-} \to \mathsf{l_B}} (|\mathsf{l_T}|_1 + |\mathsf{t}|_1) c^{\mathsf{l_B^-}\, \mathsf{b}\, \mathsf{r_B}}_{m(\mathsf{l_B^-})\, \mathsf{l_T}\, \mathsf{t}, m(\mathsf{t})\, \mathsf{r_T}\, m(\mathsf{r_B})}$$

$$- \sum_{\mathsf{r_B^-}: \mathsf{r_B^-} \to \mathsf{r_B}} (R_1(\mathsf{r_B^-}, \mathsf{r_B}) + 1) c^{\mathsf{l_B}\, \mathsf{b}\, \mathsf{r_B^-}}_{m(\mathsf{l_B})\, \mathsf{l_T}\, \mathsf{t}, m(\mathsf{t})\, \mathsf{r_T}\, m(\mathsf{r_B^-})}.$$

(2) *The number of oriented HFPLs with boundary* $(\mathsf{l_T}, \mathsf{t}, \mathsf{r_T}; \mathsf{l_B}, \mathsf{b}, \mathsf{r_B})$ *to which one of the moves in* $\{B, RR, RB\}$ *can be applied is given by*

$$\sum_{\mathsf{r_T^+}: \mathsf{r_T} \to \mathsf{r_T^+}} (L_0(\mathsf{r_T}, \mathsf{r_T^+}) + |\mathsf{t}|_0) c^{\mathsf{l_B}\, \mathsf{b}\, \mathsf{r_B}}_{m(\mathsf{l_B})\, \mathsf{l_T}\, \mathsf{t}, m(\mathsf{t})\, \mathsf{r_T^+}\, m(\mathsf{r_B})} + \sum_{\mathsf{r_B^-}: \mathsf{r_B^-} \to \mathsf{r_B}} (|\mathsf{t}|_0 + |\mathsf{r_T}|_0) c^{\mathsf{l_B}\, \mathsf{b}\, \mathsf{r_B^-}}_{m(\mathsf{l_B})\, \mathsf{l_T}\, \mathsf{t}, m(\mathsf{t})\, \mathsf{r_T}\, m(\mathsf{r_B^-})}$$

$$- \sum_{\mathsf{l_B^-}: \mathsf{l_B^-} \to \mathsf{l_B}} L_0(\mathsf{l_B^-}, \mathsf{l_B}) c^{\mathsf{l_B^-}\, \mathsf{b}\, \mathsf{r_B}}_{m(\mathsf{l_B^-})\, \mathsf{l_T}\, \mathsf{t}, m(\mathsf{t})\, \mathsf{r_T}\, m(\mathsf{r_B})}.$$

(3) *The number of oriented HFPLs with boundary* $(\mathsf{l_T}, \mathsf{t}, \mathsf{r_T}; \mathsf{l_B}, \mathsf{b}, \mathsf{r_B})$ *to which one of the moves in* $\{BB, BR\}$ *can be applied is given by*

$$\sum_{\mathsf{r_T^+}: \mathsf{r_T} \to \mathsf{r_T^+}} (|\mathsf{t}|_1 + L_1(\mathsf{r_T}, \mathsf{r_T^+}) + 1) c^{\mathsf{l_B}\, \mathsf{b}\, \mathsf{r_B}}_{m(\mathsf{l_B})\, \mathsf{l_T}\, \mathsf{t}, m(\mathsf{t})\, \mathsf{r_T^+}\, m(\mathsf{r_B})} + \sum_{\mathsf{r_B^-}: \mathsf{r_B^-} \to \mathsf{r_B}} (|\mathsf{t}|_1 + |\mathsf{r_T}|_1) c^{\mathsf{l_B}\, \mathsf{b}\, \mathsf{r_B^-}}_{m(\mathsf{l_B})\, \mathsf{l_T}\, \mathsf{t}, m(\mathsf{t})\, \mathsf{r_T}\, m(\mathsf{r_B^-})}$$

$$- \sum_{\mathsf{l_B^-}: \mathsf{l_B^-} \to \mathsf{l_B}} (L_1(\mathsf{l_B^-}, \mathsf{l_B}) + 1) c^{\mathsf{l_B^-}\, \mathsf{b}\, \mathsf{r_B}}_{m(\mathsf{l_B^-})\, \mathsf{l_T}\, \mathsf{t}, m(\mathsf{t})\, \mathsf{r_T}\, m(\mathsf{r_B})}.$$

(4) *The number of oriented HFPLs with boundary* $(\mathsf{l_T}, \mathsf{t}, \mathsf{r_T}; \mathsf{l_B}, \mathsf{b}, \mathsf{r_B})$ *to which the move* $R$ *can be applied is given by*

$$\sum_{\mathsf{l_T^+}: \mathsf{l_T} \to \mathsf{l_T^+}} R_1(\mathsf{l_T}, \mathsf{l_T^+}) c^{\mathsf{l_B}\, \mathsf{b}\, \mathsf{r_B}}_{m(\mathsf{l_B})\, \mathsf{l_T^+}\, \mathsf{t}, m(\mathsf{t})\, \mathsf{r_T}\, m(\mathsf{r_B})} + \sum_{\mathsf{l_B^-}: \mathsf{l_B^-} \to \mathsf{l_B}} (|\mathsf{l_T}|_1 + L_1(\mathsf{l_B^-}, \mathsf{l_B})) c^{\mathsf{l_B^-}\, \mathsf{b}\, \mathsf{r_B}}_{m(\mathsf{l_B^-})\, \mathsf{l_T}\, \mathsf{t}, m(\mathsf{t})\, \mathsf{r_T}\, m(\mathsf{r_B})}$$

$$- \sum_{\mathsf{r_T^+}: \mathsf{r_T} \to \mathsf{r_T^+}} L_1(\mathsf{r_T}, \mathsf{r_T^+}) c^{\mathsf{l_B}\, \mathsf{b}\, \mathsf{r_B}}_{m(\mathsf{l_B})\, \mathsf{l_T}\, \mathsf{t}, m(\mathsf{t})\, \mathsf{r_T^+}\, m(\mathsf{r_B})} - \sum_{\mathsf{r_B^-}: \mathsf{r_B^-} \to \mathsf{r_B}} (R_1(\mathsf{r_B^-}, \mathsf{r_B}) + |\mathsf{r_T}|_1) c^{\mathsf{l_B}\, \mathsf{b}\, \mathsf{r_B^-}}_{m(\mathsf{l_B})\, \mathsf{l_T}\, \mathsf{t}, m(\mathsf{t})\, \mathsf{r_T}\, m(\mathsf{r_B^-})}.$$

(5) *The number of oriented HFPLs with boundary* $(l_T, t, r_T; l_B, b, r_B)$ *where the defect is of type BD or RD is given by*

$$\sum_{l_T^+ : l_T \to l_T^+} (R_1(l_T, l_T^+) + |t|_1 + 1) c^{l_B \, b \, r_B}_{m(l_B) \, l_T^+ \, t, m(t) \, r_T \, m(r_B)}$$

$$+ \sum_{r_T^+ : r_T \to r_T^+} (L_0(r_T, r_T^+) + |t|_0 + 1) c^{l_B \, b \, r_B}_{m(l_B) \, l_T \, t, m(t) \, r_T^+ \, m(r_B)}$$

$$+ \sum_{r_B^- : r_B^- \to r_B} (|t|_0 + |r_T|_0 - R_1(r_B^-, r_B)) c^{l_B \, b \, r_B^-}_{m(l_B) \, l_T \, t, m(t) \, r_T \, m(r_B^-)}$$

$$+ \sum_{l_B^- : l_B^- \to l_B} (|l_T|_1 + |t|_1 - L_0(l_B^-, l_B)) c^{l_B^- \, b \, r_B}_{m(l_B^-) \, l_T \, t, m(t) \, r_T \, m(r_B)}.$$

The proof of Proposition 5.45 follows the same ideas as presented in Section 6.3 in [**11**] and therefore will not be given in this thesis. In the next subsection, the third and the fourth statement of the previous proposition will be needed to give formulae for the number of oriented HFPLs of excess 1 with a defect of type DHD and DHU.

**5.6.3. Configurations of excess 1 with a defect of type DHD or DHU.** The key observation for the study of oriented HFPLs of excess 1 with a defect of type DHD (*resp.* DHU) is indicated in Figure 5.20; they can be identified with oriented HFPLs of excess 1 with a defect of type BD (*resp.* RD) to which the move BR (*resp.* RB) can be applied. The number of oriented HFPLs with boundary $(l_T, t, r_T; l_B, b, r_B)$ of excess 1 to which the move BR can be applied and the number of oriented HFPLs with the same boundary to which the move RB can be applied are related as follows:

LEMMA 5.46. *Let* $l_T, t, r_T, r_B, b, l_B$ *be words with* $\mathrm{exc}(l_T, t, r_T; l_B, b, r_B) = 1$. *Subtracting the number of oriented HFPLs with boundary* $(l_T, t, r_T; l_B, b, r_B)$ *to which the move RB can be applied from the number of oriented HFPLs with the same boundary to which the move BR can be applied gives*

$$\sum_{r_T^+ : r_T \to r_T^+} c^{l_B \, b \, r_B}_{m(l_B) \, l_T \, t, m(t) \, r_T^+ \, m(r_B)} - \sum_{r_B^- : r_B^- \to r_B} c^{l_B \, b \, r_B^-}_{m(l_B) \, l_T \, t, m(t) \, r_T \, m(r_B^-)}.$$

Lemma 5.46 follows by an argument similar to the one that leads to Proposition 6.11(1) in [**11**] which states the analogous for oriented TFPLs of excess 1. This is why a proof of Lemma 5.46 will not be given. As a result of the previous lemma it suffices to enumerate oriented HFPLs of excess 1 to which the move BR can be applied in order to derive formulae for both the number of oriented HFPLs of excess 1 with a defect of type DHD and the number of oriented HFPLs of excess 1 with a defect of type DHU. Furthermore, due to Proposition 5.45(3) in order to achieve a formula for the number of oriented HFPLs of excess 1 to which the move BR can be applied it remains to find a formula for the number of oriented HFPLs of excess 1 to which the move BB can be applied. The finding of such a formula relies on the following crucial observation: rotating a BD-puzzle to

which the move BB can be applied by $-120°$ gives an RD-puzzle to which the move $R^{-1}$ can be applied. This relation is illustrated in Figure 5.6.3. Considering the corresponding rotated puzzles allows the use of Proposition 5.45(4) to obtain a formula for the number of BD-puzzles to which the move $BB$ can be applied.
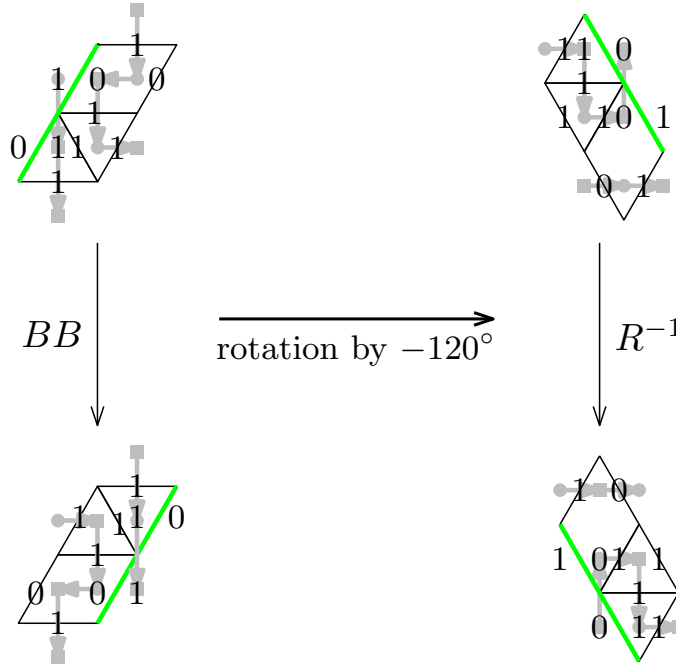


FIGURE 5.22. The move BB in terms of puzzles and its image under rotation by $-120°$, which is the move $R^{-1}$.

LEMMA 5.47. *Let* $I_T, t, r_T, I_B, b, r_B$ *be words with* $exc(I_T, t, r_T; I_B, b, r_B) = 1$. *The number of BD-puzzles with boundary* $(I_T, t, r_T; I_B, b, r_B)$ *to which the move BB can be applied is given by*

$$\sum_{b^- : b^- \to b} L_1(b^-, b) c^{I_B\, b^-\, r_B}_{m(I_B)\, I_T\, t, m(t)\, r_T\, m(r_B)} + \sum_{r_B^- : r_B^- \to r_B} (|b|_1 + L_1(r_B^-, r_B)) c^{I_B\, b\, r_B^-}_{m(I_B)\, I_T\, t, m(t)\, r_T\, m(r_B^-)}$$

$$- \sum_{I_T^+ : I_T \to I_T^+} L_1(I_T, I_T^+) c^{I_B\, b\, r_B}_{m(I_B)\, I_T^+\, t, m(t)\, r_T\, m(r_B)} - \sum_{t^+ : t \to t^+} (|r_T|_1 + R_1(t, t^+)) c^{I_B\, b\, r_B}_{m(I_B)\, I_T\, t^+, m(t^+)\, r_T\, m(r_B)}.$$

The previous results give rise to the following expressions for the number of oriented HFPLs of excess 1 with a defect of type DHD and the number of oriented HFPLs of excess 1 with a defect of type DHU in terms of Littlewood-Richardson coefficients.

PROPOSITION 5.48. *Let* $I_T, t, r_T, I_B, b, r_B$ *be a words with* $exc(I_T, t, r_T; I_B, b, r_B) = 1$.

(1) *The number of oriented HFPLs with boundary* $(l_T, t, r_T; l_B, b, r_B)$ *where the defect is of type DHD equals*

$$\sum_{l_T^+ : l_T \to l_T^+} L_1(l_T, l_T^+) c^{l_B\, b\, r_B}_{m(l_B)\, l_T^+\, t, m(t)\, r_T\, m(r_B)} + \sum_{t^+ : t \to t^+} (|r_T|_1 + R_1(t, t^+)) c^{l_B\, b\, r_B}_{m(l_B)\, l_T\, t^+, m(t^+)\, r_T\, m(r_B)}$$

$$+ \sum_{r_T^+ : r_T \to r_T^+} (|t|_1 + L_1(r_T, r_T^+) + 1) c^{l_B\, b\, r_B}_{m(l_B)\, l_T\, t, m(t)\, r_T^+\, m(r_B)}$$

$$- \sum_{l_B^- : l_B^- \to l_B} (L_1(l_B^-, l_B) + 1) c^{l_B^-\, b\, r_B}_{m(l_B^-)\, l_T\, t, m(t)\, r_T\, m(r_B)}$$

$$+ \sum_{r_B^- : r_B^- \to r_B} (|l_B|_1 - L_1(r_B^-, r_B)) c^{l_B\, b\, r_B^-}_{m(l_B)\, l_T\, t, m(t)\, r_T\, m(r_B^-)} - \sum_{b^- : b^- \to b} L_1(b^-, b) c^{l_B\, b^-\, r_B}_{m(l_B)\, l_T\, t, m(t)\, r_T\, m(r_B)}.$$

(2) *The number of oriented HFPLs with boundary* $(l_T, t, r_T; l_B, b, r_B)$ *where the defect is of type DHU is given by*

$$\sum_{l_T^+ : l_T \to l_T^+} L_1(l_T, l_T^+) c^{l_B\, b\, r_B}_{m(l_B)\, l_T^+\, t, m(t)\, r_T\, m(r_B)} + \sum_{t^+ : t \to t^+} (|r_T|_1 + R_1(t, t^+)) c^{l_B\, b\, r_B}_{m(l_B)\, l_T\, t^+, m(t^+)\, r_T\, m(r_B)}$$

$$+ \sum_{r_T^+ : r_T \to r_T^+} (|t|_1 + L_1(r_T, r_T^+)) c^{l_B\, b\, r_B}_{m(l_B)\, l_T\, t, m(t)\, r_T^+\, m(r_B)} - \sum_{l_B^- : l_B^- \to l_B} L_1(l_B^-, l_B) c^{l_B^-\, b\, r_B}_{m(l_B^-)\, l_T\, t, m(t)\, r_T\, m(r_B)}$$

$$+ \sum_{r_B^- : r_B^- \to r_B} (|l_B|_1 - L_1(r_B^-, r_B)) c^{l_B\, b\, r_B^-}_{m(l_B)\, l_T\, t, m(t)\, r_T\, m(r_B^-)} - \sum_{b^- : b^- \to b} L_1(b^-, b) c^{l_B\, b^-\, r_B}_{m(l_B)\, l_T\, t, m(t)\, r_T\, m(r_B)}.$$

**5.6.4. Enumeration of configurations of excess 1.** In this subsection the results of the previous subsections are combined to formulae for the number of oriented HFPLs with boundary $(l_T, t, r_T; l_B, b, r_B)$ of excess 1 and for the number of ordinary HFPLs with boundary $(l_T, t, r_T; l_B, b, r_B)$ of excess 1.

THEOREM 5.49. *Let* $(l_T, t, r_T; l_B, b, r_B)$ *be words of lengths* $(K, L, M; M + N - K, K + L - N, N)$ *respectively such that* $\text{exc}(l_T, t, r_T; l_B, b, r_B) = 1$.

(1) *The number of oriented HFPLs with boundary* $(\mathsf{l_T}, \mathsf{t}, \mathsf{r_T}; \mathsf{l_B}, \mathsf{b}, \mathsf{r_B})$ *equals*

$$\sum_{\mathsf{l_T^+}:\mathsf{l_T}\longrightarrow \mathsf{l_T^+}} (|\mathsf{l_T}|_1 + |\mathsf{t}|_1 + L_1(\mathsf{l_T}, \mathsf{l_T^+}))c_{m(\mathsf{l_B})\, \mathsf{l_T^+}\, \mathsf{t}, m(\mathsf{t})\, \mathsf{r_T}\, m(\mathsf{r_B})}^{\mathsf{l_B}\, \mathsf{b}\, \mathsf{r_B}}$$

$$+ \sum_{\mathsf{t^+}:\mathsf{t}\longrightarrow \mathsf{t^+}} 2(|\mathsf{r_T}|_1 + R_1(\mathsf{t}, \mathsf{t^+}))c_{m(\mathsf{l_B})\, \mathsf{l_T}\, \mathsf{t^+}, m(\mathsf{t})\, \mathsf{r_T}\, m(\mathsf{r_B})}^{\mathsf{l_B}\, \mathsf{b}\, \mathsf{r_B}}$$

$$+ \sum_{\mathsf{r_T^+}:\mathsf{r_T}\longrightarrow \mathsf{r_T^+}} (L + |\mathsf{t}|_1 + L(\mathsf{r_T}, \mathsf{r_T^+}) + L_1(\mathsf{r_T}, \mathsf{r_T^+}) + 1)c_{m(\mathsf{l_B})\, \mathsf{l_T}\, \mathsf{t}, m(\mathsf{t})\, \mathsf{r_T^+}\, m(\mathsf{r_B})}^{\mathsf{l_B}\, \mathsf{b}\, \mathsf{r_B}}$$

$$+ \sum_{\mathsf{r_B^-}:\mathsf{r_B^-}\longrightarrow \mathsf{r_B}} (L + M + |\mathsf{l_B}|_1 + 1 - |\mathsf{r_B}|_1 - |\mathsf{b}|_1 - L_1(\mathsf{r_B^-}, \mathsf{r_B}))c_{m(\mathsf{l_B})\, \mathsf{l_T}\, \mathsf{t}, m(\mathsf{t})\, \mathsf{r_T}\, m(\mathsf{r_B})}^{\mathsf{l_B}\, \mathsf{b}\, \mathsf{r_B^-}}$$

$$- \sum_{\mathsf{b^-}:\mathsf{b^-}\longrightarrow \mathsf{b}} 2L_1(\mathsf{b^-}, \mathsf{b})c_{m(\mathsf{l_B})\, \mathsf{l_T}\, \mathsf{t}, m(\mathsf{t})\, \mathsf{r_T}\, m(\mathsf{r_B})}^{\mathsf{l_B}\, \mathsf{b^-}\, \mathsf{r_B}}$$

$$+ \sum_{\mathsf{l_B^-}:\mathsf{l_B^-}\longrightarrow \mathsf{l_B}} (|\mathsf{l_T}|_1 + |\mathsf{t}|_1 - L(\mathsf{l_B^-}, \mathsf{l_B}) - L_1(\mathsf{l_B^-}, \mathsf{l_B}))c_{m(\mathsf{l_B})\, \mathsf{l_T}\, \mathsf{t}, m(\mathsf{t})\, \mathsf{r_T}\, m(\mathsf{r_B})}^{\mathsf{l_B^-}\, \mathsf{b}\, \mathsf{r_B}}.$$

(2) *The weighted enumeration of oriented HFPLs with boundary* $(\mathsf{l_T}, \mathsf{t}, \mathsf{r_T}; \mathsf{l_B}, \mathsf{b}, \mathsf{r_B})$ *equals*

$$\sum_{\mathsf{l_T^+}:\mathsf{l_T}\longrightarrow \mathsf{l_T^+}} (R_1(\mathsf{l_T}, \mathsf{l_T^+}) + |\mathsf{t}|_1 + 1 + (q + q^{-1})L_1(\mathsf{l_T}, \mathsf{l_T^+}))c_{m(\mathsf{l_B})\, \mathsf{l_T^+}\, \mathsf{t}, m(\mathsf{t})\, \mathsf{r_T}\, m(\mathsf{r_B})}^{\mathsf{l_B}\, \mathsf{b}\, \mathsf{r_B}}$$

$$+ \sum_{\mathsf{t^+}:\mathsf{t}\longrightarrow \mathsf{t^+}} (q + q^{-1})(|\mathsf{r_T}|_1 + R_1(\mathsf{t}, \mathsf{t^+}))c_{m(\mathsf{l_B})\, \mathsf{l_T}\, \mathsf{t^+}, m(\mathsf{t})\, \mathsf{r_T}\, m(\mathsf{r_B})}^{\mathsf{l_B}\, \mathsf{b}\, \mathsf{r_B}}$$

$$+ \sum_{\mathsf{r_T^+}:\mathsf{r_T}\longrightarrow \mathsf{r_T^+}} (|\mathsf{t}|_0 + 1 + L_0(\mathsf{r_T}, \mathsf{r_T^+}) + (q + q^{-1})(|\mathsf{t}|_1 + L_1(\mathsf{r_T}, \mathsf{r_T^+})) + q)c_{m(\mathsf{l_B})\, \mathsf{l_T}\, \mathsf{t}, m(\mathsf{t})\, \mathsf{r_T^+}\, m(\mathsf{r_B})}^{\mathsf{l_B}\, \mathsf{b}\, \mathsf{r_B}}$$

$$+ \sum_{\mathsf{r_B^-}:\mathsf{r_B^-}\longrightarrow \mathsf{r_B}} (|\mathsf{t}|_0 + |\mathsf{r_T}|_0 - R_1(\mathsf{r_B^-}, \mathsf{r_B}) + (q + q^{-1})(|\mathsf{l_B}|_1 - L_1(\mathsf{r_B^-}, \mathsf{r_B})))c_{m(\mathsf{l_B})\, \mathsf{l_T}, m(\mathsf{t})\, \mathsf{r_T}\, m(\mathsf{r_B})}^{\mathsf{l_B}\, \mathsf{b}\, \mathsf{r_B^-}}$$

$$- \sum_{\mathsf{b^-}:\mathsf{b^-}\longrightarrow \mathsf{b}} (q + q^{-1})L_1(\mathsf{b^-}, \mathsf{b})c_{m(\mathsf{l_B})\, \mathsf{l_T}\, \mathsf{t}, m(\mathsf{t})\, \mathsf{r_T}\, m(\mathsf{r_B})}^{\mathsf{l_B}\, \mathsf{b^-}\, \mathsf{r_B}}$$

$$+ \sum_{\mathsf{l_B^-}:\mathsf{l_B^-}\longrightarrow \mathsf{l_B}} (|\mathsf{l_T}|_1 + |\mathsf{t}|_1 - L_0(\mathsf{l_B^-}, \mathsf{l_B}) - (q + q^{-1})L_1(\mathsf{l_B^-}, \mathsf{l_B}) - q)c_{m(\mathsf{l_B})\, \mathsf{l_T}\, \mathsf{t}, m(\mathsf{t})\, \mathsf{r_T}\, m(\mathsf{r_B})}^{\mathsf{l_B^-}\, \mathsf{b}\, \mathsf{r_B}}.$$

(3) *The number of HFPLs with boundary* $(\mathsf{l_T}, \mathsf{t}, \mathsf{r_T}; \mathsf{l_B}, \mathsf{b}, \mathsf{r_B})$ *equals*

$$\sum_{\mathsf{l_T^+}:\mathsf{l_T}\longrightarrow \mathsf{l_T^+}} (|\mathsf{l_T}|_1 + |\mathsf{t}|_1) c^{\mathsf{l_B}\, \mathsf{b}\, \mathsf{r_B}}_{\mathrm{m}(\mathsf{l_B})\,\mathsf{l_T^+}\,\mathsf{t},\mathrm{m}(\mathsf{t})\,\mathsf{r_T}\,\mathrm{m}(\mathsf{r_B})}$$

$$+ \sum_{\mathsf{t^+}:\mathsf{t}\longrightarrow \mathsf{t^+}} (|\mathsf{r_T}|_1 + R_1(\mathsf{t},\mathsf{t^+}) - 1) c^{\mathsf{l_B}\, \mathsf{b}\, \mathsf{r_B}}_{\mathrm{m}(\mathsf{l_B})\,\mathsf{l_T}\,\mathsf{t^+},\mathrm{m}(\mathsf{t})\,\mathsf{r_T}\,\mathrm{m}(\mathsf{r_B})}$$

$$+ \sum_{\mathsf{r_T^+}:\mathsf{r_T}\longrightarrow \mathsf{r_T^+}} (L + L(\mathsf{r_T},\mathsf{r_T^+})) c^{\mathsf{l_B}\, \mathsf{b}\, \mathsf{r_B}}_{\mathrm{m}(\mathsf{l_B})\,\mathsf{l_T}\,\mathsf{t},\mathrm{m}(\mathsf{t})\,\mathsf{r_T^+}\,\mathrm{m}(\mathsf{r_B})}$$

$$+ \sum_{\mathsf{r_B^-}:\mathsf{r_B^-}\longrightarrow \mathsf{r_B}} (|\mathsf{t}|_0 + |\mathsf{r_T}|_0 + |\mathsf{l_B}|_1 - |\mathsf{r_B}|_1 + 1) c^{\mathsf{l_B}\, \mathsf{b}\, \mathsf{r_B^-}}_{\mathrm{m}(\mathsf{l_B})\,\mathsf{l_T}\,\mathsf{t},\mathrm{m}(\mathsf{t})\,\mathsf{r_T}\,\mathrm{m}(\mathsf{r_B})}$$

$$- \sum_{\mathsf{b^-}:\mathsf{b^-}\longrightarrow \mathsf{b}} L_1(\mathsf{b^-},\mathsf{b}) c^{\mathsf{l_B}\, \mathsf{b^-}\, \mathsf{r_B}}_{\mathrm{m}(\mathsf{l_B})\,\mathsf{l_T}\,\mathsf{t},\mathrm{m}(\mathsf{t})\,\mathsf{r_T}\,\mathrm{m}(\mathsf{r_B})}$$

$$+ \sum_{\mathsf{l_B^-}:\mathsf{l_B^-}\longrightarrow \mathsf{l_B}} (|\mathsf{l_T}|_1 + |\mathsf{t}|_1 - L(\mathsf{l_B^-},\mathsf{l_B}) + 1) c^{\mathsf{l_B^-}\, \mathsf{b}\, \mathsf{r_B}}_{\mathrm{m}(\mathsf{l_B})\,\mathsf{l_T}\,\mathsf{t},\mathrm{m}(\mathsf{t})\,\mathsf{r_T}\,\mathrm{m}(\mathsf{r_B})}.$$

Theorem 5.45 implies the following enumeration result for TFPLs with boundary $(u, v; w)$ of excess 1 which is the content of Theorem 6.20 in [**11**].

COROLLARY 5.50. *Let $u, v, w$ be words of the same length with $\mathrm{exc}(u, v; w) = 1$. The number of TFPLs with boundary $(u, v; w)$ is given by*

$$\sum_{u^+:u\to u^+} |u|_1 c^w_{u^+,v} + \sum_{v^+:v\to v^+} L(v,v^+) c^w_{u,v^+} - \sum_{w^-:w^-\to w} L_1(w^-,w) c^w_{u,v}.$$

PROOF. The first two identities follow from Proposition 5.45(5) and Proposition 5.48; for the second identity also Proposition 5.41 needs to be considered. It remains to prove the third part of the theorem. First, note that in the excess-1-case (5.3) simplifies to

$$\overrightarrow{h}^{\mathsf{l_T},\mathsf{t},\mathsf{r_T}}_{\mathsf{l_B},\mathsf{b},\mathsf{r_B}}(q) = \overline{h}^{\mathsf{l_T},\mathsf{t},\mathsf{r_T}}_{\mathsf{l_B},\mathsf{b},\mathsf{r_B}}(q) + q^{-1}\sum_{\mathsf{t^+}:\mathsf{t}\to \mathsf{t^+}} \overline{h}^{\mathsf{l_T},\mathsf{t^+},\mathsf{r_T}}_{\mathsf{l_B},\mathsf{b},\mathsf{r_B}}(q) + q\sum_{\mathsf{b^-}:\mathsf{b^-}\to \mathsf{b}} \overline{h}^{\mathsf{l_T},\mathsf{t},\mathsf{r_T}}_{\mathsf{l_B},\mathsf{b^-},\mathsf{r_B}}(q).$$

Furthermore, it has to hold $\mathrm{exc}(\mathsf{l_T}, \mathsf{t^+}, \mathsf{r_T}; \mathsf{l_B}, \mathsf{b}, \mathsf{r_B}) = \mathrm{exc}(\mathsf{l_T}, \mathsf{t}, \mathsf{r_T}; \mathsf{l_B}, \mathsf{b^-}, \mathsf{r_B}) = 0$ if $\mathsf{t} \to \mathsf{t^+}$ and $\mathsf{b^-} \to \mathsf{b}$. Thus, $\overline{h}^{\mathsf{l_T},\mathsf{t^+},\mathsf{r_T}}_{\mathsf{l_B},\mathsf{b},\mathsf{r_B}}(q) = h^{\mathsf{l_T},\mathsf{t^+},\mathsf{r_T}}_{\mathsf{l_B},\mathsf{b},\mathsf{r_B}}$ and $\overline{h}^{\mathsf{l_T},\mathsf{t},\mathsf{r_T}}_{\mathsf{l_B},\mathsf{b^-},\mathsf{r_B}}(q) = h^{\mathsf{l_T},\mathsf{t},\mathsf{r_T}}_{\mathsf{l_B},\mathsf{b^-},\mathsf{r_B}}$ by Proposition 5.34. Therefore,

$$\overline{h}^{\mathsf{l_T},\mathsf{t},\mathsf{r_T}}_{\mathsf{l_B},\mathsf{b},\mathsf{r_B}}(q) = \overrightarrow{h}^{\mathsf{l_T},\mathsf{t},\mathsf{r_T}}_{\mathsf{l_B},\mathsf{b},\mathsf{r_B}}(q) - q^{-1}\sum_{\mathsf{t^+}:\mathsf{t}\to \mathsf{t^+}} c^{\mathsf{l_B}\, \mathsf{b}\, \mathsf{r_B}}_{\mathrm{m}(\mathsf{l_B})\,\mathsf{l_T}\,\mathsf{t^+},\mathrm{m}(\mathsf{t})\,\mathsf{r_T}\,\mathrm{m}(\mathsf{r_B})} - q\sum_{\mathsf{b^-}:\mathsf{b^-}\to \mathsf{b}} c^{\mathsf{l_B}\, \mathsf{b^-}\, \mathsf{r_B}}_{\mathrm{m}(\mathsf{l_B})\,\mathsf{l_T}\,\mathsf{t},\mathrm{m}(\mathsf{t})\,\mathsf{r_T}\,\mathrm{m}(\mathsf{r_B})}.$$

Finally, in order to derive $h^{\mathsf{r_B},\mathsf{b^-},\mathsf{l_B}}_{\mathsf{l_T},\mathsf{t},\mathsf{r_T}}$ from the weighted enumeration in Theorem 5.49 with the help of Lemma 5.18 one last identity is needed:

$$\sum_{b^-:\, b^-\to b} c^{\,l_B\; b^-\; r_B}_{m(l_B)\, l_T\, t,m(t)\, r_T\; m(r_B)} + \sum_{l_B^-:\, l_B^-\to l_B} c^{\,l_B^-\; b\; r_B}_{m(l_B^-)\, l_T\, t,m(t)\, r_T\; m(r_B)}$$

$$= \sum_{r_T^+:\, r_T\to r_T^+} c^{\,l_B\; b\; r_B}_{m(l_B)\, l_T\, t,m(t)\, r_T^+\; m(r_B)} + \sum_{t^+:\, t\to t^+} c^{\,l_B^-\; b\; r_B}_{m(l_B)\, l_T\, t^+,m(t^+)\, r_T\; m(r_B)}.$$

Its proof is analogous to the proof of the identity $\displaystyle\sum_{v^+:\, v\to v^+} c^{w}_{u,v^+} = \sum_{w^-:\, w^-\to w} c^{w^-}_{u,v}$ in [**11**]. $\square$

## 5.7. Outlook

In the previous chapters we have advanced the study of TFPLs. These advances may too be achieved for HFPLs. To begin with, Wieland drift for HFPLs can be defined as the generalisation of Wieland drift for TFPLs. For HFPLs it then ought to possess similar properties as it does for TFPLs. For instance, it should be eventually stable with period one. If the latter is true it should be possible to obtain an expression for the number of HFPLs of excess 2 in terms of stable HFPLs. This expression then must generalise the expression obtained in Theorem 4.2.

# Bibliography

[1] F. C. Alcaraz, M. N. Barber and M. T. Batchelor. Conformal invariance, the XXZ chain and the operator content of two-dimensional critical systems. *Ann. Phys.* NY 182:280–343.

[2] M. F. Ashley, W. F. Giauque. Molecular rotation in ice at 10°K. Free energy of formation and entropy of water. *Physical Review*, 43:81–82, 1933.

[3] M. T. Batchelor, H. W. J. Blöte, B. Nienhuis and C. M. Yung. Critical behaviour of the fully packed loop model on the square lattice. *J. Phys. A*, 29:L399–L404, 1996.

[4] R. Behrend, I. Fischer, M. Konvalinka. Diagonally and antidiagonally symmetric alternating sign matrices of odd order. *arXiv:1512.06030*, 2016.

[5] S. Beil. Combinatorics of hexagonal fully packed loop configurations. *Adv. Appl. Math.*, 69:109–147, 2015.

[6] S. Beil. Triangular fully packed loop configurations of excess 2 (extended abstract). *Discr. Math. Theoret. Comput. Science*, Proceedings of FPSAC 2015 (2015).

[7] S. Beil. Triangular fully packed loop configurations of excess 2. *Elect. J. Comb.*, accepted April 2016.

[8] S. Beil, I. Fischer and P. Nadeau. Wieland drift for triangular fully packed loop configurations, *Elect. J. Comb.*, 22(1), 2015

[9] L. Cantini and A. Sportiello. Proof of the Razumov–Stroganov conjecture, *J. Combinatorial Theory Ser. A*, 118(5):1549–1574, 2011.

[10] F. Caselli, C. Krattenthaler, B. Lass and P. Nadeau. On the number of fully packed loop configurations with a fixed associated matching. *Elect. J. Comb.*, 11(2), 2004.

[11] I. Fischer, P. Nadeau. Fully Packed Loops in a triangle: matchings, paths and puzzles. *J. Combinanorial Theory Ser. A*, 130:64–118, 2015.

[12] A. Knutson, T. Tao. Puzzles and (equivariant) cohomology of Grassmannians. *Duke Math. J.*, 119:221–260, 2003.

[13] V. E. Korepin. Calculation of norms of Bethe wave functions. *Commun. Math. Phys.*, 86:391–418, 1982.

[14] G. Kuperberg. Another proof of the alternating sign matrix conjecture. *Internat. Math. Res. Notices*, 139–150, 1996.

[15] E. H. Lieb. Residual entropy of square ice. *Physical Review*, 162(1):162–172, 1967.

[16] W. H. Mills, D. P. Robbins, H. Rumsey. Proof of the MacDonald conjecture. *Invent. Math.*, 66:73–87, 1982.

[17] W. H. Mills, D. P. Robbins, H. Rumsey. Alternating-sign matrices and descending plane partitions. *J. Combinatorial Theory Ser. A*, 34:340–359, 1983.

[18] S. Mitra, B. Nienhuis, J. de Gier, M. T. Batchelor. Exact expressions for correlations in the ground state of the dense $\mathcal{O}(1)$ loop model. *J. Stat. Mech. Theory Exp.*, P09010, 2004.

[19] P. Nadeau. Fully packed loop configurations in a triangle. *J. Combinanorial Theory Ser. A*, 120(8):2164–2188, 2013.

[20] P. Nadeau. Fully packed loop configurations in a triangle and Littlewood–Richardson coefficients. *J. Combinatorial Theory Ser. A*, 120(8):2137–2147, 2013.

[21] J. F. Nagle. Lattice statistics of hydrogen bonded crystals. I. The residual entropy of ice. *J. Math. Phys.*, 7(8):1484–1491, 1966.

[22] L. Pauling. The structure and entropy of ice and other crystals with some randomness of atomic arrangement. *J. Am. Chem. Soc.*, 57(12): 2680–2684, 1935.

[23] P. A. Pearce, V. Rittenberg, J. de Gier, B. Nienhuis. Temperley-Lieb stochastic processes. *J. Phys. A.*, 35:L661–L668, 2002.

[24] J. Propp. The many faces of alternating–sign matrices. *Discrete models: combinatorics, computation, and geometry (Paris, 2001)*, Discrete Math. Theor. Comput. Sci. Proc., AA, pages 043–058 (electronic). Maison Inform. Math. Discrèt. (MIMD), Paris, 2001. 45:175–188, 2009.

[25] A. V. Razumov and Y. G. Stroganov. Combinatorial nature of ground state vector of O(1) loop model. *Theor. Math. Phys.*, 138:333–337, 2004.

[26] D. Romik. Connectivity patterns in loop percolation I: the rationality phenomen and constant term identities. *Comm. Math. Phys.*, 330(2), 2013.

[27] J. C. Slater. Theory of the transition in $KH_2PO_4$. *J. Chem. Phys.*, 9(1):16–33, 1941.

[28] R. P. Stanley. Theory and applications of plane partitions: Part 2. Stud. Appl. Math., 50:259–279, 1971.

[29] J. Thapper. Refined counting of fully packed loop configurations. *Séminaire Lotharingien de Combinatoire*, 56:B56e:27, 2007.

[30] B. Wieland. A large dihedral symmetry of the set of alternating sign matrices. *Elect. J. Comb.*, 7: Research paper 37, 2000.

[31] D. Zeilberger. Proof of the alternating sign matrix conjecture. *Elect. J. Comb.*, 3(2): Research paper 13, 1996.

[32] P. Zinn-Justin. Littlewood-Richardson coefficients and integrable tilings. *Elect. J. Comb.*, 16: Research paper 12, 2009.

[33] P. Zinn-Justin. Six-vertex, loop and tiling models: integrability and combinatorics. *Lap Lambert Acad. Publ.*, 2010.

[34] P. Zinn-Justin. A conjectured formula for fully packed loop configurations in a triangle. *Elect. J. Comb.*, 17: Research paper 107, 2010.

[35] J. B. Zuber. On the counting of fully packed loop configurations: Some new conjectures. *Elect. J. Comb.*, 11(1): Research paper 13, 2004.